UCSF
UC San Francisco Electronic Theses and Dissertations

Title
Pharmacogenetic studies of membrane transporters relevant to anti-cancer drug therapy

Permalink
https://escholarship.org/uc/item/7h03t9km

Author
Badagnani, Ilaria

Publication Date
2006

Peer reviewed|Thesis/dissertation

eScholarship.org Powered by the California Digital Library
University of California

Pharmacogenetic Studies Of Membrane Transporters Relevant To Anti-Cancer Drug Therapy

by

Ilaria Badagnani

DISSERTATION

Submitted in partial satisfaction of the requirements for the degree of

DOCTOR OF PHILOSOPHY

in

Pharmaceutical Sciences and Pharmacogenomics

in the

GRADUATE DIVISION

of the

UNIVERSITY OF CALIFORNIA, SAN FRANCISCO



ACKNOWLEDGEMENTS

Graduate school was quite an adventure characterized by great excitements, but also some frustrating times. While at UCSF, I have grown professionally and personally thanks to many friends and colleagues who have given me support and devoted their time to training and teaching me. They have also encouraged me to explore new opportunities and challenges and have been instrumental in many of my achievements.

First and foremost, I would like to thank my research advisor, Dr. Kathleen Giacomini, for being an outstanding teacher and mentor throughout my graduate career. She has helped me develop as a scientist and has given me ample opportunities to explore new areas of research, while at the same time offering valuable advice to keep my research projects on course. Kathy has also been instrumental in expanding my presentation and writing skills and has devoted considerable time during my graduate career to ensure that my research and scientific endeavors were successful. In addition, I have appreciated the kind words of encouragement and the emotional support I have received from Kathy throughout my graduate studies.

I also want to thank the other members of my thesis committee, Dr. Deanna Kroetz and Dr. Laura Bull, for their helpful advice and critique of my research projects and dissertation. In addition, Dr. Leslie Benet, who was a member of my oral qualifying committee, was instrumental in my decision to come to UCSF and join the PSPG program. He was an invaluable resource when I was trying to decide on the next step in my career. Throughout graduate school, Les was a fantastic teacher and an outstanding mentor.

I thank everyone in the Pharmacogenetics of Membrane Transporters project, especially Travis Taylor, Elaine Carlson, Doug Stryke, Conrad Huang, Michiko Kawamoto, Susan Johns, and Dr. Claire Brett, for their invaluable assistance in the genomics and bioinformatics aspects of my research projects. In addition, my collaborators at St. Jude Children's Research Hospital, Dr. Mary Relling, Dr. Cheng Cheng, and Dr. Ching-Hon Pui were instrumental in helping me develop the clinical portion of my dissertation and provided outstanding technical and scientific advice.

I would like to thank all of the members of the Giacomini and Kroetz lab, especially Ryan, Tom, Jim, Chaline, Cheryl, Lara, Maya, Leah, Marco, Kim, Val, and Tan, for their friendship, encouragement, and assistance in the technical and scientific aspects of my research. Graduate school would have truly been an unhappy place without any one of them.

I give my warmest thanks to my parents for the boundless love, emotional support, and great advice they have given me throughout my life. They have been instrumental in many of my career decisions and have always provided great encouragement. I also give special thanks to my great friends, Liat, Sis, and Julie, for being there for me throughout graduate school in both the happy and difficult moments. They have provided countless words of encouragement and have been cheering me on since my first day at UCSF. I could not have done this without them.

A very special recognition goes to James who has enriched my life in the past several months. I could not have found a better person to share this exciting time of my life with. He has given me great advice, emotional support, and a stress-free environment when I needed it the most.

Subject: RE: The Pharmacogenomics Journal - Reprint permission

Date: Mon, 12 Jun 2006 13:48:55 +0100

From: "ajpermissions" <ajpermissions@nature.com> Add to Address Book Add Mobile Alert

To: "Ilaria Badagnani" <ibadagnani@yahoo.com>

Dear Requestor -

If you are the author (or the author's designated agent) of the NPG material you wish to reproduce, you probably do not need to seek permission for re-use, so long as the journal is credited with initial publication. Please see the bottom of this message for further details.

If you are not the author (or the author's designated agent), I am pleased to inform you that Nature Publishing Group has now partnered with Copyright Clearance Center's Rightslink service, which allows permissions to be requested and purchased online.

To obtain your permission, please access the following URL

http://search.nature.com/search/?sp-a=sp1001702d&sp-t=expanded&sp-q=

and use the search facility to find the NPG paper from which you wish to reproduce material.

Beneath the listing for the paper (when found through the search), you will find a clickable option 'Rights and Permissions', which will take you to the order entry page from which you can request your permission.

During the process, you will set up an account with Rightslink, who will invoice you for any fees incurred. You will be able to use your Rightslink account in the future to request (and pay for) permissions online both from Nature Publishing Group and from other participating publishers. Rightslink will also email you confirmation that permission has been granted, in the form of a printable licence.

I hope you will find Rightslink a quick and efficient way of obtaining permissions. If Rightslink cannot provide the permission you require (for example, if the material you require pre-dates our online archives), of if you have any questions or comments, please contact me at ajpermissions@nature.com .

With best regards -

Jo Webber

Permissions Manager
Academic Journals Division
Nature Publishing Group

Author Requests

If you are the author of this content (or his/her designated agent) please read the following.
Ownership of copyright in the article remains with the Authors, and provided that, when reproducing the Contribution or extracts from it, the Authors acknowledge first and reference publication in the Journal, the Authors retain the following non-exclusive rights:

a) To reproduce the Contribution in whole or in part in any printed volume (book or thesis) of which they are the author(s).

b) They and any academic institution where they work at the time may reproduce the Contribution for the purpose of course teaching.

c) To reuse figures or tables created by them and contained in the Contribution in other works created by them.

d) To post a copy of the Contribution as accepted for publication after peer review (in Word or Tex format) on the Author's own web site, or the Author's institutional repository, or the Author's funding body's archive, six months after publication of the printed or online edition of the Journal, provided that they also link to the Journal article on NPG's web site (eg through the DOI).

NPG encourages the self-archiving of the accepted version of your manuscript in your funding agency's or institution's repository, six months after publication. This policy complements the recently announced policies of the US National Instutes of Health, Wellcome Trust and other research funding bodies around the world. NPG recognises the efforts of funding bodies to increase access to the research they fund, and we strongly encourage authors to participate in such efforts.

Authors wishing to use the published version of their article for promotional use or on a web site must request in the normal way.

If you require further assistance please read NPG's online author reuse guidelines.

-----Original Message-----
From: Ilaria Badagnani [mailto:ibadagnani@yahoo.com]
Sent: 09 June 2006 23:55
To: ajpermissions
Subject: The Pharmacogenomics Journal - Reprint permission

To NPG Permissions Controller,

I am writing to request a permission to reprint in my Ph.D. thesis an article that was accepted for publication in 2005 entitled: "Functional analysis of genetic variants in the human concentrative nucleoside transporter 3 (CNT3; SLC28A3)" written by I Badagnani, W Chan, R A Castro, C M Brett, C C Huang, D Stryke, M Kawamoto, S J Johns, T E Ferrin, E J Carlson, E G Burchard and K M Giacomini. It appeared in the Pharmacogenomics Journal in volume 5, pages 157−165 (doi: 10.1038/sj.tpj.6500303).
I would be very grateful if you could fax me (415-514-4361) or e-mail me (ibadagnani@yahoo.com) a letter of authorization.
Thank you very much for your assistance.
Sincerely,

Ilaria Badagnani
Department of Biopharmaceutical Sciences
University of California, San Francisco
1550 Fourth Street, Rock Hall, RH 581, Box 2911
phone: 415-514-4363
fax: 415-514-4361
e-mail: ibadagnani@yahoo.com
San Francisco, CA 94158-2324

aspet
100 YEARS 1908—2008

Council

Elaine Sanders-Bush
President
Vanderbilt University

Kenneth P. Minneman
President-Elect
Emory University

James E. Barrett
Past President
Adolor Corporation

Lynn Wecker
Secretary/Treasurer
University of South Florida

Annette E. Fleckenstein
Secretary/Treasurer-Elect
University of Utah

Patricia K. Sonsalla
Past Secretary/Treasurer
University of Medicine & Dentistry of New Jersey

Bryan F. Cox
Councilor
Abbott Laboratories

Ronald N. Hines
Councilor
Medical College of Wisconsin

Terrence J. Monks
Councilor
University of Arizona

Brian M. Cox
Board of Publications Trustees
Uniformed Services University of the Health Sciences

Jack Bergman
Program Committee
Harvard Medical School - McLean Hospital

Sharon G. Hoffmann
Long Range Planning Committee
Emory University

Christine K. Carrico
Executive Officer

9650 Rockville Pike
Bethesda, MD 20814-3995

Phone: (301) 634-7060
Fax: (301) 634-7061

info@aspet.org
www.aspet.org

August 4, 2006

Ilaria Badagnani
Dept. of Biopharmaceutical Sciences
University of California, SF
1550Fourth Street, Rock Hall, RH 581
Box 2911
San Francisco, CA 94158-2324

Dear Dr. Badagnani:

This is to grant you permission to reproduce the following article in your dissertation:

Ilaria Badagnani, Richard A. Castro, Travis R. Taylor, Claire M. Brett, Conrad C. Huang, Douglas Stryke, Michiko Kawamoto, Susan J. Johns, Thomas E. Ferrin, Elaine J. Carlson, Esteban G. Burchard, and Kathleen M. Giacomini entitled, "**Interaction of Methotrexate with Organic-Anion Transporting Polypeptide 1A2 and Its Genetic Variants**", *Journal of Pharmacology and Experimental Therapeutics*, vol. 318, no. 2, pp. 521-529, August 2006.

On the first page of each copy of the article, please add the following:

> Reprinted with permission of the American Society for Pharmacology and Experimental Therapeutics. All rights reserved.

In addition, the original copyright line published with the paper must be shown on the copies included with your dissertation.

Sincerely yours,

Richard Dodenhoff

Richard Dodenhoff
Journals Director

American Society for Pharmacology and Experimental Therapeutics

ABSTRACT

Pharmacogenetic Studies Of Membrane Transporters Relevant To Anti-Cancer Drug Therapy

Ilaria Badagnani

Membrane transporters are important determinants of drug disposition and response. The goals of this dissertation are to examine the interaction of membrane transporters with anti-cancer drugs, in particular cladribine, fludarabine, and methotrexate, and to analyze their genetic and functional diversity. We showed that the human concentrative nucleoside transporter CNT3 (*SLC28A3*), which transports nucleoside analogs, is under negative selective pressure. The rare variant, protein reference sequence (p.) Gly367Arg, exhibited reduced transport of nucleosides, whereas common non-synonymous variants of CNT3 exhibited no change in their transport of nucleosides, suggesting that common coding region variants of CNT3 do not contribute to common variation in the efficacy of cladribine and fludarabine. Methotrexate exhibits variable pharmacokinetics and renal toxicity. We showed that the human organic anion transporting polypeptide, OATP1A2 (*SLCO1A2*) transports methotrexate in a pH-dependent manner. Since the human organic anion transporter OAT3 (*SLC22A8*) and OATP1A2 are expressed in the renal tubule, they may play a role in the elimination and nephrotoxicity of methotrexate. We identified four protein-altering variants in OATP1A2 and six in OAT3 that had altered transport of methotrexate, suggesting that these variants may contribute to variation in the renal disposition and toxicity of methotrexate. We characterized the mechanism of transport and identified critical amino acid residues in OATP1A2 that are responsible for methotrexate uptake. The enhanced transport at

acidic pH resulted from increased substrate affinity and did not depend on the proton gradient. Conserved cationic residues in OATP1A2 were important in methotrexate recognition and uptake. Lastly, we initiated collaborative studies to examine the characteristics of methotrexate elimination in patients with acute lymphoblastic leukemia (ALL). Methotrexate pharmacokinetics were non-linear and highly variable. Increased exposure to methotrexate was associated with delayed elimination. In future studies, we will genotype ALL patients for 11 variants and 16 haplotypes in 6 kidney transporters to analyze the contribution of kidney transporters to variation in MTX pharmacokinetics and renal toxicity. These studies have enhanced our understanding of how membrane transporters interact with anti-cancer drugs and, thereby, control their systemic and tissue levels. Genetic variation in these transporters may contribute to variation in the efficacy and toxicity of anti-cancer drugs.

Kathleen M. Giacomini

Nov 20, 2006

TABLE OF CONTENTS

Title Page i

Acknowledgements iii

Abstract ix

Table of Contents xi

List of Tables xviii

List of Figures xx

Chapter 1

Pharmacogenetics Of The Human *SLCO* (OATP) Transporter Family 1

Introduction – The *SLCO* (OATP) uptake transporter family 1

SLCO1A2 (OATP1A2; OATP-A) 7

SLCO1B1 (OATP1B1; OATP-C) 19

SLCO1B3 (OATP1B3; OATP8) 31

SLCO1C1 (OATP1C1; OATP-F) 32

SLCO2A1 (OATP2A1; hPGT) 33

SLCO2B1 (OATP2B1; OATP-B) 33

SLCO3A1 (OATP3A1; OATP-D) 34

SLCO4A1 (OATP4A1; OATP-E) 35

SLCO4C1 (OATP4C1; OATP-H) 35

SLCO5A1 (OATP5A1; OATP-J) 36

SLCO6A1 (OATP6A1; OATP-I) 36

Future directions 36

Summary of dissertation chapters 37

Chapter 2 37

Chapter 3 38

Chapter 4 39

Chapter 5 39

Chapter 6 40

References 41

Chapter 2

Interaction Of Anti-Cancer Nucleoside Analog Drugs With CNT3 And Its Genetic Variants 52

Introduction 52

Materials and Methods 54

Identification of *SLC28A3* variants 54

Genetic analysis of *SLC28A3* 54

Construction of *SCL28A3* variants 55

Functional studies of *SLC28A3* variants in oocytes 55

Results 56

Analysis of genetic variation in *SLC28A3* 56

Analysis of *SLC28A3* haplotypes 61

Functional characterization of non-synonymous variants in CNT3 63

Discussion 70

References 76

Chapter 3

Interaction Of Methotrexate, An Organic Anion Drug, With OATP1A2 And Its Genetic Variants 84

Introduction 84

Materials and Methods 86

Materials 86

Xenopus laevis oocyte expression assay 87

Saturation Kinetics of ^{3}H-MTX 88

MTX transport by OATP1A2 is sensitive to extracellular pH 88

Identification of *SLCO1A2* variants 89

Construction of *SLCO1A2* variants for *X. laevis* oocyte studies 89

Functional studies of *SLCO1A2* variants 90

Results 91

OATP1A2 interacts with the folate antagonists, MTX and 7-OH-MTX 91

Transport of MTX by OATP1A2 is sensitive to extracellular pH (pH_o) 92

Genetic variation in human SLCO1A2 97

Functional alterations in ES and MTX transport by protein-altering variants in OATP1A2 100

Discussion 106

References 111

Chapter 4

Interaction of Methotrexate With OAT3 (*SLC22A8*) And Its Genetic Variants **116**

Introduction 116

Material and Methods 117

Materials 117

Transport of folates and folate antagonists by OAT3 118

Saturation kinetics of ^{3}H-MTX 119

Genetic analysis of *SLC22A8* 119

Functional analysis of variants in *SLC22A8* in HEK293 cells 120

Results 121

Interaction of folates and folate antagonists with OAT3 121

Analysis of genetic variation in *SLC22A8* 124

Haplotype analysis of *SLC22A8* 128

Functional characterization of MTX transport by protein-altering variants in OAT3 129

Discussion 136

References 142

Chapter 5

Mechanisms Of Transport And Structural Determinants Of Specificity of OATP1A2 147

Introduction 147

Material and Methods 149

Materials 149

HEK293 cell culture and transfection 149

Xenopus laevis oocyte expression assay 150

Effect of pH, sodium dependency, and membrane potential on ^{3}H-ES uptake 151

pH-dependent kinetics of ^{3}H-ES uptake 152

Effect of FCCP, GSH, HCO_3^-, and OH^- on ^{3}H-ES uptake 152

Effect of Intracellular GSH concentration on ^{3}H-ES uptake 154

Construction and functional studies of PDZ consensus sequence mutants in OATP1A2 154

Effect of cationic residues in OATP1A2 on ^{3}H-ES and/or ^{3}H-MTX uptake 155

Effect of mutating charged residues in OATP1A2 to the corresponding ones in rat Oatp1a1/Oatp1a4 on ^{3}H-ES transport 157

Results 157

Transport of ES by OATP1A2 is sensitive to extracellular pH (pH_o) 157

OATP1A2-mediated transport of ES does not depend on intracellular pH (pH_i) or the proton gradient 158

OATP1A2-mediated transport of ES does not depend on the sodium 163

gradient or membrane potential

OATP1A2-mediated transport of ES is not sensitive to intracellular concentrations of GSH, HCO_3^-, or OH^- 163

PDZ consensus sequence in C-terminus of OATP1A2 is not required for organic anion transport 165

Chemical modification of histidine residues inhibits ES transport by OATP1A2 177

Functional analysis of arginine, lysine, and histidine replacements in OATP1A2 on organic anion transport 177

Functional analysis of charged amino acid replacements in OATP1A2 to uncharged or oppositely charged ones in rOatp1a1/Oatp1a4 on ES transport 179

Discussion 183

Functional analysis of pH-sensitive transport of ES by OATP1A2 184

Effect of membrane potential on ES transport mediated by OATP1A2 185

Effect of intracellular GSH, HCO_3^-, or OH^- on ES uptake by OATP1A2 185

Functional analysis of PDZ consensus sequence in C-terminus of OATP1A2 on organic anion transport 186

Functional analysis of arginine, lysine, and histidine replacements in OATP1A2 on organic anion transport 187

Functional analysis of charged amino acid replacements in 187

OATP1A2 to uncharged or oppositely charged ones in rOatp1a1/Oatp1a4 on ES transport

References 189

Chapter 6

Role Of Genetic Variation In Kidney Transporters In Methotrexate Disposition And Toxicity **194**

Introduction 194

Material and Methods 196

Study Population 196

Pharmacokinetic Analysis 198

Genotyping 199

Pharmacoepidemiological Analysis 200

Results 200

ALL study population 200

Kidney transporter genotyping 203

Pharmacoepidemiological analysis of ALL population 208

Discussion 222

References 228

Chapter 7

Summary And Conclusions **235**

References 249

LIST OF TABLES

Chapter 1

Table 1	Summary of the characteristics of human members of the *SLCO*/OATP transporter superfamily	2
Table 2	Tissue distribution of human OATP transporters	4
Table 3	Summary of genetic variants in *SLCO* genes encoding OATP transporters	8
Table 4	Summary of functional consequence of genetic variation in *SLCO1B1* on drug transport *in vitro*	22
Table 5	Clinical consequence of genetic variation in *SLCO1B1* on drug efficacy and disposition in humans	27

Chapter 2

Table 1	Summary of coding region variants in CNT3 identified in ethnically diverse population	58
Table 2	Estimates of the neutral parameter (θ), nucleotide diversity (π), and Tajima's D for *SLC28A3*	59
Table 3	Kinetics of interaction of adenosine and its analogs with CNT3 and its three common non-synonymous variants	69

Chapter 3

Table 1	Summary of protein-altering variants in OATP1A2 identified in ethnically diverse populations	99
Table 2	Summary of interaction kinetics of ES with OATP1A2	104

and the common protein-altering variants, p. Ile13Thr and p. Thr668Ser

Chapter 4

Table 1 Summary of variants in the coding region of OAT3 identified in ethnically diverse populations 125

Table 2 Estimates of the neutral parameter (θ), nucleotide diversity (π), and Tajima's D for *SLC22A8* 127

Table 3 Summary of transport kinetics of MTX with OAT3 and the 3 common protein-altering variants, p. Val281Ala, p. Ile305Phe, and p. Val448Ile 135

Chapter 5

Table 1 Transport of ES by OATP1A2 in *X. laevis* oocytes is not sensitive to the proton gradient or intracellular concentrations of GSH, $HCO3^-$, or OH^- 162

Chapter 6

Table 1 ALL patient characteristics 201

Table 2 Summary of 23 SNPs in 6 kidney membrane transporter genes 204

LIST OF FIGURES

Chapter 1

Figure 1	Schematic of the localization of human OATP transporters in the hepatocyte	6
Figure 2	Structure and population frequency of 28 haplotypes of *SLCO1A2* estimated in 270 ethnically diverse healthy individuals	18
Figure 3	Schematic representation of *SLCO1B1* variant alleles	20

Chapter 2

Figure 1	Secondary structure of CNT3 showing the position of the 16 coding region variants	60
Figure 2	Structure and population frequency of 35 haplotypes of *SLC28A3*	62
Figure 3	Uptake of nucleosides (inosine and thymidine) in *X. laevis* oocytes expressing CNT3-reference and its non-synonymous variants	64
Figure 4	Uptake of adenosine analogs in *X. laevis* oocytes expressing CNT3-reference and its non-synonymous variants, p. Ser5Asn, p. Tyr113Cys, and p. Ile328Val	65
Figure 5.	Kinetics of inhibition of ^{3}H-Inosine uptake by adenosine in *X. laevis* oocytes expressing CNT3-reference and the common non-synsonymous variants p. Ser5Asn, p. Tyr113Cys, and p. Ile328Val	66

Figure 6 Kinetics of inhibition of ^{3}H-Inosine uptake by cladribine in *X. laevis* oocytes expressing CNT3-reference and the common non-synsonymous variants p. Ser5Asn, p. Tyr113Cys, and p. Ile328Val 67

Figure 7 Kinetics of inhibition of ^{3}H-Inosine uptake by fludarabine in *X. laevis* oocytes expressing CNT3-reference and the common non-synsonymous variants p. Ser5Asn, p. Tyr113Cys, and p. Ile328Val 68

Chapter 3

Figure 1 MTX and its metabolite, 7-OH-MTX, are transported by OATP1A2 93

Figure 2 Kinetics of MTX transport in *X. laevis* oocytes expressing OATP1A2 94

Figure 3 Transport of MTX by OATP1A2 is sensitive to extracellular pH 95

Figure 4 Transport of MTX by OATP1A2 is independent of the proton gradient 96

Figure 5 Secondary structure of OATP1A2 showing the location of the 12 protein-altering variants 98

Figure 6 Two common (p. Ile13Thr and p. Glu172Asp) and two rare (p. Arg168Cys and p. Asn278DEL) protein-altering variants of OATP1A2 show altered transport function of ES and/or MTX 102

Figure 7 Kinetics of interaction of ES with OATP1A2 and the common protein-altering variants, Ile13Thr and Thr668Ser 103

Figure 8 Kinetics of interaction of ES with OATP1A2 and the common protein-altering variant, Glu172Asp 105

Chapter 4

Figure 1 Folates and folate antagonists inhibit OAT3 122

Figure 2 Transport kinetics of MTX in HEK293 cells expressing OAT3 123

Figure 3 Secondary structure prediction of OAT3 showing the location of the 10 protein-altering variants 126

Figure 4 Structure and population frequency of 20 haplotypes of *SLC22A8* 130

Figure 5 Cladogram of the 20 common haplotypes of *SLC22A8* 131

Figure 6 Uptake of ES and MTX in HEK293 cells expressing OAT3 and its 10 protein-altering variants 133

Figure 7 Kinetics of interaction of MTX with OAT3 and its 3 common protein-altering variants 134

Chapter 5

Figure 1 Transport of ES by OATP1A2 in transiently transfected HEK293 cells is sensitive to extracellular pH 159

Figure 2 Kinetics of ES transport by OATP1A2 at pH_o 5.0 shows dramatic decrease in K_m compared to pH_o 7.4 in transiently transfected HEK293 cells 160

Figure 3	Transport of ES by OATP1A2 is not sensitive to intracellular pH in transiently transfected HEK293 cells	161
Figure 4	Transport of ES by OATP1A2 is not sensitive to the sodium gradient or membrane potential in transiently transfected HEK293 cells	164
Figure 5	Multiple sequence alignment of human and rat OATPs/Oatps	166
Figure 6	Predicted secondary structure model of OATP1A2	170
Figure 7	pH-dependent transport of ES by C-terminus PDZ consensus sequence mutants of OATP1A2 in transiently transfected HEK293 cells	171
Figure 8	Overexpression of the PDZ proteins, PDZK1 and IKEPP, along with OATP1A2 does not enhance ES or MTX transport in *X. laevis* oocytes	172
Figure 9	Effect of the amino acid-modifying reagents, PGO, TNBS, and DEPC on ES uptake in transiently transfected HEK293 cells	174
Figure 10	Functional effects of arginine and lysine replacements in OATP1A2 on ES transport in transiently transfected HEK293 cells	175
Figure 11	Functional analysis of the effect of single histidine replacement in OATP1A2 on MTX transport in *X. laevis* oocytes	176
Figure 12	Multiple sequence alignment of human OATP1A2 and rat	180

Oatp1a1 and Oatp1a4

Figure 13 Functional effect of mutating conserved charged residues in OATP1A2 to the corresponding uncharged or oppositely charged ones in rat Oatp1a1/Oatp1a4 on ES transport in transiently transfected HEK293 cells 182

Chapter 6

Figure 1 Diagram of membrane transporters expressed in the human proximal and distal tubule cells of the kidney that interact with MTX 197

Figure 2 Ethnic and gender distribution of ALL population 202

Figure 3 Structure and population frequency of the most common haplotypes in 4 kidney transporters (*SLC22A8*, *SLCO1A2*, ABCC2, and ABCG2), which are used to subgroup the ALL population 206

Figure 4 Median MTX systemic clearance estimated in 564 ALL patients 209

Figure 5 Median plasma MTX concentration measured 42 hours after start of MTX infusion in 511 ALL patients 210

Figure 6 Median plasma MTX C_{42h} is negatively correlated with median MTX CL in 511 ALL patients 211

Figure 7 Median MTX AUC is positively correlated with plasma MTX C_{42h} in 511 ALL patients 212

Figure 8 Median MTX CL is positively correlated with MTX dose 213

in 565 ALL patients

Figure 9 Median MTX volume of distribution for the central compartment (V_c) is negatively correlated with plasma MTX dose in 565 ALL patients 214

Figure 10 Median SCr measured before and after MTX in 511 ALL patients 216

Figure 11 Median GFR measured before and after MTX in 404 ALL patients 217

Figure 12 Median total bilirubin measured before and after MTX in 364 ALL patients 218

Figure 13 Median ALT measured before and after MTX in 155 ALL patients 219

Figure 14 Median AST measured before and after MTX in 154 ALL patients 220

Chapter 7

Figure 1 Determinants of anti-cancer drug action 237

Figure 2 Schematic diagram depicting disposition of anti-cancer drugs in the kidney (left panel) and cancer cells (right panel) based on findings from Chapter 2, 3, and 4 246

CHAPTER 1

PHARMACOGENETICS OF THE HUMAN *SLCO* (OATP) TRANSPORTER FAMILY

1. Introduction – The *SLCO* (OATP) uptake transporter family

Transporters are critical determinants in controlling the uptake and efflux of endogenous compounds, xenobiotics, and clinically used drugs from cells and tissues throughout the body. In particular, transport proteins that are expressed in epithelial tissues, including the intestine, liver, and kidney, are critical modulators of the efficacy, disposition, and toxicity of drugs (1, 2). It is well recognized that there is considerable inter-individual variability in drug response and adverse effects from drugs and that a significant portion of such variation can be explained by an individual's genes (3). Pharmacogenetics research has focused primarily on drug metabolizing enzymes, though more recently it has expanded to include the identification and characterization of genetic variation in other proteins that interact with drugs, such as drug transporters and drug receptors to examine the impact on the observed inter-individual variability in drug therapy (4-6).

Among uptake transporters, transport proteins belonging to the organic anion-transporting polypeptide (*SLCO*; OATP) family interact with a diverse set of endogenous and therapeutic compounds (Table 1) and are expressed in multiple tissues (Table 2), suggesting that they play a critical role in cellular homeostasis and in modulating drug therapy (7, 8). There are 11 human OATPs that have been identified to date, which belong to five sub-families, OATP1-5, based on their evolutionary relationship and the

Table 1. Summary of the characteristics of human members of the *SLCO*/OATP transporter superfamily

Transporter	Synonyms	% Sequence Identity[1]	Endogenous Substrates	Drug Substrates (K_m in μM)	GenBank	Reference
***SLCO1A2*/ OATP1A2**	OATP-A, OATP	100	bile salts, steroid and thyroid hormones, eicosanoids	methotrexate (460), fexofenadine (6), saquinavir (36), rocuronium, rosuvastatin (2.6)	NM_021094 NM_134431	(9-23)
***SLCO1B1*/ OATP1B1**	OATP-C, OATP2, LST-1	44	bile salts, steroid and thyroid hormones, eicosanoids, bilirubin	benzylpenicillin, atorvastatin, cerivastatin, fluvastatin, pitavastatin (3), pravastatin (35), rosuvastatin, methotrexate, nateglinide, repaglinide, rifampin (2), SN-38	AB026257, AJ132573, NM_006446	(11, 16, 24-38)
***SLCO1B3*/ OATP1B3**	OATP8	42	bile salts, steroid thyroid and peptide hormones, eicosanoids	digoxin, docetaxel, fexofenadine (108), fluvastatin, pravastatin, pitavastatin, methotrexate (25), paclitaxel (7), rifampin (2)	NM_019844	(11, 16, 26, 27, 29-31, 33, 39-42)
***SLCO1C1*/ OATP1C1**	OATP-F	48	steroid and thyroid hormones		NM_017435	(43)
***SLCO2A1*/ OATP2A1**	hPGT	38	eicosanoids		NM_005621	(44, 45)
***SLCO2B1*/ OATP2B1**	OATP-B	34	steroid hormones	benzylpenicillin, fexofenadine, fluvastatin, pravastatin (2250)	NM_007256	(11, 24, 33, 46, 47)
***SLCO3A1*/ OATP3A1**	OATP-D	36	steroid hormones, eicosanoids		NM_013272	(24, 48)

Table 1 (cont.)

Transporter	Synonyms	% Sequence Identity[1]	Endogenous Substrates	Drug Substrates (K_m in μM)	GenBank	Reference
***SLCO4A1*/ OATP4A1**	OATP-E	32	steroid and thyroid hormones, eicosanoids		NM_016354	(12, 24)
***SLCO4C1*/ OATP4C1**	OATP-H	32	thyroid hormones	digoxin (8), methotrexate	NM_180991	(49)
***SLCO5A1*/ OATP5A1**	OATP-J	34	not determined	not determined	NM_030958	(7, 8)
***SLCO6A1*/ OATP6A1**	OATP-I, GST	24	steroid and thyroid hormones		NM_173488	(50)

[1]amino acid sequence identities were calculated by comparing each *SLCO* transporter to *SLCO1A2* using the program BESTFIT.

Table 2. Tissue distribution of human OATP transporters

	OATP1A2	OATP1B1	OATP1B3	OATP1C1	OATP2A1	OATP2B1	OATP3A1	OATP4A1	OATP4C1	OATP6A1
Brain	+++	-	-	+++	+	-/+	++	+	-	-
Heart		-	-	-/+	+++	-/+	++	++	-	-
Intestine	-/+	-	-	-	++	+/++	-	+		-
Kidney	++	-	-	-	++	+	+	++	+++	-
Liver	+/++	+++	+++	-	++	+++	-	+	-	-
Lung	+	-	-	-	+	++	+	+++	-	-
Pancreas	-	-	-	-	+++	+++	+	++	-	NA
Placenta	-	-	-	-	+	+	-	+++	-	NA
Prostate	+	-	-	-	++	-	-	++	-	NA
Ovary	-	-	-	-	+++	+/++	++	-	-	NA
Spleen	-	-	-	-	+	++	-	+	-	NA
Testis	+	-	-	++	+++	+/++	+++	+	-	+++

Relative quantitation of mRNA levels for a particular OATP was inferred from the available literature: +++, indicates high expression; ++, indicates moderate expression; +, indicates low expression; -, indicates no expression; NA, indicates information not available.

presence of a highly conserved consensus sequence, [-D-X-R-W-(I,V)-G-A-W-W-X-G-(F,L)-L-], between extracellular loop 3 and transmembrane domain (TMD) 6 (7, 8). All OATPs have similar predicted membrane topology with 12 TMDs, the N- and C-terminus located intracellularly, and a large extracellular loop between TMD 9 and TMD 10 with several predicted glycosylation sites (7, 8). OATPs have partially overlapping as well as distinct substrate specificity mediating the transport of a structurally diverse set of positively charged, negatively charged, and uncharged amphipathic compounds including bile salts, steroid hormones, thyroid hormones, eicosanoids, oligopeptides, xenobiotics, and clinically used drugs (10, 11, 51). As shown in Table 2, there are 3 human OATPs, OATP2A1 (hPGT), OATP3A1 (OATP-D), and OATP4A1 (OATP-E), which are widely expressed, while 5 human OATPs have very restricted tissue expression (7, 8). Specifically, OATP1B1 (OATP-C) and OATP1B3 (OATP8) are exclusively expressed on the basolateral side of hepatocytes (Figure 1) where they enable the uptake of drugs, including cholesterol-lowering, anti-diabetic, and anti-histamine medications, into the liver, controlling their efficacy and elimination (7, 8, 15, 23, 25, 41, 52). On the other hand, OATP1C1 (OATP-F) is found in the brain and testis, OATP4C1 (OATP-H) is expressed on the basolateral side of proximal tubule cells in the kidney, and OATP6A1 (OATP-I) is exclusively found in the testis (7, 8). It has been recently demonstrated that OATP1A2 (OATP-A) is primarily expressed in endothelial cells of the blood-brain barrier (BBB) and in epithelial tissues including intestine, liver, and kidney, suggesting that this transporter plays a critical role in the absorption, distribution, and elimination of drugs, such as methotrexate and fexofenadine (9, 15, 22, 53).

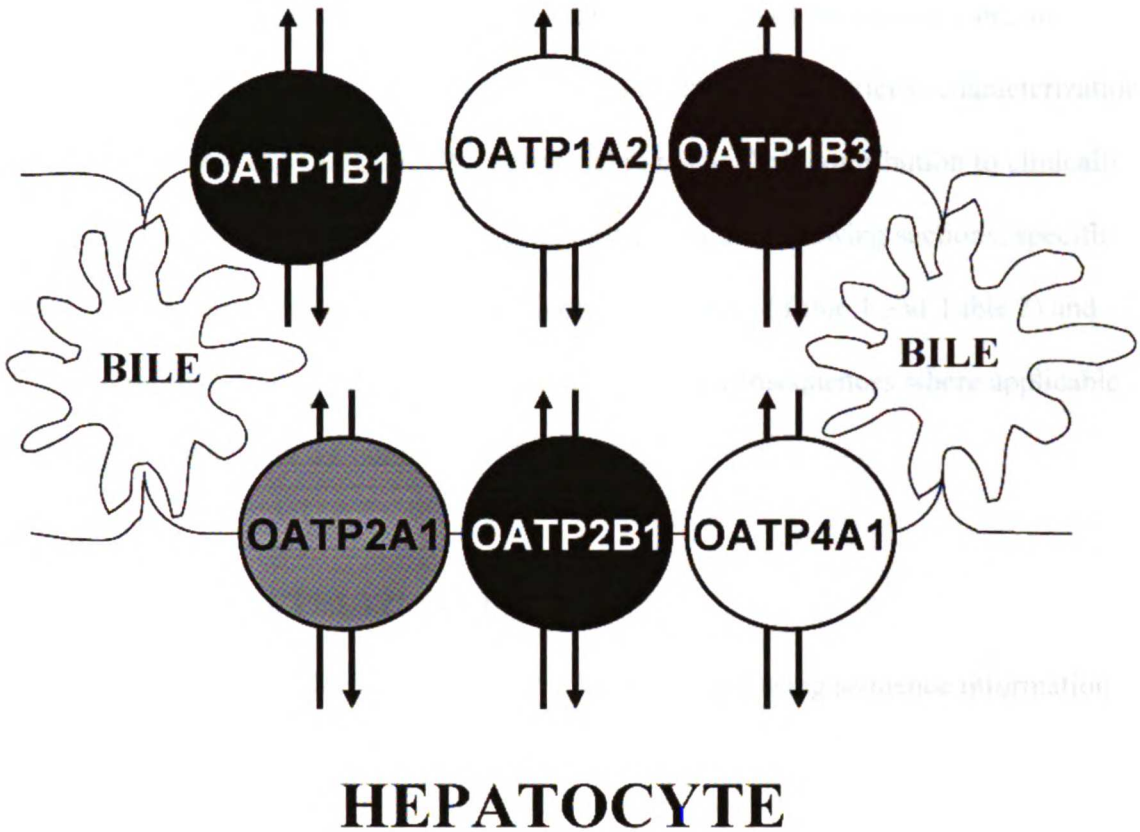

Figure 1. Schematic of the localization of human OATP transporters in the hepatocyte. The relative expression levels of each OATP transporter in the liver is denoted by the color of the circle: a black filled circle indicates the transporter is highly expressed; a gray filled circle shows moderate expression; a while filled circle denotes low expression.

Given that human OATPs interact with a diverse set of therapeutics and are localized in tissues important for drug efficacy, disposition, and toxicity, characterization of genetic variants in human OATPs is essential to assess their contribution to clinically observed inter-individual variability in drug therapy. In the following sections, specific details will be provided regarding molecular characteristics (Table 1 and Table 2) and known genetic variants and their functional and clinical consequences where applicable (Table 3) of each of the 11 human OATPs.

2. *SLCO1A2* (OATP1A2; OATP-A)

OATP1A2 was the first human OATP to be cloned using sequence information from rat Oatp1 (17). It has been shown to transport neutral, anionic, and cationic amphipathic compounds and a variety of structurally diverse therapeutics, including methotrexate, fexofenadine, saquinavir, and rocuronium (7, 9, 15, 22). OATP1A2 is expressed at the BBB and in the intestine, liver, and kidney where it likely plays an important role in regulating drug absorption, drug distribution to the central nervous system (CNS), as well as renal and non-renal drug elimination (7, 8, 14, 53). Therefore, genetic variants in *SLCO1A2*, resulting in increased or decreased expression and/or function of this transporter, may have important pharmacokinetics and pharmacological consequences.

A total of 42 single nucleotide polymorphisms (SNPs) have been identified thus far in *SLCO1A2* (Table 3) in ethnically diverse populations of healthy individuals; 5 of them occurring in the 5'-flanking region, 19 of them in exonic regions and 18 of them in the flanking intronic regions of the gene (9, 53, 54). Of the 19 exonic SNPs, 12 changed

Table 3. Summary of genetic variants in *SLCO* genes encoding OATP transporters

Transporter	Allele	Position[3]	Location	Amino Acid Change	*In Vitro* Uptake	Total MAF (%)	Ethnic Distribution (MAF as %)[4]	Reference
***SLCO1A2*/ OATP1A2**[1,2]								
		-916G>A	5'-UTR	nc				(17, 54)
		-843G>A	5'-UTR	nc				(17, 54)
		-526T>C	5'-UTR	nc				(17, 54)
		-172G>A	5'-UTR	nc				(17, 54)
		-188>ins A	5'-UTR	nc				(17, 54)
	*2	38T>C	Exon 1	Ile13Thr	ES↑, MTX↑, D↔, DP↔	6.3	EA (16), AA (2.5), ME (5)	(9, 53)
		51C>T	Exon 1	syn		0.2	AS (0.8)	(9)
		-37A>C	Intron 1	int		0.4	AS (1.7)	(9)
		-34A>T	Intron 1	int		2.9	EA (4.4), AA (5.6)	(9)
		-24C>T	Intron 1	int		0.2	EA (0.6)	(9)
		186T>C	Exon 2	syn		2.4	AA (7.5), ME(1)	(9)
		-51T>G	Intron 2	int		14	EA (29), AA (8.1), ME (15)	(9)
		+66T>C	Intron 3	int		9.2	EA (0.6), AA (1.9), AS (36)	(9)
	*5	382A>T	Exon 4	Asn128Tyr	ES↔, MTX↔ D↔, DP↔	0.5	AA (1.3), ME(1)	(9, 53)
	*6	404A>T	Exon 4	Asn135Ile	ES↓, MTX↔, D↓, DP↓	0.4	AA (1.3)	(9, 53)
		502C>T	Exon 5	Arg168Cys	ES↓, MTX↓	0.2	EA (0.6)	(9)
	*3	516A>C	Exon 5	Glu172Asp	ES↓, MTX↓, D↓, DP↓	1.1	EA (1.9), AA (0.6), ME (2)	(9, 53)

Table 3 (cont.)

Transporter	Allele	Position[3]	Location	Amino Acid Change	*In Vitro* Uptake	Total MAF (%)	Ethnic Distribution (MAF as %)[4]	Reference
	*4	559G>A	Exon 5	Ala187Thr	ES↓, MTX↔, D↔, DP↔	0.13	ME (0.5)	(9)
		+9G>A	Intron 5	int		4.9	AA (16), ME (2)	(9)
		726C>T	Exon 7	syn		1.3	AA (4.4)	(9)
		768C>T	Exon 7	syn		1.5	AA (5.1)	(9)
		830C>A	Exon 7	Thr277Asn	ES↔, MTX↔	0.2	AA (0.2)	(9)
		833A>del	Exon 7	Asn278Del	ES↓, MTX↓	0.2	AA (0.6)	(9)
		837T>G	Exon 7	syn		0.2	EA (0.6)	(9)
		841A>G	Exon 7	Ile281Val	ES↔, MTX↔	0.2	AS (0.8)	(9)
		-17T>A	Intron 7	int		0.2	AA (0.6)	(9)
		968T>C	Exon 8	Leu323Pro	ES↔, MTX↔	0.2	EA (0.6)	(9)
		1063A>G	Exon 8	Ile355Val	ES↔, MTX↔	0.5	EA (1.9)	(9)
		+43C>A	Intron 8	int		0.4	EA (1.3)	(9)
		+43C>T	Intron 8	int		0.5	EA (0.6), ME(2)	(9)
		-15T>C	Intron 8	int		1.1	AA (3.7)	(9)
		-22G>A	Intron 9	int		6.9	EA (14), AA (3.1), ME (9)	(9)
		1380A>G	Exon 10	syn		0.4	AA (1.3)	(9)
		-16T>C	Intron 10	int		2	AA (6.9)	(9)
		-13A>G	Intron 11	int		17	EA (5), AA (22), AS (38), ME (2)	(9)
		1662C>T	Exon 12	syn		2.9	EA (4.4), AA (5.6)	(9)
		+47A>C	Intron 12	int		7.2	AA (24), ME (2)	(9)

Table 3 (cont.)

Transporter	Allele	Position[3]	Location	Amino Acid Change	*In Vitro* Uptake	Total MAF (%)	Ethnic Distribution (MAF as %)[4]	Reference
		+48T>G	Intron 12	int		12	EA (0.6), AA (10), AS (38), ME (1)	(9)
		-66A>G	Intron 12	int		6.2	EA (0.6), AA (6.2), AS (17)	(9)
		-27A>ins TGAT	Intron 12	int		0.2	AA (0.6)	(9)
	*7	2003C>G	Exon 14	Thr668Ser	ES↔, MTX↔ D↓, DP↓	1.4	AA (4.4), ME(1)	(9, 53)
		+3G>T	Intron 14			1.4	AA (5)	(9)
***SLCO1B1*/ OATP1B1**[1]								
	*1b	388A>G	Exon 4	Asn130Asp	ES↔, EG↔, R↓, SN↔, P↔	44	EA (30), AA (74), AS (54)	(35, 38, 55-60)
	*1b-1	388A>G/ 1007C>G	Exon 4/ Exon 8	Asn130Asp/ Pro336Arg	ES↔, EG↔, P↔, A↔, C↓			(32)
	*1c	455G>A/ 721G>A	Exon 5/ Exon 7	Arg 152Lys/ Asp241Asn	ES↔, EG↓, R↔			(38, 55)
	*2	217T>C	Exon 2	Phe73Leu	ES↓, EG↓, R↓	2	EA (2)	(38, 55)
	*3	245T>C/ 467A>G	Exon 3/ Exon 4	Val82Ala/ Glu156Gly	ES↓, EG↓, R↓			(38, 55)
	*4	463C>A	Exon 4	Pro155Thr	ES↔, EG↔, R↔	12	EA (16), AA (2)	(38, 55)

Table 3 (cont.)

Transporter	Allele	Position[3]	Location	Amino Acid Change	*In Vitro* Uptake	Total MAF (%)	Ethnic Distribution (MAF as %)[4]	Reference
	*5	521T>C	Exon 5	Val174Ala	ES↓, EG↓, R↓, SN↔, AT↓	11	EA (14), AA (2), AS (16)	(34, 35, 38, 52, 55-57, 61-65)
	*5b	521T>C/ 1007C>G	Exon 5/ Exon 8	Val174Ala/ Pro336Arg	ES↓, EG↓, P↓, A↓, C↓			(32)
	*6	1058T>C	Exon 8	Ile353Thr	ES↓, EG↓, R↓	2	EA (2)	(38, 55)
	*7	1294A>G	Exon 9	Asn432Asp	ES↔, EG↓, R↓	1	EA (1)	(38, 55)
	*8	1385A>G	Exon 10	Asp462Gly	ES↔, EG↔, R↔	1	EA (1)	(38, 55)
	*9	1463G>C	Exon10	Gly488Ala	ES↓, EG↓, R↓, AT↓	9	AA (9)	(38, 55, 63)
	*10	1964A>G	Exon 14	Asp655Gly	ES↔, EG↔, R↔	2	EA (2)	(38, 55)
	*11	2000A>G	Exon 14	Glu667Gly	ES↔, EG↔, R↓	12	EA (2), AA (34)	(38, 55)
	*12	217T>C/ 1964A>G	Exon2/ Exon 14	Phe73Leu/ Asp655Gly	ES↓, EG↓, R↓			(38, 55)
	*13	245T>C/ 467A>G/ 2000A>G	Exon 3/ Exon 4/ Exon 14	Val82Ala/ Glu156Gly/ Glu667Gly	ES↓, EG↓, R↓			(38, 55)
	*14	388A>G/ 463C>A	Exon 4	Asn130Asp/ Pro155Thr	ES↔, EG↔, R↓			(38, 55)
	*15	388A>G/ 521T>C	Exon 4/ Exon 5	Asn130Asp/ Val174Ala	ES↓, EG↓, SN↓, AT↓	10	AS (10)	(32, 35, 56, 57, 59, 61, 63, 65, 66)

Table 3 (cont.)

Transporter	Allele	Position[3]	Location	Amino Acid Change	*In Vitro* Uptake	Total MAF (%)	Ethnic Distribution (MAF as %)[4]	Reference
	*15b	388A>G/ 521T>C/ 1007C>G	Exon 4/ Exon 5/ Exon 8	Asn130Asp/ Val174Ala/ Pro336Arg	ES↓, EG↓, P↓, A↓, C↔			(32)
	*16	452A>G	Exon 4	Asn151Ser		3.8	AS (3.8)	(57)
	*17	-11187G>A/ 388A>G/ 521T>C	5'-UTR/ Exon 4/ Exon 5	nc/ Asn130Asp/ Val174Ala		4	EA (4)	(61, 65, 67)
	*18	388A>G/ 1463G>C	Exon 4/ Exon 10	Asn130Asp/ Gly488Ala	AT↓			(63)
		-11187G>A	5'-UTR	nc		10	EA (10)	(61, 68)
		-11110T>G	5'-UTR	nc		0.4	EA (0.4)	(68)
		-10499A>C	5'-UTR	nc		8	EA (8)	(68)
		+193G>A	Intron 1	int		2	EA (2)	(61)
		+203A>T	Intron 1	int		3	EA (3)	(61)
		+160C>T	Intron 4	int		8	EA (8)	(61)
		+165A>T	Intron 4	int		32	EA (32)	(61)
		+189G>A	Intron 4	int		32	EA (32)	(61)
		+191G>A	Intron 4	int		48	EA (48)	(61)
		-108 to-113 del	Intron 4	int		40	EA (40)	(61)
		411G>A	Exon 4	syn		13	EA (13)	(68)
		571C>T	Exon 5	syn		44	EA (44)	(61)
		578T>G	Exon 5	Leu193Arg	B↓, BA↓, EG↓	0.3	EA (0.3)	(69)
		597C>T	Exon 5	syn		46	EA (46), AS(43)	(57, 68)

Table 3 (cont.)

Transporter	Allele	Position[3]	Location	Amino Acid Change	*In Vitro* Uptake	Total MAF (%)	Ethnic Distribution (MAF as %)[4]	Reference
		+33C>T	Intron 6	int		47	EA (47)	(61)
		1007C>G	Exon 8	Pro336Arg	ES↔, EG↔, P↔, A↔, C↔	1.2	AS (1.2)	(32, 57)
		-128A>del	Intron 9	int		7	EA (7)	(61)
		-104 to -105 ins CTT	Intron 9	int		44	EA (44)	(61)
		-170C>G	Intron 10	int		12	EA (12)	(61)
		-89T>C	Intron 10	int		12	EA (12)	(61)
		-75A>del	Intron 10	int		28	EA (28)	(61)
		-68G>A	Intron 10	int		4	EA (4)	(61)
		-12A>G	Intron 10	int		0.8	AS (0.8)	(57)
		1454G>T	Exon 10	Cys485Phe		0.8	AS (0.8)	(57)
		+9A>G	Intron 12	int		9	EA (9)	(61)
		-97C>A	Intron 12	int		9	EA (9)	(61)
		-159G>C	Intron 12	int		27	EA (27)	(61)
		+50T>G	Intron 13	int		0.8	AS (0.8)	(57)
		+78A>C	Intron 13	int		0.8	AS (0.8)	(57)
		1929A>C	Exon 14	Leu643Phe		9	EA (9)	(61)
		2040C>A	Exon 14	syn		0.8	AS (0.8)	(57)
***SLCO1B3*/ OATP8**[1]								
		-28 to -11 del	5'-UTR	nc		20	AS (20)	(70)
		-7 to -4 del	5'-UTR	nc		20	AS (20)	(70)

Table 3 (cont.)

Transporter	Allele	Position[3]	Location	Amino Acid Change	*In Vitro* Uptake	Total MAF (%)	Ethnic Distribution (MAF as %)[4]	Reference
		334G>T	Exon 3	Ala112Ser	B↔, BA↔, EG↔, CCK↔, D↔	25	EA (22), AS (28)	(70, 71)
		699A>G	Exon 6	Met233Ile	B↔, BA↔, EG↔, CCK↔	28	EA (29), AS (28)	(70, 71)
		1272A>G	Exon 9	syn				(54)
		1557A>G	Exon 11	syn				(54)
		1564G>T	Exon 11	Gly522Cys	B↓, BA↓, EG↔, CCK↔, D↔	2	EA (2)	(71)
		1833G>A	Exon 13	syn				(54)
***SLCO2A1*/ OATP2A1**[1]								
		$(GT)_{\sim 80}$	Intron 1	int				(45)
***SLCO2B1*/ OATP2B1**[1]								
	*2	1175C>T	Exon 7	Thr392Ile	ES↔			(56)
	*3	1457C>T	Exon 9	Ser486Phe	ES↓	31	EA (1.3), AS (31)	(24, 56, 61)
		1596C>T	Exon 10	syn		1.3	EA (1.3)	(61)

MAF, minor allele frequency; ES, estrone-3-sulfate; MTX, methotrexate; D, deltorphin II; DP, DPDE ([D-penicillamine 2,5]-enkephalin); B, bromosulftalein; BA, bile acid; EG, 17β-gluocoronosyl estradiol; CCK, cholecystokinin-8; R, rifampin; P, pravastatin; A, atorvastatin; C, cerivastatin; S, statins; SN, SN-38 (7-ethyl-10-hydroxycamptothecin); AT, atrasentan; N, nateglinide; PIT, pitavastatin; F, fexofenadine; RP, repaglinide; D, DHEAS (dehydrepiandrosterone-3-sulfate); ↔, no change in function; ↑, increase in function; ↓, decrease in function; syn, synonymous variant; nc, non-coding variant; int, intronic variant; ins, insertion; del, deletion.

[1]The GenBank accession numbers are NM_021094 and NM_134431 for OATP1A2, AB026257 and AJ132573 for OATP1B1, NM_019844 for OATP1B3, NM_007256 for OATP2B1, and NM_005630.
[2]Data are available at http://www.pharmgkb.org.
[3]Positions are relative to the ATG start site for each *SLCO* gene.
[4]EA, European-American; AA, African-American; AS, Asian-American; ME, Mexican-American

the protein sequence of OATP1A2 and were functionally characterized with regards to transport of estrone-3-sulfate (ES), methotrexate (MTX), deltorphin II (D), and [D-penicillamine 2,5]-enkephalin (DP). Three of the protein-altering variants, protein reference sequence (p.)[1] Ile13Thr, p. Glu172Asp, and p. Thr668Ser, were common and exhibited total allele frequencies ≥ 1% (9, 53). Lee *et al.* analyzed six of the protein-altering variants in SLCO1A2 in transiently trasnfected HeLa cells and determined that p. Glu172Asp and p. Asn135Ile exhibited reduced uptake of ES, D, and DP as a result of decreased surface expression (53). In addition, p. Ala187Thr and p. Thr668Ser displayed changes in substrate specificity. In particular, p. Ala187Thr showed reduced transport of ES but normal transport of D and DP, while p. Thr668Ser exhibited reduced transport of D and DP but normal transport of ES compared to OATP1A2 reference (53). Badagnani *et al.* (see Chapter 3) recently identified seven novel protein-altering variants in *SLCO1A2* in an ethnically diverse population of 270 healthy individuals and functionally characterized the 12 protein-altering variants in this transporter with respect to ES and MTX using *Xenopus laevis* oocytes and transiently transfected HEK-293 cells (9). It was determined that four of the 12 protein-altering variants exhibited alteration in the transport of ES and/or MTX. Specifically, p. Asn277del was non-functional for both ES and MTX, p. Glu172Asp and p. Arg168Cys exhibited approximately 60% reduced uptake of MTX, while p.Ile13Thr showed a 2-fold increased uptake of ES and MTX compared to OATP1A2 reference (9). Detailed characterization of the interaction kinetics of ES

[1] The nomenclature for human polymorphisms was adapted from guidelines approved by the Human Genome Variation Society (http://www.hgvs.org/mutnomen/)

with p. Ile13Thr and p. Glu172Asp demonstrated that p. Ile13Thr leads to a 2-fold increase in the maximal transport rate (V_{max}) of ES, while p. Glu172Asp leads to a 5-fold decrease in the V_{max} of ES (9). The reason for discrepancies in the number of SNPs identified and the functional assays between the studies of Lee *et al.* (53) and Badagnani *et al.* (9) may be due to differences in sample sets, methods used in screening, and cellular systems used to functionally characterize the protein-altering variants.

Using data available at http://www.pharmgkb.org on genetic variation in *SLCO1A2* and applying the Bayesian statistical method, PHASE (72), a total of 36 haplotypes could be identified in *SLCO1A2* from 25 variable sites in 540 chromosomes. Of these, 28 were present in at least two chromosomes with a combined frequency of 99% (Figure 2). The haplotypes were named using the modified convention of Nebert *et al.* according to evolutionary divergence and frequency in the sample (73). As shown in Figure 2, haplotype *1A1 occurred with the highest frequency in all four ethnic groups. Haplotype *2B1 was the second most common haplotype in European-Americans (EA), *7A1 in African-Americans (AA), *6A1 in Asian-Americans (AS), and *2B2A1 in Mexican-Americans (ME). Among the 28 haplotypes, three (*1A1, *2B1, and *2B2A1) had total frequencies of $\geq$ 5%. Only *1A1 was found in all four ethnic groups. On the other hand, 14 out of 28 haplotypes (*2A1, *2B2A2, *4A1, *4B2A1, *4B2A2, *5B2A1, *5B2A2, *6B2, *7A1, *8A2, *9A1, *9A2, *9B1, and *10A1) occurred exclusively in only one ethnic group, with the majority, 11 of 14 (79%), found in the AA sample. Six of the protein-altering variants in *SLCO1A2*, p. Ile13Thr (*2B1), p. Asn128Tyr (*11A1), p. Asn135Ile (*9A2), p. Glu172Asp (*10A1 and *10A2), p. Ile355Val (*10A2), and p.Thr668Ser (*7A2), were frequent enough to be included in the haplotype estimation.

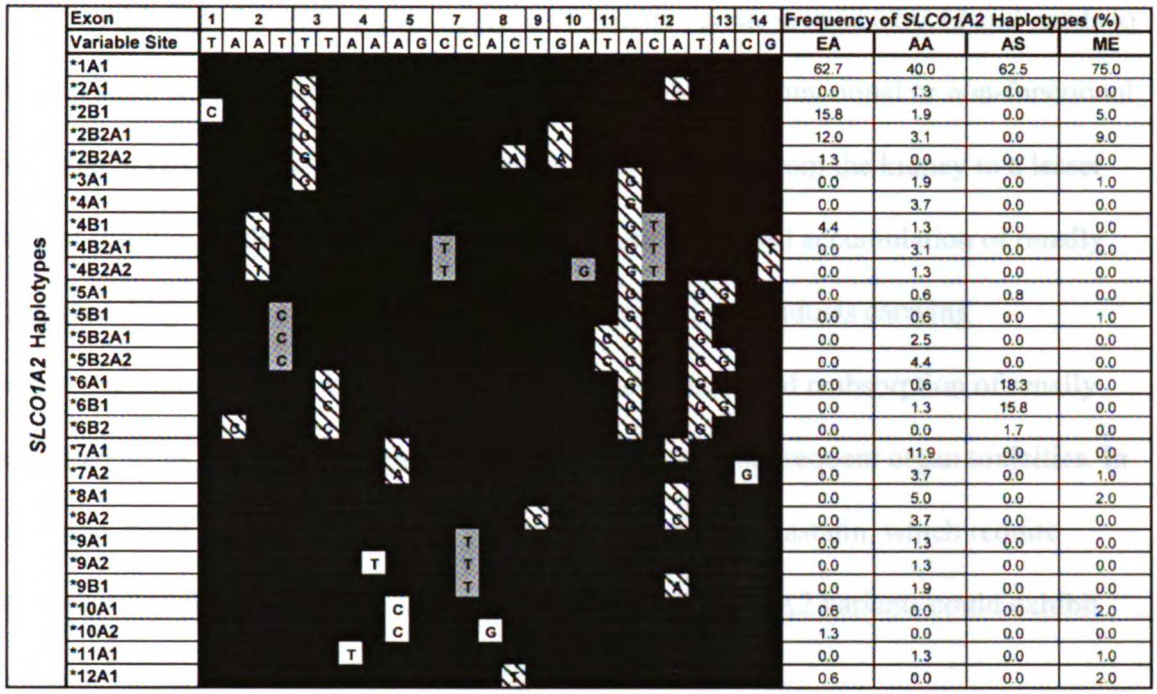

Exon	1	2		3		4		5		7		8	9	10		11	12			13	14	Frequency of *SLCO1A2* Haplotypes (%)			
Variable Site	T	A	A	T	T	A	A	A	G	C	C	A	C	T	G	A	T	A	C	A	T	A	C	G	EA	AA	AS	ME
*1A1																									62.7	40.0	62.5	75.0
*2A1				G																G					0.0	1.3	0.0	0.0
*2B1	C			G																					15.8	1.9	0.0	5.0
*2B2A1				G											G										12.0	3.1	0.0	9.0
*2B2A2				G								G			G										1.3	0.0	0.0	0.0
*3A1				G													G								0.0	1.9	0.0	1.0
*4A1				G													G								0.0	3.7	0.0	0.0
*4B1			A	A													G	T							4.4	1.3	0.0	0.0
*4B2A1			A	A						T							G	T					G		0.0	3.1	0.0	0.0
*4B2A2			A	A						T					G		G	T					G		0.0	1.3	0.0	0.0
*5A1																	G			G					0.0	0.6	0.8	0.0
*5B1		C															G			G					0.0	0.6	0.0	1.0
*5B2A1		C															G			G					0.0	2.5	0.0	0.0
*5B2A2		C															G			G					0.0	4.4	0.0	0.0
*6A1				G																G					0.0	0.6	18.3	0.0
*6B1				G													G			G					0.0	1.3	15.8	0.0
*6B2	G																G			G					0.0	0.0	1.7	0.0
*7A1								A	A											G					0.0	11.9	0.0	0.0
*7A2								A	A											G			G		0.0	3.7	0.0	1.0
*8A1																				G					0.0	5.0	0.0	2.0
*8A2													G							G					0.0	3.7	0.0	0.0
*9A1										T															0.0	1.3	0.0	0.0
*9A2						T				T															0.0	1.3	0.0	0.0
*9B1										T										G					0.0	1.9	0.0	0.0
*10A1								C																	0.6	0.0	0.0	2.0
*10A2								C				G													1.3	0.0	0.0	0.0
*11A1						T																			0.0	1.3	0.0	1.0
*12A1																									0.6	0.0	0.0	2.0

Figure 2. Structure and population frequency of 28 haplotypes of *SLCO1A2* estimated in 270 ethnically diverse healthy individuals. In the left panel are the sequences of the haplotypes at each of the 25 variable sites. Data are available at http://www.pharmgkb.org (9). The first row shows the exons of *SLCO1A2*, while the second row contains the reference allele sequence at each variable site. The remaining rows contain the 28 haplotypes clustered and named based on evolutionary divergence and population frequencies (73). A black filled square shows that there is no change from the reference allele; a gray filled square indicates a synonymous change in the coding region; a white filled square labels a non-synonymous change; changes occurring at non-coding sites are denoted by diagonally striped squares. Letters in the squares indicate the base pair change. Haplotypes were predicted using the software PHASE version 1.0.1 (72). On the right panel are the frequencies of the 28 haplotypes in the total population and in each ethnic group.

Although the clinical consequence of genetic variation in *SLCO1A2* still needs to be assessed, we can speculate that individuals carrying hypofunctional or non-functional variants in OATP1A2 could reabsorb drugs, such as MTX, from the kidney to a lesser extent resulting in decreased systemic exposure and increased accumulation of renally excreted drugs in the kidney lumen. On the other hand, individuals carrying hyperfunctional variants in OATP1A2 could exhibit increased reabsorption of renally excreted drugs resulting in higher systemic exposure and subsequent organ toxicities. In addition, since OATP1A2 interacts with drugs, such as rosuvastatin, which require transport into the liver for efficacy, individuals with OATP1A2 variants could exhibit variable response to cholesterol-lowering drugs.

3. *SLCO1B1* (OATP1B1; OATP-C)

OATP1B1 is exclusively expressed on the basolateral membrane of hepatocytes. This *SLCO* transporter exhibits broad substrate selectivity, transporting bile acids, steroid hormones, thyroid hormones, eicosanoids, and bilirubin and its conjugates (7, 8). In addition, OATP1B1 interacts with a variety of clinically important drugs, such as cholesterol-lowering drugs (atorvastatin, cerivastatin, fluvastatin, pitavastatin, pravastatin, and rosuvastatin), anti-cancer drugs (methotrexate and SN-38), anti-diabetic drugs (nateglinide and repaglinide), and anti-infective drugs (rifampicin and benzylpenicillin), suggesting that genetic variants in *SLCO1B1* may modulate the efficacy and hepatic elimination of therapeutics (7, 8, 34, 74).

A total of 18 protein-altering variants have been identified in *SLCO1B1*, with some occurring in linkage in a particular variant allele (Table 3 and Figure 3). Eight

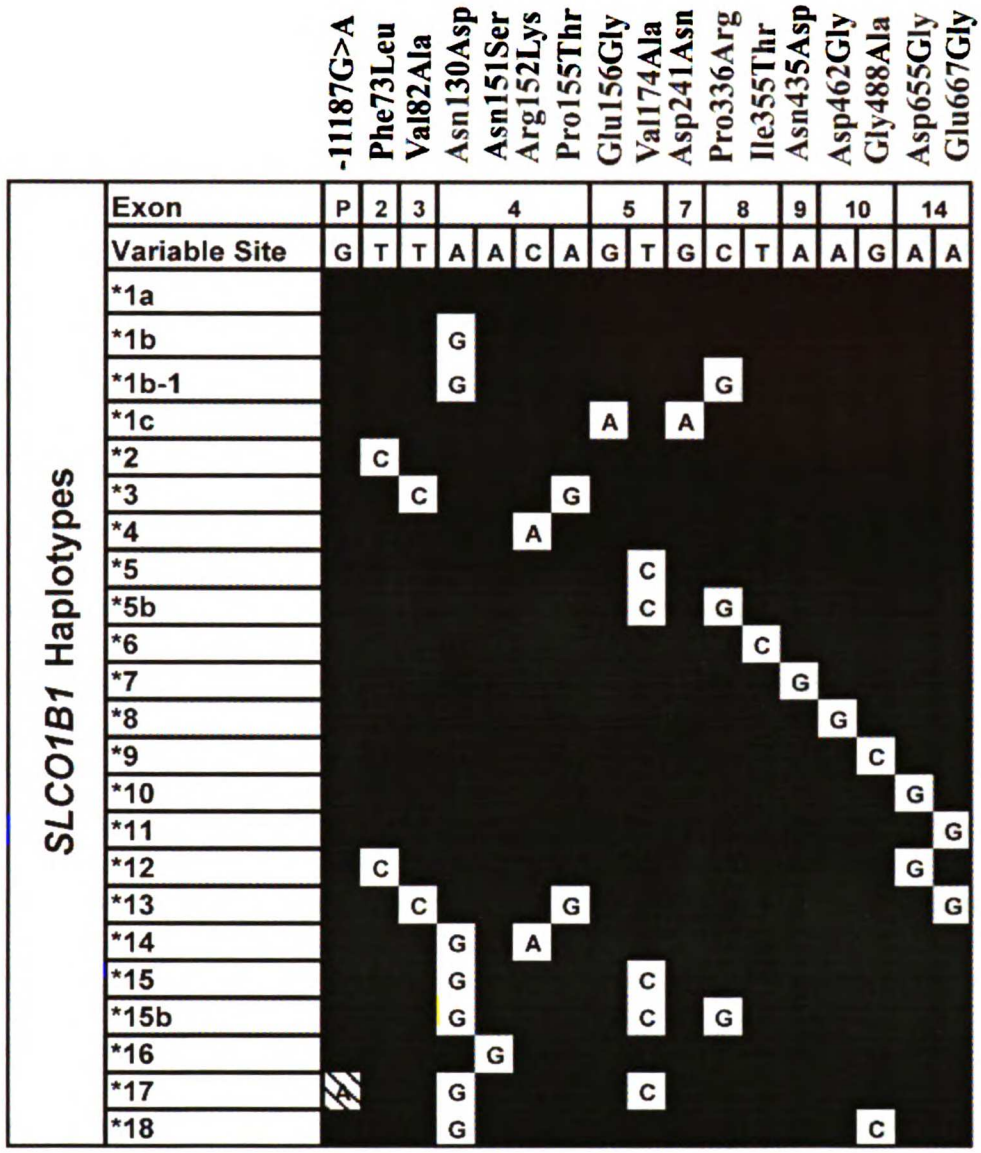

Figure 3. Schematic representation of *SLCO1B1* variant alleles. The first row contains the exons of *SLCO1B1*, while the second row contains the sequence of the reference allele (*1a) at each of 17 variable sites. The subsequent rows contain the 23 variant alleles (32, 38, 57, 61, 63). A black filled square shows that there is no change from the reference allele, a white filled square indicates a non-synonymous change, and a diagonally striped square denotes a change at a non-coding site. Letters in the squares indicate the base pair change.

protein-altering variants and one promoter variant occurred with an allele frequency of ≥ 1%: p. Phe73Leu (*2) was found exclusively in EA with an allele frequency of 2%; p. Pro155Thr (*4) was found in EA and AA with allele frequencies of 16% and 2%, respectively; p. Asn130Asp (*1b) was found in EA, AA, and AS, with allele frequencies of 30%, 74%, and 54%, respectively; p. Asn151Ser (*16) was found in AS with an allele frequency of 4%; p. Val174Ala (*5) was found in EA, AA, and AS, with allele frequencies of 14%, 2%, and 16%, respectively; p. Ile353Thr (*6) was present in EA with an allele frequency of 2%; p. Gly488Ala (*9) was present in AA with an allele frequency of 9%; p. Glu667Gly (*11) was found in EA and AA with allele frequencies of 2% and 34%, respectively; and -11187G>A was found in EA with an allele frequency of 10% (32, 38, 57, 61, 63, 69).

In vitro analysis of protein altering variants and variant alleles of *SLCO1B1* (Table 3 and Table 4) has revealed that OATP1B1 exhibits considerable functional as well as genetic diversity. Alterations in transport and substrate specificity have been associated with protein-altering variants that occur in TMDs and in extracellular loops between TMD 3 and 4 and between TMD 9 and 10 (55, 74). Specifically, variant allele *1b, which contains p. Asn130Asp, was shown to have about 50% decrease in the transport of rifampin (R), while it exhibited normal uptake of ES, 17β-gluocoronosyl estradiol (EG), and 7-ethyl-10-hydroxycamptothecin (SN38) compared to OATP1B1 reference, suggesting that this variant alters the substrate specificity of the transporter (35, 38, 55). Variant allele *1c, which contains p. Arg152Lys and p. Asp241Asn, exhibited approximately 75% of EG transport, but normal uptake of ES and R compared functional for ES, EG, and R, resulting from a dramatic decrease in the surface

Table 4. Summary of functional consequence of genetic variation in *SLCO1B1* on drug transport *in vitro*

Haplotype	Variant	Drug	*In vitro* activity	Reference
*1b	Asn130Asp	Rifampin	↓	(38)
		SN-38	↓	(35)
*1b-1	Asn130Asp, Pro336Arg	Atorvastatin	↔	(32)
		Pravastatin	↔	(32)
		Cerivastatin	↔	(32)
*1c	Arg152Lys, Asp241Asn	Rifampin	↔	(38)
		Rosuvastatin	↓	(23)
*2	Phe73Leu	Rifampin	Ø	(38)
		Rosuvastatin	Ø	(23)
*3	Val82Ala, Glu156Gly	Rifampin	Ø	(38)
*4	Pro155Thr	Rifampin	↔	(38)
*5	Val174Ala	Rifampin	Ø	(38)
		Rosuvastatin	Ø	(23)
		Atorvastatin	↓	(32)
		Pravastatin	↓	(32)
		Cerivastatin	↔	(32)
		Rosuvastatin	Ø	(23)
		Atrasentan	↓	(63)
*5b	Val174Ala, Pro336Arg	Atorvastatin	↓	(32)

Table 4 (cont.)

Haplotype	Variant	Drug	*In vitro* activity	Reference
		Pravastatin	↓	(32)
		Cerivastatin	↔	(32)
*6	Ile353Thr	Rifampin	Ø	(38)
		Rosuvastatin	↓	(23)
*7	Asn432Asp	Rifampin	↓	(38)
		Rosuvastatin	↓	(23)
*8	Asp462Gly	Rifampin	↔	(38)
*9	Gly488Ala	Rifampin	Ø	(38)
		Atrasentan	↓	(63)
*10	Asp655Gly	Rifampin	↔	(38)
*11	Glu667Gly	Rifampin	↓	(38)
*12	Phe73Leu, Asp655Gly	Rifampin	↓	(38)
		Rosuvastatin	Ø	(23)
*13	Val82Ala, Glu156Gly, Glu667Gly	Rifampin	↓	(38)
		Rosuvastatin	Ø	(23)
*14	Asn130Asp, Pro155Thr	Rifampin	↓	(38)
*15	Asn130Asp, Val174Ala	Atorvastatin	↓	(32)
		Pravastatin	↓	(32)
		Cerivastatin	↓	(32)

Table 4 (cont.)

Haplotype	Variant	Drug	*In vitro* activity	Reference
		SN-38	↓	(35)
		Rosuvastatin	Ø	(23)
		Atrasentan	↓	(63)
*15b	Asn130Asp, Val174Ala, Pro336Arg	Atorvastatin	↓	(32)
		Pravastatin	↓	(32)
		Cerivastatin	↔	(32)
	Pro336Arg	Atorvastatin	↔	(32)
		Pravastatin	↔	(32)
		Cerivastatin	↔	(32)
*18	Asn130AspGly488Ala	Rosuvastatin	Ø	(23)
		Atrasentan	↓	(63)

SN-38, 7-ethyl-10-hydroxycamptothecin. *In vitro* activity of variants and/or haplotypes of *SLCO1B1* was assessed in comparison to reference OATP1B1 (*i.e.* *1a allele), where ↔ denotes no change in function; ↓ indicates decrease in function; Ø shows non-functional variants or haplotypes.

expression of the variant protein (38, 55). Variant alleles *5 (p. Val174Ala), *5b (p. Val174Ala and p. Pro336Arg), *15 (p. Asn130Asp and p. Val174Ala), and *15b (p. Asn130Asp, p. Val174Ala, and p. Pro336Arg) exhibited a dramatic decrease in the transport of ES, EG, and the cholesterol-lowering drugs, atorvastatin, pravastatin and cerivastatin, due to significant decreases in the V_{max} values compared to OATP1B1 reference (32). Transport function was not altered when Pro336Arg and the variant allele *1b-1 (p. Asn130Asp and p. Pro336Arg) were tested, suggesting that the reduced function of *5 and *15 variant proteins is primarily a consequence of the p. Val174Ala substitution (32). Interestingly, it was found that *5, *15, and *15b proteins were found not only at the plasma membrane, but also intracellularly in significant amounts, which explains their reduced cellular transport function (32). In addition, variant allele *15 (p. Asn130Asp and p. Val174Ala) resulted in the significantly reduced transport of SN-38, which is the predominant active metabolite of the anti-cancer drug irinotecan (35).Variant alleles *12 (p. Phe73Leu and p. Asp655Gly) and *13 (p. Val82Ala, p. Glu156Gly, and p. Glu667Gly) exhibited reduced transport of ES, EG, and R, resulting from a significant decrease in the interaction (38, 55). Variant allele *7 (p. Asn432Asp) exhibited reduced transport of EG and R, but normal transport of ES compared to OATP1B1 reference (38, 55). Variant alleles *11 (p. Glu667Gly) and *14 (p. Asn130Asp and p. Pro155Thr) showed reduced uptake of R, but transported ES and EG at levels comparable to OATP1B1 reference (38, 55). The protein-altering variant p. Leu193Arg was newly identified in a human liver sample that exhibited reduced amount of OATP1B1 expression (69). P. Leu193Arg showed dramatically reduced uptake of bromosulftalein

(B), bile acids (BA), and EG, likely because this variant protein was retained intracellularly (69).

The clinical consequences of genetic variation in *SLCO1B1* has been extensively studied to assess the impact of variant alleles of OATP1B1on cholesterol-lowering, anti-diabetic, and anti-cancer therapy, particularly focusing on efficacy and pharmacokinetics (Table 5). Several variant alleles of OATP1B1, including *1b (p. Asn130Asp), *5 (p. Val174Aal), *15 (p. Asn130Asp and p. Val174Ala), and *17 (-11187G>A, p. Asn130Asp, and p. Val174Ala) have been tested for their effects on the pharmacokinetics and cholesterol-lowering response of pravastatin. Specifically, it was found that individuals heterozygous for the variant allele *1b had significantly lower AUC and C_{max} of pravastatin compared to individuals homozygous for the reference allele (*1a) (57, 58, 60). In addition, pravastatin AUC was 65% lower and pravastatin C_{max} was 65% lower in *1b/*1b subjects compared to *1a/*1a individuals (58). In that study similar trends were observed for valsartan and temocapril, though the difference did not reach statistical significance (58). On the other hand, individuals heterozygous for the variant allele *5 exhibited significantly higher AUC and C_{max} of pravastatin compared to *1a/*1a individuals. These data suggest that the *1b allele leads to increased uptake, whereas the *5 allele leads to reduced uptake of pravastatin into hepatocytes (60). Since pravastatin requires transport into the liver to exert its cholesterol-lowering effects, Gerloff *et al.* investigated the clinical consequence of carrying the *1b or *5 alleles (75). As expected from their impact on pravastatin pharmacokinetics, individuals carrying the *1b allele showed the biggest decrease in cholesterol and its precursor lathosterol, whereas individuals carrying the *5 allele exhibited the smallest decrease in both cholesterol and

Table 5. Clinical consequence of genetic variation in *SLCO1B1* on drug efficacy and disposition in humans

Haplotype	Variant	Drug	*In vivo* effect	Reference
*1b	Asn130Asp	pravastatin	↓ AUC, ↓ C_{max}	(58, 60)
		pravastatin	↑ CL[1], ↑ CL_{nr}[1]	(57)
		pravastatin	highest ↓ in cholesterol, lathosterol, lathosterol/cholesterol[2]	(75)
		pravastatin	↑ basal serum sterol[3]	(75)
		valsartan	↔ AUC	(58)
		temocapril	↔ AUC	(58)
		rosuvastatin	↑ C_{max}	(76)
*5	Val174Ala	pravastatin	↑ AUC, ↑ C_{max}	(58, 60, 61)
		pravastatin	smallest ↓ in cholesterol, lathosterol, lathosterol/cholesterol[2]	(75)
		pravastatin	↓ basal serum sterol[3]	(75)
		pravastatin	↓ efficacy	(62)
		fexofenadine	↑ AUC, ↓ CL_{nr}	(52)
		nateglinide	↑ AUC, ↑ C_{max}, ↑ t_{max}	(64)
		repaglinide	↑ AUC, ↑ C_{max}	(34)
		atrasentan	↑ AUC, ↑ AUC_{ss}, ↑ C_{max}	(63)
		rosuvastatin	↑ AUC, ↑ C_{max}	(76)
*9	Gly488Ala	atrasentan	↑ AUC, ↑ AUC_{ss}, ↑ C_{max}	(63)

Table 5 (cont.)

Haplotype	Variant	Drug	*In vivo* effect	Reference
*15	Asn130Asp, Val174Ala	pravastatin	↑ AUC, ↑ C_{max}	(61)
		pravastatin	↓ CL[1], ↓ CL_{nr}[1]	(57)
		valsartan	↔ AUC	(58)
		temocapril	↔ AUC	(58)
		pitivastatin	↑ AUC, ↑ C_{max}	(59)
		atrasentan	↑ AUC, ↑ AUC_{ss}, ↑ C_{max}	(63)
*15b	Asn130Asp, Val174Ala, Pro336Arg	pravastatin	↑ AUC	(61)
*17	-11187G>A, Asn130Asp, Val174Ala	pravastatin	↑ AUC, ↑ C_{max}	(61)
		pravastatin	smaller ↓ in cholesterol, lathosterol, lathosterol/cholesterol	(67)
*18	Asn130Asp, Gly488Ala	atrasentan	↑ AUC, ↑ AUC_{ss}, ↑ C_{max}	(63)
	-11187G>A	pravastatin	↑ AUC	(61)
		repaglinide	↑ glucose lowering effect	(34)

AUC, area under the concentration versus time curve; AUC_{ss}, area under the concentration versus time curve at steady state; C_{max}, maximum plasma concentration; CL, total clearance; CL_{nr}, non-renal clearance; $t_{1/2}$, elimination half-life. *In vivo* effects of variants and/or haplotypes in *SLCO1B1* were assessed compared to reference OATP1B1 (*i.e.* *1a allele), where ↔ denotes no change in a clinical parameter; ↑ indicates an increase in a clinical parameter; ↓ denotes a decrease in a clinical parameter.
[1]Subjects with OATP1B1 *15 allele were compared to those carrying *1b allele.
[2]Subjects with *1a/*1a haplotype had an intermediate decrease in cholesterol levels, lathosterol levels, and lathosterol-to-cholesterol ratios.
[3]Subjects with *1a/*1a haplotype had intermediate basal serum sterol levels.

to OATP1B1 reference (38, 55). Variant alleles *2 (p. Phe73Leu), *3 (p. Val82Ala and p. Glu156Gly), *5 (p. Val174Ala), *6 (p. Ile353Thr), and *9 (p. Gly488Ala) were non-lathosterol following a single dose of pravastatin compared to individuals with the reference *1a allele (75). In addition, the ratio of lathosterol to cholesterol, which is an indicator of endogenous cholesterol synthesis, decreased the most in the *1b group and the least in the *5 group following treatment with pravastatin, whereas the *1a group showed intermediate effect (75). Individuals heterozygous for the *5 allele (TC genotype) exhibited an attenuated response to the cholesterol-lowering effects of pravastatin, in particular with respect to total cholesterol, which is consistent with the finding that the p. Val174Ala variant protein results in the reduced hepatic uptake of pravastatin (62). The *1b and *5 variant alleles of *SLCO1B1* also appeared to have inverse effects on basal sterol serum levels, which were higher in the *1b group, intermediate in the *1a group, and lowest in the *5 group (75). Nishizato *et al.* investigated the effect of variant allele *15 on pravastatin kinetics, and determined that the total clearance (CL_t) and non-renal clearance (CL_{nr}) of pravastatin were significantly reduced in *1b/*15 and *15/*15 subjects compared to *1b/*1b individuals, suggesting that the protein-altering variant Val174Ala is associated with altered pravastatin elimination (57). In addition, Niemi *et al.* determined that carriers of the *15 variant allele exhibited a mean pravastatin AUC and C_{max} that were approximately 2-fold higher compared to non-carriers, while carriers of the *17 variant allele had an approximately 3-fold higher AUC and C_{max} of pravastatin compared to non-carriers (61). Similarly, when carriers of the *5, *15, and *17 alleles were compared as a group to non-carriers, pravastatin AUC and C_{max} were 2- and 3-fold higher, respectively, in the variant group compared to the control group (65). In addition,

it was recently determined that heterozygous carriers of *17 variant allele exhibited reduced response to the cholesterol-lowering effects of pravastatin, as measured by plasma lathosterol concentrations and lathosterol to cholesterol ratios. These findings suggest that presence of the *17 allele leads to higher plasma levels, but lower hepatocellular levels of pravastin, resulting in reduced inhibition of cholesterol synthesis (67). The *5 variant allele has been recently associated with altered pharmacokinetics of the anti-histamine drug, fexofenadine (F), and the anti-diabetic therapeutics, nateglinide (N), and repaglinide (RP) (34, 52, 64). Specifically, it was shown that subjects homozygous for the *5 variant allele (CC genotype) had a mean AUC of fexofenadine that was 127% higher and a CL_{nr} of fexofenadine that was lower compared to individuals who were homozygous for the reference allele (TT genotype) (52). In a different study it was determined that the AUC and C_{max} of nateglinide was approximately 80% and 110% higher, respectively, and the t_{max} 80% longer in subjects homozygous for the *5 variant allele (CC genotype) compared to individuals homozygous for the reference allele (TT genotype) (64). Subjects homozygous for the *5 variant allele (CC genotype) exhibited an approximately 200% increase in the AUC of repaglinide compared to individuals homozygous for the reference allele (TT genotype) (34). In the same study, the promoter variant -11187G>A was found to be significantly associated with the blood glucose-lowering effects of repaglinide, where carrying the GA genotype predicted the maximum decrease and mean change in blood glucose (34). Recently, it was observed that individuals carrying one *15 variant allele exhibited significantly higher AUC and C_{max} of pitavastatin, a novel member of HMG-CoA reductase inhibitors used in cholesterol-lowering therapy, compared to those individuals not carrying the *15 allele (59). The

variant alleles *1b, *5, *9, *15, and *18 in OATP1B1 were recently analyzed for their effect on the cellular uptake and pharmacokinetics of atrasentan (AT), which is an endothelin A receptor antagonist developed for the treatment of prostate cancer (63). The *5 (p. Val174Ala), *9 (p. Gly488Ala), *15 (p. Asn130Asp and p. Val174Ala), and *18 (p. Asn130Asp and p. Gly488Ala) alleles exhibited reduced uptake of AT and were classified as low-activity alleles, while the *1b allele and the reference allele *1a were classified as high-activity alleles (63). Individuals were categorized by OATP1B1 activity in 3 groups, extensive, intermediate, and poor transporters based on the number of high activity alleles (*i.e.* 0, 1, or 2) they carried. It was determined that AT AUC both after one dose and at steady-state and AT C_{max} were significantly associated with OATP1B1 transport activity class, suggesting that individuals who have poor OATP1B1 transport phenotype, based on carrying the *5, *9, *15, or *18 variant allele, exhibit increased exposure to AT (63).

4. *SLCO1B3* (OATP1B3; OATP8)

OATP1B3, similarly to OATP1B1, is exclusively expressed on the basolateral membrane of hepatocytes, where it interacts with a broad range of endogenous compounds and therapeutics (7, 8). Compared to other human OATPs, OATP1B3 is the only known member, in addition to OATP4C1, to transport digoxin, which is a drug used in the treatment of cardiovascular disease, and the peptide hormone cholecystokinin-8 (CCK-8) (11, 49). However, unlike OATP1A2 and OATP1B1, OATP1B3 does not interact with bile salts or unconjugated bilirubin (7, 8).

Three studies to date have identified and/or functionally characterized genetic variants in *SLCO1B3* (54, 70, 71). Specifically, 2 deletions in the 5'-flanking region were identified in AS with an allele frequency of 20% and were shown to be in complete linkage disequilibrium (70). In addition, 3 protein-altering variants, p. Ala112Ser, p. Met233Ile, and p. Gly522Cys, were identified in *SLCO1B3* (70, 71). P.Ala112Ser and p. Met233Ile were found in both EA and AS samples and these variant proteins were shown to have similar transport function compared to OATP1B3 reference (70, 71). Specifically, p.Ala112Ser occurred with allele frequencies of 22% in EA and 28% in AS, while p. Met233Ile was found at allele frequencies of 29% and 28% in EA and AS, respectively. P. Glu522Cys was only observed in EA with an allele frequency of 2% (71). This variant exhibited reduced intracellular accumulation of B and the bile acid taurocholic acid, but showed similar transport of ES, EG, CCK-8, and dehydroepiandrosterone-3-sulfate (DHEAS) compared to OATP1B3 reference (71). The mechanism for the reduced transport of some substrates by p. Glu522Cys was ascribed to the increased intracellular retention of this variant protein (71). The clinical impact of genetic variation in *SLCO1B3* on drug efficacy, disposition, and/or toxicity remains to be determined.

5. *SLCO1C1* (OATP1C1; OATP-F)

OATP1C1 has been recently cloned from a human brain library and was shown to be exclusively expressed in the brain, with the exception of the pons and cerebellum, and in the Leydig cells of the testis (43). Functional characterization of OATP1C1 in *Xenopus laevis* oocytes and CHO cells demonstrated that OATP1C1 is a high affinity thyroid hormone transporter, mediating the cellular uptake of both T_4 and reverse T_3 (rT_3) with

affinities (K_m) of 90 nM and 128 nM, respectively (43). These findings suggest that OATP1C1 is involved in thyroid hormone homeostasis, especially in the brain and testis. Identification of genetic variants in OATP1C1 and characterization of their impact on thyroid hormone disposition still needs to be performed.

6. *SLCO2A1* (OATP2A1; hPGT)

OATP2A1 was cloned from a human kidney and was determined to have wide tissue distribution (44). OATP2A1 mediates the transport of a variety of eicosanoids, including prostaglandins (PGE_1, PGE_2, PGD_2, and $PGF_{2\alpha}$) and thromboxanes (TXB_2), which have important pathophysiological and pharmacological roles (44, 77). Recently, a repetitive sequence of dinucleotide repeats, $(GT)_{\sim 80}$, in intron 1 of *SLCO2A1* was identified in 49 unrelated individuals (45). There remains a need to identify SNPs in *SLCO2A1* and assess their impact on prostanoid homeostasis and the disposition of synthetic prostaglandin analogs.

7. *SLCO2B1* (OATP2B1; OATP-B)

OATP2B1 is predominantly expressed in the liver, kidney, and intestine (7, 8). In particular, it has been recently shown that OATP2B1 is localized to the apical membrane of human intestinal epithelial cells, where it mediates the pH-dependent uptake of organic anions, including ES, DHEAS, BA (taurocholic acid), fexofenadine, and pravastatin (46, 47). The increased transport of organic anions by OATP2B1 at acidic pH was ascribed to a 7-fold increase in the maximal transport rate and it appeared to be dependent on the proton gradient (46). This is clinically relevant because the physiological pH in the

intestinal lumen can vary anywhere from 4.0 to 8.0, suggesting that OATP2B1 is a critical determinant of the absorption and pharmacokinetics of organic anion drugs.

Three coding variants have been identified thus far in *SLCO2B1*; 2 of them alter the protein sequence (p. Thr392Ile and p. Ser486Phe) and 1 leads to a silent substitution (1596C>T) (24, 56, 61). P. Ser486Phe (*3 variant allele) was found in both EA and AS samples with an allele frequency of 1.3 and 31%, respectively (56, 61). The variant 1596C>T was observed in the EA sample with an allele frequency of 1.3% (61). Functional characterization of the protein-altering variants in OATP2B1, demonstrated that p. Thr392Ile (*2 variant allele) transported ES similarly to OATP2B1 reference, while Ser486Phe exhibited approximately 50% decrease in the maximal transport rate for ES corrected for expression levels of the variant and reference protein (56).

Preliminary assessment of the impact of p. Ser486Phe on pravastatin pharmacokinetics suggests that this variant does not appear to be associated with elevated pravastatin AUC (61). Further characterization of the clinical effects of genetic variation in *SLCO2B1*on the absorption and disposition of organic anion drugs remains to be carried out.

8. *SLCO3A1* (OATP3A1; OATP-D)

OATP3A1 was isolated from a human brain and was shown to be ubiquitously expressed, with a similar distribution at the protein level compared to OAP2A1 (44, 48). OATP3A1 mediates the transport of prostaglandins, including PGE_1, PGE_2, and $PGF_{2\alpha}$ with slightly better affinity (K_m ~ 50 nM) compared to OATP2A1 (K_m ~100 nM) (44, 48). This suggests that both OATP3A1 and OATP2A1 act in a coordinated fashion to

modulate the disposition and homeostasis of endogenous prostanoids. Identification of genetic variants in OATP3A1 and characterization of their impact on eicosanoids disposition still needs to be performed.

9. *SLCO4A1* (OATP4A1; OATP-E)

OATP4A1 was cloned from human brain and was shown to be abundantly expressed in a variety of tissues (12). OATP4A1 mediated the cellular transport of T_3 with an affinity (K_m) of approximately 0.9 μM, while it interacted weakly with T_4 and rT_3 (12). This suggests that OATP4A1 plays an important role in the cellular and tissue homeostasis of thyroid hormones. Identification of genetic variants in OATP4A1 and characterization of their effects on thyroid hormones disposition still needs to be addressed.

10. *SLCO4C1* (OATP4C1; OATP-H)

OATP4C1 was recently cloned and shown to be predominantly expressed in the kidney (49). The rat ortholog was localized to the basolateral membrane of proximal tubule cells of the kidney (49). OATP4C1 mediated the transport of cardiac glycosides, such as digoxin (K_m = 8 μM) and ouabain (K_m = 0.4 μM), thyroid hormones, such as T_3 (K_m = 6 μM) and T_4, and methotrexate (49). These findings suggest that OATP4C1 may play an important role in the renal elimination of neutral and anionic drugs. Identification of genetic variants in OATP4C1 and characterization of their impact on drug disposition and renal elimination still needs to be performed.

11. *SLCO5A1* (OATP5A1; OATP-J)

OATP5A1 has yet to be cloned and functionally characterized.

12. *SLCO6A1* (OATP6A1; OATP-I)

OATP6A1 was cloned from human testis and was shown to be predominantly expressed in Sertoli cells, spermatogonia, and Leydig cells of the testis (50). The rat orthologs, GST-1 and GST-2, were functionally characterized in the same study and were found to transport DHEAS, BA (taurocholic acid), and T_4 with affinities (K_m) in the low μM range (50). The functional analysis of OATP6A1 remains to be determined and no information is available to date on SNPs in *SLCO6A1* and their clinical consequences.

13. Future directions

Uptake transporters, including members of the OATP superfamily, play critical roles in the efficacy, disposition, and toxicity of drugs. Significant progress has been made in the identification and functional characterization of genetic variation in OATP1A2, OATP1B1, OATP1B3, and OATP2B1. Additional studies are needed to investigate the impact of genetic variants in OATP1A2, OATP1B3, and OATP2B1 on inter-individual variability in drug response and pharmacokinetics. Furthermore, the genetic and functional diversity of the remaining 7 human OATP members remains to be addressed. The data published thus far suggest that genetic variants in human OATPs are likely to contribute to inter-individual variability in drug therapy. In particular, there is preliminary clinical evidence that genetic variation in hepatic OATPs influences the efficacy and disposition of cholesterol-lowering drugs. More recently, it has also been

appreciated that genetic variation in OATPs expressed in the intestine and kidney may play an important role in variable intestinal absorption and/or renal elimination of organic anion drugs. Therefore, additional genetic and functional studies with human OATPs would advance our efforts in successfully optimizing drug therapy regimens.

14. Summary of dissertation chapters

Membrane transporters act as gatekeepers to mediate the uptake and efflux of endogenous substances, xenobiotics, and therapeutics into and out of cells and tissues of the human body, thereby influencing nutrient homeostasis and drug disposition. The studies in this dissertation are focused on identifying and characterizing membrane transporters that interact with anti-cancer drugs to examine their role in controlling systemic and tissue levels of anti-cancer drugs. In addition, genetic and functional diversity of various transporter proteins was analyzed to elucidate the contribution of genetic variation in membrane transporters to the observed inter-individual variability in the efficacy, disposition, and toxicity of anti-cancer drugs. The objectives of the dissertation studies are as follows:

Chapter 2. Functional analysis of genetic variants in the human concentrative nucleoside transporter 3 (CNT3; *SLC28A3*)

To understand the genetic basis for inter-individual differences in the disposition and response to anti-cancer nucleoside analogs, the genetic and functional diversity of CNT3 was examined in an ethnically diverse population of 270 healthy individuals. Population genetic analysis suggested that *SLC28A3* is under negative selection. The 10 protein-

altering variants in CNT3 were expressed in *Xenopus laevis* oocytes and were shown to transport both purine and pyrimidine model substrates, except for the rare variant c. 1099G>A (p. Gly367Arg), which alters an evolutionarily conserved site in the putative substrate recognition domain of CNT3. The genetic analysis and functional characterization of CNT3 variants suggest that this transporter does not tolerate non-synonymous changes and is important for human fitness.

Chapter 3. Interaction of methotrexate, an organic anion drug, with OATP1A2 and its genetic variants

This chapter examines the interaction of the anti-cancer drug methotrexate with a human organic anion transporting polypeptide transporter, OATP1A2, which is expressed in tissues important for MTX disposition and toxicity. OATP1A2 exhibited saturable transport of methotrexate, which was sensitive to extracellular pH. Seven novel protein-altering variants were identified in 270 ethnically diverse DNA samples. Four protein-altering variants in OATP1A2 exhibited altered transport of methotrexate and the 2 common variants, p. Ile13Thr and p.Glu172Asp, showed significant changes in the maximum transport rate (V_{max}) of estrone-3-sulfate. Because of its expression on the apical membrane of the distal tubule and in tissues relevant to MTX disposition and toxicity, these findings suggest that OATP1A2 may play a role in active tubular reabsorption of MTX and in MTX-induced toxicities. Furthermore, genetic variation in OATP1A2 may contribute to variation in MTX therapy.

UCSF LIBRARY

Chapter 4. Interaction of methotrexate with OAT3 (*SLC22A8*) and its genetic variants

Since OAT3 has been shown to play an important role in the renal tubular secretion of methotrexate, this chapter provides a comprehensive genetic and functional analysis of OAT3 in an ethnically diverse population of 270 healthy individuals to better understand the genetic factors that influence inter-individual variability in methotrexate disposition, elimination, and toxicity. Population genetic analysis indicated that there are significant evolutionary constraints on this protein and that it shows reduced genetic diversity at sites that alter the amino acid sequence of the protein. Five of the 10 protein-altering variants in OAT3, which were expressed in human embryonic kidney cells, exhibited significant reduction in the cellular uptake of methotrexate. Rare protein-altering variants in OAT3 may contribute to variable renal secretion and pharmacokinetic parameters of methotrexate.

Chapter 5. Mechanisms of transport of organic anions by OATP1A2 and structural determinants of organic anions interaction with OATP1A2

The driving force of substrate transport by OATP1A2 was examined using estrone-3-sulfate and methotrexate as the model organic anion substrates. Transport of organic anions by OATP1A2 was found to be extremely sensitive to extracellular acidic pH, as a result of increased substrate affinity. The pH-dependent transport of organic anions did not rely on the pH gradient, or exchange with intracellular anions, such as HCO_3^-, OH^-, or GSH. Analysis of the structural determinants of the interaction of organic

anions with OATP1A2 suggested that arginine (R49, R168, R240, R556, R590, and R609) and histidine (H107) residues have essential structural and/or functional roles.

Chapter 6. Role of genetic variation in kidney transporters in methotrexate disposition and toxicity

Since MTX is primarily excreted unchanged in the urine and its elimination depends on saturable secretion and reabsorption in the kidney, it was hypothesized that genetic variation in kidney transporters that interact with MTX contributes to the variation in MTX therapy. This chapter provides an initial pharmacogenetics and pharmacopedemiological analysis of 565 leukemia patients enrolled between 1991 and 1998 at St. Jude Children's Research Hospital treated with methotrexate. Eleven SNPs and 16 haplotypes in 6 kidney transporters were selected for association with methotrexate clearance and plasma concentration 42 hours after dosing, and biomarkers of renal function. Delayed elimination of methotrexate was negatively correlated with methotrexate plasma levels, which was in turn positively correlated with increased exposure to methotrexate. Methotrexate pharmacokinetics, in particular clearance and volume of distribution, exhibited a non-linear relationship with dose. Methotrexate was shown to have a negative impact on clinical biomarkers of renal and hepatic function, which could lead to variable methotrexate disposition and result in methotrexate-induced nephrotoxicity and hepatotoxicity.

References

1. Ayrton A, Morgan P. Role of transport proteins in drug absorption, distribution and excretion. Xenobiotica 2001; **31**: 469-97.

2. Lee VH. Membrane transporters. Eur J Pharm Sci 2000; **11 Suppl 2**: S41-50.

3. Kalow W, Endrenyi L, Tang B. Repeat administration of drugs as a means to assess the genetic component in pharmacological variability. Pharmacology 1999; **58**: 281-4.

4. Meyer UA. Pharmacogenetics - five decades of therapeutic lessons from genetic diversity. Nat Rev Genet 2004; **5**: 669-76.

5. Evans WE, McLeod HL. Pharmacogenomics--drug disposition, drug targets, and side effects. N Engl J Med 2003; **348**: 538-49.

6. Kerb R. Implications of genetic polymorphisms in drug transporters for pharmacotherapy. Cancer Lett 2006; **234**: 4-33.

7. Hagenbuch B, Meier PJ. The superfamily of organic anion transporting polypeptides. Biochim Biophys Acta 2003; **1609**: 1-18.

8. Hagenbuch B, Meier PJ. Organic anion transporting polypeptides of the OATP/ SLC21 family: phylogenetic classification as OATP/ SLCO superfamily, new nomenclature and molecular/functional properties. Pflugers Arch 2004; **447**: 653-65.

9. Badagnani I, Castro RA, Taylor TR, Brett CM, Huang CC, Stryke D, et al. Interaction Of Methotrexate With OATP1A2 And Its Genetic Variants. J Pharmacol Exp Ther 2006.

10. Meier PJ, Eckhardt U, Schroeder A, Hagenbuch B, Stieger B. Substrate specificity of sinusoidal bile acid and organic anion uptake systems in rat and human liver. Hepatology 1997; **26**: 1667-77.

11. Kullak-Ublick GA, Ismair MG, Stieger B, Landmann L, Huber R, Pizzagalli F, et al. Organic anion-transporting polypeptide B (OATP-B) and its functional comparison with three other OATPs of human liver. Gastroenterology 2001; **120**: 525-33.

12. Fujiwara K, Adachi H, Nishio T, Unno M, Tokui T, Okabe M, et al. Identification of thyroid hormone transporters in humans: different molecules are involved in a tissue-specific manner. Endocrinology 2001; **142**: 2005-12.

13. van Montfoort JE, Hagenbuch B, Fattinger KE, Muller M, Groothuis GM, Meijer DK, et al. Polyspecific organic anion transporting polypeptides mediate hepatic uptake of amphipathic type II organic cations. J Pharmacol Exp Ther 1999; **291**: 147-52.

14. Gao B, Hagenbuch B, Kullak-Ublick GA, Benke D, Aguzzi A, Meier PJ. Organic anion-transporting polypeptides mediate transport of opioid peptides across blood-brain barrier. J Pharmacol Exp Ther 2000; **294**: 73-9.

15. Cvetkovic M, Leake B, Fromm MF, Wilkinson GR, Kim RB. OATP and P-glycoprotein transporters mediate the cellular uptake and excretion of fexofenadine. Drug Metab Dispos 1999; **27**: 866-71.

16. Fischer WJ, Altheimer S, Cattori V, Meier PJ, Dietrich DR, Hagenbuch B. Organic anion transporting polypeptides expressed in liver and brain mediate uptake of microcystin. Toxicol Appl Pharmacol 2005; **203**: 257-63.

17. Kullak-Ublick GA, Hagenbuch B, Stieger B, Schteingart CD, Hofmann AF, Wolkoff AW, et al. Molecular and functional characterization of an organic anion transporting polypeptide cloned from human liver. Gastroenterology 1995; **109**: 1274-82.

18. Kullak-Ublick GA, Glasa J, Boker C, Oswald M, Grutzner U, Hagenbuch B, et al. Chlorambucil-taurocholate is transported by bile acid carriers expressed in human hepatocellular carcinomas. Gastroenterology 1997; **113**: 1295-305.

19. Kullak-Ublick GA, Fisch T, Oswald M, Hagenbuch B, Meier PJ, Beuers U, et al. Dehydroepiandrosterone sulfate (DHEAS): identification of a carrier protein in human liver and brain. FEBS Lett 1998; **424**: 173-6.

20. Bossuyt X, Muller M, Meier PJ. Multispecific amphipathic substrate transport by an organic anion transporter of human liver. J Hepatol 1996; **25**: 733-8.

21. Pascolo L, Cupelli F, Anelli PL, Lorusso V, Visigalli M, Uggeri F, et al. Molecular mechanisms for the hepatic uptake of magnetic resonance imaging contrast agents. Biochem Biophys Res Commun 1999; **257**: 746-52.

22. Su Y, Zhang X, Sinko PJ. Human organic anion-transporting polypeptide OATP-A (SLC21A3) acts in concert with P-glycoprotein and multidrug resistance protein 2 in the vectorial transport of Saquinavir in Hep G2 cells. Mol Pharm 2004; **1**: 49-56.

23. Ho RH, Tirona RG, Leake BF, Glaeser H, Lee W, Lemke CJ, et al. Drug and bile acid transporters in rosuvastatin hepatic uptake: function, expression, and pharmacogenetics. Gastroenterology 2006; **130**: 1793-806.

24. Tamai I, Nezu J, Uchino H, Sai Y, Oku A, Shimane M, et al. Molecular identification and characterization of novel members of the human organic anion transporter (OATP) family. Biochem Biophys Res Commun 2000; **273**: 251-60.

25. Hsiang B, Zhu Y, Wang Z, Wu Y, Sasseville V, Yang WP, et al. A novel human hepatic organic anion transporting polypeptide (OATP2). Identification of a liver-specific human organic anion transporting polypeptide and identification of rat and human hydroxymethylglutaryl-CoA reductase inhibitor transporters. J Biol Chem 1999; **274**: 37161-8.

26. Cui Y, Konig J, Leier I, Buchholz U, Keppler D. Hepatic uptake of bilirubin and its conjugates by the human organic anion transporter SLC21A6. J Biol Chem 2001; **276**: 9626-30.

27. Abe T, Kakyo M, Tokui T, Nakagomi R, Nishio T, Nakai D, et al. Identification of a novel gene family encoding human liver-specific organic anion transporter LST-1. J Biol Chem 1999; **274**: 17159-63.

28. Nakai D, Nakagomi R, Furuta Y, Tokui T, Abe T, Ikeda T, et al. Human liver-specific organic anion transporter, LST-1, mediates uptake of pravastatin by human hepatocytes. J Pharmacol Exp Ther 2001; **297**: 861-7.

29. Vavricka SR, Van Montfoort J, Ha HR, Meier PJ, Fattinger K. Interactions of rifamycin SV and rifampicin with organic anion uptake systems of human liver. Hepatology 2002; **36**: 164-72.

30. Abe T, Unno M, Onogawa T, Tokui T, Kondo TN, Nakagomi R, et al. LST-2, a human liver-specific organic anion transporter, determines methotrexate sensitivity in gastrointestinal cancers. Gastroenterology 2001; **120**: 1689-99.

31. Hirano M, Maeda K, Shitara Y, Sugiyama Y. Contribution of OATP2 (OATP1B1) and OATP8 (OATP1B3) to the hepatic uptake of pitavastatin in humans. J Pharmacol Exp Ther 2004; **311**: 139-46.

32. Kameyama Y, Yamashita K, Kobayashi K, Hosokawa M, Chiba K. Functional characterization of SLCO1B1 (OATP-C) variants, SLCO1B1*5, SLCO1B1*15 and SLCO1B1*15+C1007G, by using transient expression systems of HeLa and HEK293 cells. Pharmacogenet Genomics 2005; **15**: 513-22.

33. Kopplow K, Letschert K, Konig J, Walter B, Keppler D. Human hepatobiliary transport of organic anions analyzed by quadruple-transfected cells. Mol Pharmacol 2005; **68**: 1031-8.

34. Niemi M, Backman JT, Kajosaari LI, Leathart JB, Neuvonen M, Daly AK, et al. Polymorphic organic anion transporting polypeptide 1B1 is a major determinant of repaglinide pharmacokinetics. Clin Pharmacol Ther 2005; **77**: 468-78.

35. Nozawa T, Minami H, Sugiura S, Tsuji A, Tamai I. Role of organic anion transporter OATP1B1 (OATP-C) in hepatic uptake of irinotecan and its active metabolite, 7-ethyl-10-hydroxycamptothecin: in vitro evidence and effect of single nucleotide polymorphisms. Drug Metab Dispos 2005; **33**: 434-9.

36. Schneck DW, Birmingham BK, Zalikowski JA, Mitchell PD, Wang Y, Martin PD, et al. The effect of gemfibrozil on the pharmacokinetics of rosuvastatin. Clin Pharmacol Ther 2004; **75**: 455-63.

37. Shitara Y, Hirano M, Sato H, Sugiyama Y. Gemfibrozil and its glucuronide inhibit the organic anion transporting polypeptide 2 (OATP2/OATP1B1:SLC21A6)-mediated hepatic uptake and CYP2C8-mediated metabolism of cerivastatin: analysis of the mechanism of the clinically relevant drug-drug interaction between cerivastatin and gemfibrozil. J Pharmacol Exp Ther 2004; **311**: 228-36.

38. Tirona RG, Leake BF, Wolkoff AW, Kim RB. Human organic anion transporting polypeptide-C (SLC21A6) is a major determinant of rifampin-mediated pregnane X receptor activation. J Pharmacol Exp Ther 2003; **304**: 223-8.

39. Ismair MG, Stieger B, Cattori V, Hagenbuch B, Fried M, Meier PJ, et al. Hepatic uptake of cholecystokinin octapeptide by organic anion-transporting polypeptides OATP4 and OATP8 of rat and human liver. Gastroenterology 2001; **121**: 1185-90.

40. Konig J, Cui Y, Nies AT, Keppler D. Localization and genomic organization of a new hepatocellular organic anion transporting polypeptide. J Biol Chem 2000; **275**: 23161-8.

41. Shimizu M, Fuse K, Okudaira K, Nishigaki R, Maeda K, Kusuhara H, et al. Contribution of OATP (organic anion-transporting polypeptide) family transporters to the hepatic uptake of fexofenadine in humans. Drug Metab Dispos 2005; **33**: 1477-81.

42. Smith NF, Acharya MR, Desai N, Figg WD, Sparreboom A. Identification of OATP1B3 as a high-affinity hepatocellular transporter of paclitaxel. Cancer Biol Ther 2005; **4**: 815-8.

43. Pizzagalli F, Hagenbuch B, Stieger B, Klenk U, Folkers G, Meier PJ. Identification of a novel human organic anion transporting polypeptide as a high affinity thyroxine transporter. Mol Endocrinol 2002; **16**: 2283-96.

44. Lu R, Kanai N, Bao Y, Schuster VL. Cloning, in vitro expression, and tissue distribution of a human prostaglandin transporter cDNA(hPGT). J Clin Invest 1996; **98**: 1142-9.

45. Lu R, Schuster VL. Molecular cloning of the gene for the human prostaglandin transporter hPGT: gene organization, promoter activity, and chromosomal localization. Biochem Biophys Res Commun 1998; **246**: 805-12.

46. Nozawa T, Imai K, Nezu J, Tsuji A, Tamai I. Functional characterization of pH-sensitive organic anion transporting polypeptide OATP-B in human. J Pharmacol Exp Ther 2004; **308**: 438-45.

47. Kobayashi D, Nozawa T, Imai K, Nezu J, Tsuji A, Tamai I. Involvement of human organic anion transporting polypeptide OATP-B (SLC21A9) in pH-dependent transport across intestinal apical membrane. J Pharmacol Exp Ther 2003; **306**: 703-8.

48. Adachi H, Suzuki T, Abe M, Asano N, Mizutamari H, Tanemoto M, et al. Molecular characterization of human and rat organic anion transporter OATP-D. Am J Physiol Renal Physiol 2003; **285**: F1188-97.

49. Mikkaichi T, Suzuki T, Onogawa T, Tanemoto M, Mizutamari H, Okada M, et al. Isolation and characterization of a digoxin transporter and its rat homologue expressed in the kidney. Proc Natl Acad Sci U S A 2004; **101**: 3569-74.

50. Suzuki T, Onogawa T, Asano N, Mizutamari H, Mikkaichi T, Tanemoto M, et al. Identification and characterization of novel rat and human gonad-specific organic anion transporters. Mol Endocrinol 2003; **17**: 1203-15.

51. Kullak-Ublick GA, Stieger B, Hagenbuch B, Meier PJ. Hepatic transport of bile salts. Semin Liver Dis 2000; **20**: 273-92.

52. Niemi M, Kivisto KT, Hofmann U, Schwab M, Eichelbaum M, Fromm MF. Fexofenadine pharmacokinetics are associated with a polymorphism of the SLCO1B1 gene (encoding OATP1B1). Br J Clin Pharmacol 2005; **59**: 602-4.

53. Lee W, Glaeser H, Smith LH, Roberts RL, Moeckel GW, Gervasini G, et al. Polymorphisms in human organic anion-transporting polypeptide 1A2 (OATP1A2): implications for altered drug disposition and central nervous system drug entry. J Biol Chem 2005; **280**: 9610-7.

54. Iida A, Saito S, Sekine A, Mishima C, Kondo K, Kitamura Y, et al. Catalog of 258 single-nucleotide polymorphisms (SNPs) in genes encoding three organic anion transporters, three organic anion-transporting polypeptides, and three NADH:ubiquinone oxidoreductase flavoproteins. J Hum Genet 2001; **46**: 668-83.

55. Tirona RG, Leake BF, Merino G, Kim RB. Polymorphisms in OATP-C: identification of multiple allelic variants associated with altered transport activity among European- and African-Americans. J Biol Chem 2001; **276**: 35669-75.

56. Nozawa T, Nakajima M, Tamai I, Noda K, Nezu J, Sai Y, et al. Genetic polymorphisms of human organic anion transporters OATP-C (SLC21A6) and OATP-B (SLC21A9): allele frequencies in the Japanese population and functional analysis. J Pharmacol Exp Ther 2002; **302**: 804-13.

57. Nishizato Y, Ieiri I, Suzuki H, Kimura M, Kawabata K, Hirota T, et al. Polymorphisms of OATP-C (SLC21A6) and OAT3 (SLC22A8) genes: consequences for pravastatin pharmacokinetics. Clin Pharmacol Ther 2003; **73**: 554-65.

58. Maeda K, Ieiri I, Yasuda K, Fujino A, Fujiwara H, Otsubo K, et al. Effects of organic anion transporting polypeptide 1B1 haplotype on pharmacokinetics of pravastatin, valsartan, and temocapril. Clin Pharmacol Ther 2006; **79**: 427-39.

59. Chung JY, Cho JY, Yu KS, Kim JR, Oh DS, Jung HR, et al. Effect of OATP1B1 (SLCO1B1) variant alleles on the pharmacokinetics of pitavastatin in healthy volunteers. Clin Pharmacol Ther 2005; **78**: 342-50.

60. Mwinyi J, Johne A, Bauer S, Roots I, Gerloff T. Evidence for inverse effects of OATP-C (SLC21A6) 5 and 1b haplotypes on pravastatin kinetics. Clin Pharmacol Ther 2004; **75**: 415-21.

61. Niemi M, Schaeffeler E, Lang T, Fromm MF, Neuvonen M, Kyrklund C, et al. High plasma pravastatin concentrations are associated with single nucleotide polymorphisms and haplotypes of organic anion transporting polypeptide-C (OATP-C, SLCO1B1). Pharmacogenetics 2004; **14**: 429-40.

62. Tachibana-Iimori R, Tabara Y, Kusuhara H, Kohara K, Kawamoto R, Nakura J, et al. Effect of genetic polymorphism of OATP-C (SLCO1B1) on lipid-lowering response to HMG-CoA reductase inhibitors. Drug Metab Pharmacokinet 2004; **19**: 375-80.

63. Katz DA, Carr R, Grimm DR, Xiong H, Holley-Shanks R, Mueller T, et al. Organic anion transporting polypeptide 1B1 activity classified by SLCO1B1 genotype influences atrasentan pharmacokinetics. Clin Pharmacol Ther 2006; **79**: 186-96.

64. Zhang W, He YJ, Han CT, Liu ZQ, Li Q, Fan L, et al. Effect of SLCO1B1 genetic polymorphism on the pharmacokinetics of nateglinide. Br J Clin Pharmacol 2006.

65. Igel M, Arnold KA, Niemi M, Hofmann U, Schwab M, Lutjohann D, et al. Impact of the SLCO1B1 polymorphism on the pharmacokinetics and lipid-lowering efficacy of multiple-dose pravastatin. Clin Pharmacol Ther 2006; **79**: 419-26.

66. Iwai M, Suzuki H, Ieiri I, Otsubo K, Sugiyama Y. Functional analysis of single nucleotide polymorphisms of hepatic organic anion transporter OATP1B1 (OATP-C). Pharmacogenetics 2004; **14**: 749-57.

67. Niemi M, Neuvonen PJ, Hofmann U, Backman JT, Schwab M, Lutjohann D, et al. Acute effects of pravastatin on cholesterol synthesis are associated with SLCO1B1 (encoding OATP1B1) haplotype *17. Pharmacogenet Genomics 2005; **15**: 303-9.

68. Pasanen MK, Backman JT, Neuvonen PJ, Niemi M. Frequencies of single nucleotide polymorphisms and haplotypes of organic anion transporting polypeptide 1B1 SLCO1B1 gene in a Finnish population. Eur J Clin Pharmacol 2006; **62**: 409-15.

69. Michalski C, Cui Y, Nies AT, Nuessler AK, Neuhaus P, Zanger UM, et al. A naturally occurring mutation in the SLC21A6 gene causing impaired membrane localization of the hepatocyte uptake transporter. J Biol Chem 2002; **277**: 43058-63.

70. Tsujimoto M, Hirata S, Dan Y, Ohtani H, Sawada Y. Polymorphisms and linkage disequilibrium of the OATP8 (OATP1B3) gene in Japanese subjects. Drug Metab Pharmacokinet 2006; **21**: 165-9.

71. Letschert K, Keppler D, Konig J. Mutations in the SLCO1B3 gene affecting the substrate specificity of the hepatocellular uptake transporter OATP1B3 (OATP8). Pharmacogenetics 2004; **14**: 441-52.

72. Stephens M, Smith NJ, Donnelly P. A new statistical method for haplotype reconstruction from population data. Am J Hum Genet 2001; **68**: 978-89.

73. Nebert DW. Proposal for an allele nomenclature system based on the evolutionary divergence of haplotypes. Hum Mutat 2002; **20**: 463-72.

74. Konig J, Seithel A, Gradhand U, Fromm MF. Pharmacogenomics of human OATP transporters. Naunyn Schmiedebergs Arch Pharmacol 2006; **372**: 432-43.

75. Gerloff T, Schaefer M, Mwinyi J, Johne A, Sudhop T, Lutjohann D, et al. Influence of the SLCO1B1*1b and *5 haplotypes on pravastatin's cholesterol lowering capabilities and basal sterol serum levels. Naunyn Schmiedebergs Arch Pharmacol 2006; **373**: 45-50.

76. Lee E, Ryan S, Birmingham B, Zalikowski J, March R, Ambrose H, et al. Rosuvastatin pharmacokinetics and pharmacogenetics in white and Asian subjects residing in the same environment. Clin Pharmacol Ther 2005; **78**: 330-41.

77. Goodman LS, Hardman JG, Limbird LE, Gilman AG. Goodman & Gilman's the pharmacological basis of therapeutics. 10th / ed. New York: McGraw-Hill Medical Pub. Division; 2001.

CHAPTER 2

FUNCTIONAL ANAYSIS OF GENETIC VARIANTS IN THE HUMAN CONCENTRATIVE NUCLEOSIDE TRANSPORTER 3 (CNT3; *SLC28A3*)*

Introduction

Nucleosides serve as intermediates for essential biosynthetic cellular pathways, are important regulators of neurotransmission and cardiovascular activity, and act as signaling molecules (1). Many synthetic analogs of purine and pyrimidine nucleosides are currently used in cancer and viral chemotherapy. Naturally occurring nucleosides and most synthetic nucleoside analogs are hydrophilic and require nucleoside transporters to traverse biological membranes. Therefore, nucleoside transporters are critical determinants of cellular and whole body homeostasis of naturally occurring nucleosides and are important players in the tissue specific disposition and pharmacokinetics of nucleoside analog drugs.

CNT3 is one of three recently cloned members of the SLC28 concentrative nucleoside transporter family (2). In contrast to CNT1 and CNT2, CNT3 is broadly selective, transporting both purine and pyrimidine nucleosides. Among the cloned human SLC28 transporters, CNT3 is primarily responsible for the transport of several anti-leukemic drugs, such as cladribine and fludarabine (2, 3). CNT3 has a 2:1

---

* This chapter was published in *The Pharmacogenomics Journal* 5:157-165, 2005. Permission from the publisher can be found in the "Acknowledgements" section.

Na^+/nucleoside coupling ratio, allowing it to concentrate nucleosides intracellularly ten times more efficiently than CNT1 or CNT2, which have a 1:1 Na^+/nucleoside coupling ratio (2). Its localization to the apical membrane of intestine and liver epithelia suggests that CNT3 plays an important role in the absorption and disposition of nucleosides and synthetic nucleoside analogs (3).

A major clinical problem in cancer treatment is intrinsic resistance to the initial drug regimen selected. Although nucleoside analogs (e.g., cladribine, fludarabine, and cytarabine) are highly active in lymphoproliferative disorders, a significant portion of patients is resistant to these agents (4, 5). This heterogeneous response to treatment could be explained, at least in part, by inter-individual variability in the expression and/or activity of nucleoside transporters. For example, recent studies have shown that variation in the intracellular transport of fludarabine correlated with its chemosensitivity (6). In addition, analysis of expression levels of nucleoside transporters in leukemic cells suggests that CNT3 has the highest inter-individual variability (6). Gray *et al.* recently reported that several genetic variants of CNT1 exhibited altered interaction with gemcitabine, suggesting that common CNT1 variants may contribute to variation in systemic and intracellular levels of pyrimidine nucleoside analog drugs (7).

Because CNT3 is an important determinant of the disposition of physiological nucleosides and nucleoside analogs, we proposed to undertake a comprehensive genetic and functional analysis of CNT3 in ethnically diverse populations. Our study had two major goals: (1) to identify and analyze genetic variation in *SLC28A3*, and (2) to functionally characterize the protein altering variants of CNT3.

Material and Methods

Identification of *SLC28A3* variants

Genomic DNA samples were collected from unrelated healthy individuals in the San Francisco Bay Area as part of the Studies of Pharmacogenetics in Ethnically Diverse Populations (SOPHIE) project. *SLC28A3* variants were identified by direct sequencing of genomic DNA as previously described (8) from an ethnically diverse population of 270 individuals: 80 African-Americans, 80 European-Americans, 60 Asian-Americans (50 Chinese-Americans and 10 Japanese-Americans), and 50 Mexican-Americans. The Genomics Core and Bioinformatics Core of the Pharmacogenetics of Membrane Transporters project were responsible for the resequencing of *SLC28A3* and for the analysis of genetic variation of *SLC28A3*, respectively. The reference cDNA sequence of *SLC28A3* was obtained from GenBank (http://www.ncbi.nlm.nih.gov, accession number AF305210). Primers were designed manually to span the exons and 50-200 bp of flanking intronic sequence. The primer sequences can be found at http://www.pharmgkb.org. The genomic structure of *SLC28A3* was based on a recent analysis by Toan *et al.* (9). Variant positions are relative to the ATG start site and are based on the reference cDNA sequence of *SLC28A3.*

Genetic analysis of *SLC28A3*

The neutral parameter (θ), nucleotide diversity (π), and Tajima's D statistic were calculated as described by Tajima (10). Each parameter was determined for various sites within the coding region of *SLC28A3* (e.g. synonymous and non-synonymous sites, and sites within transmembrane domains and loops) for the entire population and for each ethnic group. Synonymous and non-synonymous sites were defined as described by Hartl

and Clark (11). Haplotypes were inferred from variant sites using the Bayesian statistical method of PHASE (12). Before PHASE analysis, all singleton samples were removed. Only haplotypes that were found in at least 7 of 10 PHASE runs were reported.

Construction of *SCL28A3* variants

Human CNT3 cDNA (GenBank accession number AF305210.1) was subcloned into the mammalian expression vector pOX to obtain CNT3-reference. CNT3-reference corresponds to the coding region in the *SCL28A3* *1A1 haplotype (reference haplotype), which had the highest frequency in all ethnic groups. The QuikChange site-directed mutagenesis kit (Stratagene, La Jolla, CA) was used to construct each amino acid variant of CNT3 following the manufacturer protocol. In all cases CNT3-reference in pOX was used as the template, except for CNT3: p. Gly367Arg-reversed, which used CNT3: p. Gly367Arg as the template. The variants were confirmed by DNA sequencing and were fully sequenced to verify that they only had the desired change.

Functional studies of *SLC28A3* variants in oocytes

Healthy stage V and VI *Xenopus laevis* oocytes were injected with 10-30 ng of capped cRNA transcribed *in vitro* using T3 RNA polymerase (mCAP RNA capping kit; Stratagene) from *NotI*-linearized pOX plasmids containing reference or variant CNT3 cDNA. Before injection, an aliquot of the cRNA was run on an agarose gel to verify that none of the RNA was degraded. RNA concentrations were measured using a spectrophotometer. The injected oocytes were stored in modified Barth's medium at 18°C for 72 h prior to transport experiments. Groups of seven to nine oocytes were incubated in the presence of Na^+ in buffer containing 0.1 μM ^{3}H-inosine (30 Ci/mmol; Moravek), ^{3}H-thymidine (61 Ci/mmol; Moravek), ^{3}H-adenosine (24 Ci/mmol; Moravek),

^{3}H-cladribine (17 Ci/mmol; Moravek), or ^{3}H-fludarabine (6 Ci/mmol; Moravek) and 1 μM of the respective unlabeled substrate at room temperature for 60 min. Uptake was stopped by washing the oocytes five times with ice-cold Na^+ free buffer in which Na^+ was replaced by choline. Oocytes were then lysed individually with 100 μL of 10% SDS and the radioactivity associated with each oocyte was determined. Variant data were normalized to the uptake of CNT3-reference for each experiment. Data are presented as mean of normalized value ± SE. Uninjected oocytes, oocytes injected with CNT3-reference, and oocytes incubated with Na^+ free buffer containing ^{3}H-inosine served as controls within each batch of oocytes. For inhibition kinetic studies, oocytes were incubated with 0.1 μM ^{3}H-inosine (30 Ci/mmol; Moravek) and varying concentrations of unlabeled adenosine (0-500 μM), cladribine (0-1500 μM), or fludarabine (0-6800 μM) at room temperature for 5-20 min. All experiments were repeated two to three times using different batches of oocytes. Uninjected oocytes served as controls within each batch of oocytes. Data are reported as mean ± SE. To determine apparent K_i values, data were fit using non-linear regression analysis as previously described (13). Statistical analysis for the functional studies was carried out by comparing the raw uptake data or K_i values of each variant to those of CNT3-reference using the unpaired Student's t test (Primer of Biostatistics software, Version 3, written by Stanton A. Glantz, McGraw-Hill Companies, 1991). In each case, Bonferroni correction was applied to adjust for multiple testing.

Results

Analysis of genetic variation in *SLC28A3*

Genetic variants of *SLC28A3* were identified as part of a large study, the Pharmacogenetics of Membrane Transporters project, which entails identifying variants in membrane transporter genes that may determine differences in drug response and disposition. The 18 coding exons of *SLC28A3* and 50-200 bp of flanking intronic sequence were screened in a collection of 270 ethnically diverse genomic DNA samples. The data can be found at http://www.pharmgkb.org. Fifty-six variants were identified in a total of 5997 bp screened, with a frequency of approximately ten single nucleotide polymorphisms (SNPs) per kb of sequence (Table 1). Forty variable sites were found in the non-coding intronic regions of the gene. Of the 16 coding region variants, ten altered the protein sequence. Twelve of the 16 coding region variants (cSNPs) were not previously reported in dbSNP (http://www.ncbi.nlm.nih.gov/SNP). Figure 1 shows the position of the 16 cSNPs in the proposed topology of CNT3 (2). The majority of non-synonymous variants were found in intracellular or extracellular loops (seven out of 10).

Three non-synonymous variants (c. 338A>G; c. 14G>A; c. 982A>G) had total allele frequencies of ≥ 1% (Table 1). c. 338A>G (p. Tyr113Cys) was found in all populations sampled; c. 14G>A (p. Ser5Asn) was present in both the African-American and European-American population samples; and c. 982A>G (p. Ile328Val) was only found in the African-American population sample. p. Tyr113Cys was the only protein altering variant with a particularly high allele frequency in all the ethnic groups (10.4%). The other seven protein altering variants were singletons, meaning that they were found on only one of 540 chromosomes.

Table 2 provides a summary of the estimates for the neutral parameter (θ), nucleotide diversity (π), and Tajima's D statistic. These were calculated for the entire

Table 1. Summary of coding region variants in CNT3 identified in ethnically diverse populations

SNP #	CDS Position[1]	Nucleotide Change	Amino Acid Position[1]	Amino Acid Change	Grantham[2]	EC/EU[3]	Allele Frequency (%)[4]			
							AA (n=160)	EA (n=160)	AS (n=120)	ME (n=100)
1.4	*11*	*G→A*	*4*	*Arg→Lys*	*26*	*EC*	*0*	*0*	*0*	*1.0*
1.5	**14**	**G→A**	**5**	**Ser→Asn**	**46**	**EU**	**5.6**	**1.3**	**0**	**0**
2.2	96	A→G	32	syn	-	EU	2.5	0	0	0
3.1	*184*	*G→C*	*62*	*Asp→His*	*81*	*EU*	*0.6*	*0*	*0*	*0*
3.2	*200*	*G→A*	*67*	*Arg→Lys*	*26*	*EU*	*0.6*	*0*	*0*	*0*
4.1	267	G→A	89	syn	-	EC	26.9	72.5	47.4	40.6
5.2	**338**	**A→G**	**113**	**Tyr→Cys**	**194**	**EU**	**16.9**	**8.7**	**9.2**	**4.0**
9.2	*870*	*G→A*	*290*	*syn*	-	*EC*	*0*	*0*	*0*	*1.0*
10.5	**982**	**A→G**	**328**	**Ile→Val**	**29**	**EC**	**5.6**	**0**	**0**	**0**
11.1	*1046*	*G→A*	*349*	*Arg→Gln*	*43*	*EU*	*0*	*0*	*0.8*	*0*
11.2	*1099*	*G→A*	*367*	*Gly→Arg*	*125*	*EC*	*0*	*0*	*0.8*	*0*
11.3	1122	C→T	374	syn	-	EC	2.5	0	0	1.0
12.6	*1252*	*C→A*	*418*	*Leu→Ile*	*5*	*EC*	*0.6*	*0*	*0*	*0*
13.3	1381	C→T	461	syn	-	EC	30.0	13.1	13.2	25.0
15.2	1674	C→T	558	syn	-	EC	0.6	0	5.0	0
16.1	*1754*	*G→A*	*585*	*Arg→His*	*29*	*EC*	*0.6*	*0*	*0*	*0*

Data are available at http://www.pharmgkb.org. Common non-synonymous variants (≥5% in any ethnic group) are shown in bold. Singletons are shown in italics. The reduced function variant is shown in red.

[1]Positions are relative to the ATG start site and are based on the cDNA sequence from GenBank accession number AF305210.

[2]Grantham values range from 5 to 215, where low values indicate chemical similarity and high values indicate radical differences.

[3]EC/EU classifies coding variants as being evolutionarily conserved (EC) or evolutionarily unconserved (EU) based on sequence alignments with mammalian orthologs.

[4]Some samples contained amplicons that could not be sequenced. Allele frequencies were calculated from actual DNA samples sequenced. \AA, African-American; EA, European-American; AS, Asian-American; ME, Mexican-American; n, number of chromosomes.

Table 2. Estimates of the neutral parameter (θ), nucleotide diversity (π), and Tajima's D for *SLC28A3*[1]

Population	SNP type	Base pairs Screened	n[2]	No. variable sites	θ (x 10^4)	π (x 10^4)	D
Total[3]	All	5997	540	56	12.6 ± 2.9	6.1 ± 3.4	-2.36
	Non-coding	3974		40	13.4 ± 3.4	6.4 ± 3.8	-1.94
	Coding	2023		16	11.2 ± 3.5	5.5 ± 4.0	-1.18
	Synonymous	463		6	18.4 ± 8.3	18.1 ± 14.2	-0.02
	Non-synonymous	1560		10	9.1 ± 3.3	1.8 ± 2.1	-1.39
AA	All	5997	160	40	10.7 ± 3.0	7.6 ± 4.2	-1.24
	Non-coding	3974		28	10.9 ± 3.3	7.9 ± 4.6	-0.95
	Coding	2023		12	10.2 ± 3.8	7.1 ± 4.8	-0.71
	Synonymous	463		5	18.7 ± 9.4	19.6 ± 15.0	0.06
	Non-synonymous	1560		7	7.7 ± 3.4	3.4 ± 3.1	-0.92
EA	All	5997	160	17	5.0 ± 1.7	3.7 ± 2.3	-0.73
	Non-coding	3974		12	5.9 ± 2.1	3.6 ± 2.5	-0.93
	Coding	2023		5	3.4 ± 1.9	3.9 ± 3.1	0.17
	Synonymous	463		2	7.5 ± 5.6	13.3 ± 11.6	0.55
	Non-synonymous	1560		3	2.2 ± 1.6	1.2 ± 1.7	-0.34
AS	All	5997	60	24	6.7 ± 2.1	5.7 ± 3.3	-0.42
	Non-coding	3974		18	7.2 ± 2.5	6.3 ± 3.8	-0.34
	Coding	2023		6	5.4 ± 2.6	4.7 ± 3.7	-0.20
	Synonymous	463		3	11.8 ± 7.4	16.3 ± 13.3	0.38
	Non-synonymous	1560		3	3.5 ± 2.2	1.3 ± 1.7	-0.63
ME	All	5997	50	24	7.8 ± 2.5	5.9 ± 3.4	-0.88
	Non-coding	3974		18	8.9 ± 3.0	6.6 ± 4.0	-0.82
	Coding	2023		6	5.6 ± 2.7	4.7 ± 3.5	-0.27
	Synonymous	463		4	16.3 ± 9.1	18.3 ± 14.4	0.15
	Non-synonymous	1560		2	2.4 ± 1.8	0.61 ± 1.2	-0.58

[1]θ, π, and Tajima's D were calculated as described in Methods and Materials
[2] n, number of chromosomes
[3]Total, entire sample; AA, African-American; EA, European-American; AS, Asian-American; ME, Mexican-American. Data are mean ± SD.

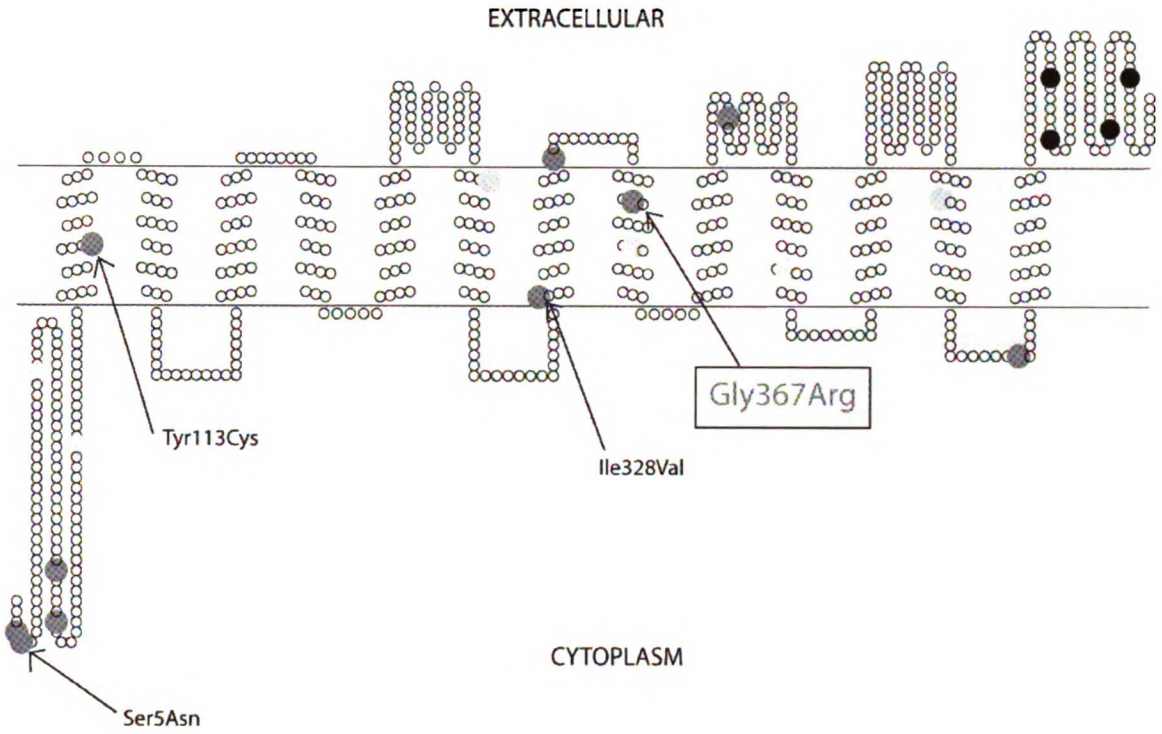

Figure 1. Secondary structure of CNT3 showing the position of the 16 coding region variants. The transmembrane topology diagram was rendered using TOPO [S. J. Johns (UCSF, San Francisco) and R. C. Speth (Washington State University, Pullman), transmembrane protein display software available at the UCSF Sequence Analysis Consulting Group website, http://www.sacs.ucsf.edu/TOPO/topo.html]. Non-synonymous amino acid changes are shown in dark gray; synonymous changes are shown in light gray; putative N-glycosylation sites are shown in black. The three most common non-synonymous variants, which have been kinetically characterized, are indicated by arrows. The reduced function variant is boxed.

population and for each ethnic group. For the entire sample, θ (x 10^4) and π (x 10^4) were 12.6 ± 2.93 and 6.11 ± 3.43, respectively. These estimates are consistent with a previous analysis of 24 membrane transporter genes (14). The π (x 10^4) for synonymous (π_S) and non-synonymous (π_{NS}) sites were 18.1 ± 14.2 and 1.81 ± 2.13, respectively, suggesting that selection is acting against amino acid changes in CNT3. Because most values of θ were greater than π, values for Tajima's D statistic were mostly negative, which is consistent with either recent population expansion or negative selection. Nucleotide diversity in both loop and transmembrane domain (TMD) regions was low ($\pi_{loop\text{-}NS}$ = 0.62 x 10^4 versus $\pi_{TMD\text{-}NS}$ = 3.72 x 10^4), suggesting that there are evolutionary constraints on both regions of the protein.

Analysis of *SLC28A3* haplotypes

Haplotypes of *SLC28A3* were inferred from 32 population variable sites using the Bayesian statistical method of PHASE (12). A total of 52 haplotypes were identified, of which 35 occurred on at least two chromosomes (Figure 2). Because the combined frequency of the 35 haplotypes was over 95%, we focused our analysis on this group. The haplotypes were named according to a modified convention of Nebert following two main criteria: evolutionary divergence and frequency in the sample (15).

Haplotype *1A1 was the most common haplotype accounting for about 40% of the total sample. Seventeen of the 35 haplotypes (49%) were found only in one ethnic group. In contrast, only four of the 35 haplotypes (11%), *1A1, *2A1B, *3A1, and *4A1, were present in all ethnic groups. As expected, the African-American population had the greatest number of haplotypes (24 out of 35), as well as the greatest number of ethnic

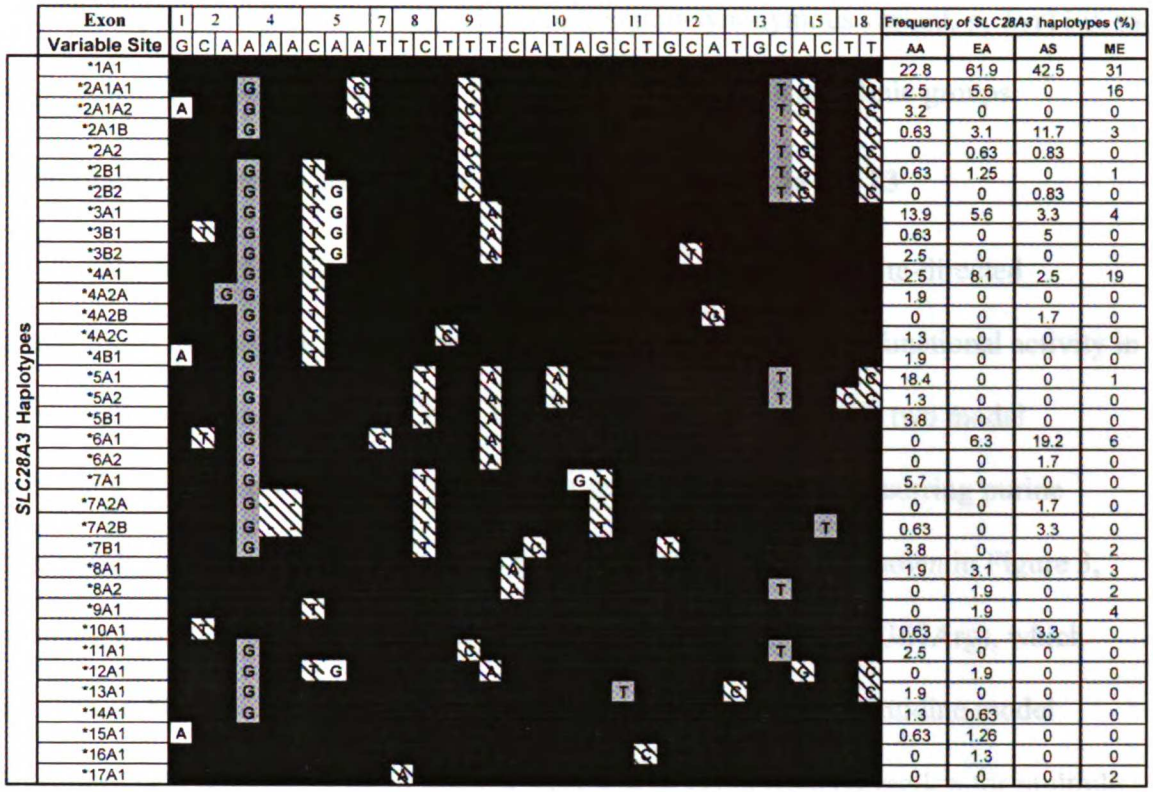

Exon	1	2	4	5	7	8	9	10	11	12	13	15	18	Frequency of *SLC28A3* haplotypes (%)			
Variable Site	G	C	A A A	C	A	A	T	T C	T	T	T C A T A G	C	T	G C A	T G C	A C	T T	AA	EA	AS	ME
*1A1														22.8	61.9	42.5	31
*2A1A1			G	G							T G			2.5	5.6	0	16
*2A1A2	A		G	G							T G			3.2	0	0	0
*2A1B			G								T G			0.63	3.1	11.7	3
*2A2											T G		G	0	0.63	0.83	0
*2B1			G								T G			0.63	1.25	0	1
*2B2			G	G							T G		G	0	0	0.83	0
*3A1			G	G										13.9	5.6	3.3	4
*3B1			G	G										0.63	0	5	0
*3B2			G	G										2.5	0	0	0
*4A1			G											2.5	8.1	2.5	19
*4A2A		G	G											1.9	0	0	0
*4A2B			G											0	0	1.7	0
*4A2C			G											1.3	0	0	0
*4B1	A		G											1.9	0	0	0
*5A1			G								T		G	18.4	0	0	1
*5A2			G								T		G	1.3	0	0	0
*5B1			G											3.8	0	0	0
*6A1			G											0	6.3	19.2	6
*6A2			G											0	0	1.7	0
*7A1			G					G						5.7	0	0	0
*7A2A			G											0	0	1.7	0
*7A2B			G									T		0.63	0	3.3	0
*7B1			G											3.8	0	0	2
*8A1														1.9	3.1	0	3
*8A2											T			0	1.9	0	2
*9A1														0	1.9	0	4
*10A1														0.63	0	3.3	0
*11A1			G								T			2.5	0	0	0
*12A1			G	G									G	0	1.9	0	0
*13A1			G						T				G	1.9	0	0	0
*14A1			G											1.3	0.63	0	0
*15A1	A													0.63	1.26	0	0
*16A1														0	1.3	0	0
*17A1														0	0	0	2

Figure 2. Structure and population frequency of 35 haplotypes of *SLC28A3*. Left panel, sequences of the haplotypes at each of the 32 variable sites. The first row shows the exons of *SLC28A3*; the second row indicates the sequence of the reference allele at each site. The subsequent rows show each of the 35 haplotypes clustered and named according to their evolutionary divergence and population frequencies using a modified convention of Nebert (15). A black filled square indicates that there is no change from the reference allele; a gray filled square denotes a synonymous change in the coding region; a white filled square indicates a non-synonymous change; changes at non-coding sites are indicated by diagonal lines within a square. Letters in the squares indicate the base pair change and a "-" indicates a deletion. Haplotypes were predicted using PHASE software version 1.0.1 as previously described (12). Right panel, frequencies of each haplotype in the total population and in each ethnic group.

specific haplotypes (11 out of 17). The common non-synonymous variant, p. Tyr113Cys, was present in a common haplotype (*3A1) that was found in all ethnic groups.

Functional characterization of non-synonymous variants in CNT3

The ten protein altering variants of CNT3 were obtained by site-directed mutagenesis of the CNT3-reference template and were screened for functional activity in *Xenopus laevis* oocytes. Since CNT3 has broad substrate selectivity, two model substrates were used for the initial functional screen: the naturally occurring purine nucleoside, inosine, and the pyrimidine nucleoside, thymidine. As shown in Figure 3, with the exception of one of the 10 non-synonymous variants (p. Gly367Arg), which showed an 80-85% reduction in the transport of both purine and pyrimidine model substrates ($P < 0.0001$, unpaired Student's t-test with Bonferroni correction for multiple testing), all variants of CNT3 transported both inosine and thymidine. p. Gly367Arg changed an evolutionarily conserved site, which is also conserved in the two human paralogs, CNT1 and CNT2. This variant was found on a single chromosome in the Asian-American sample and results in a radical chemical change (Grantham value of 125) (16). In addition, this variant occurred in the middle of TMD 8, which is considered to be part of the substrate recognition domain for CNTs (17). Functional transport of the p. Gly367Arg variant was restored to normal levels after the variant sequence was changed to the reference sequence demonstrating that this amino acid change was responsible for the reduced activity (Figure 3, *Gly367Arg reversed*).

We examined the functional consequences of the three common non-synonymous variants (p. Ser5Asn, p. Tyr113Cys, and p. Ile328Val) using the anti-leukemic adenosine analogs, cladribine and fludarabine. We first determined that the transport profile of the

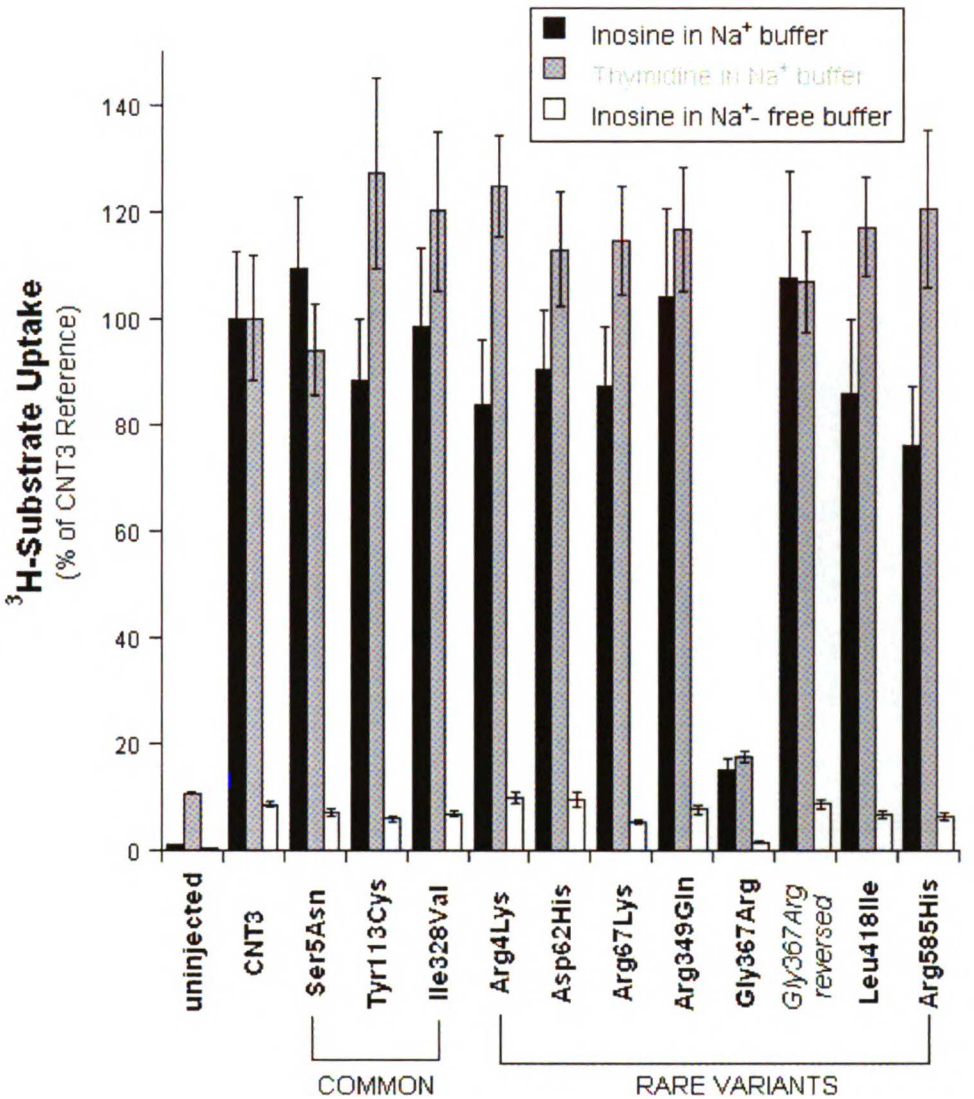

Figure 3. Uptake of nucleosides (inosine and thymidine) in *X. laevis* oocytes expressing CNT3-reference and its non-synonymous variants. Inosine uptake in the absence of Na^+ is shown by the open bars; inosine and thymidine uptake in the presence of sodium is shown by the black and gray filled bars, respectively. Oocytes were injected with 10-30 ng of RNA. Uptake of ^{3}H-substrate (0.1 μM of labeled and 1 μM unlabeled substrate) was measured after incubation for 60 min. Each value represents mean ± SE from 7-9 oocytes.

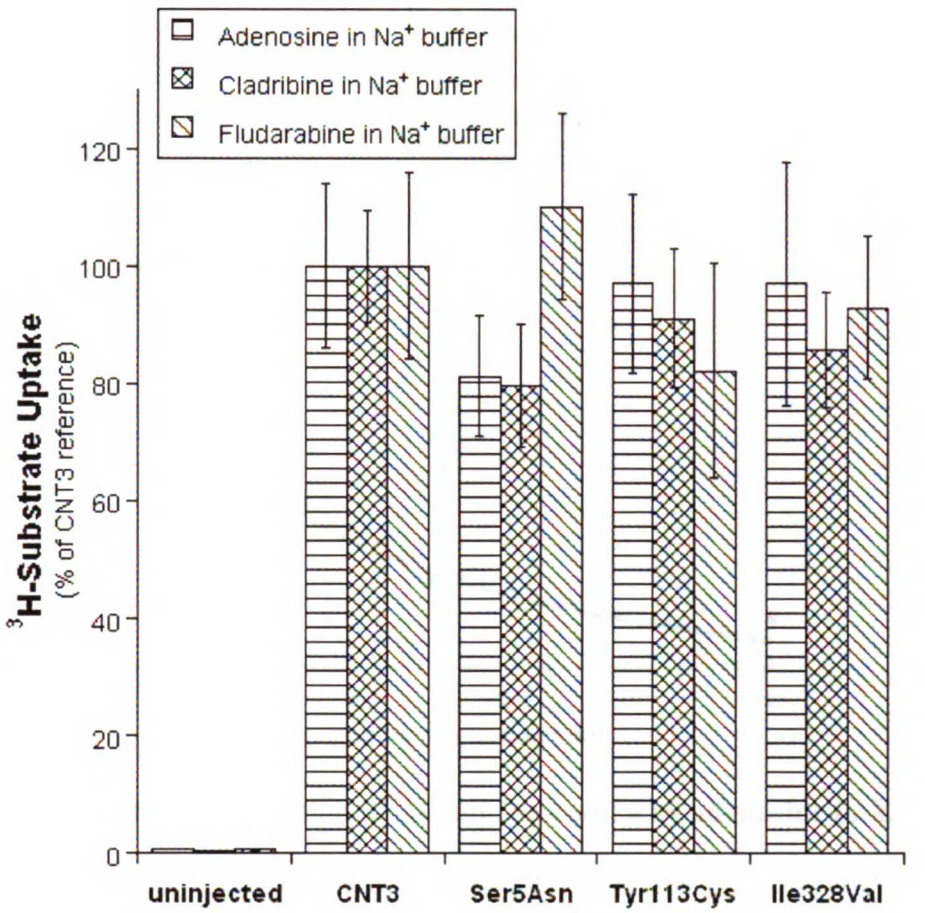

Figure 4. Uptake of adenosine analogs in *X. laevis* oocytes expressing CNT3-reference and its non-synonymous variants, p. Ser5Asn, p. Tyr113Cys, and p. Ile328Val. Adenosine, cladribine, and fludarabine uptake is shown by the horizontally striped bars, hatched bars, and diagonally striped bars, respectively. Oocytes were injected with 10-30 ng of RNA. Uptake of ^{3}H-substrate (0.1 μM of labeled and 1 μM unlabeled substrate) was measured after incubation for 60 min. Each value represents mean ± SE from 7-9 oocytes.

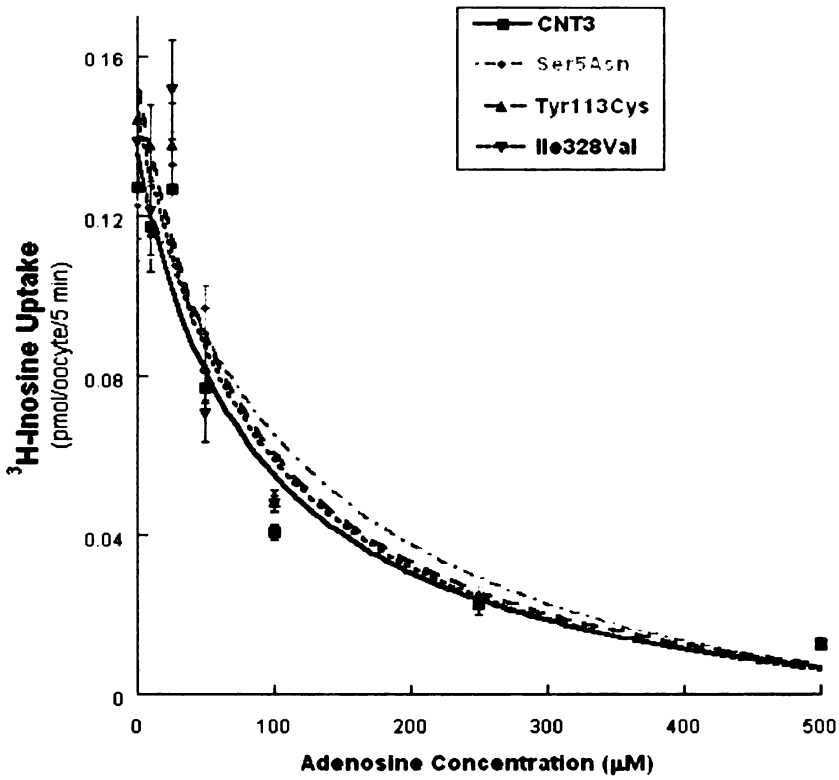

Figure 5. Kinetics of inhibition of ^{3}H-Inosine uptake by adenosine in *X. laevis* oocytes expressing CNT3-reference (■) and the common non-synsonymous variants p. Ser5Asn (♦), p. Tyr113Cys (▲), and p. Ile328Val (▼). Oocytes were injected with 10 ng of CNT3-reference or variant RNA, and uptake of ^{3}H-inosine in the presence of increasing concentrations of substrate was measured after incubation for 5-20 min. Data are representative of experiments carried out with 2-3 different batches of oocytes. Each value represents the mean ± SE from 7-9 oocytes. Uninjected oocytes serve as the negative control. The uptake of inosine (mean ± SE) in the absence of inhibitors in oocytes expressing CNT3-reference was 0.13 ± 0.013 pmol and in uninjected oocytes was 0.0021 ± 0.00021 pmol.

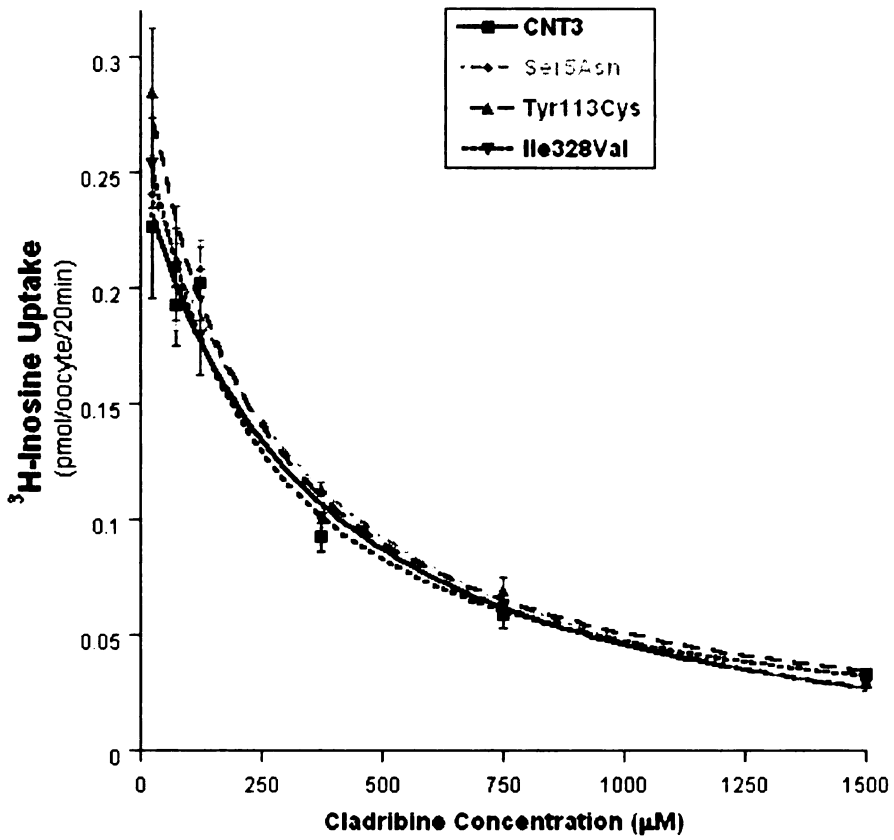

Figure 6. Kinetics of inhibition of ^{3}H-Inosine uptake by cladribine in *X. laevis* oocytes expressing CNT3-reference (■) and the common non-synsonymous variants p. Ser5Asn (♦), p. Tyr113Cys (▲), and p. Ile328Val (▼). Oocytes were injected with 10 ng of CNT3-reference or variant RNA, and uptake of ^{3}H-inosine in the presence of increasing concentrations of substrate was measured after incubation for 5-20 min. Data are representative of experiments carried out with 2-3 different batches of oocytes. Each value represents the mean ± SE from 7-9 oocytes. Uninjected oocytes serve as the negative control. The uptake of inosine (mean ± SE) in the absence of inhibitors in oocytes expressing CNT3-reference was 0.23 ± 0.031 pmol and in uninjected oocytes was 0.0038 ± 0.00025 pmol.

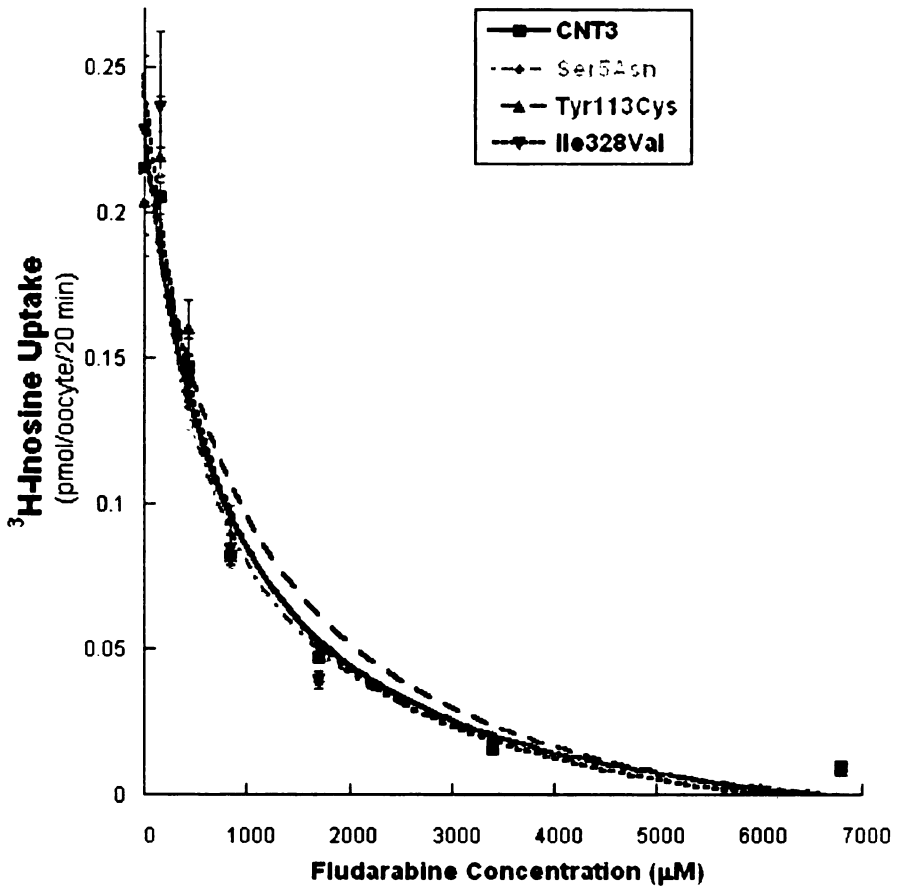

Figure 7. Kinetics of inhibition of ^{3}H-Inosine uptake by fludarabine in *X. laevis* oocytes expressing CNT3-reference (■) and the common non-synsonymous variants p. Ser5Asn (♦), p. Tyr113Cys (▲), and p. Ile328Val (▼). Oocytes were injected with 10 ng of CNT3-reference or variant RNA, and uptake of ^{3}H-inosine in the presence of increasing concentrations of substrate was measured after incubation for 5-20 min. Data are representative of experiments carried out with 2-3 different batches of oocytes. Each value represents the mean ± SE from 7-9 oocytes. Uninjected oocytes serve as the negative control. The uptake of inosine (mean ± SE) in the absence of inhibitors in oocytes expressing CNT3-reference was 0.21 ± 0.022 pmol and in uninjected oocytes was 0.0029 ± 0.00020 pmol.

Table 3. Kinetics of interaction of adenosine and its analogs with CNT3 and its three common non-synonymous variants

Variant	Adenosine K_i (μM)	Cladribine K_i (μM)	Fludarabine K_i (μM)
CNT3-reference	68.7 ± 11	274 ± 65	1066 ± 283
p. Ser5Asn	91.2 ± 24	241 ± 123	870 ± 183
p. Tyr113Cys	77.5 ± 8.9	195 ± 23	1193 ± 168
p. Ile328Val	94.4 ± 3.4	230 ± 11	856 ± 155

three common variants for adenosine and its analogs was similar to CNT3-reference (Figure 4). Then, the uptake of 0.1 μM ^{3}H-inosine in the presence of increasing concentrations of unlabeled adenosine, cladribine, or fludarabine, was measured in oocytes expressing the reference and variant constructs. For these kinetic studies we selected time based on initial transport rates where substrate uptake is linear (5 min for adenosine and 20 min for cladribine and fludarabine). Figures 5-7 show representative graphs of the interaction kinetics of p. Ser5Asn, p. Tyr113Cys, and p. Ile328Val with adenosine and its synthetic analogs. The K_i values for each variant revealed no substantial differences in the interaction affinity of adenosine and its analogs for the three common protein altering variants of CNT3 (Table 3; $P > 0.0167$, unpaired Student's t-test with Bonferroni correction for multiple testing).

Discussion

To better understand inter-individual differences in the disposition of and response to anti-cancer nucleoside analog drugs, we undertook a comprehensive genetic and functional analysis of variation in the coding region of the human concentrative nucleoside transporter, CNT3, encoded by *SLC28A3*. Population genetic analysis of *SLC28A3* and functional characterization of protein altering variants suggest that CNT3 is under negative selective pressure and is important for human fitness.

Our data shows that nucleotide diversity at non-synonymous sites ($\pi_{NS\text{-}total}$ (x 10^4): 1.81 ± 2.13) was consistently lower than at synonymous sites ($\pi_{S\text{-}total}$ (x 10^4): 18.1 ± 14.2) for the entire sample and for each ethnic group. The ratio of π_{NS}/π_S was 0.1, which is lower than 0.23 reported in a recent analysis of variation in 24 membrane transporter

genes (14). These observations suggest that CNT3 is under strong negative selection, which is acting to preserve its amino acid sequence more so than in the case of many membrane transporters. Strong negative selection is also suggested by the values of Tajima's D for non-synonymous sites, which were consistently negative compared to the corresponding values for synonymous sites, which were always positive for each of the ethnic groups analyzed. In addition, the majority of non-synonymous variants in CNT3 occurred at a lower allele frequency than synonymous variants, where seven out of ten protein altering changes compared to just one out of six synonymous changes were singletons. Furthermore, a greater proportion of non-synonymous variants was population specific (eight out of ten) compared to synonymous variants (two out of six). This is consistent with the theory that deleterious mutations (which are more likely to be at non-synonymous sites) are kept at low frequency and should not easily spread to multiple populations (18). The fact that CNT3 has few non-synonymous changes may be ascribed to important endogenous roles of this transporter in regulating cellular and whole organ homeostasis of physiological nucleosides (19).

A total of 52 haplotypes were identified in *SLC28A3*, which is consistent with a report by Stephens *et al.*, where the 313 genes analyzed had between two and 53 haplotypes (20). Most haplotypes had only synonymous or intronic changes, while only nine of 35 haplotypes contained one amino acid altering variant. None of the haplotypes contained two or more amino acid changes.

Of the ten non-synonymous variants identified in CNT3, one showed severely reduced functional transport of both purine and pyrimidine model substrates (Figure 3). p. Gly367Arg changed an evolutionarily conserved residue, which is also conserved in

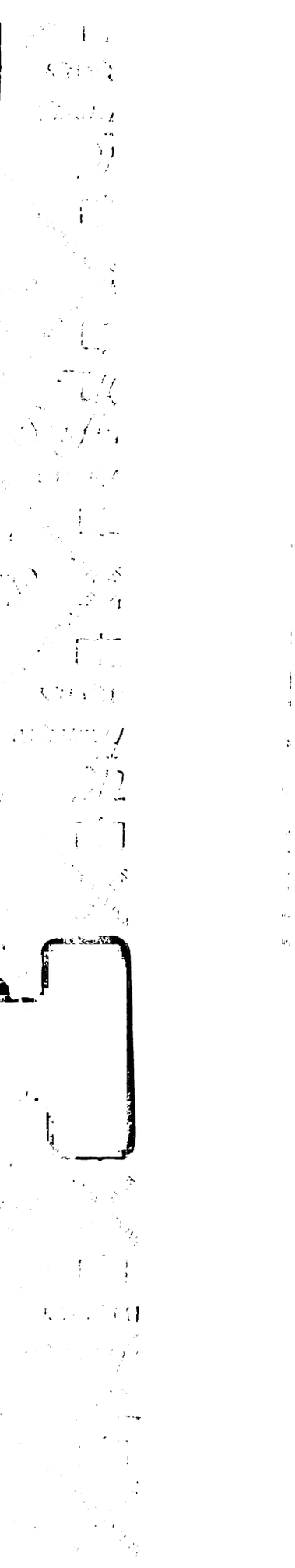

human paralogs of CNT3, and was found on a single chromosome in the Asian-American sample. In addition, this variant results in a radical chemical change with a Grantham value of 125 and is found in the middle of TMD 8, which is part of the putative substrate recognition domain of CNTs (16, 17). These observations are consistent with findings that rare variants are more likely to affect function than common variants and that changes at evolutionarily conserved sites are more likely to be deleterious to protein function (14, 21). In addition, Shu *et al.* analyzed protein altering variants of the organic cation transporter, OCT1 and found that combining evolutionary conservation with Grantham values was a stronger predictor of function (22).

Interestingly, TMD 8 of CNT3 has four glycines, including Gly367, which are conserved not only among mammals, but also in the other two human paralogs (CNT1 and CNT2), suggesting that these residues may be particularly important for the function of the concentrative nucleoside transporter family. A similar observation was also recently reported by Shu *et al.* for the organic cation transporter family, where all three of the non-functional variants of OCT1 altered evolutionarily conserved glycine residues (22). Vitkup *et al.* estimated that mutations at glycine residues are responsible for about 20% of genetic diseases and changes at glycine residues have the third highest probability (behind changes at cysteine and tryptophan, respectively) of causing an altered phenotype (23). This may be related to the important structural roles played by this residue (24). In particular, glycine is frequently found at the turns of alpha-helices and if mutated may result in backbone strain, which may negatively impact the structural stability of a protein (25). Partridge *et al.* recently reported that the Gly → Arg change accounts for approximately 5% of all phenotypic mutations in TMDs of various membrane proteins

and occurs statistically more frequently in TMDs than in soluble domains (26). This is not surprising, since glycine residues are involved in van der Waals mediated packing of transmembrane helices (27). Introducing an arginine residue in place of a glycine would then have dual deleterious effects of disrupting helix-helix interactions and introducing non-native electrostatic interactions.

Comparison of nucleoside transporters suggests that there is a continuum in the genetic diversity, haplotype structure, and functional variation of these transporters. ENT1 (in the SLC29 equilibrative nucleoside transporter family), which has the least genetic and functional variation and is most constrained, is at one end of the spectrum, while CNT1, which has the most genetic and functional variation and is least constrained, is at the opposite extreme, with CNT3 in between (7, 28). It is interesting that CNT3 has less genetic and functional diversity than its paralog, CNT1, suggesting that it is more critical for human fitness. The fact that both purine and pyrimidine nucleosides are substrates of CNT3, while only pyrimidine nucleosides are substrates of CNT1, suggests that CNT3 is able to replace the function of CNT1 in tissues where these transporters are co-expressed, whereas the reverse is not true. Moreover, because of its more favorable Na^+/nucleoside stoichiometry, CNT3 is capable of concentrating its substrates ten fold more than CNT1. Thus, CNT3 may be a more important transporter in terms of human fitness than CNT1 and as a result, it tolerates less genetic and functional diversity. Non-synonymous variants of CNT3, as well as of ENT1 and CNT1, have less functional diversity than those of the xenobiotic transporter, OCT1 (7, 22, 28). A possible explanation for this phenomenon could be that transporters with a primary role in xenobiotic detoxification may be functionally less constrained compared to transporters,

like CNT3, which though involved in xenobiotic disposition, function primarily to maintain homeostasis of endogenous compounds.

CNT3 plays an important role in modulating the disposition and entry of nucleoside analog drugs into target tissues (3). CNT3 has been shown to interact with a variety of purine and pyrimidine analogs, including the anti-leukemic agents, cladribine and fludarabine (2). These agents are currently considered the first drugs of choice in the treatment of a variety of lymphoproliferative disorders, such as chronic lymphocytic leukemia (4, 5). Recently, Molina-Arcas *et al.* showed that leukemic cancer cells had varying abilities to concentrate fludarabine intracellularly and this correlated with fludarabine cytotoxicity (6). These same cells had variable expression levels of nucleoside transporters, with CNT3 showing the highest inter-individual variation (6). Therefore, in this study we examined the potency of interaction of cladribine and fludarabine with CNT3 and the three common protein altering variants, p. Ser5Asn, p. Tyr113Cys, and p. Ile328Val (Figures 5-7). No significant differences were observed in the potency of any of the compounds tested in inhibiting CNT3-reference and its three non-synonymous polymorphisms (Table 3). Although studies in heterologous expression systems, such as *X. laevis* oocytes, can accurately assess substrate and inhibitor potencies (K_i) and may reflect *in vivo* potencies in various tissues, the same is not the case for maximum transport rates. The maximum transport rate (V_{max}) of a substrate is a function of both the expression level of the transporter on the plasma membrane and its turnover rate constant. In oocytes, V_{max} is controlled by the quantity of mRNA injected, its stability in the cells, and the rate of translation, trafficking, and degradation of the transporter. Obviously, these factors would vary in different tissues in the body.

In summary, we have determined that CNT3 has a high degree of genetic and functional constraints. This transporter is under strong negative selection, which is acting to preserve its amino acid sequence. It is possible that due to its primary role in maintaining homeostasis of endogenous compounds, CNT3 is critical for human fitness. The three common amino acid variants of CNT3 (p. Ser5Asn, p. Tyr113Cys, and p. Ile328Val) interact with the anti-leukemic analogs, cladribine and fludarabine, similarly to CNT3-reference. It remains to be determined whether genetic variation in other regions of *SLC28A3* can explain the observed variation in the expression levels of this transporter and in the clinical response to the adenosine nucleoside analogs in leukemia patients.

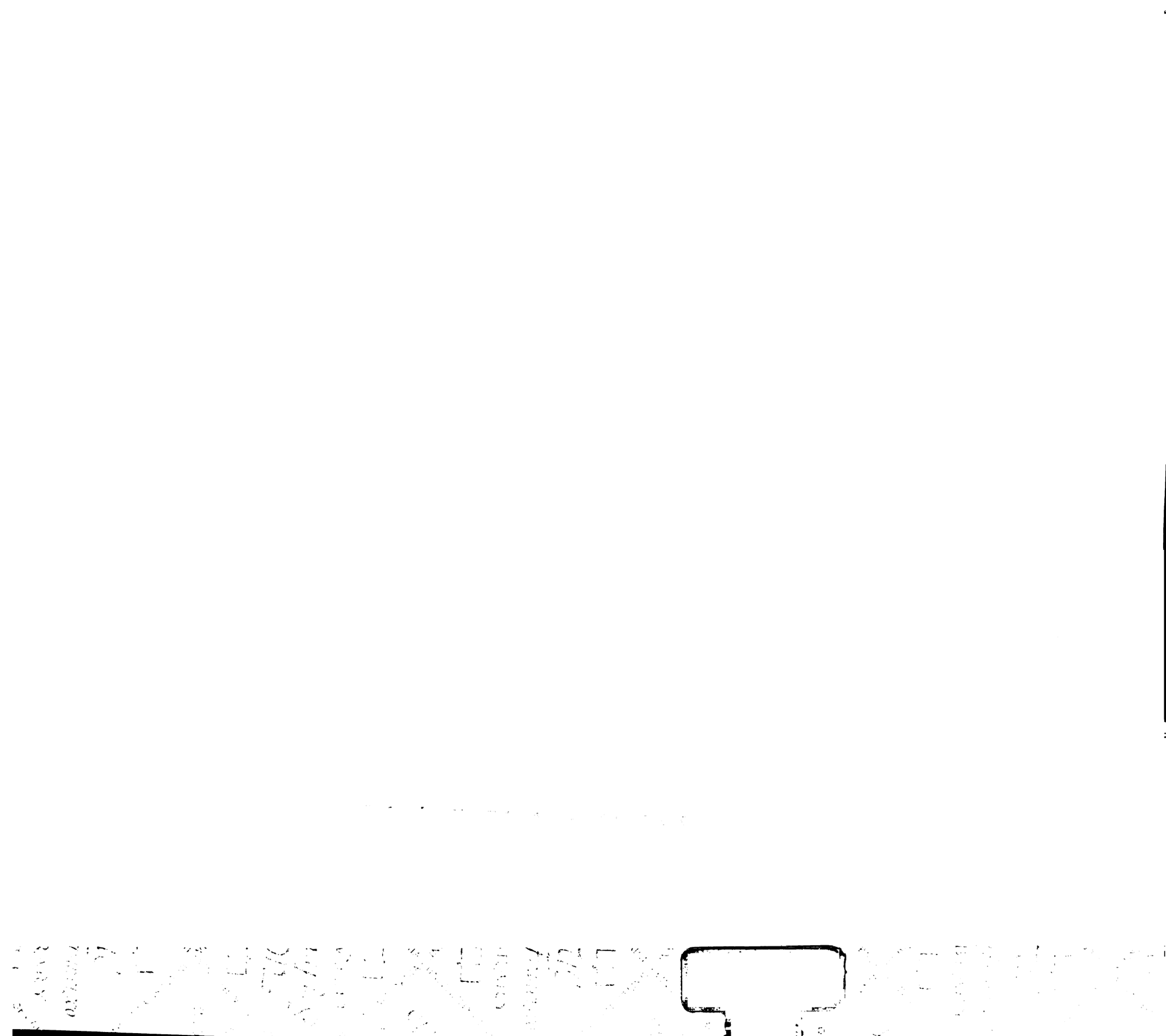

References

1. Baldwin SA, Mackey JR, Cass CE, Young JD. Nucleoside transporters: molecular biology and implications for therapeutic development. Mol Med Today 1999; **5**: 216-24.

2. Ritzel MW, Ng AM, Yao SY, Graham K, Loewen SK, Smith KM, et al. Molecular identification and characterization of novel human and mouse concentrative Na+-nucleoside cotransporter proteins (hCNT3 and mCNT3) broadly selective for purine and pyrimidine nucleosides (system cib). J Biol Chem 2001; **276**: 2914-27.

3. Mangravite LM, Badagnani I, Giacomini KM. Nucleoside transporters in the disposition and targeting of nucleoside analogs in the kidney. Eur J Pharmacol 2003; **479**: 269-81.

4. Pott C, Hiddemann W. Purine analogs in the treatment of chronic lymphocytic leukemia. Leukemia 1997; **11 Suppl 2**: S25-8.

5. Robak T. The role of nucleoside analogues in the treatment of chronic lymphocytic leukemia-lessons learned from prospective randomized trials. Leuk Lymphoma 2002; **43**: 537-48.

6. Molina-Arcas M, Bellosillo B, Casado FJ, Montserrat E, Gil J, Colomer D, et al. Fludarabine uptake mechanisms in B-cell chronic lymphocytic leukemia. Blood 2003; **101**: 2328-34.

7. Gray JH, Mangravite LM, Owen RP, Urban TJ, Chan W, Carlson EJ, et al. Functional and genetic diversity in the concentrative nucleoside transporter, CNT1, in human populations. Mol Pharmacol 2004; **65**: 512-9.

8. Leabman MK, Huang CC, Kawamoto M, Johns SJ, Stryke D, Ferrin TE, et al. Polymorphisms in a human kidney xenobiotic transporter, OCT2, exhibit altered function. Pharmacogenetics 2002; **12**: 395-405.

9. Toan SV, To KK, Leung GP, de Souza MO, Ward JL, Tse CM. Genomic organization and functional characterization of the human concentrative nucleoside transporter-3 isoform (hCNT3) expressed in mammalian cells. Pflugers Arch 2003; **447**: 195-204.

10. Tajima F. Statistical method for testing the neutral mutation hypothesis by DNA polymorphism. Genetics 1989; **123**: 585-95.

11. Hartl DL, Clark AG. Principles of population genetics. 3rd ed. Sunderland, MA: Sinauer Associates; 1997.

12. Stephens M, Smith NJ, Donnelly P. A new statistical method for haplotype reconstruction from population data. Am J Hum Genet 2001; **68**: 978-89.

13. Zhang L, Schaner ME, Giacomini KM. Functional characterization of an organic cation transporter (hOCT1) in a transiently transfected human cell line (HeLa). J Pharmacol Exp Ther 1998; **286**: 354-61.

14. Leabman MK, Huang CC, DeYoung J, Carlson EJ, Taylor TR, de la Cruz M, et al. Natural variation in human membrane transporter genes reveals evolutionary and functional constraints. Proc Natl Acad Sci U S A 2003; **100**: 5896-901.

15. Nebert DW. Proposal for an allele nomenclature system based on the evolutionary divergence of haplotypes. Hum Mutat 2002; **20**: 463-72.

16. Grantham R. Amino acid difference formula to help explain protein evolution. Science 1974; **185**: 862-4.

17. Wang J, Giacomini KM. Molecular determinants of substrate selectivity in Na+-dependent nucleoside transporters. J Biol Chem 1997; **272**: 28845-8.

18. Fay JC, Wyckoff GJ, Wu CI. Positive and negative selection on the human genome. Genetics 2001; **158**: 1227-34.

19. Gray JH, Owen RP, Giacomini KM. The concentrative nucleoside transporter family, SLC28. Pflugers Arch 2004; **447**: 728-34.

20. Stephens JC, Schneider JA, Tanguay DA, Choi J, Acharya T, Stanley SE, et al. Haplotype variation and linkage disequilibrium in 313 human genes. Science 2001; **293**: 489-93.

21. Miller MP, Kumar S. Understanding human disease mutations through the use of interspecific genetic variation. Hum Mol Genet 2001; **10**: 2319-28.

22. Shu Y, Leabman MK, Feng B, Mangravite LM, Huang CC, Stryke D, et al. Evolutionary conservation predicts function of variants of the human organic cation transporter, OCT1. Proc Natl Acad Sci U S A 2003; **100**: 5902-7.

23. Vitkup D, Sander C, Church GM. The amino-acid mutational spectrum of human genetic disease. Genome Biol 2003; **4**: R72.

24. Majewski J, Ott J. Amino acid substitutions in the human genome: evolutionary implications of single nucleotide polymorphisms. Gene 2003; **305**: 167-73.

25. Wang Z, Moult J. SNPs, protein structure, and disease. Hum Mutat 2001; **17**: 263-70.

26. Partridge AW, Therien AG, Deber CM. Polar mutations in membrane proteins as a biophysical basis for disease. Biopolymers 2002; **66**: 350-8.

27. Russ WP, Engelman DM. The GxxxG motif: a framework for transmembrane helix-helix association. J Mol Biol 2000; **296**: 911-9.

28. Osato DH, Huang CC, Kawamoto M, Johns SJ, Stryke D, Wang J, et al. Functional characterization in yeast of genetic variants in the human equilibrative nucleoside transporter, ENT1. Pharmacogenetics 2003; **13**: 297-301.

29. Goodman LS, Hardman JG, Limbird LE, Gilman AG. Goodman & Gilman's the pharmacological basis of therapeutics. 10th / ed. New York: McGraw-Hill Medical Pub. Division; 2001.

30. Hendel J, Nyfors A. Nonlinear renal elimination kinetics of methotrexate due to saturation of renal tubular reabsorption. Eur J Clin Pharmacol 1984; **26**: 121-4.

31. Shen DD, Azarnoff DL. Clinical pharmacokinetics of methotrexate. Clin Pharmacokinet 1978; **3**: 1-13.

32. Bourke RS, Chheda G, Bremer A, Watanabe O, Tower DB. Inhibition of renal tubular transport of methotrexate by probenecid. Cancer Res 1975; **35**: 110-6.

33. Huang KC, Wenczak BA, Liu YK. Renal tubular transport of methotrexate in the rhesus monkey and dog. Cancer Res 1979; **39**: 4843-8.

34. Perazella MA. Crystal-induced acute renal failure. Am J Med 1999; **106**: 459-65.

35. Perazella MA. Drug-induced renal failure: update on new medications and unique mechanisms of nephrotoxicity. Am J Med Sci 2003; **325**: 349-62.

36. el-Badawi MG, Abdalla MA, Bahakim HM, Fadel RA. Nephrotoxicity of low-dose methotrexate in guinea pigs: an ultrastructural study. Nephron 1996; **73**: 462-6.

37. Koepsell H, Endou H. The SLC22 drug transporter family. Pflugers Arch 2004; **447**: 666-76.

38. Ganapathy V, Smith SB, Prasad PD. SLC19: the folate/thiamine transporter family. Pflugers Arch 2004; **447**: 641-6.

39. Hooijberg JH, Peters GJ, Assaraf YG, Kathmann I, Priest DG, Bunni MA, et al. The role of multidrug resistance proteins MRP1, MRP2 and MRP3 in cellular folate homeostasis. Biochem Pharmacol 2003; **65**: 765-71.

40. Hagenbuch B, Meier PJ. Organic anion transporting polypeptides of the OATP/ SLC21 family: phylogenetic classification as OATP/ SLCO superfamily, new nomenclature and molecular/functional properties. Pflugers Arch 2004; **447**: 653-65.

41. Kullak-Ublick GA, Ismair MG, Stieger B, Landmann L, Huber R, Pizzagalli F, et al. Organic anion-transporting polypeptide B (OATP-B) and its functional comparison with three other OATPs of human liver. Gastroenterology 2001; **120**: 525-33.

42. Kullak-Ublick GA, Hagenbuch B, Stieger B, Schteingart CD, Hofmann AF, Wolkoff AW, et al. Molecular and functional characterization of an organic anion transporting polypeptide cloned from human liver. Gastroenterology 1995; **109**: 1274-82.

43. Lee W, Glaeser H, Smith LH, Roberts RL, Moeckel GW, Gervasini G, et al. Polymorphisms in human organic anion-transporting polypeptide 1A2 (OATP1A2): implications for altered drug disposition and central nervous system drug entry. J Biol Chem 2005; **280**: 9610-7.

44. Su Y, Zhang X, Sinko PJ. Human organic anion-transporting polypeptide OATP-A (SLC21A3) acts in concert with P-glycoprotein and multidrug resistance protein 2 in the vectorial transport of Saquinavir in Hep G2 cells. Mol Pharm 2004; **1**: 49-56.

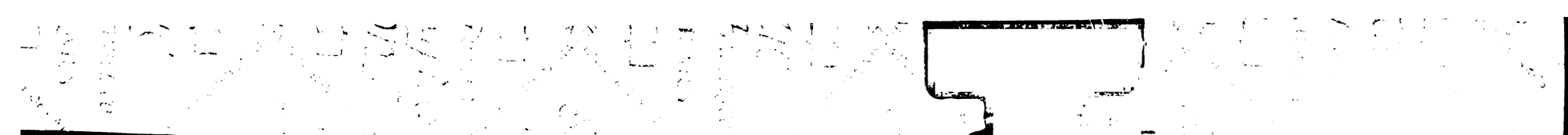

45. Gao B, Hagenbuch B, Kullak-Ublick GA, Benke D, Aguzzi A, Meier PJ. Organic anion-transporting polypeptides mediate transport of opioid peptides across blood-brain barrier. J Pharmacol Exp Ther 2000; **294**: 73-9.

46. Konig J, Hartel M, Nies AT, Martignoni ME, Guo J, Buchler MW, et al. Expression and localization of human multidrug resistance protein (ABCC) family members in pancreatic carcinoma. Int J Cancer 2005; **115**: 359-67.

47. Giacomini KM, Markovich D, Werner A, Biber J, Wu X, Murer H. Expression of a renal Na(+)-nucleoside cotransport system (N2) in Xenopus laevis oocytes. Pflugers Arch 1994; **427**: 381-3.

48. Badagnani I, Chan W, Castro RA, Brett CM, Huang CC, Stryke D, et al. Functional analysis of genetic variants in the human concentrative nucleoside transporter 3 (CNT3; SLC28A3). Pharmacogenomics J 2005; **5**: 157-65.

49. Erdman AR, Mangravite LM, Urban TJ, Lagpacan LL, Castro RA, de la Cruz M, et al. The human organic anion transporter 3 (OAT3; SLC22A8): genetic variation and functional genomics. Am J Physiol Renal Physiol 2006; **290**: F905-12.

50. Werner A, Biber J, Forgo J, Palacin M, Murer H. Expression of renal transport systems for inorganic phosphate and sulfate in Xenopus laevis oocytes. J Biol Chem 1990; **265**: 12331-6.

51. Due AD, Qu ZC, Thomas JM, Buchs A, Powers AC, May JM. Role of the C-terminal tail of the GLUT1 glucose transporter in its expression and function in Xenopus laevis oocytes. Biochemistry 1995; **34**: 5462-71.

52. Liegler DG, Henderson ES, Hahn MA, Oliverio VT. The effect of organic acids on renal clearance of methotrexate in man. Clin Pharmacol Ther 1969; **10**: 849-57.

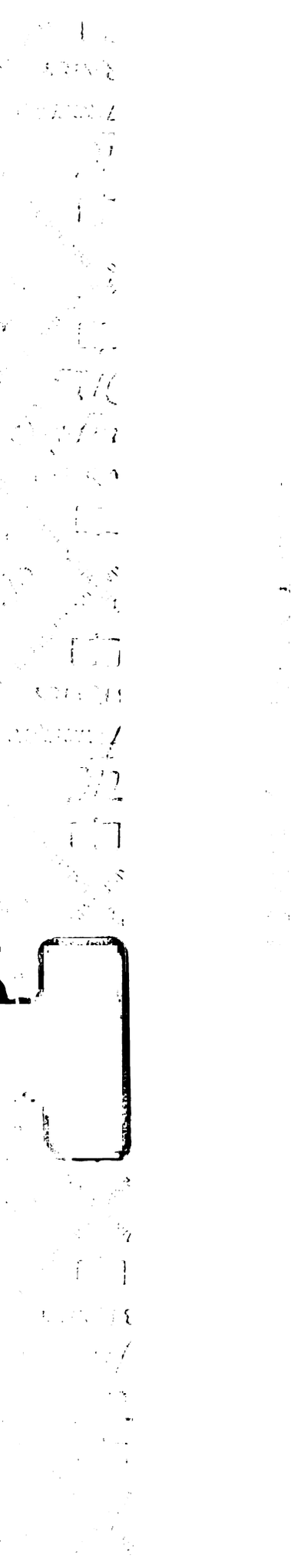

53. Chladek J, Grim J, Martinkova J, Simkova M, Vaniekova J, Koudelkova V, et al. Pharmacokinetics and pharmacodynamics of low-dose methotrexate in the treatment of psoriasis. Br J Clin Pharmacol 2002; **54**: 147-56.

54. Christophidis N, Louis WJ, Lucas I, Moon W, Vajda FJ. Renal clearance of methotrexate in man during high-dose oral and intravenous infusion therapy. Cancer Chemother Pharmacol 1981; **6**: 59-64.

55. Ferrazzini G, Sohl H, Robieux I, Johnson D, Giesbrecht E, Koren G. Diurnal variation of methotrexate disposition in children with acute leukaemia. Eur J Clin Pharmacol 1991; **41**: 425-7.

56. Kobayashi D, Nozawa T, Imai K, Nezu J, Tsuji A, Tamai I. Involvement of human organic anion transporting polypeptide OATP-B (SLC21A9) in pH-dependent transport across intestinal apical membrane. J Pharmacol Exp Ther 2003; **306**: 703-8.

57. Nozawa T, Imai K, Nezu J, Tsuji A, Tamai I. Functional characterization of pH-sensitive organic anion transporting polypeptide OATP-B in human. J Pharmacol Exp Ther 2004; **308**: 438-45.

58. Tirona RG, Leake BF, Merino G, Kim RB. Polymorphisms in OATP-C: identification of multiple allelic variants associated with altered transport activity among European- and African-Americans. J Biol Chem 2001; **276**: 35669-75.

59. Shu Y, Leabman MK, Feng B, Mangravite LM, Huang CC, Stryke D, et al. Evolutionary conservation predicts function of variants of the human organic cation transporter, OCT1. Proc Natl Acad Sci U S A 2003; **100**: 5902-7.

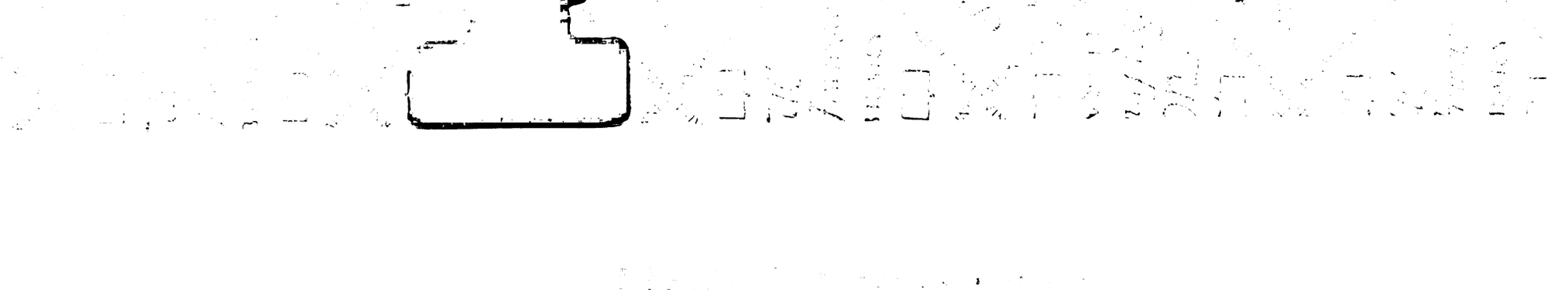

60. Owen RP, Gray JH, Taylor TR, Carlson EJ, Huang CC, Kawamoto M, et al. Genetic analysis and functional characterization of polymorphisms in the human concentrative nucleoside transporter, CNT2. Pharmacogenet Genomics 2005; **15**: 83-90.

61. Gray JH, Mangravite LM, Owen RP, Urban TJ, Chan W, Carlson EJ, et al. Functional and genetic diversity in the concentrative nucleoside transporter, CNT1, in human populations. Mol Pharmacol 2004; **65**: 512-9.

62. Erdman AR, Mangravite LM, Urban TJ, Lagpacan LL, Castro RA, de la Cruz M, et al. The human organic anion transporter 3 (OAT3; SLC22A8): genetic variation and functional genomics. Am J Physiol Renal Physiol 2005.

CHAPTER 3

INTERACTION OF METHOTREXATE, AN ORGANIC ANION DRUG, WITH OATP1A2 AND ITS GENETIC VARIANTS*

Introduction

MTX, a folate antimetabolite and a weak bicarboxylic organic anion, has been used to treat millions of patients with malignant and autoimmune diseases. Despite its high efficacy, MTX therapy can result in severe toxicity to the kidney, liver, gastrointestinal tract, hematopoietic system, and central nervous system (1). MTX is primarily excreted unchanged in the urine and its net excretion is a function of active tubular secretion and reabsorption (2-5). Because of poor solubility, MTX and its minor metabolite, 7-hydroxymethotrexate (7-OH-MTX), can precipitate in the distal kidney lumen, especially after high doses. This crystalluria can result in nephrotoxicity and delayed excretion, producing high systemic blood levels of MTX (1, 6-8). Accumulation of MTX in blood can then lead to severe system toxicity to other organs.

Organ specific toxicity of MTX as well as other drugs is often related to high systemic or tissue specific drug levels. There is evidence that systemic blood levels and

---

* This chapter was published in the *Journal of Pharmacology and Experimental Therapeutics* 318(2):521-529, 2006. Reprinted with permission of the American Society for Pharmacology and Experimental Therapeutics. All rights reserved. Copyright © 2006 by the American Society for Pharmacology and Experimental Therapeutics.

tissue specific levels of MTX are determined by membrane transporters such as the reduced folate carrier (RFC; *SLC19A1*), organic anion transporters (OATs), and ATP-binding cassette (ABC) transporters (9-11). Although several transporters that mediate MTX secretion in the proximal tubule have been identified, little is known about the transporters that are responsible for the saturable reabsorption mechanism in the distal tubule of the kidney.

Organic anion transporting polypeptides (human, OATPs; rodents, Oatps) represent a family of membrane solute carrier proteins that are expressed in a variety of organs important for drug disposition. These proteins mediate the cellular transport of a wide range of amphipathic compounds, including drugs in clinical use and other xenobiotic substances (12). Within the OATP family, OATP1A2 (*SLCO1A2*, also referred as OATP-A or OATP1) has been shown to transport the largest number of structurally diverse compounds, including bile acids, steroid hormones, neutral and anionic peptides, and bulky organic cations (13, 14). Since it is primarily expressed in epithelial cells of the kidney, liver, intestine, and in endothelial cells of the blood-brain barrier (15-17), OATP1A2 likely plays an important role in tissue-specific disposition, pharmacokinetics, and toxicity of xenobiotics. Recently, OATP1A2 has been localized to the luminal membrane of endothelial cells at the blood-brain barrier and on the apical domain of distal tubule kidney cells, suggesting that this transporter may play a role in drug toxicity in the central nervous system and kidney, as well as in drug disposition (15, 18).

In the present study, we determined that MTX is transported by OATP1A2, suggesting that this transporter is an important determinant of MTX disposition and

toxicity. Transport of MTX by OATP1A2 was found to be exquisitely sensitive to extracellular pH, but was not affected by the proton gradient across the membrane. Furthermore, we identified seven new protein-altering variants in OATP1A2 in ethnically diverse populations. Four of the twelve protein-altering variants studied, two of which had allele frequencies ≥ 1%, exhibited changes in the transport of ES and/or MTX compared to OATP1A2 reference. Interestingly, we showed that p. Ile13Thr, a common variant found in 16% of European-Americans and previously reported to have normal transport function, has a 2-fold higher transport of both ES and MTX as a result of a significant increase in V_{max}. In addition, p. Glu172Asp, which is found in 2% of European-Americans, exhibited a 3-fold and 5-fold lower maximal transport capacity for ES and MTX, respectively, compared to OATP1A2. Our data suggest that OATP1A2 plays an important role in the tissue specific and pH-dependent disposition of MTX in the body and genetic variants in this transporter may have significant pharmacokinetic and toxicological implications.

Materials and Methods

Materials

^{3}H-ES (57.3 Ci/mmol) was purchased from PerkinElmer Life Sciences (Wellesley, MA) and ^{3}H-MTX (49.6 Ci/mmol) was obtained from Moravek (Brea, CA). All unlabeled chemicals were purchased from Sigma (St. Louis, MO), except for 7-hydroxymethotrexate (7-OH-MTX), which was obtained from Schircks Laboratories (Jona, Switzerland). Human embryonic kidney cells (Flp-In™-HEK293) and the

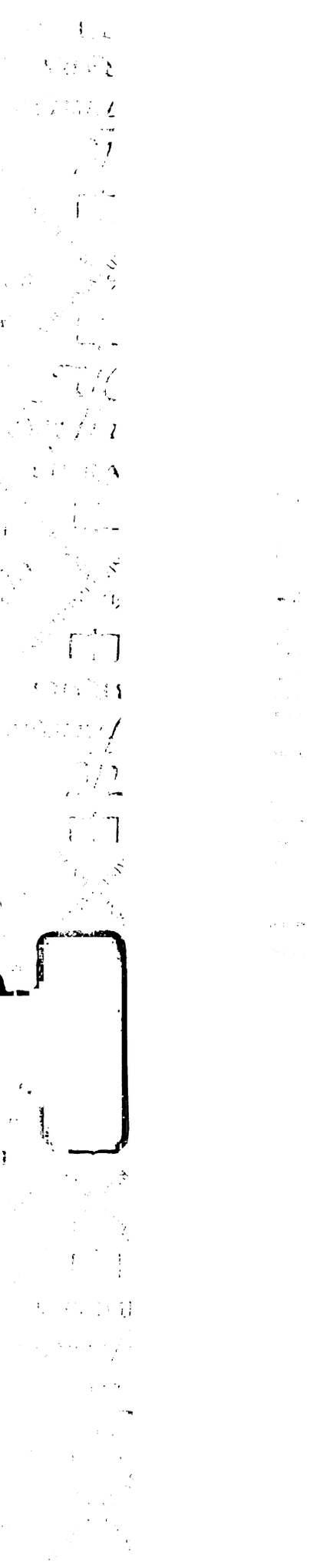

mammalian expression vector, pcDNA5/FRT were purchased from Invitrogen (Carlsbad, CA).

Xenopus laevis oocyte expression assay

The original human *SLCO1A2* plasmid containing the full-length cDNA in a pCMV expression vector was purchased from Genecopoeia (Germantown, MD). The *SLCO1A2* cDNA was subsequently subcloned into the amphibian high-expression vector pOX. Healthy stage V and VI oocytes were harvested from *X. laevis* (Xenopus One, Dexter, MI) as previously described (19). The oocytes were injected with 50-75 ng of capped cRNA transcribed *in vitro* using T3 RNA polymerase (mMESSAGE MACHINE T3 kit; Ambion, Austin, TX) from *Not I*-linearized pOX plasmid containing *SLCO1A2* cDNA. Before injection, an aliquot of the cRNA was run on 1% agarose gel to verify that the RNA was not degraded. RNA concentrations were determined using a spectrophotometer. The injected oocytes were incubated in modified Barth's medium (88 mM NaCl, 1 mM KCl, 0.82 mM $MgSO_4$, 0.41 mM $CaCl_2$, 0.33 mM $Ca(NO_3)_2$, 2.4 mM $NaHCO_3$, 10 mM HEPES/Tris, pH 7.4, supplemented with 20 mg/l gentamicin, and 50 mg/l tetracycline) at 18°C for 72 h prior to transport experiments. Groups of seven to nine oocytes were exposed to Na^+ buffer containing 20 nM ^{3}H-ES or 0.2 μM ^{3}H-MTX at room temperature for 60 min. For inhibition experiments, folate, leucovorin, MTX, and 7-OH-MTX (1 and 2 mM) were added to Na^+ buffer in the presence of 20 nM ^{3}H-ES. Uptake of both ES and MTX was linear for at least 120 min in oocytes expressing OATP1A2. The Na^+ buffer contained 100 mM NaCl, 2 mM KCl, 1 mM $CaCl_2$, 1 mM $MgCl_2$, and 10 mM HEPES/ Tris[hydroxymethyl]-aminomethane. The pH of the Na^+ buffer was adjusted to 7.4 (or any other relevant pH) using Tris[hydroxymethyl]-

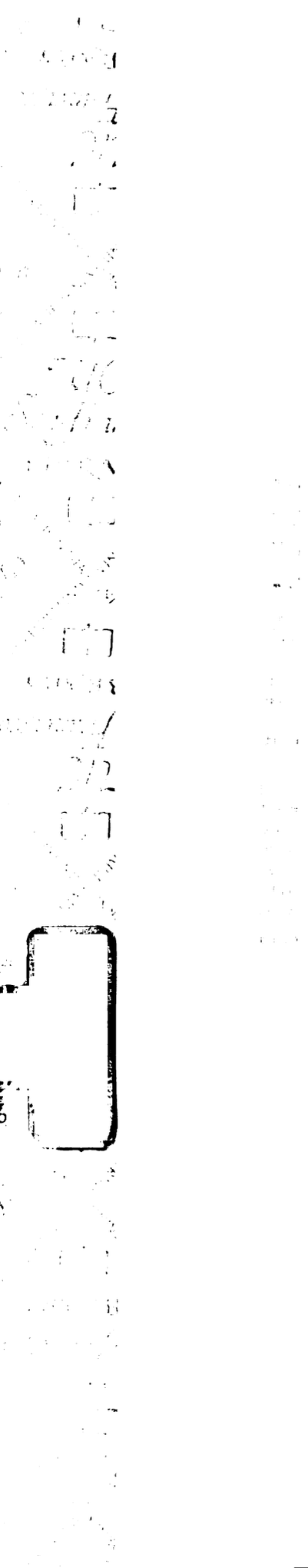

aminomethane and/or HCl. Uptake was stopped by washing the oocytes five times with ice-cold Na^+ free buffer in which Na^+ was replaced by choline chloride. Oocytes were lysed individually using 100 μL of 10% SDS and the radioactivity of each oocyte was then determined.

Saturation kinetics of ^{3}H-MTX

Oocytes injected with OATP1A2 cRNA were incubated with 0.2 μM ^{3}H-MTX in Na^+ buffer, pH 7.4, in the presence of various concentrations of unlabeled MTX at room temperature for 60 min. The kinetic curve for MTX transport by OATP1A2 was generated by fitting the data to a Michaelis-Menten curve by non-linear regression, using GraphPad Prism 4 Software. A summary of the kinetic parameters of MTX transport by OATP1A2 is given as mean ± SE from three independent experiments.

MTX transport by OATP1A2 is sensitive to extracellular pH

To test the effect of extracellular pH on OATP1A2-mediated transport of MTX, oocytes injected with OATP1A2 were incubated with 0.2 μM ^{3}H-MTX in Na^+ buffer in the presence of decreasing extracellular pH (pH_o) at room temperature for 60 min. In addition, to determine whether MTX transport by OATP1A2 was dependent on the proton gradient across the membrane, oocytes expressing OATP1A2 were exposed to the proton ionophore, carbonylcyanide *p*-trifluoromethoxyphenyl hydrazone (FCCP). Oocytes were pre-incubated in Na^+ buffer, pH 7.4, for 30 min at room temperature. Oocytes were washed three times with Na^+ buffer, pH 7.4, and then incubated with 0.2 μM ^{3}H-MTX in Na^+ buffer in the absence or presence of 20 μM FCCP at pH 7.4 or pH 5.0 for 60 min. Data are normalized to uptake of MTX by OATP1A2 at pH_o=7.4 and are presented as mean ± SE from 7-9 oocytes. Data shown are representative of three

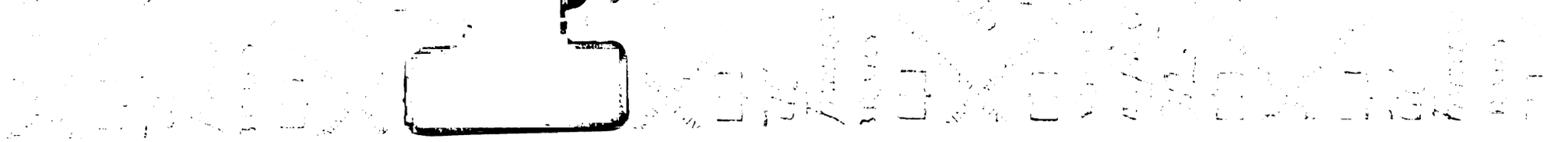

independent experiments. P values were determined by comparing uptake in the presence of FCCP to that in the absence of FCCP at each Na^+ buffer pH separately, using one-way ANOVA and Tukey's multi-comparison test with $p < 0.05$ as the criterion of significance.

Identification of *SLCO1A2* variants

Genomic DNA samples were obtained from unrelated healthy individuals in the San Francisco Bay Area, as previously described (20). The Genomics Core and Bioinformatics Core of the Pharmacogenetics of Membrane Transporters project were responsible for the resequencing of *SLCO1A2* and for the analysis of genetic variation of *SLCO1A2*, respectively. *SLCO1A2* variants were identified using automated direct sequencing in an ethnically diverse population of 270 individuals: 80 African-Americans, 80 European-Americans, 60 Asian-Americans (50 Chinese-Americans and 10 Japanese-Americans), and 50 Mexican-Americans. The reference cDNA sequence of *SLCO1A2* was acquired from GenBank (http://www.ncbi.nlm.nih.gov, accession number NM_021094). Primers were designed manually to cover the exons and at least 50 bp of flanking intronic sequence. The primer sequences can be found at http://www.pharmgkb.org. Variant positions were determined relative to the ATG start site and were based on the reference cDNA sequence of *SLCO1A2.*

Construction of SLCO1A2 variants for X. laevis oocyte studies

OATP1A2 cDNA (GenBank accession number NM_021094) was subcloned into pOX to obtain OATP1A2 reference. The sequence of OATP1A2 reference corresponds to the OATP1A2 coding region that had the highest frequency in all ethnic groups. Each of the 12 protein-altering variants in OATP1A2 was constructed by site-directed

mutagenesis of the OATP1A2-reference-containing plasmid, using the QuickChange mutagenesis protocol (Stratagene, La Jolla, CA, USA).

Functional studies of SLCO1A2 variants

Oocytes expressing reference or variant OATP1A2 were incubated in Na^+ buffer, pH 7.4, containing 20 nM ^{3}H-ES or 0.2 μM ^{3}H-MTX at room temperature for 60 min. The data are presented as percentage of ES or MTX uptake by OATP1A2 reference at pH 7.4. Each value represents the mean ± SE from 7-9 oocytes. Data are shown as a summary of three independent experiments. P values were determined in each of three experiments by comparing variant uptake to OATP1A2 reference for each substrate using one-way ANOVA and Tukey's multi-comparison test with $p < 0.05$ as the criterion of significance. The maximum transport rate (V_{max}) of ES by OATP1A2 reference and the common protein-altering variant, p. Glu172Asp, was characterized in oocytes injected with varying concentrations of OATP1A2 or variant cRNA. The data shown are representative of three independent experiments and were fitted by non-linear regression analysis using GraphPad Prism 4 Software. P values were determined by comparing uptake of p. Glu172Asp to that of OATP1A2 at each cRNA concentration using the unpaired Student's *t* test with $p < 0.05$ as the criterion of significance. In addition, kinetics studies of ES interaction with OATP1A2 and the common protein-altering variants, p. Ile13Thr and p. Thr668Ser, were performed in transiently transfected HEK293 cells. The plasmid containing human *SLCO1A2* in pSPORT1 was a generous gift from Dr. B. Stieger (University of Zurich, Zurich, Switzerland). This *SLCO1A2* clone has identical open reading frame cDNA sequence and amino acid sequence to the *SLCO1A2* clone used in *X. laevis* oocyte expression assays. The *SLCO1A2* cDNA was

subsequently subcloned into the mammalian expression vector, pcDNA5/FRT. HEK293 cells were grown and propagated as previously described (21). Cells were plated at 3 x 10^5 cells/well on poly-d-lysine 24-well plates (Becton Dickenson, Bedford, MA) 24 hr prior to transfection. Transfection was performed by incubating 1 μg/well of plasmid DNA with 3 μL of the lipid vehicle Lipofectamine 2000™ (Invitrogen, Carlsbad, CA). The transfection mixture was replaced with fresh media after 24 hr. Uptake experiments were performed 48 hr after transfection. Uptake of ES was linear for at least 2 min. HEK293 cells transiently transfected with pcDNA5/FRT, OATP1A2, p. Ile13Thr, and p. Thr668Ser were incubated with 20 nM ^{3}H-ES in Na^+ buffer at pH 7.4 in the presence of various concentrations of unlabeled ES for 2 min at 37°C. The kinetic curves were generated by fitting the data to a Michaelis-Menten curve fit, using GraphPad Prism 4 Software. A summary of the kinetic parameters of ES transport by OATP1A2 reference and variants is given as mean ± SE from three independent experiments. P values were determined by comparing K_m and V_{max} values for each variant to OATP1A2 using one-way ANOVA and Tukey's multi-comparison test with $p < 0.05$ as the criterion of significance.

Results

OATP1A2 interacts with the folate antagonists, MTX and 7-OH-MTX

The role of OATP1A2 in the cellular transport of folates and folate antagonists was examined by inhibiting ES uptake in oocytes expressing OATP1A2. Initial studies demonstrated that uptake of the model substrate, ES, and MTX was enhanced 30- and 3-fold, respectively. As shown in Figure 1, MTX and 7-OH-MTX inhibited ES transport by

UCSF LIBRARY

70% and 25%, respectively. On the other hand, folate and leucovorin, a drug used clinically to rescue normal cells from the cytotoxic effects of MTX, did not inhibit ES uptake, despite being structurally similar to MTX. Structure activity studies to examine the relationship between various functional groups and interaction with OATP1A2 are needed to identify the pharmacophores that are essential or preferred for interaction with OATP1A2. ES and MTX transport in oocytes expressing OATP1A2 was linear for at least 120 min (data not shown) and uptake times of 60 min were, therefore, used in subsequent experiments. The initial rate of uptake of MTX by OATP1A2 was saturable (Figure 2), with a mean K_m of 457 ± 118 μM and V_{max} of 17.5 ± 4.9 pmol/oocyte/60 min.

Transport of MTX by OATP1A2 is sensitive to extracellular pH (pH_o)

To characterize the mechanism of transport of MTX by OATP1A2 in tissues, such as the kidney and intestine, where luminal pH is known to vary, MTX uptake by OATP1A2 was measured at pHs ranging from 7.4 to 5.0. MTX transport significantly increased at acidic pH in oocytes expressing OATP1A2 (Figure 3). The initial rate of MTX uptake in oocytes expressing OATP1A2 was 5-7-fold higher at pH 5.0 (0.606 ± 0.0289 pmol/oocyte/60 min) compared to pH 7.4 (0.0811 ± 0.0046 pmol/oocyte/60 min). Similar findings were obtained with ES, where uptake was enhanced by 2-4 fold at pH 5.0 compared to pH 7.4 (data not shown). To examine whether the increase in MTX transport by OATP1A2 at pH 5.0 was due to the H^+ gradient across the membrane, the proton ionophore, FCCP, was used to collapse the pH gradient. The initial rate of uptake of MTX at pH 5.0 in oocytes expressing OATP1A2 and pre-incubated in pH 7.4 buffer was not significantly decreased by FCCP (20 μM) (Figure 4). We were unable to

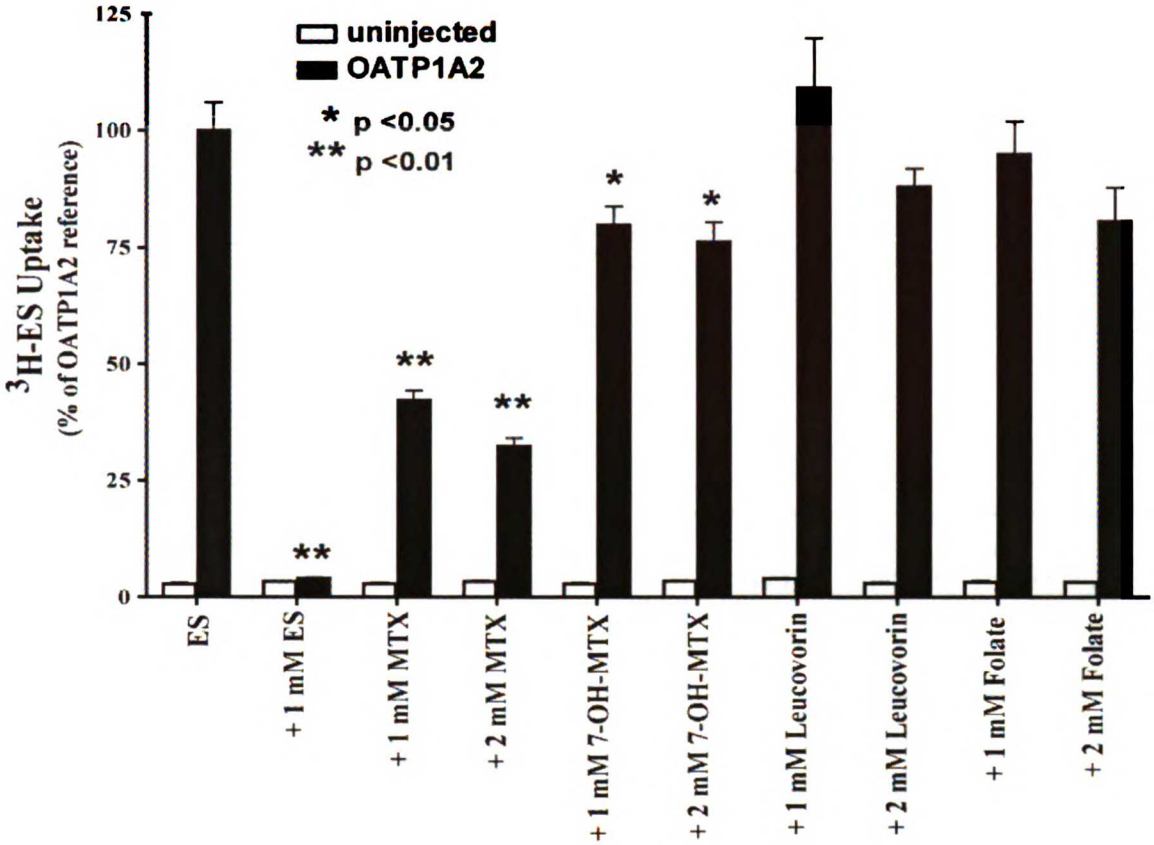

Figure 1. MTX and its metabolite, 7-OH-MTX, are transported by OATP1A2.

Inhibition of ES uptake by folates (leucovorin and folate) and folate antagonists (MTX and 7-OH-MTX) in *X. laevis* oocytes expressing OATP1A2. ES uptake by uninjected oocytes and oocytes expressing OATP1A2 is shown in the white and black bars, respectively. Oocytes were incubated for 60 min with ^{3}H-ES (20 nM) in the absence or presence of various concentrations of unlabeled compounds. Uptake is expressed as percentage of ES uptake by OATP1A2 at pH 7.4. Data are representative of experiments carried out with 3 different batches of oocytes. Each value represents the mean ± SE from 7-9 oocytes. P values were determined by comparing ES uptake in the presence of inhibitors to OATP1A2-mediated ES uptake in the absence of inhibitors using one-way ANOVA and Tukey's multi-comparison test with $p < 0.05$ as the criterion of significance.

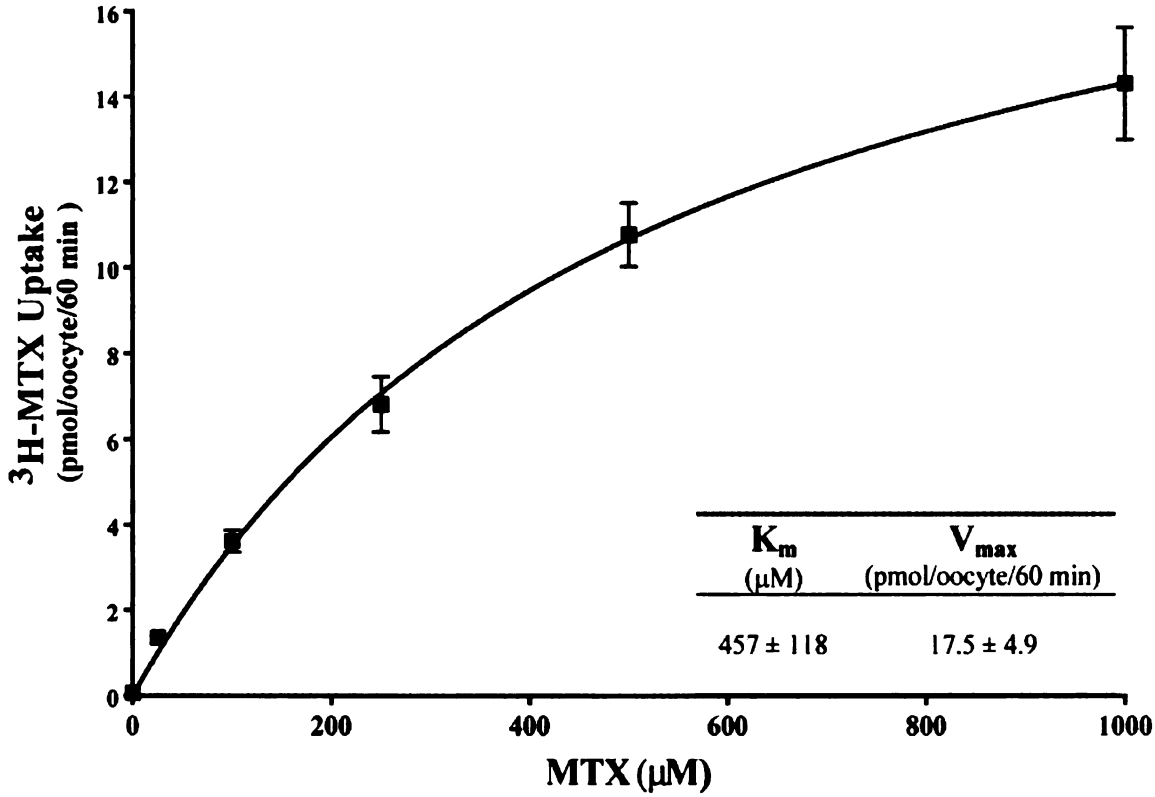

Figure 2. Kinetics of MTX transport in *X. laevis* oocytes expressing OATP1A2. Oocytes were incubated for 60 min with ^{3}H-MTX (0.2 μM) in the presence of various concentrations of unlabeled MTX. *Inset,* kinetic parameters of MTX transport by OATP1A2 were determined by fitting the data using nonlinear regression analysis and are shown as mean ± SE from 3 independent experiments. Data are representative of experiments carried out with 3 different batches of oocytes. Each value represents the mean ± SE from 7-9 oocytes.

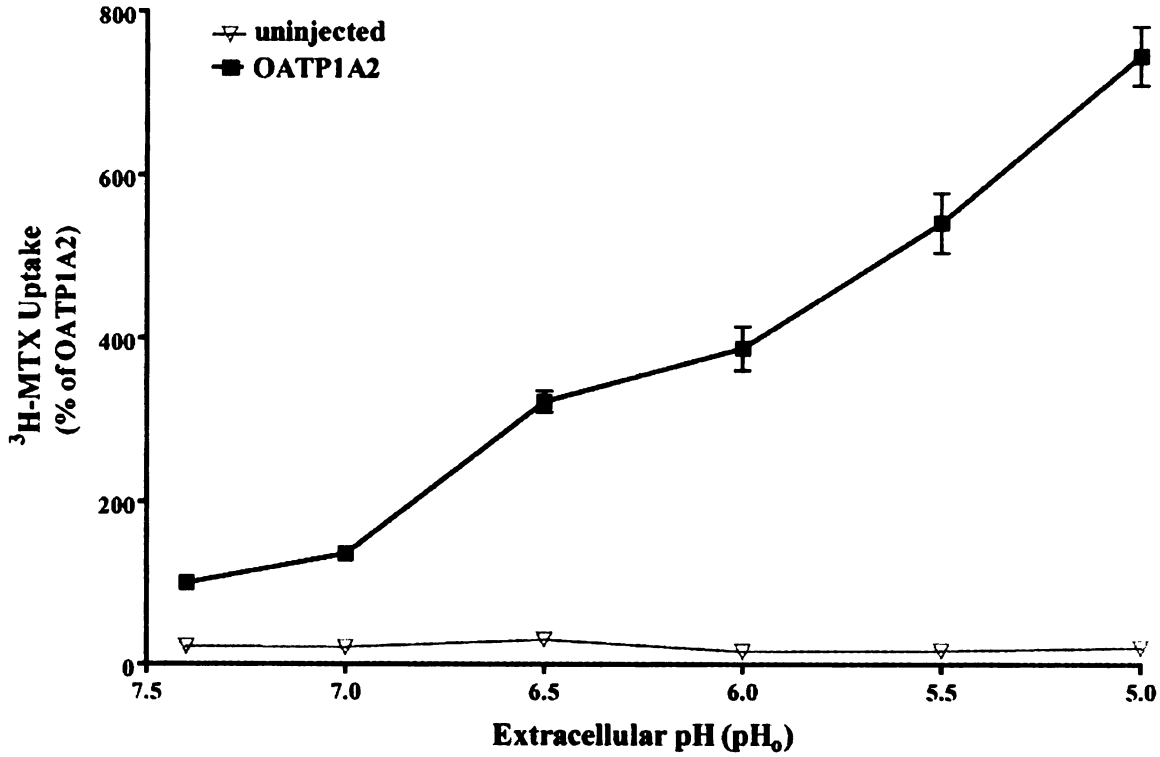

Figure 3. Transport of MTX by OATP1A2 is sensitive to extracellular pH. Uptake of ^{3}H-MTX (0.2 μM) in *X. laevis* oocytes expressing OATP1A2 (black squares) or uninjected oocytes (gray inverted triangles) as a function of decreasing extracellular pH. Oocytes were pre-incubated for 30 min with Na^+ buffer at pH 7.4. Transport of MTX was measured in Na^+ buffer over 60 min. Uptake is expressed as percentage of MTX uptake by OATP1A2 injected oocytes at pH 7.4. The pH of the Na^+ buffer was adjusted with Trizma and HCl. Data are representative of 3 independent experiments. Each value represents the mean ± SE from 7-9 oocytes.

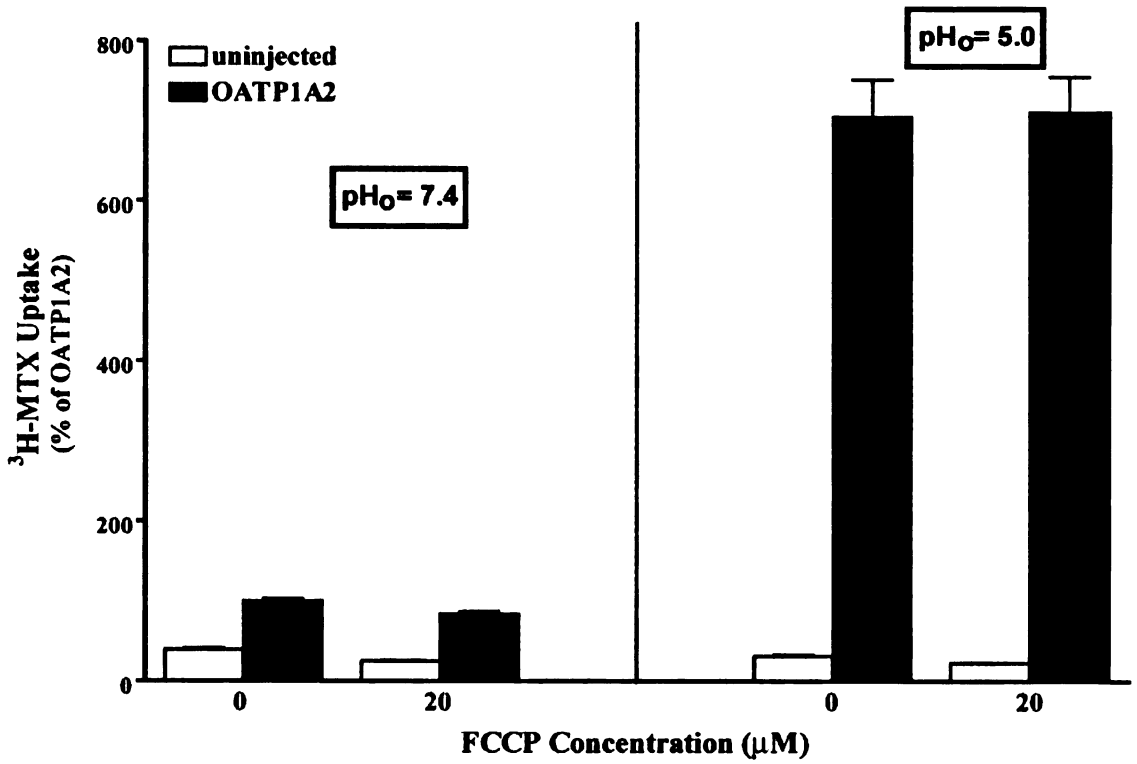

Figure 4. Transport of MTX by OATP1A2 is independent of the proton gradient.

Uptake of ^{3}H-MTX (0.2 μM) in *X. laevis* oocytes expressing OATP1A2 (black bars) or in uninjected oocytes (white bars) in the absence or presence of 20 μM FCCP at extracellular pH 7.4 and 5.0. Oocytes were pre-incubated for 30 min with Na^{+} buffer at pH 7.4. Transport of MTX was measured in Na^{+} buffer over 60 min. Uptake is expressed as percentage of MTX uptake by OATP1A2 injected oocytes at pH 7.4. The pH of the Na^{+} buffer was adjusted with Trizma and HCl. Data are representative of 3 independent experiments. Each value represents the mean ± SE from 7-9 oocytes.

determine the effect of extracellular pH on the kinetics of MTX transport by OATP1A2, because MTX was insoluble at concentrations ≥ 500 μM at acidic pH. Altogether, these data indicate that OATP1A2-mediated uptake of MTX is sensitive to extracellular pH, but that the proton gradient across the membrane does not appear to be the driving force for MTX transport by OATP1A2.

Genetic variation in human SLCO1A2

Genetic variants of *SLCO1A2* were identified as part of a large study, the Pharmacogenetics of Membrane Transporters project, which entails identifying variants in membrane transporter genes that may lead to differences in drug response and disposition. The 14 coding exons of *SLCO1A2* and 50-200 bp of flanking intronic sequence were screened in a collection of 270 ethnically diverse genomic DNA samples. The data are posted in the NIH-Pharmacogenetics and Pharmacogenomics Knowledgebase, http://www.pharmgkb.org. Forty-one variants were identified; of these, 11 altered the protein sequence of OATP1A2. As shown in Figure 5 and Table 1, the majority of non-synonymous variants were found in intracellular or extracellular loops (seven out of 11). Through this resequencing effort, seven of eleven protein-altering variants were newly identified (c. 404 A>T; c. 502 C>T; c. 830 C>A; c. 833 A>-; c. 841 A>G; c. 968 T>C; c. 1063 A>G). Six non-synonymous variants (c. 38T>C; c. 382A>T; c. 404A>T; c. 516 A>C; c. 1063 A>G; c. 2003 C>G) had allele frequencies of ≥ 1% in at least one ethnic group (Table 1). c. 38 T>C (p. Ile13Thr) was found in all populations sampled, except for Asian-Americans, with a particularly high allele frequency, especially in the European-American sample (16.3%). c. 516 A>C was present exclusively in the European- (1.9%) and Mexican-American samples (2%). This variant,

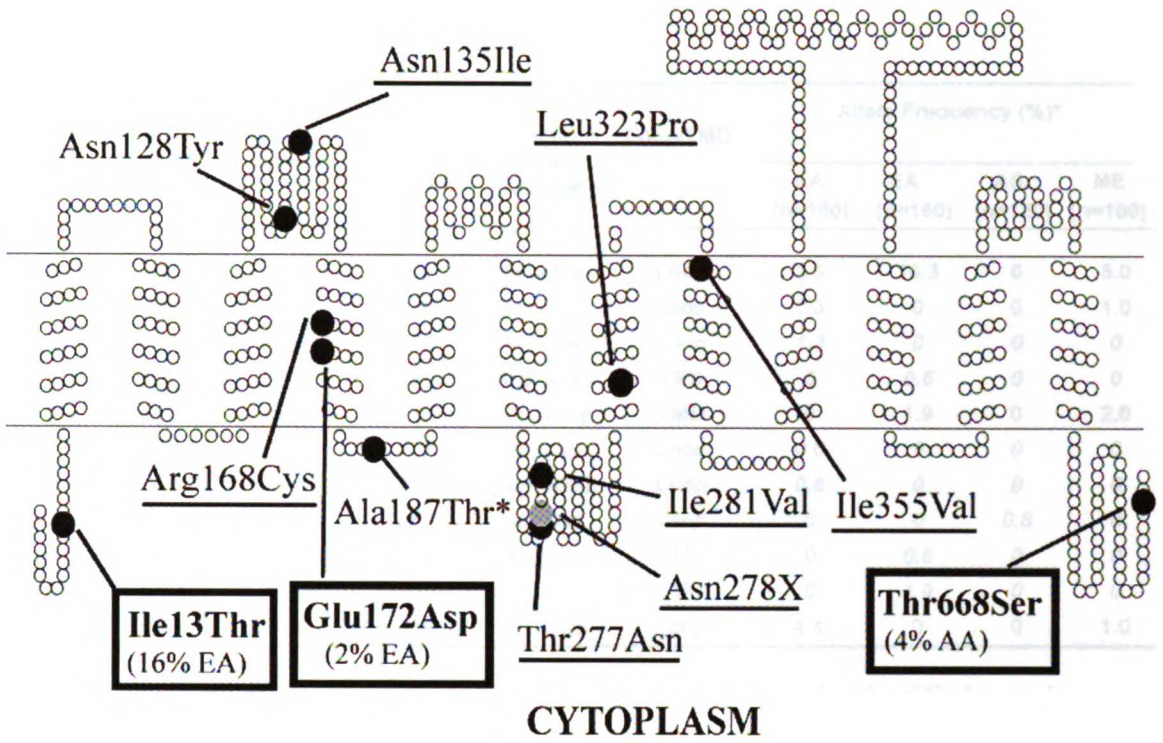

Figure 5. Secondary structure of OATP1A2 showing the location of the 12 protein-altering variants. The transmembrane topology diagram was rendered using TOPO [S. J. Johns (UCSF, San Francisco) and R. C. Speth (Washington State University, Pullman), transmembrane protein display software available at the UCSF Sequence Analysis Consulting Group website, http://www.sacs.ucsf.edu/TOPO/topo.html]. Non-synonymous variants are identified by the black circles, while the deletion variant (Asn278X) is shown in the gray circle. The seven newly identified protein-altering variants are underlined. The asterisk denotes the previously identified variant that was not found in our resequencing project. The three most common non-synonymous variants of OATP1A2, which were kinetically characterized, are shown in bold and boxed.

Table 1. Summary of protein-altering variants in OATP1A2 identified in ethnically diverse populations

SNP #	CDS Position[§]	Nucleotide Change	Amino Acid Position[§]	Amino Acid Change	Loop/TMD[†]	Allele Frequency (%)*			
						AA (n=160)	EA (n=160)	AS (n=120)	ME (n=100)
1.1	**38**	**T→C**	**13**	**Ile→Thr**	**Loop**	**2.5**	**16.3**	**0**	**5.0**
4.1	382	A→T	128	Asn→Tyr	Loop	1.3	0	0	1.0
4.2	*404*	*A→T*	*135*	*Asn→Ile*	*Loop*	*1.3*	*0*	*0*	*0*
5.1	***502***	***C→T***	***168***	***Arg→Cys***	***TMD***	***0***	***0.6***	***0***	***0***
5.2	**516**	**A→C**	**172**	**Glu→Asp**	**TMD**	**0**	**1.9**	**0**	**2.0**
7.3	*830*	*C→A*	*277*	*Thr→Asn*	*Loop*	*0.6*	*0*	*0*	*0*
7.4	***833***	***A→-***	***278***	***Asn→DEL***	***Loop***	***0.6***	***0***	***0***	***0***
7.6	*841*	***A→G***	*281*	*Ile→Val*	*Loop*	*0*	*0*	*0.8*	*0*
8.2	*968*	*T→C*	*323*	*Leu→Pro*	*TMD*	*0*	*0.6*	*0*	*0*
8.3	*1063*	*A→G*	*355*	*Ile→Val*	*TMD*	*0*	*1.9*	*0*	*0*
14.2	2003	C→G	668	Thr→Ser	Loop	4.4	0	0	1.0

Data are available at http://www.pharmgkb.org. The seven newly identified protein-altering variants are shown in italics. The four variants that exhibit a change in transport function compared to reference OATP1A2 are shown in bold.

[§]Positions are relative to the ATG start site and are based on the cDNA sequence from GenBank accession number NM_021094.

[†]Loop/TMD indicates whether a variant is located in a predicted loop or transmembrane domain region.

*Allele frequencies were calculated from actual DNA samples sequenced. AA, African-American; EA, European-American; AS, Asian-American; ME, Mexican-American; n, number of chromosomes

which was found in TMD 4 (Figure 5), has been previously reported to have an allele frequency of 5.3% in European-Americans (15). c. 2003 C>G was found in the African-American population at a high allele frequency (4.4%). Only one protein-altering variant, c. 841A>G, was observed in Asian-Americans. c. 833 A>- (p. Asn278DEL) resulted in the early truncation of the OATP1A2 protein and retained only the first six transmembrane domains. Five of the 11 protein-altering variants, c. 502 C>T, c. 830 C>A, c. 833 A>-, c. 841 A>G, and c. 968 T>C, were singletons, meaning that they were found on only one of 540 chromosomes analyzed. The previously identified singleton variant, c. 559 G>A, was not observed in our genomic DNA samples (15). In our resequencing effort we were able to identify 11 protein-altering variants in OATP1A2, only four of which, c. 38 T>C, c. 382 A> T, c. 516 A>C, and c. 2003 C>G, had been previously identified in a screen of 78 DNA samples from European- and African-American populations (15). Our data indicate that there is significant genetic variation in OATP1A2, with three protein-altering variants, p. Ile13Thr, p. Glu172Asp, and p. Thr668Ser, present at high allele frequencies in populations.

Functional alterations in ES and MTX transport by protein-altering variants in OATP1A2

The 12 protein-altering variants of OATP1A2 were constructed by site-directed mutagenesis using the OATP1A2 reference template and were screened for functional activity with the organic anions, ES and MTX, in *X. laevis* oocytes. In our initial functional screens, four of the 12 protein-altering variants, p. Ile13Thr, p. Arg168Cys, p. Glu172Asp, and Asn278DEL, exhibited significant ($p < 0.01$) altered transport of ES and/or MTX compared to OATP1A2 reference (Figure 6). Interestingly, the common

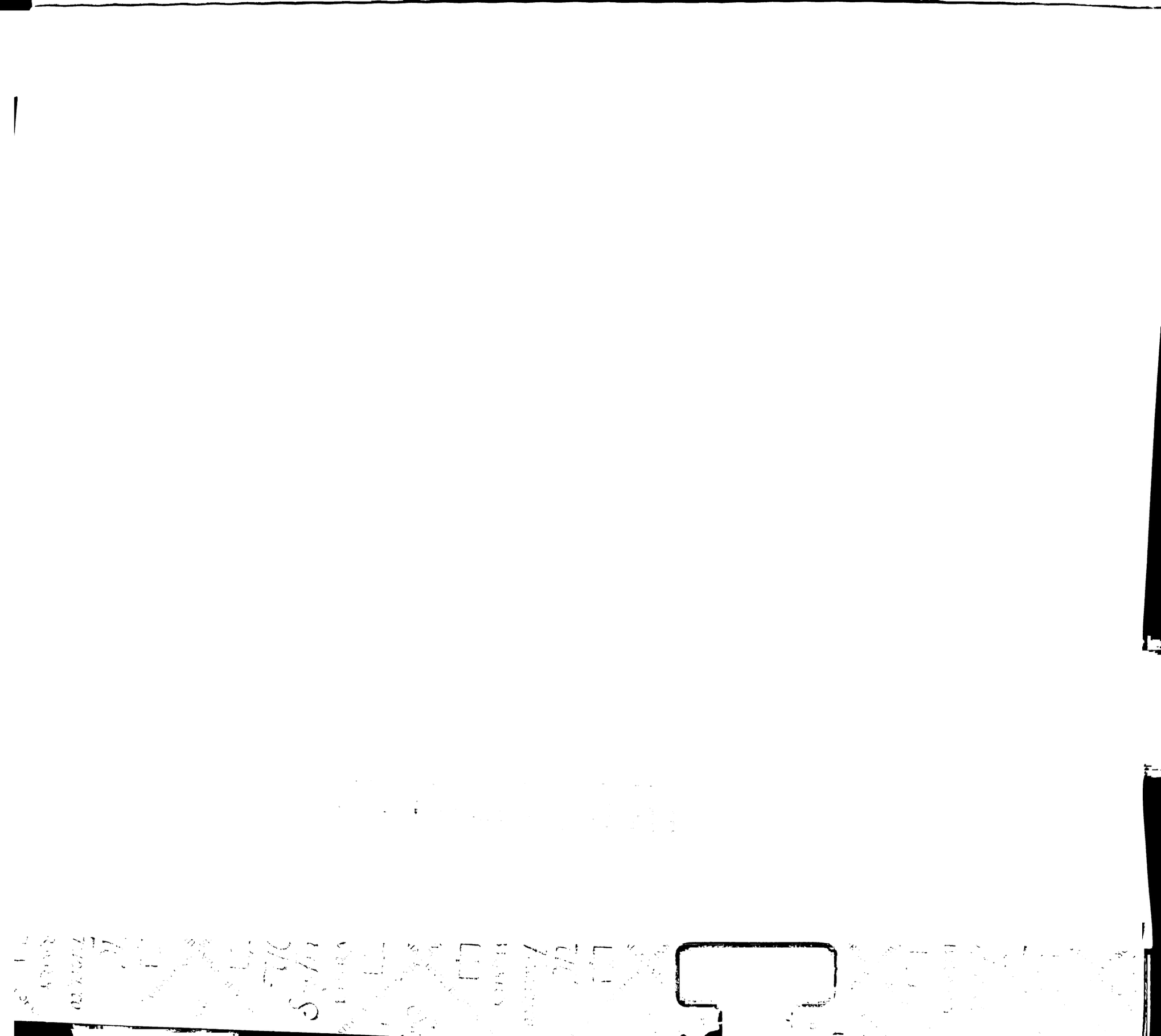

variant p. Ile13Thr, which was previously reported to have a similar function as OATP1A2 reference (15), showed approximately a 2-fold increase (ES = 168 ± 27.9 %; MTX = 174 ± 13.6 %) in the transport of both organic anions compared to OATP1A2 (ES = 100 ± 7.6 %; MTX = 100 ± 5.6 %). The common variant p. Glu172Asp (MTX = 59.1 ± 5.3 %) and the singleton variant p. Arg168Cys (MTX = 60.4 ± 5.3 %) exhibited approximately 40% reduction in the uptake of MTX. The singleton variant p. Asn278DEL, which lacks the last six of 12 transmembrane domains, was non-functional for both organic anions (ES = 4.4 ± 0.2 %; MTX = 24.7 ± 2.8 %). In contrast to a previous report (15), p. Asn135Ile transported ES and MTX similarly to OATP1A2 reference. Following these initial tests for function, the three most common protein-altering variants in OATP1A2, p. Ile13Thr, p. Glu172Asp, and p. Thr668Ser, were expressed in HEK293 cells to further examine their concentration-dependent transport kinetics of ES. As shown in Figure 7 and Table 2, cells expressing p. Ile13Thr exhibited a 2-fold increase ($p < 0.05$) in the V_{max} (258 ± 32.7 pmol/mg of protein/2 min) for ES, while the K_m (13.1 ± 2.5 μM) was not significantly different compared to cells expressing OATP1A2 (V_{max} = 127 ± 20.3 pmol/mg of protein/2 min; K_m = 13.6 ± 3.2 μM). There were no significant differences in the interaction affinity and maximal transport rate of ES between p. Thr668Ser and OATP1A2. Since, p.Glu172Asp was non-functional when expressed in HEK293 (data not shown), the kinetic studies were performed in *X. laevis* oocytes. In RNA dose-response studies, the common protein-altering variant, p. Glu172Asp, showed differences in the maximal transport rate, V_{max}, of ES compared to OATP1A2 (Figure 8). In this approach, oocytes are injected with increasing amounts of reference or variant RNA (10-150 ng). Injecting high doses of RNA allows maximal

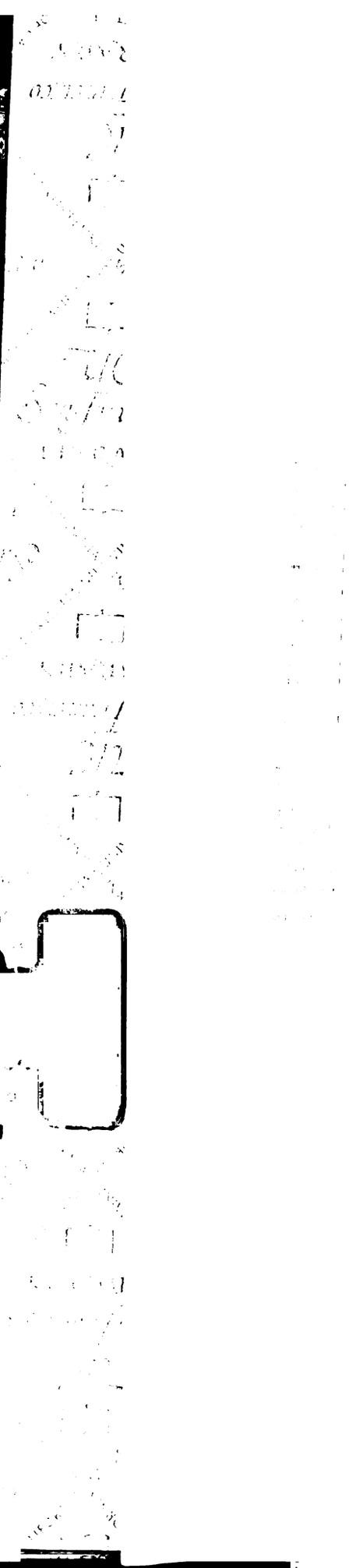

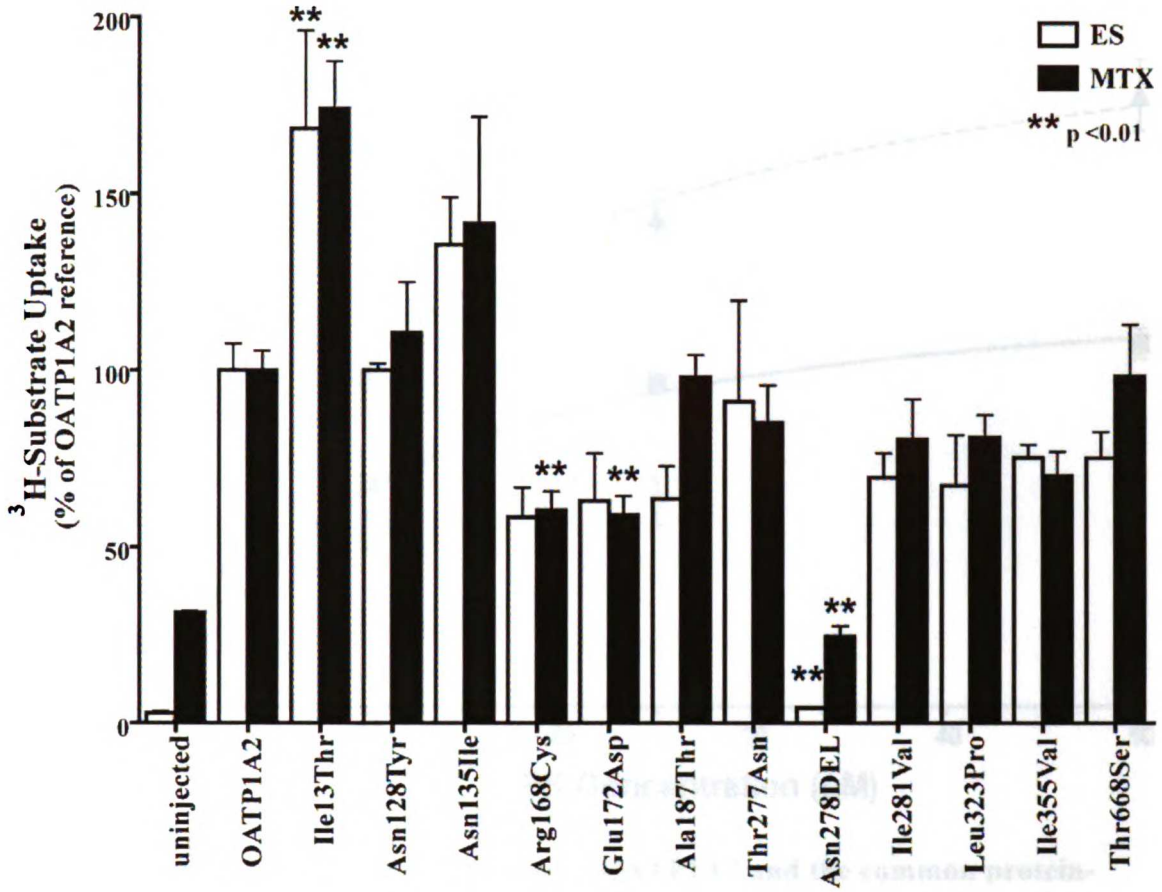

Figure 6. Two common (p. Ile13Thr and p. Glu172Asp) and two rare (p. Arg168Cys and p. Asn278DEL) protein-altering variants of OATP1A2 show altered transport function of ES and/or MTX. Uptake of 20 nM ^{3}H-ES (white bars) or 0.2 μM ^{3}H-MTX (black bars) in oocytes expressing OATP1A2 reference or the 12 protein-altering variants. Transport was measured in Na^+ buffer at pH 7.4 over 60 min. Uptake is expressed as percentage of ES and MTX uptake, respectively, by OATP1A2 injected oocytes at pH 7.4. Data shown are a summary of 3 independent experiments and are expressed as mean ± SE. P values were determined in each of 3 experiments by comparing variant uptake to OATP1A2 reference for each substrate using one-way ANOVA and Tukey's multi-comparison test with $p < 0.05$ as the criterion of significance.

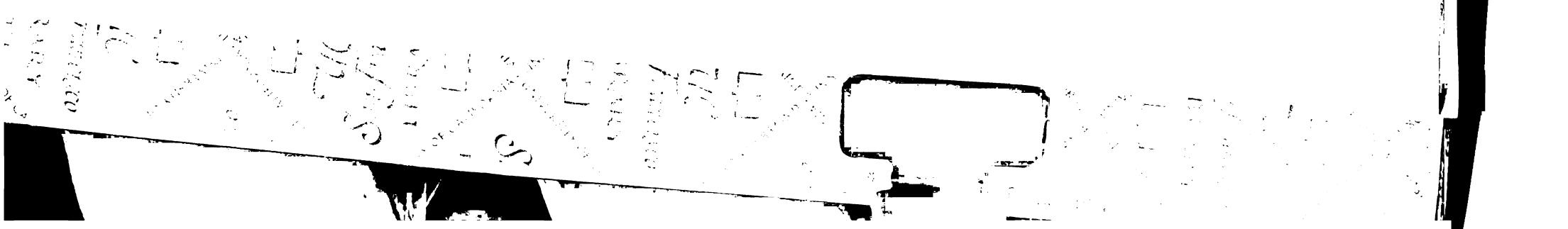

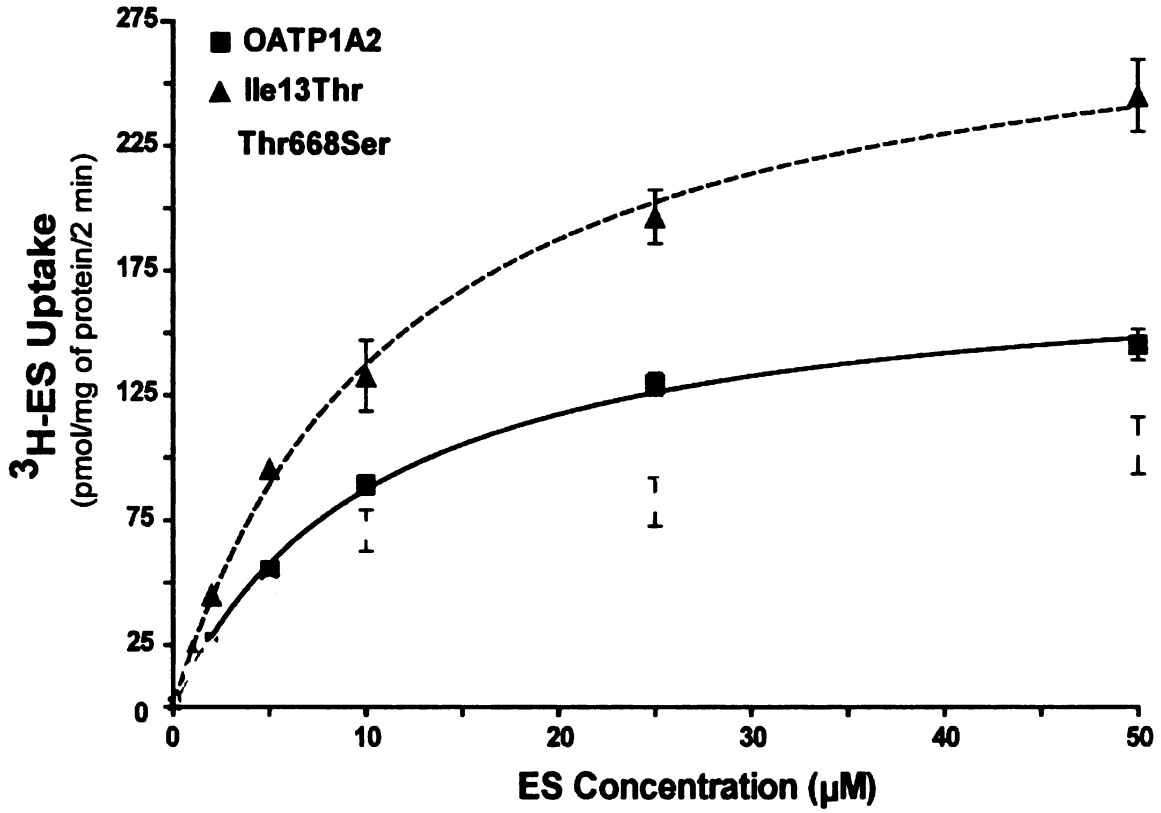

Figure 7. Kinetics of interaction of ES with OATP1A2 and the common protein-altering variants, p. Ile13Thr and p. Thr668Ser. Interaction kinetics of ^{3}H-ES in HEK293 cells transiently transfected with OATP1A2 reference (black square) and the common protein altering variants, p. Ile13Thr (dark gray triangle), and p. Thr668Ser (light gray circle). Uptake of ^{3}H-ES (20 nM) was measured in the presence of various concentrations of unlabeled ES in Na^+ buffer at pH 7.4 over 2 min. Data are representative of 3 independent experiments. Each value represents the mean ± SE from 3 wells. Transport data were fitted using nonlinear regression analysis. P values were determined by comparing kinetic parameters for each variant to OATP1A2 reference using one-way ANOVA and Tukey's multi-comparison test with $p < 0.05$ as the criterion of significance.

Table 2. Summary of interaction kinetics of ES with OATP1A2 and the common protein-altering variants, p. Ile13Thr and p. Thr668Ser

*p<0.05	OATP1A2	Ile13Thr	Thr668Ser
K_m (μM)	13.6 ± 3.2	13.1 ± 2.5	11.2 ± 2.6
V_{max} (pmol/mg of protein/2 min)	127 ± 20.3	**258 ± 32.7***	105 ± 14.4

Uptake of ^{3}H-ES (20 nM) was measured in the presence of various concentrations of unlabeled ES in Na^+ buffer at pH 7.4 over 60 min. Each value represents the mean ± SE from 3 independent experiments. Transport data was fitted using nonlinear regression analysis. Significant differences in the kinetics parameters of the variant proteins compared to OATP1A2 reference are shown in bold. P values were determined by comparing K_m and V_{max} values for each variant to OATP1A2 using one-way ANOVA and Tukey's multi-comparison test with $p < 0.05$ as the criterion of significance.

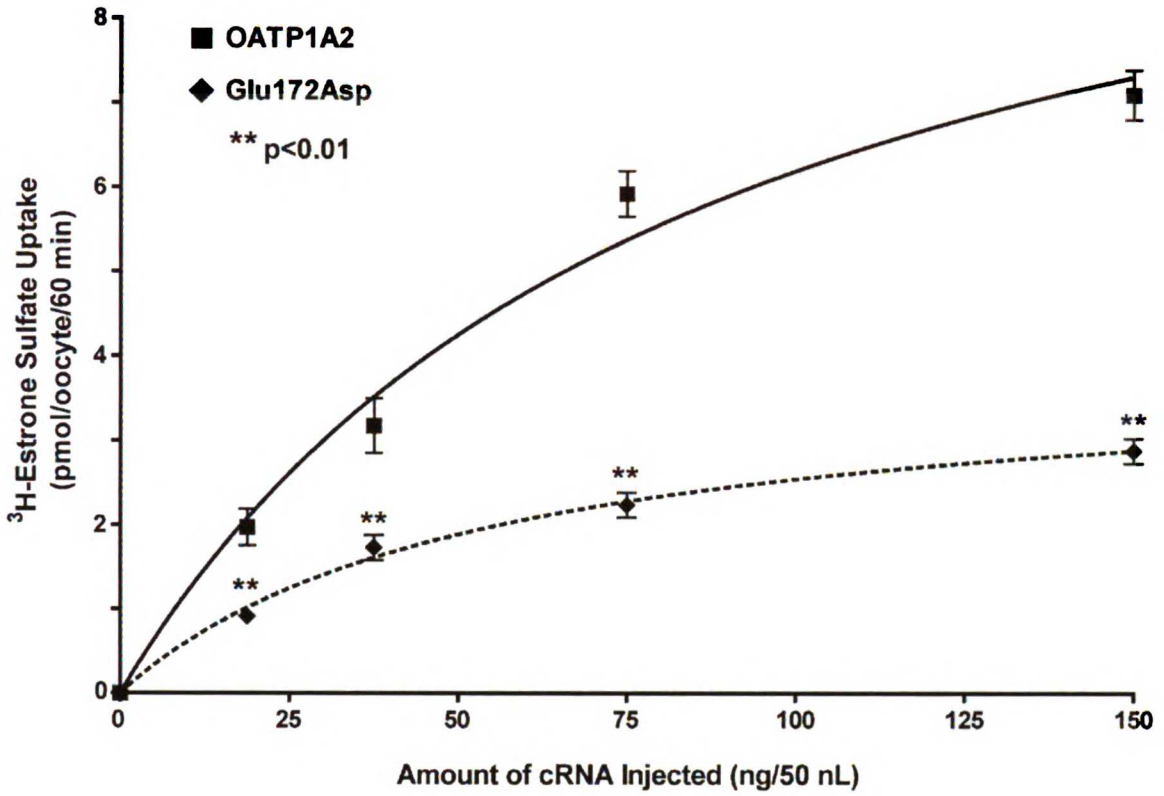

Figure 8. Kinetics of interaction of ES with OATP1A2 and the common protein-altering variant, Glu172Asp. RNA dose-dependent uptake of ES by OATP1A2 reference (square) and the common protein altering variant, p. Glu172Asp (diamond) in *X. laevis* oocytes. Uptake of ^{3}H-ES (20 nM) was measured in oocytes injected with 18.75, 37.5, 75, or 150 ng of reference or variant cRNA. Transport was measured in Na^+ buffer at pH 7.4 over 60 min. Data are representative of 3 independent experiments. Each value represents the mean ± SE from 7-9 oocytes. Transport data were fitted using nonlinear regression analysis. P values were determined by comparing uptake of p. Glu172Asp to that of OATP1A2 at each cRNA concentration using the unpaired Student's *t* test with $p < 0.05$ as the criterion of significance.

expression of the transporter protein and controls for RNA degradation that can occur during injection (22, 23). The RNA dose-response curve for p. Glu172Asp was significantly lower than that of OATP1A2 ($p < 0.01$) and p. Glu172Asp exhibited a 3-fold lower maximal transport capacity for ES (Figure 8). We also observed a similar reduction, approximately 5-7-fold, in the maximal transport capacity of p. Glu172Asp for MTX without any significant changes in the interaction affinity (data not shown). In contrast to many transporters, GFP tagging of OATP1A2 (at either the N or C terminus) produces a non-functional protein and other methods to detect the protein via tagged epitopes using confocal imaging have been unsuccessful (unpublished results in our laboratory). Thus, although differences in V_{max} have been observed between OATP1A2 and the common variants, p. Ile13Thr and p. Glu172Asp, we do not know whether these differences can be explained by changes in cell surface expression. Altogether, these data suggest that OATP1A2 exhibits significant functional variation with respect to ES and MTX.

Discussion

In the present study, we provide a comprehensive characterization of the interaction of MTX with OATP1A2, which is highly expressed in tissues important for MTX disposition and toxicity. Our data demonstrate for the first time that the bicarboxylic organic anion, MTX, and its minor metabolite, 7-OH-MTX, interact with OATP1A2 (Figure 1 and 2). Because OATP1A2 is expressed on the apical surface of distal tubule cells, our studies suggest that OATP1A2 may play a role in the saturable reabsorption of MTX in the distal tubule (2, 15, 24). Concentrations of MTX in the distal

tubule may be 100 times greater than in the plasma; therefore, a K_m of 457 ± 118 μM is consistent with expected biological concentrations in the distal tubule, which could range from 10 μM to 200,000 μM depending on luminal pH (1, 2, 25-27). Thus, OATP1A2 may play a role in controlling the levels of MTX and its minor metabolite in the distal tubule and may be an important determinant of its toxicity secondary to crystalluria (6-8).

Because urine pH may vary, particularly in the distal tubule, we determined the effect of extracellular pH on the interaction of MTX with OATP1A2 and observed that MTX uptake by OATP1A2 is extremely sensitive to extracellular pH (Figure 3). Uptake of MTX is increased by as much as 7-fold at pH 5.0 compared to pH 7.4. The apparent pH sensitivity of OATP1A2 might reflect the ionization state of MTX rather than a specific effect of pH on the carrier. Since MTX has a pK_a of 4.8 and 5.5, the majority of the drug exists as an anion at both pH 7.4 and 5.0. Thus, it is possible that OATP1A2 preferentially transports the monocarboxylic form of MTX resulting in enhanced MTX uptake at acidic pH, where the monocarboxylic form predominates over the bicarboxylic acid form. It is also possible that the acidic extracellular pH may enhance MTX transport by OATP1A2 by affecting the protonation state of amino acid side chains on the extracellular loops and/or extracellular-facing portions of transmembrane domains of OATP1A2. We also observed a pH-dependent transport of ES by OATP1A2, indicating that increased transport at acidic pH is a general property of this transporter (data not shown). Since ES has a pKa of 2 (i.e. predominantly mono-anionic at pH 5.0) and transport of ES by OATP1A2 was enhanced 2-4 fold at pH 5.0, it can be concluded that the pH-dependent transport of organic anions by OATP1A2 is likely dependent, at least in part, on the protonation state of this carrier protein. Irrespective of mechanism, the

finding that MTX transport is enhanced in acidic pHs has important clinical implications in the absorption and disposition of MTX, since the luminal pH of the intestine and kidney, where OATP1A2 is expressed, ranges from 4 to 7 and 4.5 to 8, respectively. Interestingly, another human OATP transporter, OATP2B1, which is highly expressed on the apical domain of enterocytes, has been recently shown to be sensitive to extracellular pH, but unlike OATP1A2, its pH-dependent transport relies on the proton gradient (28, 29).

Interindividual diversity in MTX efficacy and toxicity is a well-recognized obstacle in the successful clinical management of patients with malignant and autoimmune diseases. Significant genetic and functional variation in drug uptake transporters exists and may contribute to variation in MTX disposition and toxicity (20, 21, 30-35). In the present study we characterized the interaction of MTX with genetic variants in OATP1A2. The extent of genetic variation in OATP1A2 appears consistent with other drug uptake transporters, such as OAT3, OCT1, and OCT2 (21, 31, 32, 35). In comparison to the study of Lee *et al.*, we identified a greater number of variants in OATP1A2 including a number of novel variants, two of which, c. 404 A>T and c. 1063 A>G, had allele frequencies of 1.3 % and 1.9 % in the African- and European-American samples, respectively (Figure 5 and Table 1). In addition, we found that the allele frequency of c. 516 A>C was 1.9% in European-Americans, compared to 5.3% as previously reported (15). The reason for discrepancies between our study and that of Lee *et al.* may be due to differences in sample sets and methods used in screening. Lee *et al.* used single strand conformational polymorphism analysis to initially screen DNA samples from 46 European- and 32 African-Americans for variants in OATP1A2 (15).

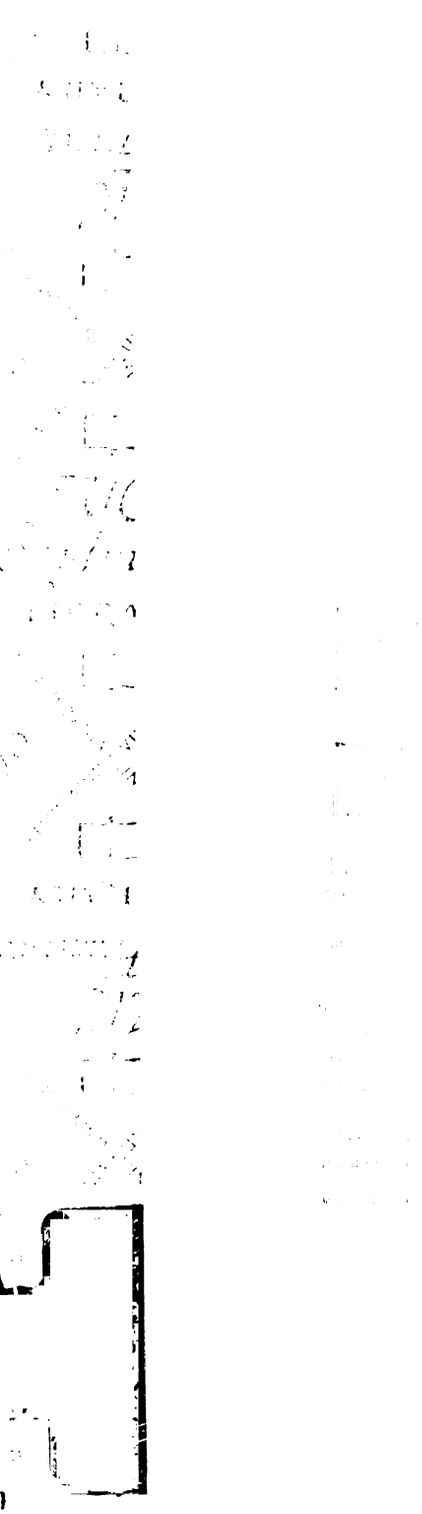

Additional DNA samples (n = 302) appeared to be used for estimation of allele frequencies. In contrast, we screened all 270 DNA samples from four ethnic groups by automated direct sequencing analysis. By initially screening a larger sample set in a greater number of ethnic populations, we discovered a greater number of variants.

Functional studies with the twelve protein-altering variants of OATP1A2 showed that four of these variants, p. Ile13Thr, p. Arg168Cys, p. Glu172Asp, and p. Asn278DEL, exhibited altered transport of ES and/or MTX (Figure 6). p. Arg168Cys was hypofunctional, while p. Asn278DEL was non-functional. Interestingly, we determined that p. Ile13Thr, which is found at allele frequencies of 16% in European-Americans, exhibited 2-fold higher transport of both ES and MTX (Figure 6). It was determined in kinetic studies that the increased transport of ES by p. Ile13Thr was due to a 2-fold greater transport capacity (*i.e.* V_{max}) with no significant effect on the interaction affinity (*i.e.* K_m) (Figure 7 and Table 2). Based on these findings, we can speculate that *in vivo* p. Ile13Thr could result in increased reabsorption of MTX from the distal tubule leading to increased exposure to MTX and subsequent systemic toxicity. However, p. Ile13Thr had been previously reported by Lee *et al.* to transport ES similarly to OATP1A2 (15). The difference between our results and that of Lee *et al.* may be explained by differences in experimental conditions. Lee *et al.* used HeLa cells infected with vaccinia, whereas we used oocytes. In the study of Lee *et al.*, ES uptake was enhanced approximately 3-fold at 30 min, a time at which ES uptake was no longer linear; therefore, differences in ES uptake between reference and variant OATP1A2 transporters may not have been detected. It is also possible that expression in oocytes may produce differences in transport of both ES and MTX between p.Ile13Thr and reference OATP1A2. To

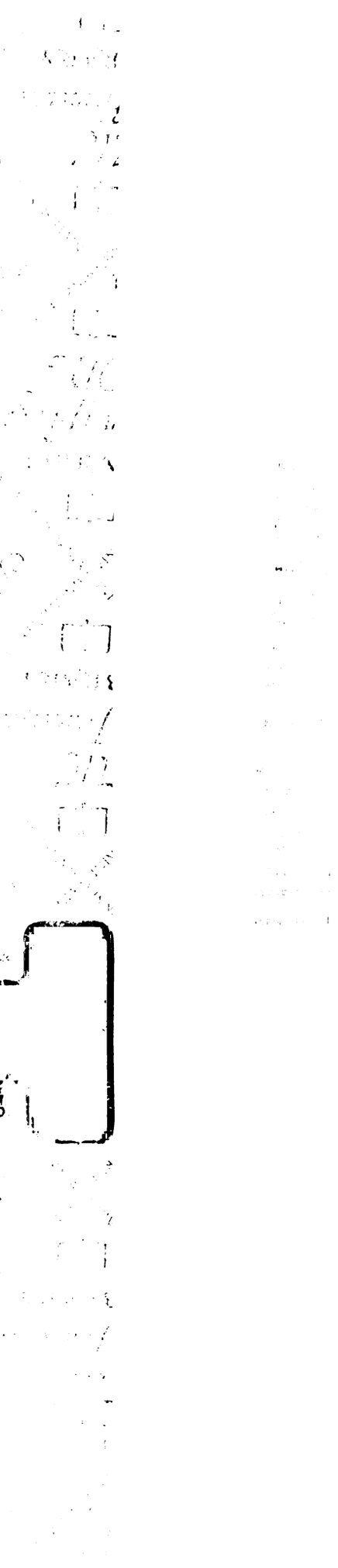

determine whether this was an artifact of the oocyte expression system, we expressed the transporter in mammalian cells and, similarly, obtained a 1.5-2-fold greater uptake and maximal transport capacity of ES by p. Ile13Thr compared to OATP1A2. These data suggest that our results demonstrating a greater uptake of ES by p. Ile13Thr are consistent between mammalian and amphibian expression systems.

p. Glu172Asp, which has an allele frequency of 1.9 % in European-Americans, exhibited 40% reduced uptake of MTX (Figure 6). We determined that the mechanism for the altered transport function of this variant was ascribed to a decrease in the maximal transport rate for both ES and MTX of 3-fold and 5-fold, respectively, compared to OATP1A2 (Figure 8). Based on these findings, we can speculate that *in vivo* p. Glu172Asp could result in lower reabsorption of MTX and higher MTX accumulation in the lumen of the distal tubule leading to crystalluria and subsequent nephrotoxicity. Our data are consistent with the study of Lee *et al.* in which p. Glu172Asp was shown to have significant loss of cell surface expression compared to OATP1A2 (15). Altogether, the genetic and functional analyses of OATP1A2 presented in this study indicate that genetic variation in OATP1A2 may play an important role in MTX disposition and toxicity.

In summary, our studies suggest that protein-altering variants in OATP1A2 may play an important role in inter-individual variation in drug disposition and toxicity. Since MTX therapy can result in severe toxicity in the kidney, liver, gastrointestinal tract, and brain, where OATP1A2 is expressed (1, 12), clinical studies of genetic variants in OATP1A2 are important to determine their significance to MTX therapy.

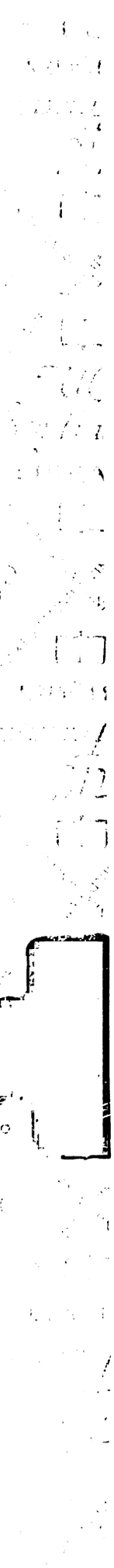

References

1. Goodman LS, Hardman JG, Limbird LE, Gilman AG. Goodman & Gilman's the pharmacological basis of therapeutics. 10th / ed. New York: McGraw-Hill Medical Pub. Division; 2001.

2. Hendel J, Nyfors A. Nonlinear renal elimination kinetics of methotrexate due to saturation of renal tubular reabsorption. Eur J Clin Pharmacol 1984; **26**: 121-4.

3. Shen DD, Azarnoff DL. Clinical pharmacokinetics of methotrexate. Clin Pharmacokinet 1978; **3**: 1-13.

4. Bourke RS, Chheda G, Bremer A, Watanabe O, Tower DB. Inhibition of renal tubular transport of methotrexate by probenecid. Cancer Res 1975; **35**: 110-6.

5. Huang KC, Wenczak BA, Liu YK. Renal tubular transport of methotrexate in the rhesus monkey and dog. Cancer Res 1979; **39**: 4843-8.

6. Perazella MA. Crystal-induced acute renal failure. Am J Med 1999; **106**: 459-65.

7. Perazella MA. Drug-induced renal failure: update on new medications and unique mechanisms of nephrotoxicity. Am J Med Sci 2003; **325**: 349-62.

8. el-Badawi MG, Abdalla MA, Bahakim HM, Fadel RA. Nephrotoxicity of low-dose methotrexate in guinea pigs: an ultrastructural study. Nephron 1996; **73**: 462-6.

9. Koepsell H, Endou H. The SLC22 drug transporter family. Pflugers Arch 2004; **447**: 666-76.

10. Ganapathy V, Smith SB, Prasad PD. SLC19: the folate/thiamine transporter family. Pflugers Arch 2004; **447**: 641-6.

11. Hooijberg JH, Peters GJ, Assaraf YG, Kathmann I, Priest DG, Bunni MA, et al. The role of multidrug resistance proteins MRP1, MRP2 and MRP3 in cellular folate homeostasis. Biochem Pharmacol 2003; **65**: 765-71.

12. Hagenbuch B, Meier PJ. Organic anion transporting polypeptides of the OATP/ SLC21 family: phylogenetic classification as OATP/ SLCO superfamily, new nomenclature and molecular/functional properties. Pflugers Arch 2004; **447**: 653-65.

13. Kullak-Ublick GA, Ismair MG, Stieger B, Landmann L, Huber R, Pizzagalli F, et al. Organic anion-transporting polypeptide B (OATP-B) and its functional comparison with three other OATPs of human liver. Gastroenterology 2001; **120**: 525-33.

14. Kullak-Ublick GA, Hagenbuch B, Stieger B, Schteingart CD, Hofmann AF, Wolkoff AW, et al. Molecular and functional characterization of an organic anion transporting polypeptide cloned from human liver. Gastroenterology 1995; **109**: 1274-82.

15. Lee W, Glaeser H, Smith LH, Roberts RL, Moeckel GW, Gervasini G, et al. Polymorphisms in human organic anion-transporting polypeptide 1A2 (OATP1A2): implications for altered drug disposition and central nervous system drug entry. J Biol Chem 2005; **280**: 9610-7.

16. Su Y, Zhang X, Sinko PJ. Human organic anion-transporting polypeptide OATP-A (SLC21A3) acts in concert with P-glycoprotein and multidrug resistance protein 2 in the vectorial transport of Saquinavir in Hep G2 cells. Mol Pharm 2004; **1**: 49-56.

17. Gao B, Hagenbuch B, Kullak-Ublick GA, Benke D, Aguzzi A, Meier PJ. Organic anion-transporting polypeptides mediate transport of opioid peptides across blood-brain barrier. J Pharmacol Exp Ther 2000; **294**: 73-9.

18. Konig J, Hartel M, Nies AT, Martignoni ME, Guo J, Buchler MW, et al. Expression and localization of human multidrug resistance protein (ABCC) family members in pancreatic carcinoma. Int J Cancer 2005; **115**: 359-67.

19. Giacomini KM, Markovich D, Werner A, Biber J, Wu X, Murer H. Expression of a renal Na(+)-nucleoside cotransport system (N2) in Xenopus laevis oocytes. Pflugers Arch 1994; **427**: 381-3.

20. Badagnani I, Chan W, Castro RA, Brett CM, Huang CC, Stryke D, et al. Functional analysis of genetic variants in the human concentrative nucleoside transporter 3 (CNT3; SLC28A3). Pharmacogenomics J 2005; **5**: 157-65.

21. Erdman AR, Mangravite LM, Urban TJ, Lagpacan LL, Castro RA, de la Cruz M, et al. The human organic anion transporter 3 (OAT3; SLC22A8): genetic variation and functional genomics. Am J Physiol Renal Physiol 2006; **290**: F905-12.

22. Werner A, Biber J, Forgo J, Palacin M, Murer H. Expression of renal transport systems for inorganic phosphate and sulfate in Xenopus laevis oocytes. J Biol Chem 1990; **265**: 12331-6.

23. Due AD, Qu ZC, Thomas JM, Buchs A, Powers AC, May JM. Role of the C-terminal tail of the GLUT1 glucose transporter in its expression and function in Xenopus laevis oocytes. Biochemistry 1995; **34**: 5462-71.

24. Liegler DG, Henderson ES, Hahn MA, Oliverio VT. The effect of organic acids on renal clearance of methotrexate in man. Clin Pharmacol Ther 1969; **10**: 849-57.

25. Chladek J, Grim J, Martinkova J, Simkova M, Vaniekova J, Koudelkova V, et al. Pharmacokinetics and pharmacodynamics of low-dose methotrexate in the treatment of psoriasis. Br J Clin Pharmacol 2002; **54**: 147-56.

26. Christophidis N, Louis WJ, Lucas I, Moon W, Vajda FJ. Renal clearance of methotrexate in man during high-dose oral and intravenous infusion therapy. Cancer Chemother Pharmacol 1981; **6**: 59-64.

27. Ferrazzini G, Sohl H, Robieux I, Johnson D, Giesbrecht E, Koren G. Diurnal variation of methotrexate disposition in children with acute leukaemia. Eur J Clin Pharmacol 1991; **41**: 425-7.

28. Kobayashi D, Nozawa T, Imai K, Nezu J, Tsuji A, Tamai I. Involvement of human organic anion transporting polypeptide OATP-B (SLC21A9) in pH-dependent transport across intestinal apical membrane. J Pharmacol Exp Ther 2003; **306**: 703-8.

29. Nozawa T, Imai K, Nezu J, Tsuji A, Tamai I. Functional characterization of pH-sensitive organic anion transporting polypeptide OATP-B in human. J Pharmacol Exp Ther 2004; **308**: 438-45.

30. Tirona RG, Leake BF, Merino G, Kim RB. Polymorphisms in OATP-C: identification of multiple allelic variants associated with altered transport activity among European- and African-Americans. J Biol Chem 2001; **276**: 35669-75.

31. Shu Y, Leabman MK, Feng B, Mangravite LM, Huang CC, Stryke D, et al. Evolutionary conservation predicts function of variants of the human organic cation transporter, OCT1. Proc Natl Acad Sci U S A 2003; **100**: 5902-7.

32. Leabman MK, Huang CC, Kawamoto M, Johns SJ, Stryke D, Ferrin TE, et al. Polymorphisms in a human kidney xenobiotic transporter, OCT2, exhibit altered function. Pharmacogenetics 2002; **12**: 395-405.

33. Owen RP, Gray JH, Taylor TR, Carlson EJ, Huang CC, Kawamoto M, et al. Genetic analysis and functional characterization of polymorphisms in the human concentrative nucleoside transporter, CNT2. Pharmacogenet Genomics 2005; **15**: 83-90.

34. Gray JH, Mangravite LM, Owen RP, Urban TJ, Chan W, Carlson EJ, et al. Functional and genetic diversity in the concentrative nucleoside transporter, CNT1, in human populations. Mol Pharmacol 2004; **65**: 512-9.

35. Erdman AR, Mangravite LM, Urban TJ, Lagpacan LL, Castro RA, de la Cruz M, et al. The human organic anion transporter 3 (OAT3; SLC22A8): genetic variation and functional genomics. Am J Physiol Renal Physiol 2005.

CHAPTER 4

INTERACTION OF METHOTREXATE WITH OAT3 (*SLC22A8*) AND ITS GENETIC VARIANTS

Introduction

The antiproliferative folate antagonist methotrexate (MTX) has been widely used at high doses in the treatment of a variety of malignancies and at low doses in the treatment of several chronic inflammatory disorders. Despite being highly efficacious, methotrexate therapy can result in serious complications, including renal dysfunction, neurotoxicity, myelosuppression, and mucositis (1). It has been determined that 50-90% of each MTX dose is excreted unchanged in the urine and net renal elimination occurs via active secretory and reabsorptive processes (2-5). MTX and its minor metabolite, 7-hydroxymethotrexate (7-OH-MTX) are poorly soluble and have been shown to precipitate in the lumen of distal tubules resulting in nephrotoxicity and delayed elimination (6-10). Accumulation of MTX in blood due to renal dysfunction and delayed clearance can then lead to severe multi-organ toxicity.

Xenobiotic membrane transporters are important determinants of systemic blood levels and tissue specific levels of drugs, such as MTX, thereby affecting their efficacy and toxicity. An important uptake transport system in humans is the *SLC22* transporter family, whose members interact with a broad variety of organic solutes and xenobiotics (11). In particular, the organic anion transporter family (OAT; *SLC22A6-8* and *SLC22A10-11*) has been shown to be a critical determinant of MTX renal tubular secretion and elimination (4, 5, 12). Furthermore, it was determined that blocking OAT

transport function using probenecid led to a significant increase in the half-life, exposure, and plasma concentrations of MTX, which are associated with MTX-induced toxicity (4, 13). Of all the human OAT transporters that have been identified and characterized, OAT3 (SLC22A8) is the most abundant in the kidney where it is located on the basolateral surface of renal proximal tubules (11, 14). This transporter is responsible for the cellular uptake of a structurally diverse set of endogenous organic anions and commonly used drugs, including MTX (11, 15-18). Recently, Erdman *et al.* identified naturally occurring variants in human OAT3 and determined that these variants exhibit significant functional differences with respect to the model substrates estrone sulfate (ES) and cimetidine (19).

Given that OAT3 plays an important role in the renal tubular secretion of MTX, we undertook a comprehensive genetic and functional analysis of OAT3 in ethnically diverse populations to gain useful insights about the genetic factors that influence inter-individual variability in MTX disposition, elimination, and toxicity.

Material and Methods

Materials

^{3}H-ES (57.3 Ci/mmol) and ^{3}H-MTX (49.6 Ci/mmol) were purchased from PerkinElmer Life Sciences (Wellesley, MA) and Moravek (Brea, CA), respectively. All unlabeled chemicals were obtained from Sigma (St. Louis, MO), except for 7-hydroxymethotrexate (7-OH-MTX), which was purchased from Schircks Laboratories (Jona, Switzerland). Human embryonic kidney cells (Flp-In™-HEK293) and the mammalian expression vector, pcDNA5/FRT were from Invitrogen (Carlsbad, CA).

Transport of folates and folate antagonists by OAT3

The original human *SLC22A8* (GenBank accession number NM_004254) was obtained by homology cloning and subcloned into the mammalian expression vector pcDNA5/FRT as previously described (19). HEK293 were propagated according to the manufacturer's instructions. They were grown at 37°C and 5% CO_2 in Dulbecco's Modified Eagle's media (DME H-21; UCSF Cell Culture Facility, San Francisco, CA) containing 10% fetal bovine serum (UCSF Cell Culture Facility), 100 μg/mL streptomycin (UCSF Cell Culture Facility), 100 units/mL penicillin G (UCSF Cell Culture Facility), and 100 μg/mL Zeocin™ (Invitrogen). Cells were seeded at 3 x 10^5 cells/well on Biocoat® poly-d-lysine-coated 24-well plates (Becton Dickenson, Bedford, MA) 24 hr before transfection. Cells were transfected with 1 μg/well of pcDNA5/FRT (empty vector) or OAT3-pcDNA5/FRT (OAT3) and 3 μL of the lipid vehicle, Lipofectamine™ 2000 (Invitrogen). Incubation with the transfection mixture was carried out overnight, which was then replaced with fresh media. Uptake studies were performed 48 hr after transfection by pre-incubating transfected cells in 5 mM glutaric acid in PBS (UCSF Cell Culture Facility) for 30 min at 37°C. This solution was then replaced with Na^+ buffer (128 mM NaCl, 4.73 mM KCl, 1.25 mM $CaCl_2$, 1.25 mM $MgSO_4$, and 5 mM Hepes or Tris, in H_2O, pH 7.4) and cells were incubated for an additional 5 min. The solution was then removed and cells were incubated for 3 min at 37°C in Na^+ buffer containing 20 nM ^{3}H-ES in the absence or presence of folate, leucovorin, or the folate antagonists, MTX and 7-OH-MTX at a final concentration of 1 or 2 mM. Uptake was terminated by washing wells three times with ice-cold Na^+ free buffer in which Na^+ was replaced by choline chloride. The cells were then lysed using 0.1 N NaOH/0.1% sodium

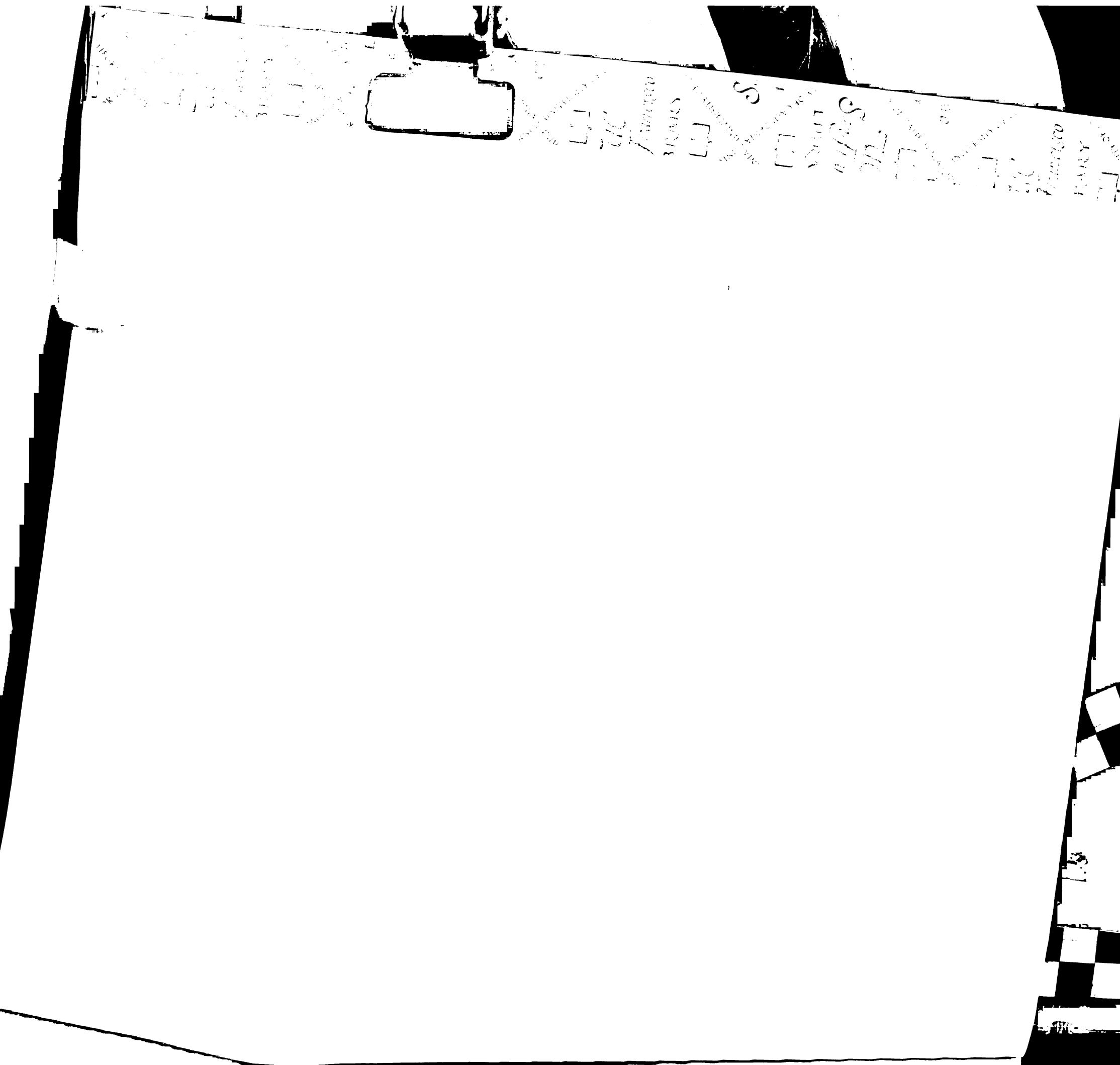

dodecyl sulfate (SDS) and incubating for at least 2 hr on an agitating platform. Radioactivity in an aliquot of the resultant mixture was then measured using a scintillation counter. Normalization for protein content was performed to correct for differences in cell number from well to well. A spectrophotometric plate reader and the BCA™ Protein Assay Kit (Pierce, Rockford IL) were used to assess protein concentrations. The inhibition data shown are representative of 2 independent experiments. P values were determined by comparing ES uptake in the presence of inhibitors to OAT3-mediated ES uptake in the absence of inhibitors using one-way ANOVA and Tukey's multi-comparison test with $p < 0.05$ as the criterion of significance.

Saturation kinetics of ^{3}H-MTX

HEK293 transiently transfected with empty vector or OAT3 were pre-incubated in 5 mM glutaric acid for 30 min at 37°C. This solution was then replaced with Na^+ buffer and cells were incubated for an additional 5 min. The solution was removed and cells were exposed for 3 min at 37°C in Na^+ buffer containing 20 nM ^{3}H-MTX in the presence of various concentrations of unlabeled MTX. The curve of MTX uptake by OAT3 was obtained by fitting the data to a Michaelis-Menten curve by non-linear regression, using GraphPad Prism 4 Software. A summary of the kinetic parameters of MTX transport by OAT3 is shown as mean ± SE from a representative experiment.

Genetic analysis of *SLC22A8*

Genetic variants in *SLC22A8* were previously identified by Erdman *et al.* (19). The neutral parameter (θ), nucleotide diversity (π), and Tajima's D statistic were determined using the methods described by Tajima (20). Each parameter was calculated

for non-coding and coding sites within *SLC22A8* (e.g. synonymous and non-synonymous sites) for the entire population and for each ethnic group. The definition of synonymous and non-synonymous sites was adapted from Hartl and Clark (21). Haplotypes were inferred from variant sites using the Bayesian statistical method of PHASE (22). Before PHASE analysis, all singleton samples were removed and only haplotypes found in at least 7 of 10 PHASE runs were reported.

Functional analysis of variants in *SLC22A8* in HEK293 cells

The sequence of OAT3 reference corresponds to the OAT3 coding sequence that occurred at the highest frequency in all ethnic groups. Each of the 10 non-synonymous OAT3 variants was constructed by site-directed mutagenesis of the OAT3 reference using the QuickChange mutagenesis protocol (Stratagene, La Jolla, CA, USA), as previously described (19). HEK293 cells transiently transfected with OAT3 or each of the non-synonymous variants in OAT3 were pre-incubated in 5 mM glutaric acid for 30 min at 37°C. This solution was then replaced with Na^+ buffer and cells were incubated for an additional 5 min. This solution was removed and cells were exposed for 3 min at 37°C in Na^+ buffer containing 20 nM ^{3}H-ES or 20 nM ^{3}H-MTX.The data are presented as percentage of ES or MTX uptake by OAT3 reference. Each value is expressed as mean ± SE for 3 wells from a representative experiment out of 3 independent experiments. P values were determined by comparing variant uptake to OAT3 reference for each substrate using one-way ANOVA and Tukey's multi-comparison test with $p < 0.05$ as the criterion of significance. Kinetic studies of MTX interaction with OAT3 and the 3 common protein-altering variants, p. Val281Ala, p. Ile305Phe, and p. Val448Ile, were performed in transiently transfected HEK293 cells. Cells transiently transfected with

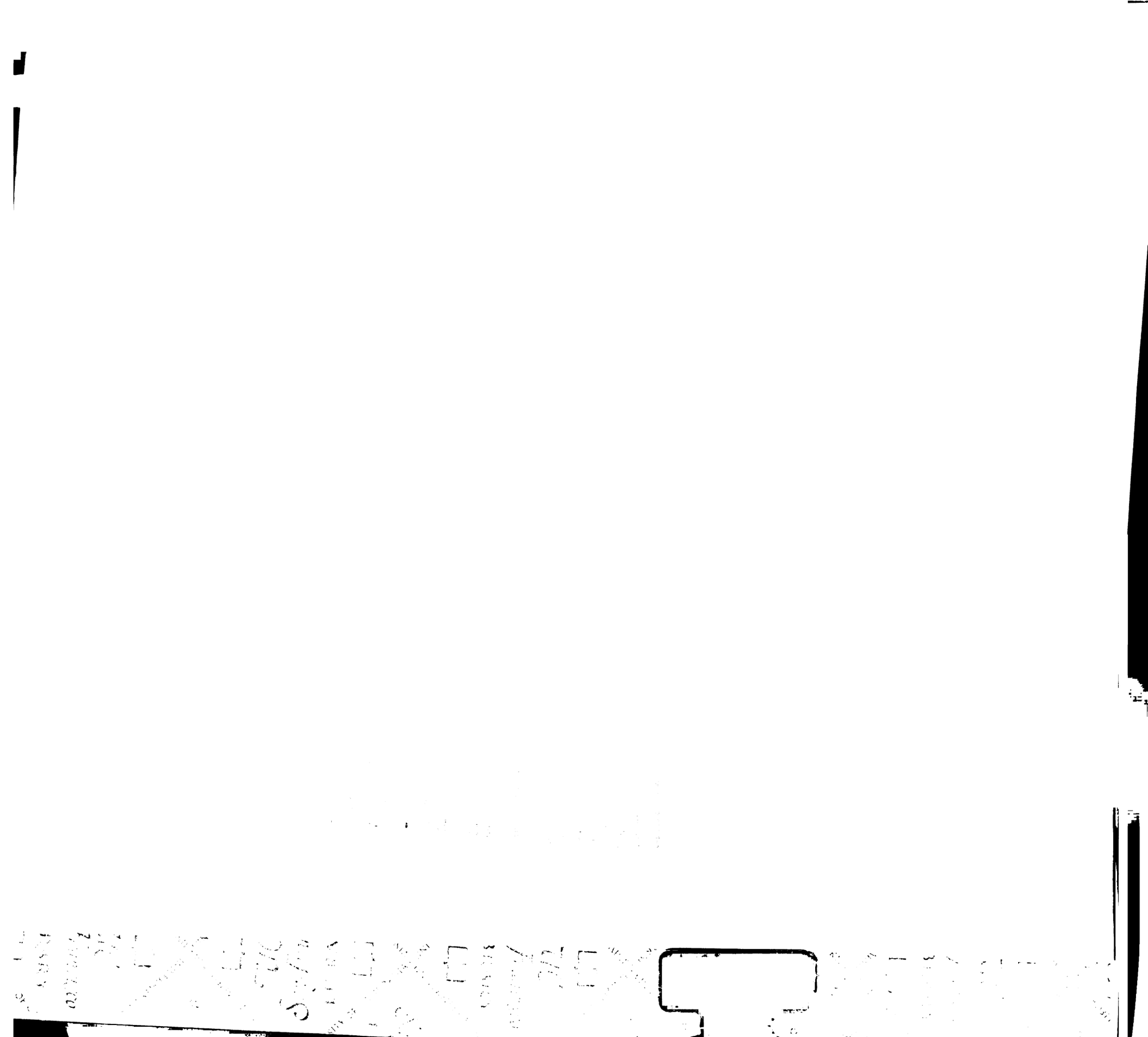

empty vector, OAT3, or each of the 3 common OAT3 protein-altering variants were pre-incubated in 5 mM glutaric acid for 30 min at 37°C. This solution was then replaced with Na^+ buffer and cells were incubated for an additional 5 min. This solution was removed and cells were exposed for 3 min at 37°C in Na^+ buffer containing 20 nM ^{3}H-MTX in the presence of various concentrations of unlabeled MTX. The kinetic curves were generated by fitting the data to a Michaelis-Menten curve fit, using GraphPad Prism 4 Software. A summary of the kinetic parameters of MTX uptake by OAT3 reference and variants is given as mean ± SE from three independent experiments. P values were determined by comparing K_m and V_{max} values for each variant to OAT3 using one-way ANOVA and Tukey's multi-comparison test with $p < 0.05$ as the criterion of significance.

Results

Interaction of folates and folate antagonists with OAT3

Folic acid and reduced folates are essential cofactors for the synthesis of nucleotides during DNA synthesis in dividing cells. This requirement has been successfully exploited in cancer therapy by the development of folic acid analogs, such as MTX, as chemotherapy agents. Since folates and folate antagonists undergo active tubular secretion in the kidney, their interaction with OAT3 was examined in transiently transfected HEK293 cells. As shown in Figure 1, both MTX and 7-OH-MTX strongly inhibited ES transport by approximately 90%. On the other hand, folate and leucovorin, which is a reduced folate drug that rescues normal cells from the cytotoxic effects of MTX, only weakly inhibited ES uptake even at concentrations of 2 mM, despite being structurally similar to MTX. Further characterization of MTX transport revealed that its

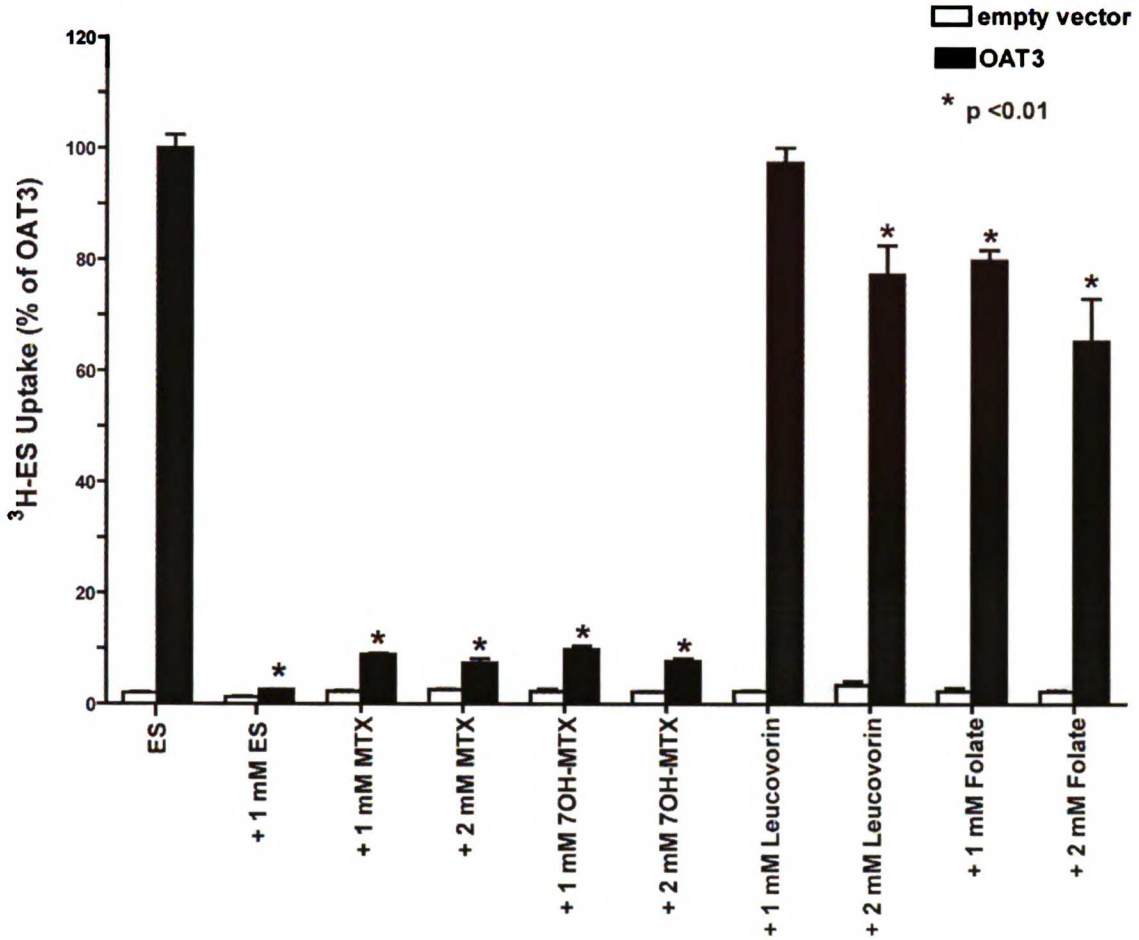

Figure 1. Folates and folate antagonists inhibit OAT3. Inhibition of ES uptake by folates (leucovorin and folate) and folate antagonists (MTX and 7-OH-MTX) in HEK293 cells transiently transfected with empty vector (white bars) or OAT3 (black bars). Cells were incubated for 3 min with ^{3}H-ES (20 nM) in the absence or presence of various concentrations of unlabeled compounds. Uptake is expressed as percentage of ES uptake by OAT3. Each value represents the mean ± SE from 3 wells in a representative experiment of 2 independent experiments. P values were determined by comparing ES uptake in the presence of inhibitors to OAT3-mediated ES uptake in the absence of inhibitors using one-way ANOVA and Tukey's multi-comparison test with $p < 0.05$ as the criterion of significance.

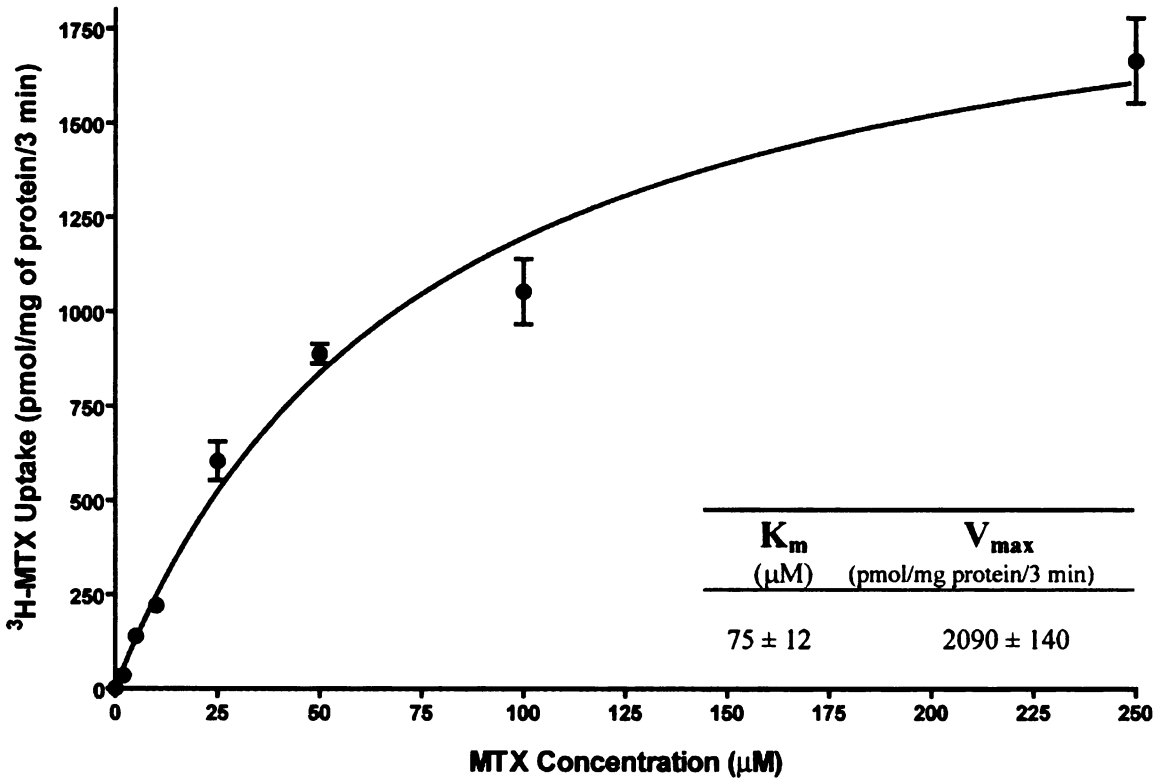

Figure 2. Transport kinetics of MTX in HEK293 cells expressing OAT3. Uptake of ^{3}H-MTX (20 nM) was measured in the presence of various concentrations of unlabeled ES in Na^+ buffer over 3 min. Each value represents the mean ± SE from 3 wells in a representative experiment. Transport data were fitted using nonlinear regression analysis.

initial rate of uptake by OAT3 was saturable (Figure 2), with a mean K_m of 75 ± 12 μM and V_{max} of 2090 ± 140 pmol/mg of protein/3 min.

Analysis of genetic variation in *SLC22A8*

Variants in *SLC22A8* were identified by direct automated sequencing of all ten *SLC22A8* exons and 50-200 bp of flanking intronic sequences by Erdman *et al.* (19) as part of a large-scale project with the goal of examining the effects of natural variation in membrane transporter genes in drug efficacy and toxicity. The variant data from 270 ethnically diverse and healthy individuals are deposited in the Pharmacogenetics and Pharmacogenomics Knowledge Base at http://www.pharmgkb.org. A total of 26 single nucleotide polymorphisms (SNPs) were found in the 3706 bp sequenced, resulting in a frequency of approximately seven SNPs per kb. This is in line with the average frequency of SNPs/kb obtained in the analysis of 24 membrane transporter genes (23). Eleven SNPs were found in the non-coding intronic regions of SLC22A8. Of the remaining 15 variable sites, ten altered the protein sequence and five were synonymous (Table 1). Three of the five synonymous variants had an allele frequency of 4% or higher in at least one ethnic group. Of the ten non-synonymous variants, 3 (p. Val281Ala, p. Ile305Phe, and p. Val448Ile) were polymorphic, occurring at a frequency of ≥ 1% in an ethnic group, and six (p. Phe129Leu, p. Gln239DEL, p. Ile260Arg, p. Arg277Trp, p. Ala310Val, and p. Ala399Ser) were singletons, meaning that they were found only once in 540 chromosomes. Six of the protein-altering variants were population specific: p. Arg277Trp and p. Val281Ala were found in African-Americans; p. Ala310Val occurred in European-Americans; p. Gln239DEL and p. Ile260Arg were identified in Asian-Americans; and p.



Table 1. Summary of variants in the coding region of OAT3 identified in ethnically diverse populations

Exon	SNP #	CDS Position[1]	Nucleotide Change	Amino Acid Position[1]	Amino Acid Change	Grantham[2]	EC/EU[3]	Allele Frequency (%)[4]			
								AA (n=160)	EA (n=160)	AS (n=120)	ME (n=100)
1	1.2	51	G→A	17	syn	-	EC	0	0	0.8	0
	1.3	153	G→A	51	syn	-	EU	40.0	5.1	8.5	3.1
2	*2.1*	*387*	*C→A*	*129*	*Phe→Leu*	*22*	*EC*	*0*	*0*	*0*	*1.0*
3	*3.1*	*445*	*C→A*	*149*	*Arg→Ser*	*110*	*EC*	*0*	*0.6*	*0.8*	*0*
4	4.1	714	G→T	238	syn	-	EC	0	0	0.8	0
	4.2	*715*	*C→T*	*239*	*Gln→DEL*	-	*EC*	*0*	*0*	*0.8*	*0*
	4.3	723	T→A	241	syn	-	EU	9.0	24.4	18.3	29.0
5	*5.1*	*779*	*T→G*	*260*	*Ile→Arg*	*97*	*EC*	*0*	*0*	*0.8*	*0*
	5.2	*829*	*C→T*	*277*	*Arg→Trp*	*101*	*EU*	*0.7*	*0*	*0*	*0*
	5.3	**842**	**T→C**	**281**	**Val→Ala**	**64**	**EU**	**6.0**	**0**	**0**	**0**
6	***6.1***	***913***	***A→T***	***305***	***Ile→Phe***	***21***	***EC***	***0***	***0***	***3.5***	***1.1***
	6.2	929	C→T	310	Ala→Val	64	EU	0	0.6	0	0
7	7.1	1195	G→T	399	Ala→Ser	99	EU	0	0	0	1.0
9	***9.3***	***1342***	***G→A***	***448***	***Val→Ile***	***29***	***EU***	***0.6***	***1.3***	***0***	***1.0***
10	10.5	1590	C→A	530	syn	-	EC	4.4	0	0	0

Data are available at http://www.pharmgkb.org. The 3 common non-synonymous variants (≥1% in any ethnic group) are shown in bold. The variants that exhibited altered transport of ES and/or MTX are shown in italics.

[1]Positions are relative to the ATG start site and are based on the cDNA sequence from GenBank accession number NM_004254.

[2]Grantham values range from 5 to 215, where low values indicate chemical similarity and high values indicate radical differences.

[3]EC/EU classifies coding variants as being evolutionarily conserved (EC) or evolutionarily unconserved (EU) based on sequence alignments with 7 mammalian orthologs.

[4]Some samples contained amplicons that could not be sequenced. Allele frequencies were calculated from actual DNA samples sequenced. AA, African-American; EA, European-American; AS, Asian-American; ME, Mexican-American; n, number of chromosomes.

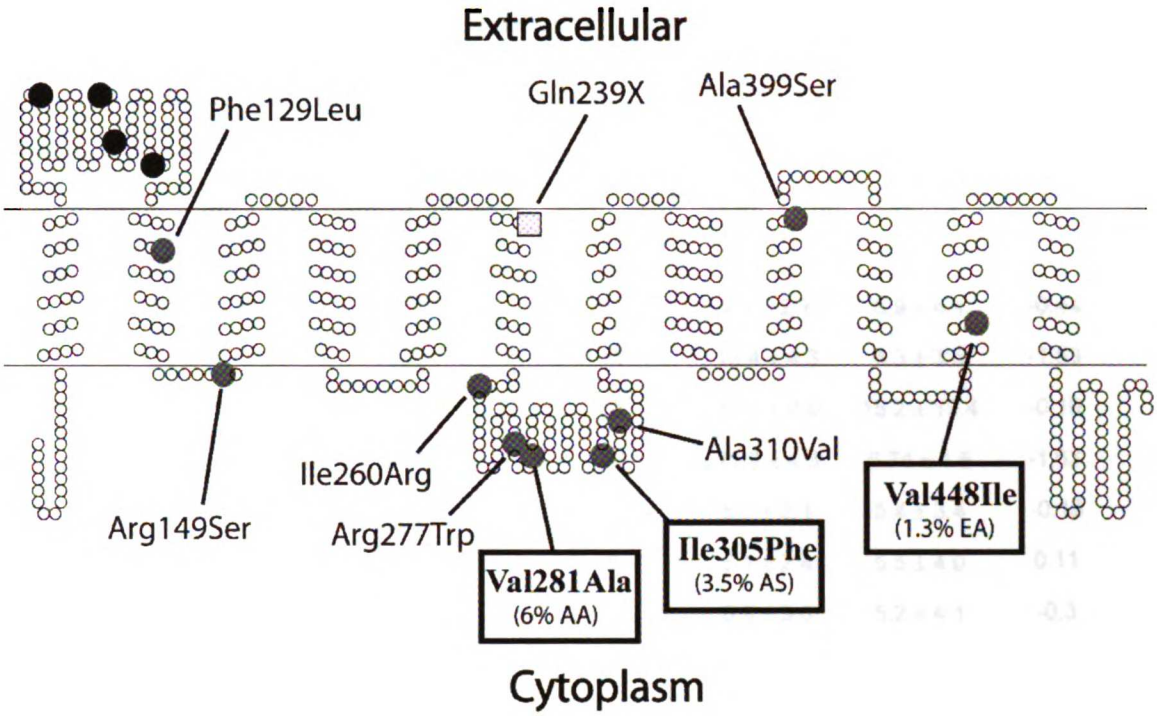

Figure 3. Secondary structure prediction of OAT3 showing the location of the 10 protein-altering variants. The transmembrane topology diagram was obtained using TOPO [S. J. Johns (UCSF, San Francisco) and R. C. Speth (Washington State University, Pullman), transmembrane protein display software available at the UCSF Sequence Analysis Consulting Group website, http://www.sacs.ucsf.edu/TOPO/topo.html]. Non-synonymous variants are labeled with dark gray circles, the deletion variant (Gln239X) is identified by the light gray square, and putative N-glycosylation sites are shown by the black circles. The three most common non-synonymous variants of OAT3, which were kinetically characterized, are shown in bold and boxed and the highest allele frequency in a given ethnic group is shown in parentheses (AA, African-American; EA, European-American; AS, Asian-American; ME, Mexican-American).

Table 2. Estimates of the neutral parameter (θ), nucleotide diversity (π), and Tajima's D for *SLC22A8*[1]

Population	SNP type	Base pairs Screened	n[2]	No. variable sites	θ (x 10^4)	π (x 10^4)	D
Total[3]	All	3706	540	26	10.1 ± 2.8	5.2 ± 3.3	-1.53
	Non-coding	2077		11	7.7 ± 2.7	5.9 ± 4.1	-0.44
	Coding	1629		15	13.4 ± 4.3	4.3 ± 3.6	-1.53
	Synonymous	395		5	18.4 ± 8.9	15.2 ± 13.4	-0.19
	Non-synonymous	1234		10	11.8 ± 4.3	0.74 ± 1.5	-1.63
AA	All	3706	160	12	5.7 ± 2.1	5.4 ± 3.4	-0.15
	Non-coding	2077		6	5.1 ± 2.4	5.5 ± 4.0	0.11
	Coding	1629		6	6.5 ± 3.0	5.2 ± 4.1	-0.3
	Synonymous	395		3	13.4 ± 8.3	18.3 ± 15.2	0.34
	Non-synonymous	1234		3	4.3 ± 2.7	1.0 ± 1.7	-0.72
EA	All	3706	160	11	5.3 ± 2.0	3.9 ± 2.6	-0.58
	Non-coding	2077		6	5.1 ± 2.4	4.4 ± 3.4	-0.21
	Coding	1629		5	5.4 ± 2.7	3.2 ± 3.0	-0.56
	Synonymous	395		2	9.0 ± 6.7	11.7 ± 11.5	0.22
	Non-synonymous	1234		3	4.3 ± 2.7	0.4 ± 1.1	-0.85
AS	All	3706	120	14	7.1 ± 2.5	5.9 ± 3.7	-0.43
	Non-coding	2077		6	5.4 ± 2.6	7.7 ± 5.1	0.66
	Coding	1629		8	9.2 ± 3.9	3.7 ± 3.3	-1.13
	Synonymous	395		4	18.9 ± 10.5	12.3 ± 11.8	-0.42
	Non-synonymous	1234		4	6.1 ± 3.4	0.9 ± 1.6	-1.02
ME	All	3706	100	13	6.8 ± 2.5	4.5 ± 3.0	-0.87
	Non-coding	2077		7	6.5 ± 2.9	5.4 ± 3.9	-0.30
	Coding	1629		6	7.1 ± 3.4	3.4 ± 3.1	-0.85
	Synonymous	395		2	9.8 ± 7.3	12.0 ± 11.6	0.17
	Non-synonymous	1234		4	6.3 ± 3.5	0.63 ± 1.4	-1.11

[1] θ, π, and Tajima's D were calculated as described in Materials and Methods
[2] n, number of chromosomes
[3] Total, entire sample; AA, African-American; EA, European-American; AS, Asian-American; ME, Mexican-American. Data are listed as mean x 10^4 ± SD.

Ala399Ser was found in Mexican-Americans. The position of each protein-altering variant in the putative membrane topology of OAT3 is shown in Figure 3. The majority of nonsynonymous variants were found in intracellular loops (six of ten), while synonymous SNPs were equally distributed between transmembrane domains (TMDs) and intracellular or extracellular loops.

Table 2 shows a summary of the estimated neutral parameter (θ), nucleotide diversity (π), and Tajima's D statistic for the total population and for each of the four ethnic groups. Overall the genetic variation in *SLC22A8* was similar to the average previously reported for 24 transporter genes, since π (x 10^4) for *SLC22A8* is 5.2 ± 3.3 compared to the average of 5.1 ± 2.4 (23). However, the ratio of π for non-synonymous sites to π for synonymous sites (π_{NS}/π_S) was considerably lower than the one previously reported (0.05 for *SLC22A8* versus 0.23 for the average of 24 transporter genes (23)), suggesting that OAT3 is under significant purifying selection acting against amino-acid changes. In addition, since most values of θ were greater than π, Tajima's D statistics were mostly negative, again consistent with negative selection acting on OAT3. Nucleotide diversity at non-synonymous sites in loops ($\pi_{NS\text{-}loop\text{-}OAT3}$ = 0.97 ± 2.2 versus 3.6 ± 1.9) and TMDs ($\pi_{NS\text{-}TMD\text{-}OAT3}$ = 0.45 ± 1.7 versus 1.6 ± 1.1) of OAT3 was considerably lower than the average for 24 transporter genes (23) and OAT3 π_{NS} for TMDs was much lower than OAT3 π_{NS} for loops, indicating that there are evolutionary constraints on both regions of the protein, but especially in TMDs.

Haplotype analysis of *SLC22A8*

A total of 30 haplotypes in *SLC22A8* were identified from 15 variable sites using the Bayesian statistical method, PHASE (22). Twenty of the 30 haplotypes occurred on at

least two chromosomes and, since their combined frequency was 98%, further analyses were conducted using this smaller haplotype set. Naming of the haplotypes was done based on the modified convention of Nebert *et al.* according to two main criteria: evolutionary divergence and frequency in the sample (24).

As shown in Figure 4, haplotype *1A1 occurred with the highest frequency in all 4 ethnic groups. Haplotype *2A1 was the second most common haplotype, except in African-Americans where *3A1 was instead more common after *1A1. Among the 20 haplotypes, 5 (*1A1, *2A1, *2B1, *3A1, and *4A1) had total frequencies of $\geq$ 5% and occurred in all ethnic groups. On the other hand, eight out of 20 haplotypes (40%) were found in only one ethnic group: *6A1 in European-Americans; *8A2, *9A1, and *9B1 in African-Americans; *4B1 and *4B2 in Asian-Americans; and *2B2 and *4A2 in Mexican-Americans. African-Americans (13 out of 20) and Asian-Americans (13 out of 20) had the greatest number of haplotypes, while African-Americans had the largest number of ethnic specific haplotypes (three out of eight). The common protein-altering variants p. Val281Ala (*8A2) and p. Ile305Phe (*4B2) were each found in an ethnic specific haplotype, while p. Val448Ile was found in haplotype *1A2.

The cladogram for OAT3 examining the relationship among the 20 haplotypes is shown in Figure 5. Several variants (i.e. SNP # 1.1, 1.3, 2.2, 2.3, 4.3, and 9.1) appear more than once, suggesting that either substitutions have arisen multiple times in evolutionary history or that recombination events have occurred.

Functional characterization of MTX transport by protein-altering variants in OAT3

We characterized the interaction of the ten naturally occurring protein-altering variants in OAT3 with MTX to determine their role in inter-individual variation in MTX

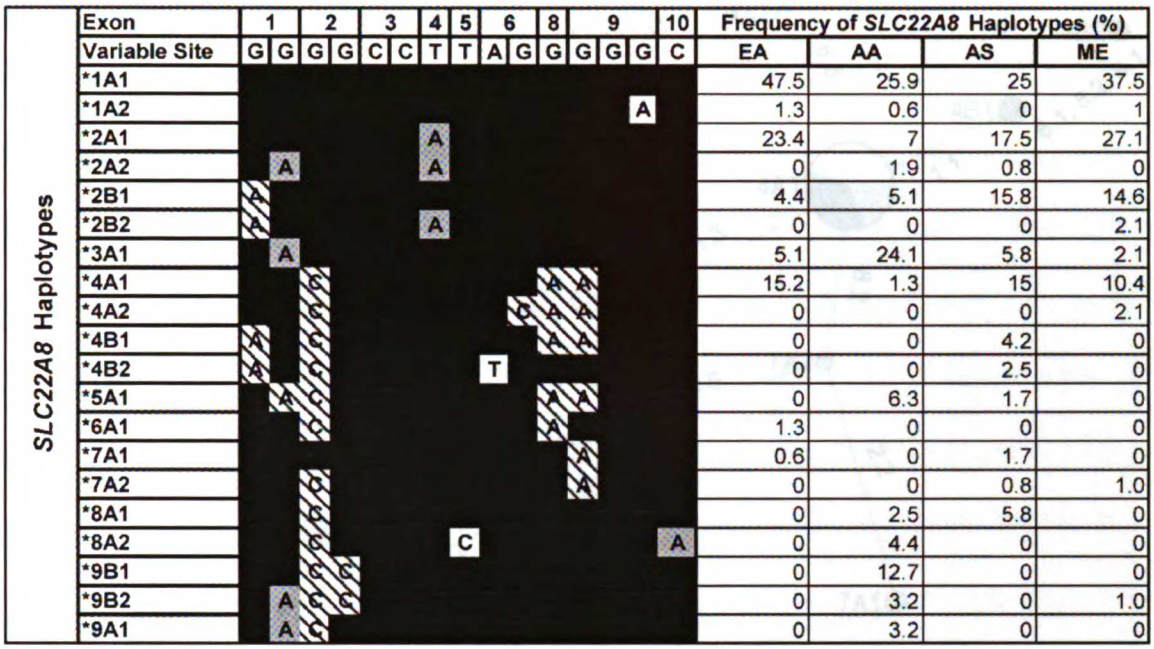

Exon	1	2	3	4	5	6	8	9	10	Frequency of *SLC22A8* Haplotypes (%)			
Variable Site	G	G G G	C C	T	T	A G	G	G G G	C	EA	AA	AS	ME
*1A1										47.5	25.9	25	37.5
*1A2									A	1.3	0.6	0	1
*2A1				A						23.4	7	17.5	27.1
*2A2	A			A						0	1.9	0.8	0
*2B1	A									4.4	5.1	15.8	14.6
*2B2	A			A						0	0	0	2.1
*3A1	A									5.1	24.1	5.8	2.1
*4A1		C					A	A		15.2	1.3	15	10.4
*4A2		C				G	A	A		0	0	0	2.1
*4B1	A	C					A	A		0	0	4.2	0
*4B2	A	C			T					0	0	2.5	0
*5A1		A C					A	A		0	6.3	1.7	0
*6A1		C					A			1.3	0	0	0
*7A1								A		0.6	0	1.7	0
*7A2		C						A		0	0	0.8	1.0
*8A1		C								0	2.5	5.8	0
*8A2		C			C				A	0	4.4	0	0
*9B1		C C								0	12.7	0	0
*9B2	A	C C								0	3.2	0	1.0
*9A1	A	C								0	3.2	0	0

Figure 4. Structure and population frequency of 20 haplotypes of *SLC22A8*. Left panel, sequences of the haplotypes at each of the 15 variable sites. The first row shows the exons of *SLC22A8*; the second row contains the sequence of the reference allele at each variable site. Each of the subsequent rows shows the 20 haplotypes clustered and named based on their evolutionary divergence and population frequencies using a modified convention of Nebert (24). A black filled square is used to indicate that there is no change from the reference allele; a gray filled square shows a synonymous change in the coding region; a white filled square indicates a non-synonymous change; changes occurring at non-coding sites are denoted by diagonally striped squares. Letters in the squares indicate the base pair change. Haplotypes were predicted using PHASE software version 1.0.1 as previously described (22). Right panel, frequencies of the 20 haplotype in each ethnic group.

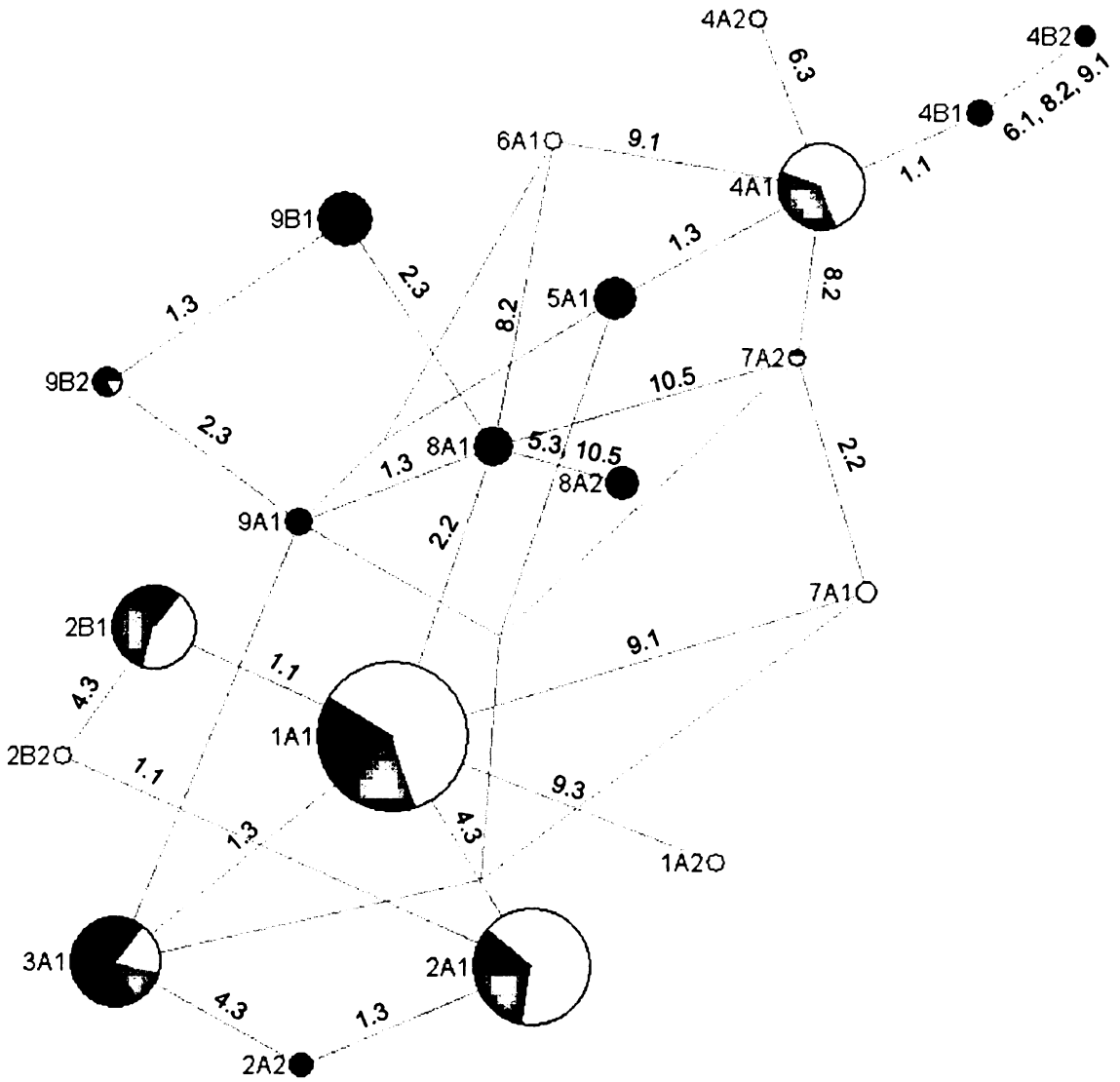

Figure 5. Cladogram of the 20 common haplotypes of *SLC22A8*. The circles for each haplotype were drawn proportional to the overall frequency at which the haplotypes were found. The SNP changes between haplotypes are indicated above the lines connecting the haplotypes. The circles are subdivided in 4 differently colored slices according to the proportion of chromosomes carrying that particular haplotype in each ethnic group: European-Americans are identified in white, African-Americans in black, Asian-Americans in dark gray, and Mexican-Americans in light gray. The *1A1 haplotype is the most common haplotype overall and in each ethnic group.

Stanford Libraries

disposition and toxicity. As shown in Figure 6, six out of ten protein-altering variants in OAT3 exhibited altered uptake of MTX and/or the model organic anion compound, ES. Specifically, the rare variants p. Arg149Ser, p. Gln239DEL, and p. Ile260Arg were non-functional, meaning their transport was not significantly different compared to HEK293 cells transiently transfected with pcDNA5/FRT (empty vector). P. Gln239DEL occurs in the beginning of TMD 6 and results in the truncation of the last 7 TMDs. On the other hand, the singleton variants p. Phe129Leu (51.2 ± 4.8 %) and p. Arg277Trp (50.7 ± 7.3 %) showed reduced MTX transport in comparison to OAT3 reference (100 ± 8.0 %). In addition, p. Ile305Phe exhibited substrate specificity changes as previously reported (19), whereby it transported MTX similarly to OAT3 reference, but showed significantly reduced uptake of ES ($p < 0.01$). It is interesting to note that, except for p. Arg277Trp, all of the protein-altering variants that exhibited altered MTX transport occurred at evolutionarily conserved (EC) sites. On the other hand, the four protein-altering variants that showed MTX uptakes similar to OAT3 reference were instead found at evolutionarily unconserved (EU) sites. Amino acid changes were classified as EC or EU based on multiple sequence alignments with seven mammalian orthologs (chimp, pongo, monkey, pig, rabbit, mouse, and rat).

Following these initial screens for function, the interaction kinetics of MTX with the three most common protein-altering variants in OAT3, p. Val281Ala, p. Ile305Phe, and p. Val448Ile, was examined in detail in HEK293 cells (Figure 7). As shown in Table 3, cells expressing p. Val448Ile exhibited an approximately 2-fold increase ($p < 0.05$) in the K_m (147 ± 19 μM) for MTX, while the V_{max} (1980 ± 190 pmol/mg of protein/3 min) was not significantly different compared to cells expressing OAT3 (K_m = 84 ± 14 μM;

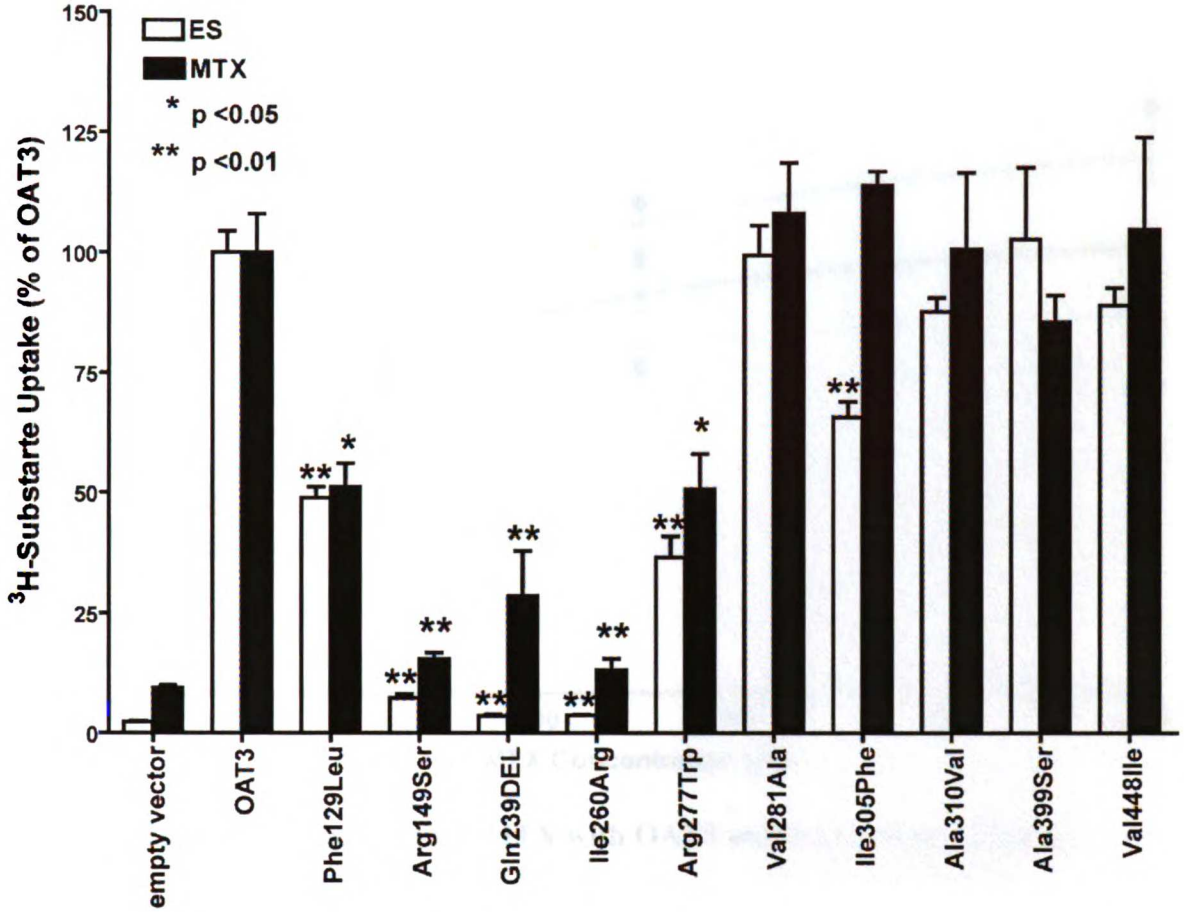

Figure 6. Uptake of ES and MTX in HEK293 cells expressing OAT3 and its 10 protein-altering variants. Uptake of 20 nM ^{3}H-ES (white bars) or 20 nM ^{3}H-MTX (black bars) in cells transiently transfected with empty vector, OAT3, or the 10 protein-altering variants. Transport was measured in Na^+ buffer at pH 7.4 over 3 min. Uptake is expressed as percentage of ES and MTX uptake, respectively, by OAT3 expressing cells. Each value is expressed as mean ± SE for 3 wells from a representative experiment out of 3 independent experiments. P values were determined by comparing variant uptake to OAT3 reference for each substrate using one-way ANOVA and Tukey's multi-comparison test with $p < 0.05$ as the criterion of significance.

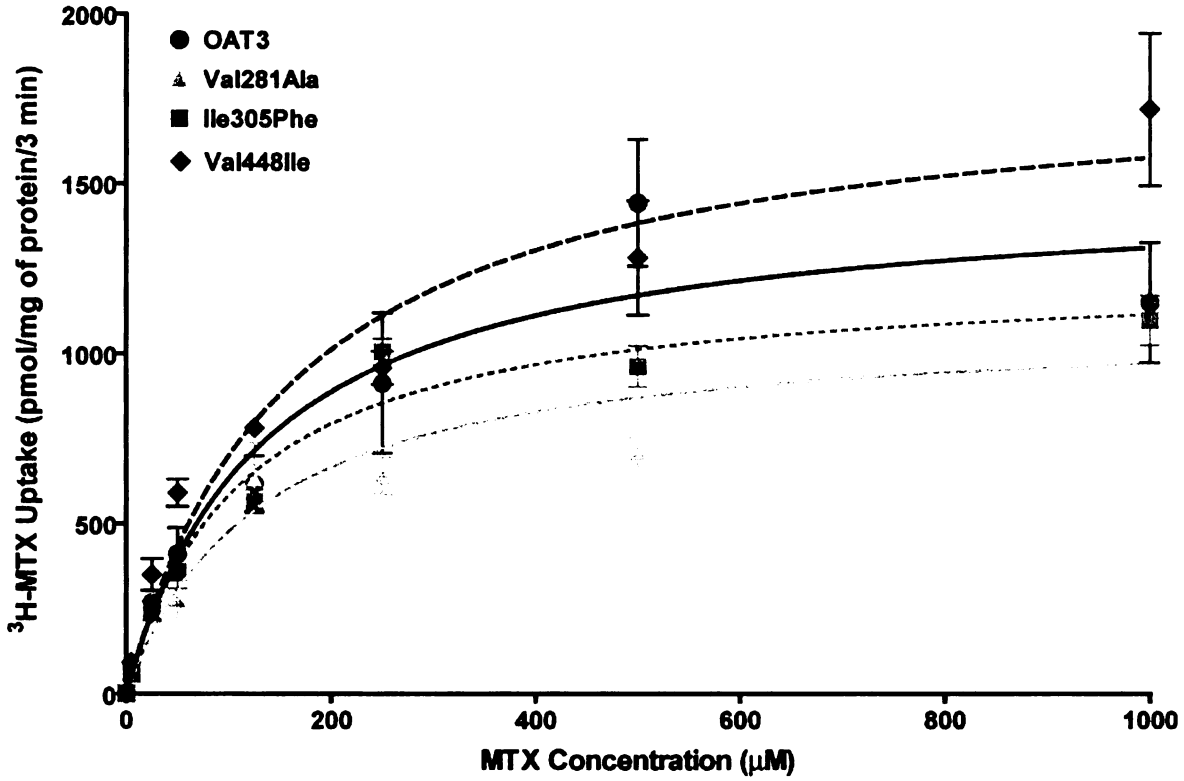

Figure 7. Kinetics of interaction of MTX with OAT3 and its 3 common protein-altering variants. Interaction kinetics of ^{3}H-MTX in HEK293 cells transiently transfected with OAT3 reference (black circle) and the common protein-altering variants, p. Val281Ala (light gray triangle), p. Ile305Phe (gray square), and p. Val448Ile (dark gray diamond). Uptake of ^{3}H-MTX (20 nM) was measured in the presence of various concentrations of unlabeled MTX in Na^+ buffer at pH 7.4 over 3 min. Data are representative of 3 independent experiments and each value represents the mean ± SE from 3 wells. Transport data were fitted using nonlinear regression analysis. P values were determined by comparing kinetic parameters for each variant to that of OAT3 reference using one-way ANOVA and Tukey's multi-comparison test with $p < 0.05$ as the criterion of significance.

Table 3. Summary of transport kinetics of MTX with OAT3 and the 3 common protein-altering variants, p. Val281Ala, p. Ile305Phe, and p. Val448Ile

	OAT3	Val281Ala	Ile305Phe	Val448Ile
K_m (μM)	84 ± 14	113 ± 12	102 ± 12	**147 ± 19***
V_{max} (pmol/mg protein/3 min)	1510 ± 141	1920 ± 415	1470 ± 262	1980 ± 190
V_{max}/K_m	17.9 ± 3.6	18.1 ± 5.4	14.5 ± 1.9	13.8 ± 1.4

Uptake of ^{3}H-MTX (20 nM) was measured in the presence of various concentrations of unlabeled MTX in Na^+ buffer at pH 7.4 over 3 min. Each value represents the mean ± SE from 3 independent experiments. Transport data was fitted using nonlinear regression analysis. Significant differences in the kinetic parameters of the variant proteins compared to OATP1A2 reference are shown in bold ($p < 0.05$). P values were determined by comparing K_m, V_{max}, and V_{max} / K_m values for each variant to OAT3 using one-way ANOVA and Dunnett's multi-comparison test with $p < 0.05$ as the criterion of significance.

V_{max} = 1510 ± 141 pmol/mg of protein/3 min). There were no significant differences in the interaction affinity and maximal transport rate of MTX between OAT3 and p. Val281Ala or p. Ile305Phe.

Discussion

MTX therapy has been extensively employed to treat a variety of malignancies and inflammatory diseases (1). However, there is considerable inter-individual variability in response, pharmacokinetic parameters, as well as development of severe organ toxicity during MTX use. Specifically, it was found that co-administration of an organic anion, probenecid, with MTX resulted in the doubling of plasma MTX levels, an increase in the MTX serum half-life, and delayed elimination, which has been associated with severe systemic toxicity (4, 25). In addition, there have been several reports of clinical drug interactions with MTX and nonsteroidal anti-inflammatory (NSAIDs) drugs, such as indomethacin and ketoprofen. Co-administration of NSAIDs with MTX led to increased MTX blood levels, decreased MTX renal clearance, and acute renal failure, primarily via inhibition of MTX secretion by NSAIDs in the proximal tubule of the kidney (5, 25-28). Since NSAIDs are organic anions which have been shown to be substrates of OATs, all these factors strongly suggest that OATs likely have important roles in MTX disposition and toxicity. In particular, among the OATs, human OAT3 is the most abundantly expressed on the basolateral side of renal proximal tubule cells (11, 14) and, therefore, is likely to be the predominant OAT responsible for MTX secretion in the kidney lumen.

Therefore, in the present study we present detailed characterization of MTX interaction with OAT3 and its naturally occurring protein-altering variants previously

identified by Erdman *et al.* (19). The comprehensive genetic and functional analysis of variation in *SLC22A8* provides evidence for the important role of OAT3 in inter-individual variation in MTX disposition and toxicity.

Our data show that the bicarboxylic organic anion, MTX, interacts with OAT3 with a K_m of 75 ± 12 μM and a V_{max} of 2090 ± 140 pmol/mg of protein/3 min (Figure 1 and 2). These data are consistent with previous reports using *Xenopus laevis* oocytes or mouse proximal tubule cells stably expressing human OATs, where human OAT3 and OAT4 were shown to interact with MTX with high affinity (K_m ~ 20 μM), whereas MTX was a low affinity substrate of human OAT1 (K_m = 550-750 μM) (15, 17). In addition, we demonstrate for the first time that the minor metabolite of MTX, 7-OH-MTX, which is also predominantly eliminated by the kidney, greatly inhibits (by more than 90%) transport of the model organic anion compound, ES, by OAT3. On the other hand, despite being structurally similar to MTX, folate and leucovorin, which is a reduced folate drug used clinically to rescue normal cells from toxic effects of MTX, only weakly interacted with OAT3. Since OAT3 is highly expressed on the basolateral surface of proximal tubule cells and interacts with MTX with 10 fold higher affinity than OAT1, our studies suggest that OAT3 plays an important and predominant role in the saturable secretion of MTX and its metabolite in the kidney proximal tubule.

We analyzed genetic variation in *SLC22A8* in an ethnically diverse population of 270 healthy individuals. A total of 26 variants were identified in *SLC22A8*: 11 were found in non-coding intronic regions and 15 in the coding regions (Table 1). Of the coding region variants, ten altered the amino acid sequence of OAT3, while five were synonymous. Two of the synonymous SNPs (c. 51 G>A and c. 723 T>A) have been

observed in a recent report by Xu *et al.* (29), which also identified a Japanese-specific protein-altering variant, p. Ala523Gly, in OAT3. This variant occurred in only one Japanese individual and was not observed in our previous resequencing effort because the Asian-American population included in our analysis was primarily a sample of Chinese-American individuals (19, 29). Compared to the study by Xu *et al.* (29) which analyzed genetic variation of OAT3 in 12 ethnic groups with ten or fewer individuals, we screened a much larger sample set (between 50 and 80 individuals) in a smaller number of ethnic populations and discovered a considerably larger number of variants, especially rare variants. As shown in Table 2, nucleotide diversity at non-synonymous sites ($\pi_{NS\text{-}total}$ (x 10^4) = 0.74 ± 1.5) was much lower than in a recently reported analysis of genetic variation ($\pi_{NS\text{-}total}$ (x 10^4) = 2.2 ± 1.1) in 24 membrane transporter genes (23). In addition, the ratio of π_{NS}/π_S, which is a measure of selection for function of a particular gene, was found to be 0.05, which again was significantly lower than the previously reported average of 0.23 for a set of membrane transporters (23). The loop regions and especially TMDs of OAT3 had low π_{NS} values, indicating that there are significant constraints on these structural regions of the transporter. Purifying selection acting on OAT3 sequence is suggested by negative Tajima's D values for nonsynonymous sites compared to positive values for synonymous sites (Table 2) and as shown in Table 1 by the lower allele frequency of protein-altering variants (6 out of 10 are singletons) compared to synonymous variants (2 out of 5 are singletons). Altogether, these data indicate that OAT3 is under strong negative selective pressure, which is acting to preserve its amino-acid sequence, and is important for human fitness.

Consistent with a previous report by Stephens *et al.*(30), where an average of 14 haplotypes was observed in the analysis of 313 genes, a total of 30 haplotypes were identified in *SLC22A8* (Figure 4 and 5). The five most common haplotypes (*1A1, *2A1, *2B1, *3A1, and *4A1), which were observed across all 4 ethnic populations studied, accounted for 82% of all haplotypes. On the other hand, a considerable number of haplotypes (8 out of 20) was found to be population-specific in African-Americans and Asian-Americans had the largest number of haplotypes (12 out of 20). Most haplotypes had only synonymous or intronic changes, while only three of 20 haplotypes (*1A2, *4B2, and *8A2) contained one amino acid altering variant. None of the 20 haplotypes had two or more amino acid changes.

Despite showing an overall relatively low degree of genetic variation, OAT3 exhibited significant functional variation in regards to MTX transport. Specifically, we identified three protein-altering variants (p. Arg149Ser, p. Gln239DEL, and p. Ile260Arg) in OAT3 which were non-functional, two protein-altering variants (p. Phe129Leu and p. Arg277Trp) which showed reduced MTX uptake, and one specificity variant (p. Ile305Phe) which transported MTX similar to OAT3 reference but showed reduced transport of ES (Figure 6). p. Gln239DEL results in the truncation of OAT3 after the first 5 TMDs (Figure 3). Its loss of transport function of organic anions, such as MTX, is consistent with previously published findings by Feng *et al.*, which showed that residues important for substrate recognition are located in the carboxyl-terminal part of OAT3 (31). The complete loss of MTX transport observed with p. Ile260Arg could be related to the fact that this mutation removes a protein kinase C (PKC) phosphorylation site with the general consensus sequence of S/T-(X)-R/K. In fact, all OATs, including

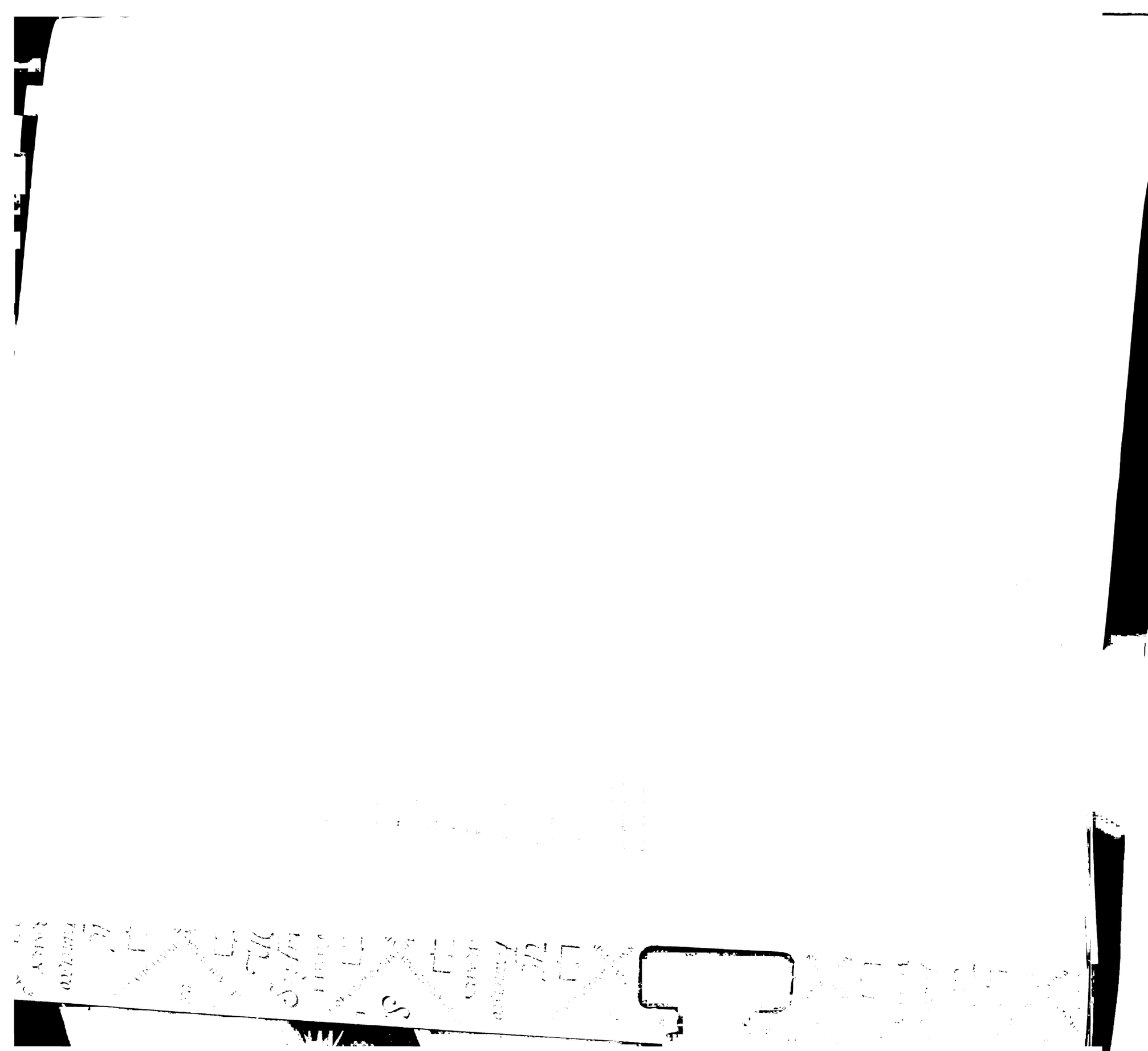

OAT3, have several phosphorylation sites by PKC in the large intracellular loop between TMD 6 and 7 (Figure 3). It has been previously reported that activation of PKC leads to altered transport function and substrate selectivity of OATs (32-34).

Interestingly, we observed that of the six protein-altering variants, which exhibited altered transport of MTX and/or ES, five occurred at EC sites (Table 1). On the other hand, all four protein-altering variants in OAT3 with transport function similar to OAT3 reference occurred at EU sites. EC residues are those that were identical in all seven members (chimp, pongo, monkey, pig, rabbit, mouse, and rat) of a set of OAT3 mammalian orthologs. This is consistent with previous reports on membrane transporter genes where evolutionary conservation was determined to be a strong predictor of both allele frequency and transport function, indicating that substitutions at EC sites are more deleterious than those at EU sites (23, 34-36).

Detailed kinetic characterization of MTX transport by the three common protein-altering variants of OAT3 (p. Val281Ala, p. Ile305Phe, and p. Val448Ile) indicated that p. Val448Ile, which is commonly found in European-Americans, interacts with MTX with a significantly lower affinity ($p < 0.05$) compared to OAT3 reference with no appreciable effect on the maximal transport rate (Table 3). Since Erdman *et al.* (19) previously showed that p. Val448Ile interacted with ES and cimetidine similarly to OAT3 reference, it can be surmised that this variant displays altered substrate specificity. Based on our kinetic findings, we can speculate that individuals carrying the p. Val448Ile variant may exhibit decreased secretion of MTX in the kidney and subsequently develop increased exposure and higher plasma concentrations of MTX, which could lead to MTX-induced toxicity. Altogether, the functional screen and kinetic data presented here

are consistent with previous studies on functional variation in membrane transporters where it has been uniformly reported that rare variants are more likely to exhibit altered transport and interaction with substrates than common variants (19, 23, 35-42).

In summary, we have determined that OAT3 shows reduced genetic diversity at sites that alter the amino acid sequence of the protein, but exhibits a high degree of functional variation in regards to MTX uptake. This transporter is under strong negative selection acting to preserve its amino acid sequence both in the loop and TMD regions, suggesting that OAT3 is critical for human fitness. Furthermore, our studies indicate that OAT3 plays an important role in the active secretion of MTX in the kidney and that protein-altering variants in OAT3 may contribute to inter-individual variation in MTX disposition and toxicity. The comprehensive genetic and functional analysis of variation in OAT3 and other transporters (37-42) suggests that in many cases rare variants should be given higher priority when selecting SNPs in membrane transporter genes to study the clinical association between genetic variants in those transporters and efficacy and toxicity of drugs, such as MTX. Since MTX therapy can result in severe toxicity in the kidney and brain, where OAT3 is expressed (1, 11), clinical studies of genetic variants in OAT3 are clearly needed to determine their significance to MTX therapy.

References

1. Goodman LS, Hardman JG, Limbird LE, Gilman AG. Goodman & Gilman's the pharmacological basis of therapeutics. 10th / ed. New York: McGraw-Hill Medical Pub. Division; 2001.

2. Hendel J, Nyfors A. Nonlinear renal elimination kinetics of methotrexate due to saturation of renal tubular reabsorption. Eur J Clin Pharmacol 1984; **26**: 121-4.

3. Huang KC, Wenczak BA, Liu YK. Renal tubular transport of methotrexate in the rhesus monkey and dog. Cancer Res 1979; **39**: 4843-8.

4. Bourke RS, Chheda G, Bremer A, Watanabe O, Tower DB. Inhibition of renal tubular transport of methotrexate by probenecid. Cancer Res 1975; **35**: 110-6.

5. Liegler DG, Henderson ES, Hahn MA, Oliverio VT. The effect of organic acids on renal clearance of methotrexate in man. Clin Pharmacol Ther 1969; **10**: 849-57.

6. el-Badawi MG, Abdalla MA, Bahakim HM, Fadel RA. Nephrotoxicity of low-dose methotrexate in guinea pigs: an ultrastructural study. Nephron 1996; **73**: 462-6.

7. Gronroos M, Chen M, Jahnukainen T, Capitanio A, Aizman RI, Celsi G. Methotrexate induces cell swelling and necrosis in renal tubular cells. Pediatr Blood Cancer 2005.

8. Perazella MA. Crystal-induced acute renal failure. Am J Med 1999; **106**: 459-65.

9. Perazella MA. Drug-induced renal failure: update on new medications and unique mechanisms of nephrotoxicity. Am J Med Sci 2003; **325**: 349-62.

10. Stoller RG, Hande KR, Jacobs SA, Rosenberg SA, Chabner BA. Use of plasma pharmacokinetics to predict and prevent methotrexate toxicity. N Engl J Med 1977; **297**: 630-4.

11. Koepsell H, Endou H. The SLC22 drug transporter family. Pflugers Arch 2004; **447**: 666-76.

12. Huffman DH, Wan SH, Azarnoff DL, Hogstraten B. Pharmacokinetics of methotrexate. Clin Pharmacol Ther 1973; **14**: 572-9.

13. McLeod HL. Clinically relevant drug-drug interactions in oncology. Br J Clin Pharmacol 1998; **45**: 539-44.

14. Burckhardt BC, Burckhardt G. Transport of organic anions across the basolateral membrane of proximal tubule cells. Rev Physiol Biochem Pharmacol 2003; **146**: 95-158.

15. Takeda M, Khamdang S, Narikawa S, Kimura H, Hosoyamada M, Cha SH, et al. Characterization of methotrexate transport and its drug interactions with human organic anion transporters. J Pharmacol Exp Ther 2002; **302**: 666-71.

16. Uwai Y, Saito H, Inui K. Interaction between methotrexate and nonsteroidal anti-inflammatory drugs in organic anion transporter. Eur J Pharmacol 2000; **409**: 31-6.

17. Uwai Y, Taniguchi R, Motohashi H, Saito H, Okuda M, Inui K. Methotrexate-loxoprofen interaction: involvement of human organic anion transporters hOAT1 and hOAT3. Drug Metab Pharmacokinet 2004; **19**: 369-74.

18. Nozaki Y, Kusuhara H, Endou H, Sugiyama Y. Quantitative evaluation of the drug-drug interactions between methotrexate and nonsteroidal anti-inflammatory drugs in the renal uptake process based on the contribution of organic anion transporters and reduced folate carrier. J Pharmacol Exp Ther 2004; **309**: 226-34.

19. Erdman AR, Mangravite LM, Urban TJ, Lagpacan LL, Castro RA, de la Cruz M, et al. The human organic anion transporter 3 (OAT3; SLC22A8): genetic variation and functional genomics. Am J Physiol Renal Physiol 2006; **290**: F905-12.



20. Tajima F. Statistical method for testing the neutral mutation hypothesis by DNA polymorphism. Genetics 1989; **123**: 585-95.

21. Hartl DL, Clark AG. Principles of population genetics. 3rd ed. Sunderland, MA: Sinauer Associates; 1997.

22. Stephens M, Smith NJ, Donnelly P. A new statistical method for haplotype reconstruction from population data. Am J Hum Genet 2001; **68**: 978-89.

23. Leabman MK, Huang CC, DeYoung J, Carlson EJ, Taylor TR, de la Cruz M, et al. Natural variation in human membrane transporter genes reveals evolutionary and functional constraints. Proc Natl Acad Sci U S A 2003; **100**: 5896-901.

24. Nebert DW. Proposal for an allele nomenclature system based on the evolutionary divergence of haplotypes. Hum Mutat 2002; **20**: 463-72.

25. Aherne GW, Piall E, Marks V, Mould G, White WF. Prolongation and enhancement of serum methotrexate concentrations by probenecid. Br Med J 1978; **1**: 1097-9.

26. Maiche AG. Acute renal failure due to concomitant action of methotrexate and indomethacin. Lancet 1986; **1**: 1390.

27. Perrin A, Milano G, Thyss A, Cambon P, Schneider M. Biochemical and pharmacological consequences of the interaction between methotrexate and ketoprofen in the rabbit. Br J Cancer 1990; **62**: 736-41.

28. Thyss A, Milano G, Kubar J, Namer M, Schneider M. Clinical and pharmacokinetic evidence of a life-threatening interaction between methotrexate and ketoprofen. Lancet 1986; **1**: 256-8.

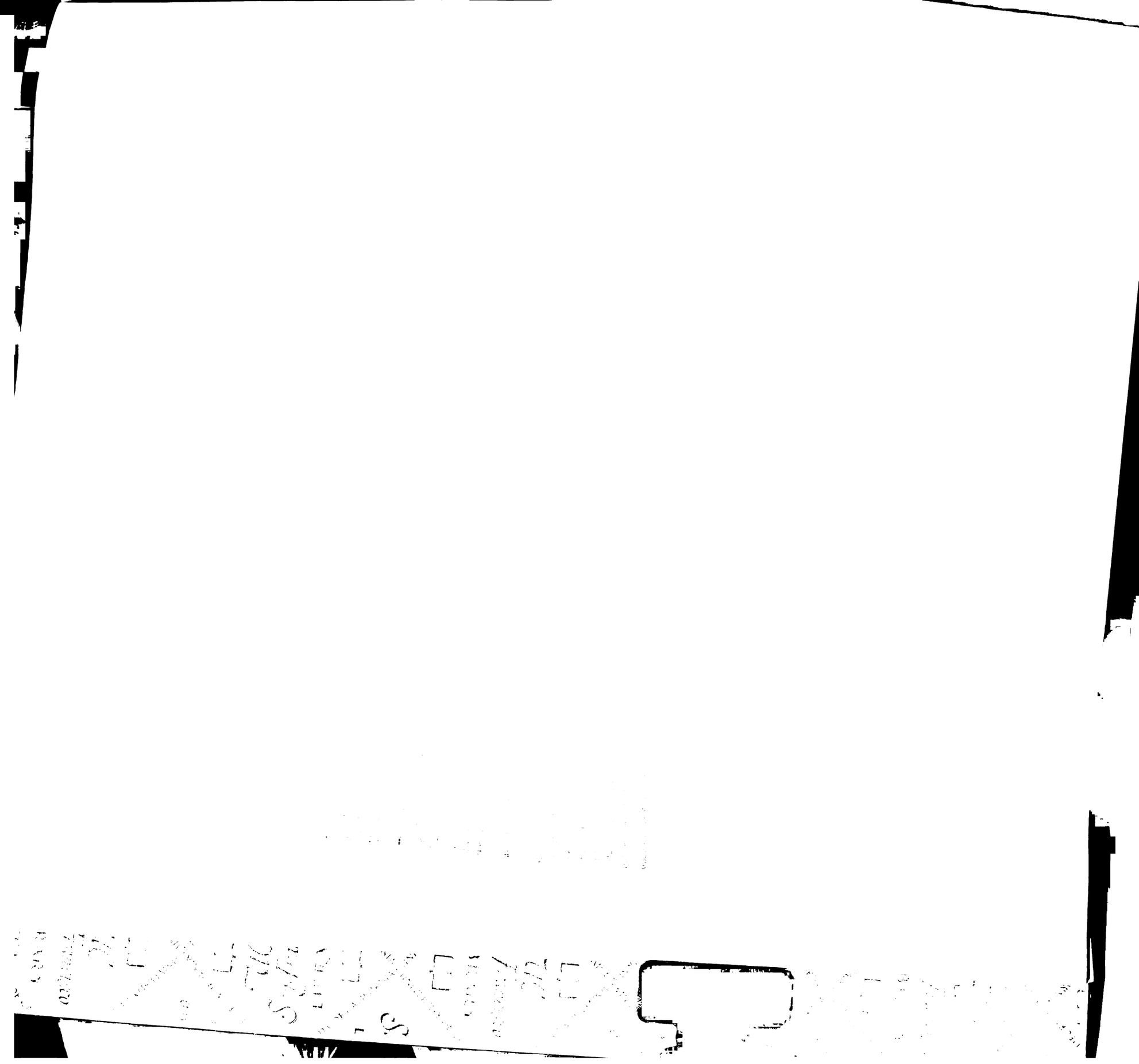

29. Xu G, Bhatnagar V, Wen G, Hamilton BA, Eraly SA, Nigam SK. Analyses of coding region polymorphisms in apical and basolateral human organic anion transporter (OAT) genes [OAT1 (NKT), OAT2, OAT3, OAT4, URAT (RST)]. Kidney Int 2005; **68**: 1491-9.

30. Stephens JC, Schneider JA, Tanguay DA, Choi J, Acharya T, Stanley SE, et al. Haplotype variation and linkage disequilibrium in 313 human genes. Science 2001; **293**: 489-93.

31. Feng B, Dresser MJ, Shu Y, Johns SJ, Giacomini KM. Arginine 454 and lysine 370 are essential for the anion specificity of the organic anion transporter, rOAT3. Biochemistry 2001; **40**: 5511-20.

32. Lu R, Chan BS, Schuster VL. Cloning of the human kidney PAH transporter: narrow substrate specificity and regulation by protein kinase C. Am J Physiol 1999; **276**: F295-303.

33. You G, Kuze K, Kohanski RA, Amsler K, Henderson S. Regulation of mOAT-mediated organic anion transport by okadaic acid and protein kinase C in LLC-PK(1) cells. J Biol Chem 2000; **275**: 10278-84.

34. Wolff NA, Thies K, Kuhnke N, Reid G, Friedrich B, Lang F, et al. Protein kinase C activation downregulates human organic anion transporter 1-mediated transport through carrier internalization. J Am Soc Nephrol 2003; **14**: 1959-68.

35. Shu Y, Leabman MK, Feng B, Mangravite LM, Huang CC, Stryke D, et al. Evolutionary conservation predicts function of variants of the human organic cation transporter, OCT1. Proc Natl Acad Sci U S A 2003; **100**: 5902-7.

36. Urban TJ, Giacomini KM, Risch N. Haplotype structure and ethnic-specific allele frequencies at the OCTN locus: implications for the genetics of Crohn's disease. Inflamm Bowel Dis 2005; **11**: 78-9.

37. Owen RP, Gray JH, Taylor TR, Carlson EJ, Huang CC, Kawamoto M, et al. Genetic analysis and functional characterization of polymorphisms in the human concentrative nucleoside transporter, CNT2. Pharmacogenet Genomics 2005; **15**: 83-90.

38. Owen RP, Lagpacan LL, Taylor TR, De La Cruz M, Huang CC, Kawamoto M, et al. Functional characterization and haplotype analysis of polymorphisms in the human equilibrative nucleoside transporter, ENT2. Drug Metab Dispos 2006; **34**: 12-5.

39. Badagnani I, Chan W, Castro RA, Brett CM, Huang CC, Stryke D, et al. Functional analysis of genetic variants in the human concentrative nucleoside transporter 3 (CNT3; SLC28A3). Pharmacogenomics J 2005; **5**: 157-65.

40. Leabman MK, Huang CC, Kawamoto M, Johns SJ, Stryke D, Ferrin TE, et al. Polymorphisms in a human kidney xenobiotic transporter, OCT2, exhibit altered function. Pharmacogenetics 2002; **12**: 395-405.

41. Osato DH, Huang CC, Kawamoto M, Johns SJ, Stryke D, Wang J, et al. Functional characterization in yeast of genetic variants in the human equilibrative nucleoside transporter, ENT1. Pharmacogenetics 2003; **13**: 297-301.

42. Fujita T, Urban TJ, Leabman MK, Fujita K, Giacomini KM. Transport of drugs in the kidney by the human organic cation transporter, OCT2 and its genetic variants. J Pharm Sci 2006; **95**: 25-36.

CHAPTER 5

MECHANISMS OF TRANSPORT AND STRUCTURAL DETERMINANTS OF SPECIFICITY OF OATP1A2

Introduction

Organic anion transporting polypeptides (human, OATPs; rodents, Oatps) are a large family of transmembrane proteins, which mediate the cellular transport of a wide range of amphipathic compounds, including clinically used drugs and xenobiotics (1). Members of this superfamily are characterized by a high degree of amino acid similarity and show partially overlapping as well as distinct substrate preferences (2). Within the OATP family, OATP1A2 (*SLCO1A2*, also referred as OATP-A or OATP1) was the first human member to be cloned and functionally characterized (3). It transports the largest number of structurally diverse compounds, including bile acids, steroid hormones, neutral and anionic peptides, and bulky organic cations (4). OATP1A2 mRNA and protein has been detected in epithelial cells of the kidney, liver, and intestine, and in endothelial cells of the blood brain barrier (5-7), indicating that it plays an important role in the tissue-specific disposition, pharmacokinetics, and toxicity of xenobiotics.

Despite considerable functional characterization of Oatps/OATPs, the mechanisms by which they mediate substrate transport across the membrane are still poorly understood, especially with respect to human members such as OATP1A2. OATP1A2 and OATP2B1 (OATP-B) are sensitive to extracellular pH, although a detailed analysis of whether movement of protons across the membrane or exchange of endogenous anions provides a driving force for these transporters remains to be

CHAPTER 5

MECHANISMS OF TRANSPORT AND STRUCTURAL DETERMINANTS OF SPECIFICITY OF OATP1A2

Introduction

Organic anion transporting polypeptides (human, OATPs; rodents, Oatps) are a large family of transmembrane proteins, which mediate the cellular transport of a wide range of amphipathic compounds, including clinically used drugs and xenobiotics (1). Members of this superfamily are characterized by a high degree of amino acid similarity and show partially overlapping as well as distinct substrate preferences (2). Within the OATP family, OATP1A2 (*SLCO1A2*, also referred as OATP-A or OATP1) was the first human member to be cloned and functionally characterized (3). It transports the largest number of structurally diverse compounds, including bile acids, steroid hormones, neutral and anionic peptides, and bulky organic cations (4). OATP1A2 mRNA and protein has been detected in epithelial cells of the kidney, liver, and intestine, and in endothelial cells of the blood brain barrier (5-7), indicating that it plays an important role in the tissue-specific disposition, pharmacokinetics, and toxicity of xenobiotics.

Despite considerable functional characterization of Oatps/OATPs, the mechanisms by which they mediate substrate transport across the membrane are still poorly understood, especially with respect to human members such as OATP1A2. OATP1A2 and OATP2B1 (OATP-B) are sensitive to extracellular pH, although a detailed analysis of whether movement of protons across the membrane or exchange of endogenous anions provides a driving force for these transporters remains to be

performed (8-10). Uptake of substrates by rodent Oatps has been reported to involve exchange with intracellular HCO_3^-, GSH, and/or may be sensitive to intracellular pH (11-14).

Structural studies with Oatps/OATPs have focused on the interaction between the carboxylic terminus and PDZ-domain containing proteins, suggesting that OATP1A2 expression and function may depend upon such interactions (15). It was recently demonstrated that interaction of rat Oatp1a1 with PDZK1 was required for its proper subcellular localization and function (16). However, rodent Oatps in the 1A subfamily probably arose by gene duplication and display significant differences in tissue distribution and substrate specificities compared to OATP1A2 (1). Therefore, mechanistic studies using Oatps may not reflect the transport mechanisms and structural determinants of the homologous human transporters.

In this study, we tested the hypothesis that transport of organic anion substrates by OATP1A2 involves a driving force. In particular, we determined whether extracellular pH, intracellular pH, the pH gradient, and endogenous anions (*i.e.* OH^-, HCO_3^-, and GSH) were able to drive organic anion transport by OATP1A2. Further, we assessed the effect of conserved cationic residues (*i.e.* arginine, lysine, and histidine residues) on the interaction of anionic substrates with OATP1A2. Our data demonstrate that transport of estrone-3-sulfate (ES) and methotrexate (MTX) by OATP1A2 is exquisitively sensitive to extracellular acidic pH, as a result of increased substrate affinity. Analysis of the structural determinants of organic anion interaction with OATP1A2 suggests that arginine (R49, R168, R240, R556, R590, and R609) and histidine (H107) residues are critical for substrate transport.

Materials and Methods

Materials

Radiolabeled ^{3}H-ES (57.3 Ci/mmol) was purchased from PerkinElmer Life Sciences (Wellesley, MA) and ^{3}H-MTX (49.6 Ci/mmol) was obtained from Moravek (Brea, CA). All unlabeled chemicals were purchased from Sigma (St. Louis, MO). Human embryonic kidney cells (Flp-In™-293) and the pcDNA5/FRT mammalian expression vector were purchased from Invitrogen (Carlsbad, CA).

HEK293 cell culture and transfection

The original human *SLCO1A2* plasmid containing the full-length open-reading frame in the pSPORT1 vector was a generous gift from Dr. B. Stieger (University of Zurich, Zurich, Switzerland). The *SLCO1A2* cDNA was subcloned into the mammalian expression vector, pcDNA5/FRT. HEK293 were propagated according to the manufacturer's protocol. They were grown at 37°C and 5% CO_2 in Dulbecco's Modified Eagle's media (DME H-21; UCSF Cell Culture Facility, San Francisco, CA) containing 10% fetal bovine serum (UCSF Cell Culture Facility), 100 μg/mL streptomycin (UCSF Cell Culture Facility), 100 units/mL penicillin G (UCSF Cell Culture Facility), and 100 μg/mL Zeocin™ (Invitrogen). Cells were plated at 3 x 10^5 cells/well on Biocoat® poly-d-lysine-coated 24-well plates (Becton Dickenson, Bedford, MA) 24 hr before transfection. The cells in individual wells were then transfected with 1 μg/well of pcDNA5/FRT (empty vector) or OATP1A2-pcDNA5/FRT and 3 μL of the lipid vehicle, Lipofectamine™ 2000 (Invitrogen). Cells were incubated overnight in the transfection mixture prior to replacement with fresh media. Uptake studies were performed 48 hr after transfection by incubating transfected cells in the presence of Na^+ buffer containing 20

nM ^{3}H-ES for 2 min at 37°C. Uptake of ES was linear for at least 2 min when measured at pH 5.0. The Na^+ buffer contained 128 mM NaCl, 5 mM KCl, 1.25 mM $CaCl_2$, 1.25 mM $MgSO_4$, and 5 mM HEPES/Tris. The pH of the Na^+ buffer was adjusted to 7.4 (or any other relevant pH unless otherwise specified) using Trizma and/or HCl. Uptake was stopped by washing the wells three times with ice-cold Na^+ free buffer in which Na^+ was replaced by choline chloride. The cells were then lysed by incubation in a solution of 0.1 N NaOH/0.1% sodium dodecyl sulfate (SDS) for at least 2 hr on an agitating platform. Radioactivity in an aliquot of the resultant mixture was then determined using a scintillation counter. The resultant uptake values were normalized for protein content to correct for differences in cell number from well to well. Protein assays were conducted on a spectrophotometric plate reader, using the BCA™ Protein Assay Kit (Pierce, Rockford IL).

***Xenopus laevis* oocyte expression assay**

The full-length *SLCO1A2* cDNA plasmid in a pCMV expression vector was purchased from Genecopoeia (Germantown, MD) and subcloned into the amphibian high-expression vector pOX. Stage V and VI oocytes were harvested from *X. laevis* (Xenopus One, Dexter, MI) as previously described (17). The oocytes were injected with 50-75 ng of capped cRNA, which was transcribed *in vitro* using T3 RNA polymerase (mMESSAGE MACHINE T3 kit; Ambion, Austin, TX) from Not I-linearized pOX plasmid containing *SLCO1A2* cDNA. The injected oocytes were stored in modified Barth's medium at 18°C for 72 h before transport experiments. Groups of seven to nine oocytes were incubated in the presence of Na^+ in buffer containing ^{3}H-ES (20 nM) or ^{3}H-MTX (0.2 μM) at room temperature for 60 min. Uptake of ES and MTX was linear for at

least 120 min. The Na^+ buffer contained 100 mM NaCl, 2 mM KCl, 1 mM $CaCl_2$, 1 mM $MgCl_2$, and 10 mM HEPES/Tris. The pH of the Na^+ buffer was adjusted to 7.4 (or any other relevant pH unless otherwise specified) using Trizma and/or HCl. Uptake was stopped by washing the oocytes five times with ice-cold Na^+ free buffer in which Na^+ was replaced by choline chloride. Oocytes were then lysed individually with 100 µL of 10% SDS and the radioactivity associated with each oocyte was determined.

Effect of pH, sodium dependency, and membrane potential on ^{3}H-ES uptake

To test the effect of extracellular pH on OATP1A2-mediated transport, cells transiently transfected with pcDNA5/FRT or OATP1A2 were pre-incubated in Na^+ buffer, pH 7.4, for 30 min at 37°C. Cells were washed with PBS and then incubated with 20 nM ^{3}H-ES in Na^+ buffer in the presence of decreasing extracellular pH (pH_o) for 2 min at 37°C. To test the effect of intracellular pH (pH_i) on ES uptake by OATP1A2, cells transiently transfected with pcDNA5/FRT or OATP1A2 were pre-incubated in Na^+ buffer with pH ranging from 7.4 to 5.0 for 30 min at 37°C. Cells were washed with PBS and then incubated with 20 nM ^{3}H-ES in Na^+ buffer at pH 7.4 or 5.0 for 2 min at 37°C. In addition, to determine whether ES transport by OATP1A2 was dependent on the proton gradient across the membrane, oocytes expressing OATP1A2 were exposed to the proton ionophore, carbonylcyanide *p*-trifluoromethoxyphenyl hydrazone (FCCP). Oocytes were pre-incubated in Na^+ buffer, pH 7.4, for 30 min at room temperature. Oocytes were washed three times with Na^+ buffer, pH 7.4, and then incubated with 20 nM ^{3}H-ES in Na^+ buffer in the absence or presence of 20 µM FCCP at pH 7.4 or pH 5.0 for 60 min. To test whether Na^+ is required for OATP1A2-dependent transport, N-methyl-D-glucamine (NMDG) was used to replace NaCl. Cells transiently transfected with pcDNA5/FRT or

OATP1A2 were pre-incubated in Na^+ buffer, pH 7.4, for 25 min at 37°C. The preload solution was then replaced with NMDG-containing buffer, pH 7.4 for an additional 5 min. Cells were then incubated with 20 nM ^{3}H-ES in NMDG-containing buffer at pH 7.4 or pH 5.0 for 2 min at 37°C. To test the effect of membrane potential on OATP1A2-mediated transport, NaCl was substituted with a high concentration of KCl (128 mM) as previously described (11, 18, 19). Cells were pre-incubated in Na^+ buffer, pH 7.4, for 25 min at 37°C. The preload solution was then replaced with KCl-containing buffer, pH 7.4 for an additional 5 min. Cells were then incubated with 20 nM ^{3}H-ES in KCl-containing buffer at pH 7.4 or pH 5.0 for 2 min at 37°C. Data are normalized to uptake of ES by OATP1A2 at pH_o=7.4 or pH_{in}/pH_o=7.4/7.4 and are presented as mean ± SE. Data shown are representative of 3 independent experiments.

pH-dependent kinetics of ^{3}H-ES uptake

Cells transiently transfected with pcDNA5/FRT or OATP1A2 were incubated with 20 nM ^{3}H-ES in Na^+ buffer at pH 7.4 or pH 5.0 in the presence of various concentrations of unlabeled ES for 2 min at 37°C. The kinetic curves for ES transport by OATP1A2 were generated by fitting the data by non-linear regression to a Michaelis-Menten curve fit, using GraphPad Prism 4 Software. A summary of the kinetic parameters of ES transport by OATP1A2 at pH 7.4 and 5.0 is given as mean ± SE from 3 independent experiments. P values were determined by comparing kinetic parameters at pH 5.0 to pH 7.4 using the unpaired Student's *t* test with $p < 0.05$ as the criterion of significance.

Effect of FCCP, GSH, HCO_3^-, and OH^- on ^{3}H-ES uptake

To test whether ES transport by OATP1A2 is dependent on the pH gradient, oocytes injected with OATP1A2, were pre-incubated in Na^+ buffer, pH 7.4, for 30 min at room temperature. Oocytes were washed three times with Na^+ buffer, pH 7.4, and then incubated with 20 nM ^{3}H-ES in Na^+ buffer in the absence or presence of 5 or 20 μM carbonylcyanide *p*-trifluoromethoxyphenyl hydrazone (FCCP) at pH 7.4 or pH 5.0 for 60 min. To test the effect of intracellular GSH on OATP1A2-mediated transport, oocytes injected with OATP1A2, were pre-incubated in Na^+ buffer in the absence or presence of 25 or 50 mM GSH with 0.5 mM acivicin, pH 7.4, for 30 min at room temperature. Oocytes were washed three times with Na^+ buffer, pH 7.4, and then incubated with 20 nM ^{3}H-ES in Na^+ buffer, pH 7.4, for 60 min. To test the effect of intracellular HCO_3^- on OATP1A2-mediated transport, oocytes injected with OATP1A2, were pre-incubated in buffer where NaCl was partially or completely substituted with 50 or 100 mM $NaHCO_3$, for 30 min at room temperature. Oocytes were washed three times with Na^+ buffer, pH 7.4, and then incubated with 20 nM ^{3}H-ES in Na^+ buffer, pH 7.4, for 60 min. To test the effect of intracellular OH^- on OATP1A2-mediated transport, oocytes injected with OATP1A2, were pre-incubated in Na^+ buffer in the absence or presence of 2 mM NaOH, pH 8.5, for 30 min at room temperature. Oocytes were washed three times with Na^+ buffer, pH 7.4, and then incubated with 20 nM ^{3}H-ES in Na^+ buffer, pH 7.4 or pH 5.0, for 60 min. The data is presented as percentage of control uptake by OATP1A2 injected oocytes measured in Na^+ buffer at either pH 7.4 or pH 5.0 after correction for the uptake of uninjected oocytes. Data are representative of 2-3 independent experiments. Each value represents the mean ± SE from 7-9 oocytes. P values were determined by comparing uptake under each condition to the control uptake at each Na^+ buffer pH,

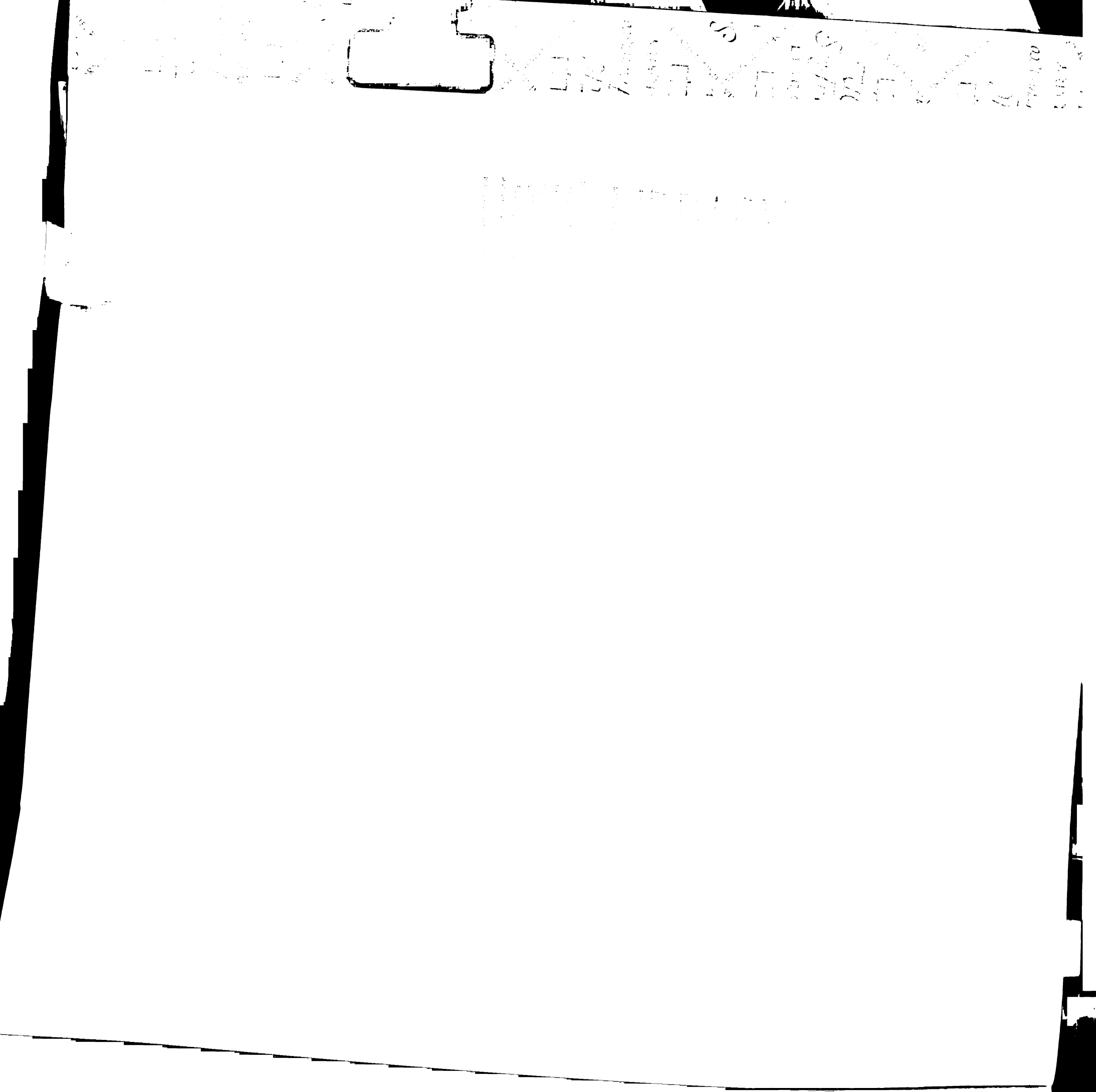

separately, using one-way ANOVA and Tukey's multi-comparison test with $p < 0.05$ as the criterion of significance.

Effect of Intracellular GSH concentration on ^{3}H-ES uptake

Endogenous GSH concentration in oocytes is approximately 2.5 mM (12). To increase GSH intracellularly, oocytes were injected with increasing concentrations of stock solutions of GSH, as previously described (12). After injection, oocytes were incubated in Na^+ buffer, pH 7.4, for 30 min in the presence of 0.5 mM acivicin to inhibit γ-glutamyl transpeptidase activity before they were used in the transport experiment. Oocytes were washed three times with Na^+ buffer, pH 7.4, and then incubated with 20 nM ^{3}H-ES in Na^+ buffer, pH 7.4, for 60 min. The data are presented as percentage of control uptake by OATP1A2 injected oocytes measured in Na^+ buffer at either pH 7.4 or pH 5.0 after correction for the uptake of uninjected oocytes. Each value represents the mean ± SE from 7-9 oocytes. P values were determined by comparing each GSH condition to the control uptake (2.5 mM endogenous GSH and no GSH injection) using one-way ANOVA and Tukey's multi-comparison test with $p < 0.05$ as the criterion of significance.

Construction and functional studies of PDZ consensus sequence mutants in OATP1A2.

Mutants in the PDZ consensus sequence in the C-terminus of OATP1A2 were constructed by site-directed mutagenesis of OATP1A2-pcDNA5/FRT. Mutants were verified by sequencing. HEK293 cells were transiently transfected with pcDNA5/FRT, OATP1A2 reference, and the OATP1A2 PDZ motif mutants, p. Thr668Ala, p. Thr668Asn, and p. DEL 667-670 (which has the last 4 amino acids in the OATP1A2

protein deleted). The cells were incubated with 20 nM ^{3}H-ES in Na^{+} buffer at pH 7.4 or pH 5.0 for 2 min. The data are presented as percentage of ES uptake by OATP1A2 reference, pH 7.4, and are representative of 3 independent experiments. Each value represents the mean ± SE from 3 wells. P values were determined by comparing mutant uptake to OATP1A2 reference for each buffer pH using one-way ANOVA and Tukey's multi-comparison test with $p < 0.05$ as the criterion of significance. Mammalian expression clones of the PDZ domain containing 1 protein (PDZK1; NM_002614) and the intestinal and kidney enriched PDZ protein (IKEPP; NM_024791), in pCMV vectors were purchased from OriGene Technologies Inc. (Rockville, MD). PDZK1 and IKEPP were linearized with Sac II and transcribed *in vitro* using T7 RNA polymerase (mMESSAGE MACHINE T7 kit; Stratagene). Oocytes we coinjected with equal concentrations (75 ng/50 nL) of OATP1A2 and PDZK1 or IKEPP cRNA to test the effect of PDZ proteins on OATP1A2-mediated transport of ES and MTX. After injection, oocytes were incubated in Na^{+} buffer at pH 7.4 or 5.0 containing 20 nM ^{3}H-ES or 0.2 μM ^{3}H-MTX at room temperature for 60 min. The data are presented as mean ± SE from 7-9 oocytes.

Functional analysis of cationic residues in OATP1A2 on ^{3}H-ES and/or ^{3}H-MTX uptake

To assess the importance of cationic residues in OATP1A2-mediated transport of ES, the amino acid-modifying reagents, phenylglyoxal (PGO), trinitrobenzenesulfonic acid (TNBS), and diethyl pyrocarbonate (DEPC) were used to irreversibly inhibit arginine, lysine, and histidine residues, respectively. HEK293 cells transiently transfected with pcDNA5/FRT or OATP1A2 were pre-incubated in Na^{+} buffer in the absence or

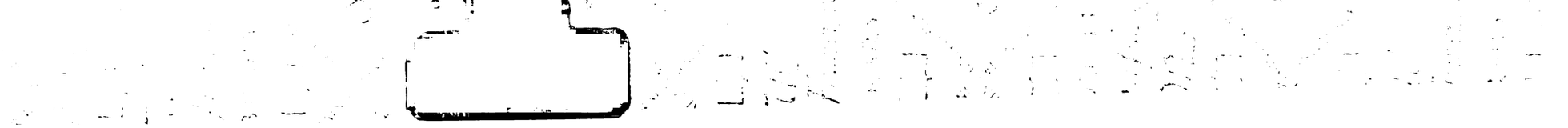

presence of 1 mM of PGO, TNBS, or DEPC for 30 min. Cells were washed twice with PBS and then incubated with 20 nM ^{3}H-ES in Na^{+} buffer at pH 7.4 or 5.0 for 2 min at 37°C. The data are presented as percentage of ES uptake by OATP1A2 in the absence of inhibitors and each value represents the mean ± SE from 3 wells. P values were determined by comparing uptake in the presence to that in the absence of an inhibitor using one-way ANOVA and Tukey's multi-comparison test with $p < 0.05$ as the criterion of significance. Arginine and lysine residues in OATP1A2 that occur in transmembrane domains or in extracellular loops were altered to alanine by site-directed mutagenesis of OATP1A2-pcDNA5/FRT. Mutants were verified by sequencing. HEK293 cells transiently transfected with pcDNA5/FRT, OATP1A2, or the mutant transporters were incubated with 20 nM ^{3}H-ES in Na^{+} buffer at pH 7.4 or 5.0 for 2 min at 37°C. The data are presented as percentage of ES uptake by OATP1A2 reference, pH 7.4. Each value represents the mean ± SE from 3 wells. P values were determined by comparing mutant uptake to OATP1A2 reference for each buffer pH using one-way ANOVA and Tukey's multi-comparison test with $p < 0.05$ as the criterion of significance. In addition, all histidine residues in OATP1A2 were mutated to alanine by mutagenesis of OATP1A2-pOX. Oocytes injected with OATP1A2 or the mutant transporters were incubated in Na^{+} buffer at pH 7.4 or 5.0 containing 0.2 μM ^{3}H-MTX at room temperature for 60 min. The data are presented as percentage of MTX uptake by OATP1A2 reference at pH 7.4. Each value represents the mean ± SE from 7-9 oocytes. P values were determined by comparing mutant uptake to OATP1A2 reference for each buffer pH using one-way ANOVA and Tukey's multi-comparison test with $p < 0.05$ as the criterion of significance.

Functional analysis of charged amino acid replacements in OATP1A2 to uncharged or oppositely charged ones in rOatp1a1/Oatp1a4 on ^{3}H-ES transport

To identify the amino acid residues responsible for pH-dependent transport of organic anions by OATP1A2, charged residues found in transmembrane domains and extracellular loops of OATP1A2 were altered by site-directed mutagenesis of OATP1A2-pcDNA5/FRT to the corresponding ones found in both rat Oatp1a1 (NM_017111) and rat Oatp1a4 (NM_131906), whose transport mechanism seems to be independent of extracellular pH (11-14). Mutants were verified by sequencing. HEK293 cells transiently transfected with pcDNA5/FRT, OATP1A2, or the mutant transporters were incubated with 20 nM ^{3}H-ES in Na^{+} buffer at pH 7.4 or 5.0 for 2 min at 37°C. The data are presented as percentage of ES uptake by OATP1A2 reference, pH 7.4. Each value represents the mean ± SE from 3 wells. P values were determined by comparing mutant uptake to OATP1A2 reference for each buffer pH using one-way ANOVA and Tukey's multi-comparison test with $p < 0.05$ as the criterion of significance.

RESULTS

Transport of ES by OATP1A2 is sensitive to extracellular pH (pH_o)

ES transport was significantly increased at acidic pH in OATP1A2 expressing cells. ES uptake was 3-fold greater at pH 5.0 (2.50 ± 0.18 pmol/mg of protein/2 min) in comparison to pH 7.4 (0.85 ± 0.03 pmol/mg of protein/2 min). The uptake by cells transfected with empty vector was not significantly affected by pH. Transport of ES in cells expressing OATP1A2 was linear for up to 2 min at pH 5.0 (data not shown). Therefore, an incubation time of 2 min was chosen for all subsequent experiments. ES

transport by OATP1A2 exhibited saturation at both pH 7.4 and pH 5.0. The K_m of ES for OATP1A2 at pH 7.4 increased by 7-fold ($p < 0.05$) compared to that at pH 5.0 (Figure 2). There was a significant decrease ($p< 0.05$) in the maximal transport rate of ES by OATP1A2 at pH 5.0 compared to pH 7.4. The K_m and V_{max} values at pH 7.4 were 13.6 ± 3.2 μM and 127 ± 20.3 pmol/mg of protein/2 min, respectively, and those at pH 5.0 were 1.94 ± 0.5 μM and 66.8 ± 3.9 pmol/mg of protein/2 min, respectively. These data suggest that increased ES uptake at extracellular acidic pH by OATP1A2 results primarily from higher affinity of ES for OATP1A2.

OATP1A2-mediated transport of ES does not depend on intracellular pH (pH_i) or the proton gradient

As shown in Figure 3, changing the intracellular pH while keeping the extracellular pH constant did not significantly decrease OATP1A2-mediated transport of ES. Specifically, when either the pH gradient across the membrane was reversed or eliminated, ES transport by OATP1A2 remained unchanged compared to the uptake in the presence of an inwardly directed pH gradient (pH_{in}/pH_{out} = 7.4/5.0). As shown in Table 1, in the presence of an initial inwardly directed proton gradient (pH_{in}/pH_{out} = 7.4/5.0) the uptake of ES by OATP1A2 was not significantly decreased when 5 and 20 μM FCCP, a proton ionophore, were used in the uptake buffer. Similar data were obtained in HEK293 cells transiently transfected with OATP1A2 and are consistent with our previous studies showing that MTX transport by OATP1A2 is also not sensitive to the proton gradient (10). Altogether these data suggest that the pH-sensitive transport of organic anions by OATP1A2 does not depend on the proton gradient or movement of

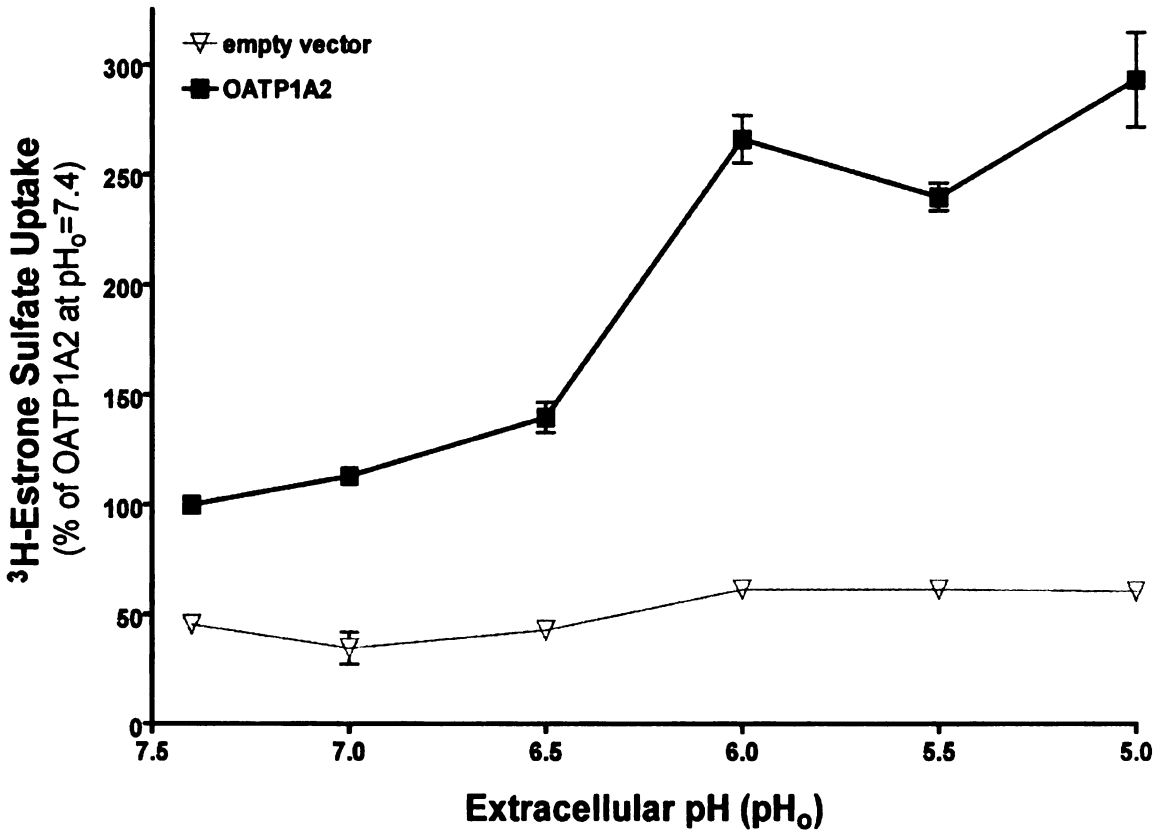

Figure 1. Transport of ES by OATP1A2 in transiently transfected HEK293 cells is sensitive to extracellular pH. Uptake of 20 nM ^{3}H-ES in HEK293 cells transiently transfected with empty vector (gray inverted triangles) or OATP1A2 (black squares) in the presence of decreasing extracellular pH. Transport of ES was measured in Na^+ buffer over 2 min. Uptake is expressed as percentage of ES uptake by OATP1A2 transfected cells at pH 7.4. The pH of the uptake buffer was adjusted with Trizma and HCl. Data are representative of 3 independent experiments. Each value represents the mean ± SE from 3 wells.

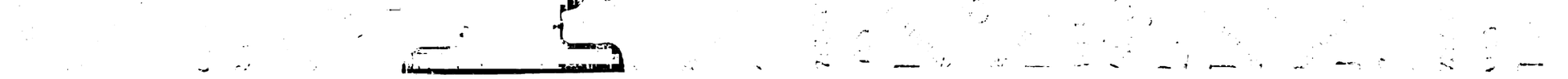

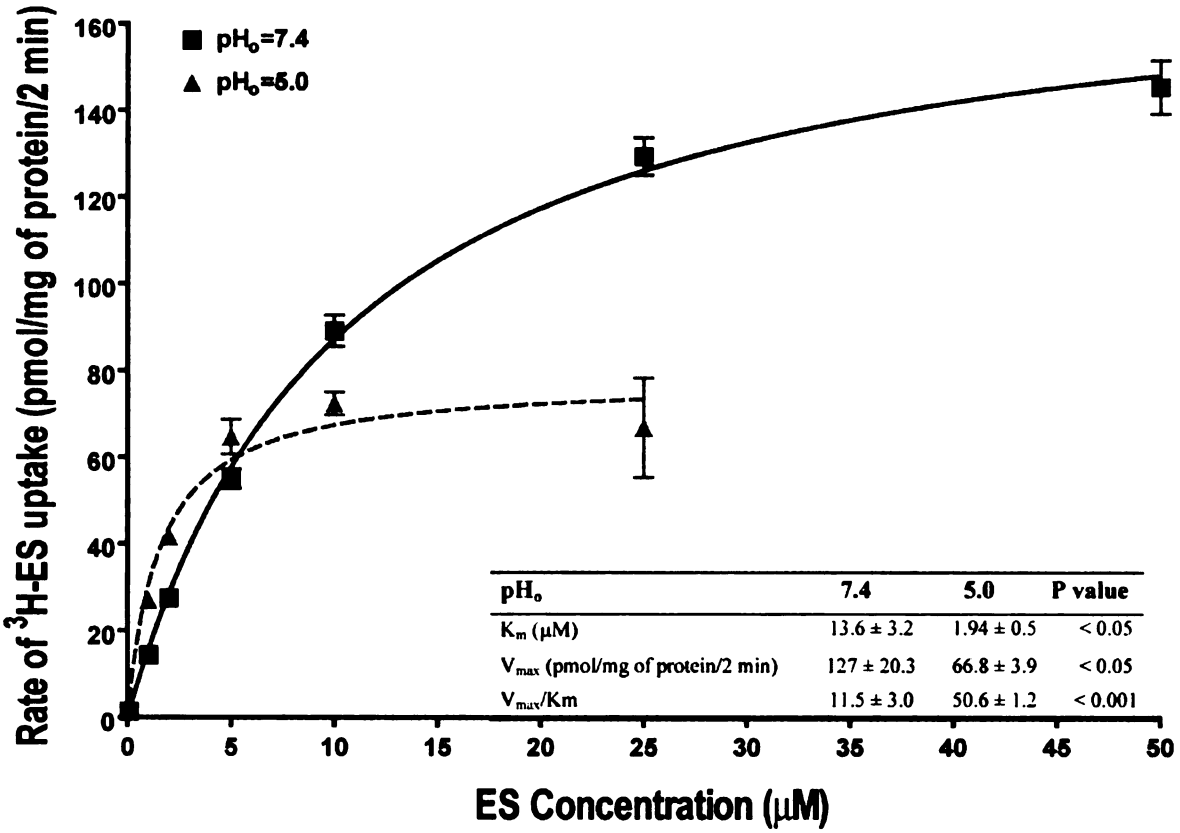

pH$_o$	7.4	5.0	P value
K_m (μM)	13.6 ± 3.2	1.94 ± 0.5	< 0.05
V_{max} (pmol/mg of protein/2 min)	127 ± 20.3	66.8 ± 3.9	< 0.05
V_{max}/Km	11.5 ± 3.0	50.6 ± 1.2	< 0.001

Figure 2. Kinetics of ES transport by OATP1A2 at pH$_o$ 5.0 shows dramatic decrease in K_m compared to pH$_o$ 7.4 in transiently transfected HEK293 cells. Uptake of 20 nM ^{3}H-ES in HEK293 cells transiently transfected with OATP1A2 was measured over 2 min in the presence of increasing concentrations of unlabeled ES in Na^+ buffer at pH 7.4 (squares) or pH 5.0 (triangles). Data are representative of 3 independent experiments. Each value represents the mean ± SE from 3 wells. *Inset,* kinetic parameters of ES transport by OATP1A2 were determined by fitting the data using nonlinear regression analysis. Data is presented as mean ± SE of 3 independent experiments. P values were determined by comparing kinetic parameters at pH 5.0 to pH 7.4 using the unpaired Student's *t* test with $p < 0.05$ as the criterion of significance.

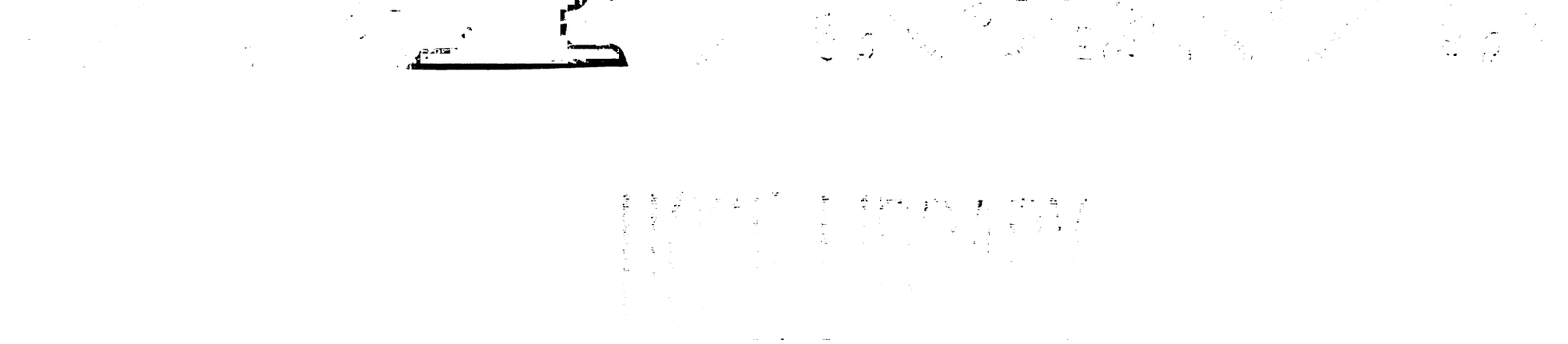

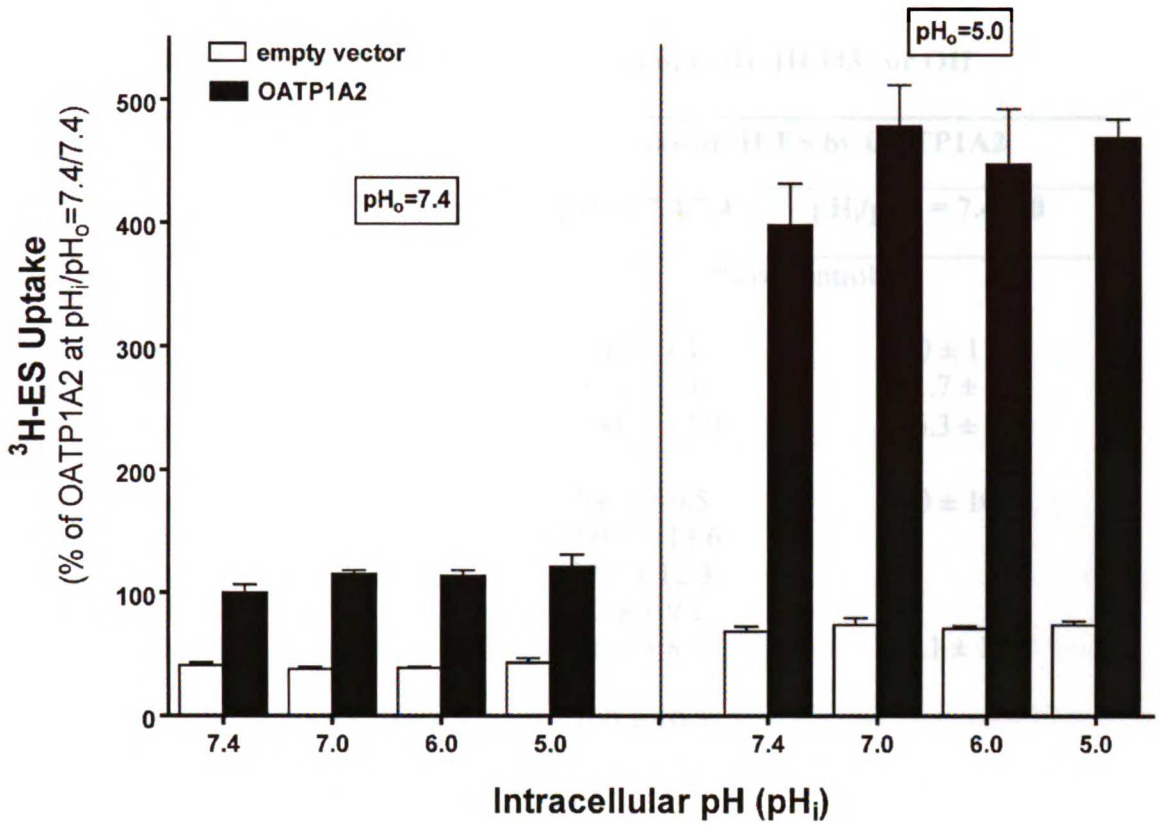

Figure 3. Transport of ES by OATP1A2 is not sensitive to intracellular pH in transiently transfected HEK293 cells. Uptake of 20 nM ^{3}H-ES in HEK293 cells transiently transfected with empty vector (white bars) or OATP1A2 (black bars) in the presence of decreasing intracellular pH. Cells were preloaded with Na^+ buffer at various pHs for 30 min to establish intracellular pH (pH_i). Transport of ES was measured in Na^+ buffer at pH 7.4 or 5.0 over 2 min. Uptake is expressed as percentage of ES uptake by OATP1A2 in Na^+ buffer at pH_i/pH_o=7.4/7.4. Data are representative of 3 independent experiments. Each value represents the mean ± SE from 3 wells. P values were determined using one-way ANOVA and Tukey's multi-comparison test with $p < 0.05$ as the criterion of significance.

Table 1. Transport of ES by OATP1A2 in *X. laevis* oocytes is not sensitive to the proton gradient or intracellular concentrations of GSH, $HCO3^-$, or OH^-

	Uptake of ^{3}H-ES by OATP1A2	
	pH_i/pH_o = 7.4/7.4	pH_i/pH_o = 7.4/5.0
	% of control	
No FCCP (control)	100 ± 7.1	100 ± 11.1
5 μM FCCP	130.1 ± 10.2	111.7 ± 9.6
20 μM FCCP	139.6 ± 14.9	116.3 ± 9.2
NaCl Preload (control)	100 ± 10.5	100 ± 10.4
25 mM GSH	109.1 ± 13.6	
50 mM GSH	87.2 ± 12.3	
50 mM $NaHCO_3$	82.8 ± 9.2	
100 mM $NaHCO_3$	86.9 ± 8.3	110.1 ± 10.6
2.5 mM intracellular GSH (control)	100 ± 10.5	
5 mM intracellular GSH	75.6 ± 10.3	
10 mM intracellular GSH	74.3 ± 11.1	
20 mM intracellular GSH	91.3 ± 19.7	
30 mM intracellular GSH	88.3 ± 14.5	
40 mM intracellular GSH	91.0 ± 12.2	
NaCl Preload (control)	100 ± 9.4	100 ± 10.6
2 mM NaOH (pH 8.5)	96.9 ±10.7	113.4 ± 12.2

Uninjected oocytes and oocytes injected with 75 ng of OATP1A2 cRNA were preincubated for 30 min at 25°C in NaCl, NaCl + GSH, $NaHCO_3$ buffers at pH 7.4, or NaCl + NaOH buffer at pH 8.5. The preload Na^+ buffer with GSH contained 0.5 mM acivicin. The oocytes were washed with Na^+ buffer, pH 7.4, before incubation with 20 nM ^{3}H-ES for 60 min in Na^+ buffer at pH 7.4 or 5.0. The proton ionophore, FCCP, was used in Na^+ buffer in the presence of ^{3}H-ES at pH 7.4 and 5.0 to eliminate the proton gradient across the membrane. To increase intracellular GSH oocytes were injected with various GSH stock solutions. Oocytes were then incubated in Na^+ buffer, pH 7.4, for 30 min in the presence of 0.5 mM acivicin before the transport experiment was initiated. The results are shown as percentage of control uptake measured in Na^+ uptake buffer after correction for the uptake of uninjected oocytes. Data are representative of 2-3 independent experiments. Each value represents the mean ± SE from 7-9 oocytes. P values were determined by comparing uptake under each condition to the control uptake at each Na^+ buffer pH, separately, using one-way ANOVA and Tukey's multi-comparison test with $p < 0.05$ as the criterion of significance.

protons across the membrane.

OATP1A2-mediated transport of ES does not depend on the sodium gradient or membrane potential

As shown in Figure 4, uptake of ES in the absence of sodium (NMDG) was not significantly different compared to that in the presence of sodium (NaCl) at either extracellular pH 7.4 or 5.0. These data confirm that transport of organic anions by OATP1A2 is sodium-independent. To assess whether OATP1A2-mediated transport is driven by the potential across the membrane, ES uptake was measured in cells expressing OATP1A2 under altered K^+ permeability conditions, adapted from methods previously described (11, 18, 19). In this approach, the membrane potential was depolarized by increasing the concentration of K^+ (128 mM) and reducing the concentration of Na^+ (1 mM) simultaneously in the uptake buffer, in effect decreasing the outwardly directed K^+ gradient across the membrane. As shown in Figure 4, transport of ES by OATP1A2 in the presence of high K^+ buffer did not significantly differ from that in the presence of low K^+ buffer at either pH 7.4 or 5.0. Uptake of ES in the presence of high K^+ (102 mM) and low Na^+ (1 mM) in the uptake buffer at pH 7.4 and 5.0 was also performed in oocytes expressing OATP1A2 with similar results (data not shown). These data indicate that the pH-sensitive transport of organic anions by OATP1A2 does not depend on the membrane potential and that OATP1A2 mechanism of transport is not potential-sensitive.

OATP1A2-mediated transport of ES is not sensitive to intracellular concentrations of GSH, HCO_3^-, or OH^-

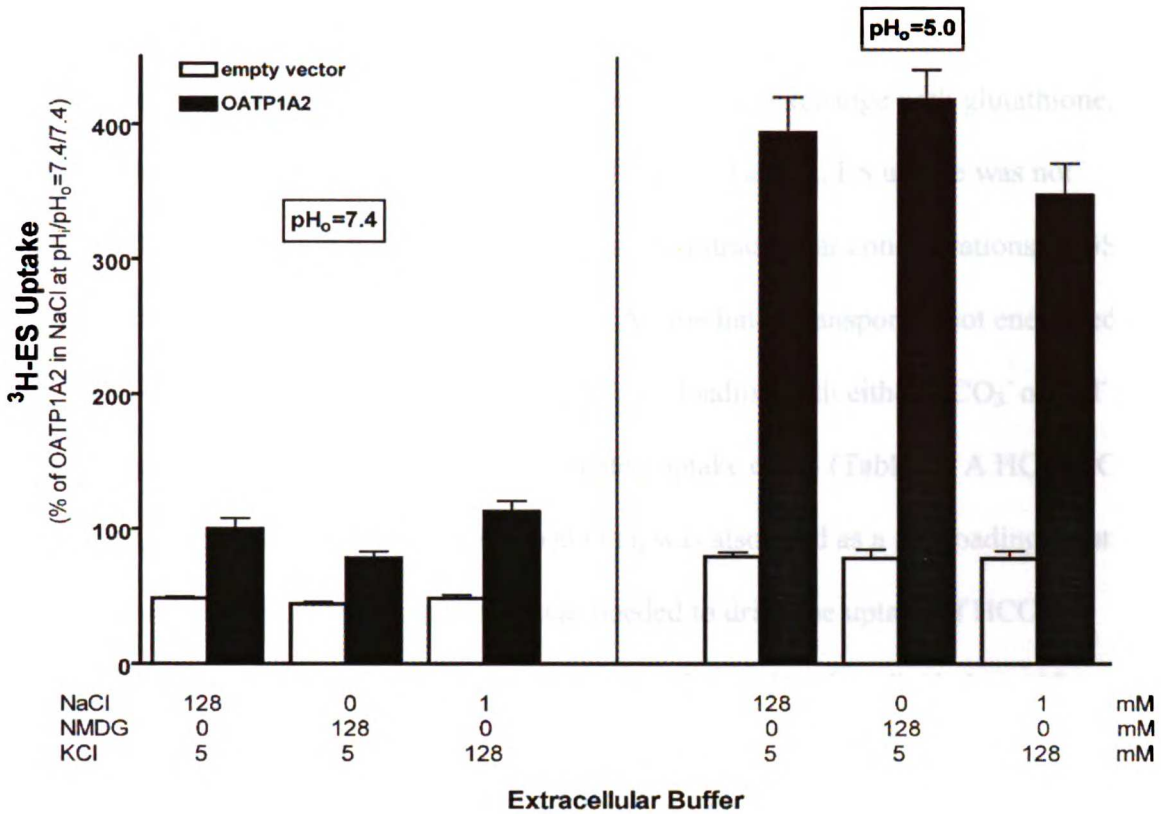

Figure 4. Transport of ES by OATP1A2 is not sensitive to the sodium gradient or membrane potential in transiently transfected HEK293 cells. Uptake of 20 nM ^{3}H-ES in HEK293 cells transiently transfected with empty vector (white bars) or OATP1A2 (black bars) in the presence of sodium (NaCl), in the absence of sodium (NMDG), or in the presence of potassium (KCl) at high concentrations to short-circuit the membrane potential. Cells were preloaded with Na^+ buffer, pH 7.4, for 25 min followed by sodium-free or high potassium buffer at pH 7.4 for an additional 5 min. Transport of ES was measured over 2 min in Na^+ buffer at pH 7.4 or 5.0. Uptake is expressed as percentage of ES uptake by OATP1A2 in Na^+ buffer at pH_i/pH_o=7.4/7.4. Data are representative of 3 independent experiments. Each value represents the mean ± SE from 3 wells. P values were determined using one-way ANOVA and Tukey's multi-comparison test with $p < 0.05$ as the criterion of significance.

UCSF LIBRARY

Previous functional studies with rat Oatps have suggested that the mechanism for organic anion transport across the membrane could involve exchange with glutathione, bicarbonate, and/or hydroxyl ions (11-14). As shown in Table 1, ES uptake was not significantly stimulated in the presence of increasing intracellular concentrations of GSH injected into the oocyte, suggesting that OATP1A2-mediated transport is not energized by efflux of intracellular GSH. Further, intracellular loading with either HCO_3^- or OH^- did not significantly enhance OATP1A2-mediated uptake of ES (Table 1). A HCO_3^-, Cl^--free buffer, prepared as previously described (11), was also used as a pre-loading solution in the event that the HCO_3^-/Cl^-exchanger was needed to drive the uptake of HCO_3^- intracellularly. However, similar observations were obtained as described above (data not shown). Altogether these data indicate that, unlike rat Oatps, transport of organic anions by OATP1A2 is not driven by exchange with intracellular GSH, HCO_3^-, or OH^-.

PDZ consensus sequence in C-terminus of OATP1A2 is not required for organic anion transport

Recently, it was determined that the C-terminus of OATP1A2 contains a PDZ consensus sequence that interacts *in vitro* with PDZ domain-containing proteins, such as PDZK1 and IKEPP (15). Furthermore, rodent Oatp1a1 was shown to interact with PDZK1 *in vivo* and this interaction affected the proper subcellular localization and function of this transporter (16). The PDZ consensus sequence in OATP1A2 is proposed to contain the last 6 amino acids of OATP1A2 (-ELKTKL), where T/S-X-L is considered to be a Class I PDZ domain binding motif (20) (Figure 5 and 6). As previously described (10), the naturally occurring variant p. Thr668Ser occurs at one of the amino acids in the

```
OATP1A2         ------------------------------------------------------------
rOatp1a1        ------------------------------------------------------------
rOatp1a3        ------------------------------------------------------------
rOatp1a4        ------------------------------------------------------------
rOatp1a5        ------------------------------------------------------------
OATP1B1         ------------------------------------------------------------
OATP1B3         ------------------------------------------------------------
rOatp1b2        ------------------------------------------------------------
OATP1C1         ------------------------------------------------------------
OATP2B1         ------------------------------------------------------MGPRI  5
OATP3A1         ------------------------------------------------------------
OATP4A1         MPLHQLGDKPLTFPSPNSAMENGLDHTPPSRRASPGTPLSPGSLRSAAHSPLDTSKQPLC  60

                                  *                                1     **
OATP1A2         -MGETEK-------RIETHRIR----------------CLSKLKMFLLAITCAFVSKTLS  36
rOatp1a1        -MEETEK-------KIATQEGR----------------LFSKMKVFLLSLTCACLTKSLS  36
rOatp1a3        -MGDLEK-------GAATHGAG----------------CFAKIKVFLMALTCAYVSKSLS  36
rOatp1a4        -MGKSEK-------RVATHGVR----------------CFAKIKMFLLALTCAYVSKSLS  36
rOatp1a5        -MGETEK-------RVATHEVR----------------CFSKIKMFLLALTWAYVSKSLS  36
OATP1B1         -MDQNQHLN-----KTAEAQPSE----------NKKTRYCNGLKMFLAALSLSFIAKTLG  44
OATP1B3         -MDQHQHLN-----KTAESASSE----------KKKTRRCNGFKMFLAALSFSYIAKALG  44
rOatp1b2        -MDHTQQSR-----KAAEAQPSR----------SKQTRFCDGFKLFLAALSFSYICKALG  44
OATP1C1         -MDTSSKENIQLFCKTSVQPVGRPSFKTEYPSSEEKQPCCGELKVFLCALSFVYFAKALA  59
OATP2B1         GPAGEVPQVPDKETKATMGTENTPGGKASPDPQDVRPSVFHNIKLFVLCHSLLQLAQLMI  65
OATP3A1         -MQGKKPGGSSGGGRSGELQGDEAQRNKK---KKKKVSCFSNIKIFLVSECALMLAQGTV  56
OATP4A1         QLWAEKHGARGTHEVRYVSAGQSVACGWWAFAPPCLQVLNTPKGILFFLCAAAFLQGMTV 120

                ***                2                *
OATP1A2         GSYMNSMLTQIERQFNIPTSLVGFINGSFEIGNLLLIIFVSYFGTKLHRPIMIGIGCVVM  96
rOatp1a1        GVYMNSMLTQIERQFDISTSVAGLINGSFEIGNLFFIVFVSYFGTKLHRPVVIGIGCVIM  96
rOatp1a3        GTFMSSMLTQIERQFGIPTAIVGFINGSFEIGNLLLIIFVSYFGMKLHRPIVIGVGCAVM  96
rOatp1a4        GTYMNSMLTQIERQFGIPTSIVGLINGSFEIGNLLLIIFVSYFGTKLHRPIMIGVGCAVM  96
rOatp1a5        GIYMNTMLTQIERQFDIPTSIVGFINGSFEIGNLLLIIFVSYFGTKLHRPIMIGVGCVIM  96
OATP1B1         AIIMKSSIIHIERRFEISSSLVGFIDGSFEIGNLLVIVFVSYFGSKLHRPKLIGIGCFIM 104
OATP1B3         GIIMKISITQIERRFDISSSLAGLIDGSFEIGNLLVIVFVSYFGSKLHRPKLIGIGCLLM 104
rOatp1b2        GVVMKSSITQIERRFDIPSSISGLIDGGFEIGNLLVIVFVSYFGSKLHRPKLIGIGCFIM 104
OATP1C1         EGYLKSTITQIERRFDIPSSLVGVIDGSFEIGNLLVITFVSYFGAKLHRPKIIGAGCVIM 119
OATP2B1         SGYLKSSISTVEKRFGLSSQTSGLLASFNEVGNTALIVFVSYFGSRVHRPRMIGYGAILV 125
OATP3A1         GAYLVSVLTTLERRFNLQSADVGVIASSFEIGNLALILFVSYFGARGHRPRLIGCGGIVM 116
OATP4A1         NGFINTVITSLERRYDLHSYQSGLIASSYDIAACLCLTFVSYFGGSGHKPRWLGWGVLLM 180

                3     *
OATP1A2         GLGCFLKSLPHFLMN--QYEYESTVSVSGNLSSNSFLCMENGTQILRPTQDPS------E 148
rOatp1a1        GLGCLLMSLPHFFMG--RYEYETTISPTGNLSSNSFLCMENRTQTLKPTQDPA------E 148
rOatp1a3        GLGCFIISLPHFLMG--RYEYETTILPTSNLSSNSFLCMENQTQTLNPAQDPA------E 148
rOatp1a4        GLGCFLISLPHFLMG--QYEYET-ILPTSNVSSNSFFCVENRSQTLNPTQDPS------E 147
rOatp1a5        GLGCFLMSLPHFLMG--RYEYETTISPTSNLSSNSFLCMENRSQTLKPTQDPA------E 148
OATP1B1         GIGGVLTALPHFFMGYYRYSKETNIDSSENSTSTLSTCLINQILSLNRASPEIVGK---G 161
OATP1B3         GTGSILTSLPHFFMGYYRYSKETHINPSENSTSSLSTCLINQTLSFNGTSPEIVEK---D 161
rOatp1b2        GIGSILTALPHFFMGYYKYAKENDIGSLGNST---LTCFINQMTSPTGPSPEIVEK---G 158
OATP1C1         GVGTLLIAMPQFFME--QYKYERYSPSSNSTLSISPCLLESSSQLPVSVMEKSKSKISNE 177
OATP2B1         ALAGLLMTLPHFISEP--YRYDNTSPEDMPQDFKASLCLPTTSAPASAPSNGNCSS---- 179
OATP3A1         ALGALLSALPEFLTH----QYKYEAGEIRWGAEGRDVCAANGSGGDEGPDPDLICR---- 168
OATP4A1         GTGSLVFALPHFTAG--RYEVELDAGVRTCPANPGAVCADSTSG---------------- 222
```

```
                    **          ***     4                              5
OATP1A2         CTKEVKSLMWVYVLVGNIVRGMGETPILPLGISYIEDFAKFENSPLYIGLVETGAIIGPL 208
rOatp1a1        CVKEMKSLMWICVMVGNIIRGIGETPIVPLGISYIEDFAKSENSPLYIGILEMGKVAGPI 208
rOatp1a3        CVKEVKSLMWIYVLVGNIIRGIGETPIMPLGVSYIENFAKSENSPLYIGILETGKMIGPI 208
rOatp1a4        CVKEMKSLMWIYVLVGNIIRGIGETPIMPLGISYIEDFAKSENSPLYIGILETGMTIGPL 207
rOatp1a5        CIKEMKSLMWIYVLVGNIIRGIGETPIMPLGISYIEDFAKSENSPLYIGILETGKVFGPI 208
OATP1B1         CLKESGSYMWIYVFMGNMLRGIGETPIVPLGLSYIDDFAKEGHSSLYLGILNAIAMIGPI 221
OATP1B3         CVKESGSHMWIYVFMGNMLRGIGETPIVPLGISYIDDFAKEGHSSLYLGSLNAIGMIGPV 221
rOatp1b2        CEKGLKSHMWIYVLMGNMLRGIGETPIVPLGISYLDDFAKEGHTSMHLGTLHTIAMIGPI 218
OATP1C1         CEVDTSSSMWIYVFLGNLLRGIGETPIQPLGIAYLDDFASEDNAAFYIGCVQTVAIIGPI 237
OATP2B1         YTETQHLSVVGIMFVAQTLLGVGGVPIQPFGISYIDDFAHNSNSPLYLGILFAVTMMGPG 239
OATP3A1         -NRTATNMMYLLLIGAQVLLGIGATPVQPLGVSYYDDHVRRKDSSLYIGILFTMLVFGPA 227
OATP4A1         -----LSRYQLVFMLGQFLHGVGATPLYTLGVTYLDENVKSSCSPVYIAIFYTAAILGPA 277

                                    ***          6
                IGLLLASFCANVYVDTGFVNTDDLIITPTDTRWVGAWWFGFLICAGVNVLTAIPFFFLPN 268
rOatp1a1        FGLLLGSYCAQIYVDIGSVNTDDLTITPSDTRWVGAWWIGFLVCAGVNILTSIPFFFLPK 268
rOatp1a3        FGLLLGSFCASIYVDTGSVNTDDLTITPTDIRWVGAWWIGFLVCAGVNILISIPFFFFPK 268
rOatp1a4        IGLLLASSCANIYVDIESVNTDDLTITPTDTRWVGAWWIGFLVCAGVNILTSFPFFFFPK 267
rOatp1a5        VGLLLGSFCASIYVDTGSVNTDDLTITPTDTRWVGAWWIGFLICAGVNILSSIPFFFFPK 268
OATP1B1         IGFTLGSLFSKMYVDIGYVDLSTIRITPTDSRWVGAWWLNFLVSGLFSIISSIPFFFLPQ 281
OATP1B3         IGFALGSLFAKMYVDIGYVDLSTIRITPKDSRWVGAWWLGFLVSGLFSIISSIPFFFLPK 281
rOatp1b2        LGFIMSSVFAKIYVDVGYVDLNSVRITPNDARWVGAWWLSFIVNGLLCITSSIPFFFLPK 278
OATP1C1         FGFLLGSLCAKLYVDIGFVNLDHITITPKDPQWVGAWWLGYLIAGIISLLAAVPFWYLPK 297
OATP2B1         LAFGLGSLMLRLYVDINQMPEGGISLTIKDPRWVGAWWLGFLIAAGAVALAAIPYFFFPK 299
OATP3A1         CGFILGSFCTKIYVDAVFIDTSNLDITPDDPRWIGAWWGGFLLCGALLFFSSLLMFGFPQ 287
OATP4A1         AGYLIGGALLNIYTEMGRR----TELTTESPLWVGAWWVGFLGSGAAAFFTAVPILGYPR 333

OATP1A2         TLPKEGLETNADIIK--------NENEDKQKEEVKKEKYGITKDFLPF------------ 308
rOatp1a1        ALPKKGQQENVAVTK--------DGKVEKYGGQAREENLGITKDFLTF------------ 308
rOatp1a3        TLPKEGLQENVDGTE--------NAKEESTEKRPRKKNRGITKDFFPF------------ 308
rOatp1a4        TLPKEGLQENVDGTE--------NAKEKKHRKKAKEEKRGITKDFFVF------------ 307
rOatp1a5        TLPKEGLQDDVDGTN--------NDKEEKHREKAKEENRGITKDFLPF------------ 308
OATP1B1         -TPNKPQKERKASLSLHVLETNDEKDQTANLTNQGKNITKNVTGFFQS------------ 328
OATP1B3         -NPNKPQKERKISLSLHVLKTNDDRNQTANLTNQGKNVTKNVTGFFQS------------ 328
rOatp1b2        -IPKRSQEERKNSVSLHAPKTDEEKKHMTNLTKQEEQDPSNMTGFLRS------------ 325
OATP1C1         SLPRSQSREDSNSSSEKSKFIIDDHTDYQTPQGENAKIMEMARDFLPS------------ 345
OATP2B1         EMPKEKRELQFRRKVLAVTDSPARKGKDSPSKQSPGESTKKQDGLVQIAPNLTVIQFIKV 359
OATP3A1         SLPPHSDPAMESEQAMLSEREYERPKPSNGVLRHPLEPDSSASCFQQLRV---------- 337
OATP4A1         QLPGSQRYAVMRAAEMH------QLKDSSRGEASNPDFGKTIRDLPLS375---------- 

                                7                **              8
OATP1A2         ----MKSLSCNPIYMLFILVSVIQFNAFVNMISFMPKYLEQQYGISSSDAIFLMGIYNLP 364
rOatp1a1        ----MKRLFCNPIYMLFILTSVLQVNGFINKFTFLPKYLEQQYGKSTAEAIFLIGVYSLP 364
rOatp1a3        ----LKSPVLQPDLHAVHPYKVLQVNAFNIYFSFLPKYLENQYGKSTAEVIFLMGVYNLP 364
rOatp1a4        ----MKSLSCNPIYMLFILISVLQFNAFINSFTFMPKYLEQQYGKSTAEVVFLMGLYMLP 363
rOatp1a5        ----MKSLSCNPIYMLLILTSVLQINAFINMFTFLPKYLEQQYGKSTAEVVLLIGVYNLP 364
OATP1B1         ----FKSILTNPLYVMFVLLTLLQVSSYIGAFTYVFKYVEQQYGQPSSKANILLGVITIP 384
OATP1B3         ----LKSILTNPLYVIFLLLTLLQVSSFIGSFTYVFKYMEQQYGQSASHANFLLGIITIP 384
rOatp1b2        ----LRSILTNEIYVIFLILTLLQVSGFIGSFTYLFKFIEQQFGRTASQANFLLGIITIP 381
OATP1C1         ----LKNLFGNPVYFLYLCTSTVQFNSLFGMVTYKPKYIEQQYGQSSSRANFVIGLINIP 401
OATP2B1         FPRVLLQTLRHPIFLLVVLSQVCLSSMAAGMATFLPKFLERQFSITASYANLLIGCLSFP 419
OATP3A1         IPKVTKHLLSNPVFTCIILAACMEIAVVAGFAAFLGKYLEQQFNLTTSSANQLLGMTAIP 397
OATP4A1         ----IWLLLKNPTFILLCLAGATEATLITGMSTFSPKFLESQFSLSASEAATLFGYLVVP 431
```

```
                                  *          9
                  ---------------  ----------
OATP1A2           PICIGYIIGGLIMKKFKITVKQAAHIGCWLSLLEYLLYFLSFLMTCENSSVVGINTSYEG 424
rOatp1a1          PICLGYLIGGFIMKKFKITVKKAAYLAFCLSVFEYLLFLCHFMLTCDNAAVAGLTTSYKG 424
rOatp1a3          AICIGYLIAGFMMKKFKITVKTAAFLRFCLSLSEYSFGFCNFLITCDNVPVAGLTNSYER 424
rOatp1a4          PICLGYLIGGLIMKKFKVTVKKAAHLAFWLCLSEYLLSFLSYVMTCDNFPVAGLTTSYEG 423
rOatp1a5          PICIGYLLIGFIMKKFKITVKKAAYMAFCLSLFEYLLYFLHFMITCDNFPVAGLTASYEG 424
OATP1B1           IFASGMFLGGYIIKKFKLNTVGIAKFSCFTAVMSLSFYLLYFFILCENKSVAGLTMTYDG 444
OATP1B3           TVATGMFLGGFIIKKFKLSLVGIAKFSFLTSMISFLFQLLYFPLICESKSVAGLTLTYDG 444
rOatp1b2          TMATAMFLGGYIVKKFKLTSVGIAKFVFFTSSVAYAFQFLYFPLLCENKPFAGLTLTYDG 441
OATP1C1           AVALGIFSGGIVMKKFRISVCGAAKLYLGSSVFGYLLFLSLFALGCENSDVAGLTVSYQG 461
OATP2B1           SVIVGIVVGGVLVKRLHLGPVGCGALCLLGMLLCLFFSLPLFFIGCSSHQIAGITHQTSA 479
OATP3A1           CACLGIFLGGLLVKKLSLSALGAIRMAMLVNLVSTACYVSFLFLGCDTGPVAGVTVPY-G 456
OATP4A1           AGGGGTFLGGFFVNKLRLRGSAVIKFCLFCTVVS-LLGILVFSLHCPSVPMAGVTASYGG 490


OATP1A2           IPQDLYVENDIFADCNVDCNCPSKIWDPVCG-NNGLSYLSACLAGCETSIGTGIN----M 479
rOatp1a1          VQHQLHVESKVLADCNTRCSCSTNTWDPVCG-DNGVAYMSACLAGCKKFVGTGTN----M 479
rOatp1a3          DQKPLYLENNVLADCNTRCSCLTKTWDPVCG-DNGLAYMSACLAGCEKSVGTGTN----M 479
rOatp1a4          VQHQLYVENKVLADCNTRCNCSTNTWDPVCG-DNGLAYMSACLAGCEKSVGTGTN----M 478
rOatp1a5          VHHPLYVENKVLADCNRGCSCSTNSWDPVCG-DNGLAYMSACLAGCKKSVGTGTN----M 479
OATP1B1           NNPVTSHRDVPLSYCNSDCNCDESQWEPVCG-NNGITYISPCLAGCKSSSGNKKP----I 499
OATP1B3           NNSVASHVDVPLSYCNSECNCDESQWEPVCG-NNGITYLSPCLAGCKSSSGIKKH----T 499
rOatp1b2          MNPVDSHIDVPLSYCNSDCSCDKNQWEPICG-ENGVTYISPCLAGCKSFRGDKKPNN--T 498
OATP1C1           TKPVSYHERALFSDCNSRCKCSETKWEPMCG-ENGITYVSACLAGCQTSNRSGKN----I 516
OATP2B1           HPG-----LELSPSCMEACSCPLDGFNPVCDPSTRVEYITPCHAGCSSWVVQDALDNSQV 534
OATP3A1           NSTAPGSALDPYSPCNNNCECQTDSFTPVCG-ADGITYLSACFAGCNSTN---------- 505
OATP4A1           SLLPEG-HLNLTAPCNAACSCQPEHYSPVCG-SDGLMYFSLCHAGCPAATETNVDGQ--K 546

                                  **                    10
                                                        ----------
OATP1A2           VFQNCSCI----QTSGNSSAVLGLCDKGPDCSLMLQYFLILSAMSSFIYSLAAIPGYMVL 535
rOatp1a1          VFQDCSCI----QSLGNSSAVLGLCKKGPECANRLQYFLILTIIISFIYSLTAIPGYMVF 535
rOatp1a3          VFHNCSCI----QSPGNSSAVLGLCNKGPECTNKLQYLLILSGFLSILYSFAAIPGYMVF 535
rOatp1a4          VFQNCSCI----QSSGNSSAVLGLCNKGPDCANKLQYFLIIAIFGCFIYSLAGIPGYMVL 534
rOatp1a5          VFQNCSCI----RSSGNSSAVLGLCKKGPECANKLQYFLIMSVIGSFIYSITAIPGYMVL 535
OATP1B1           VFYNCSCLEVTGLQNRNYSAHLGECPRDDACTRKFYFFVAIQVLNLFFSALGGTSHVMLI 559
OATP1B3           VFYNCSCVEVTGLQNRNYSAHLGECPRDNTCTRKFFIYVAIQVINSLFSATGGTTFILLT 559
rOatp1b2          EFYDCSCISNSG----NNSAHLGECPR-YKCKTNYYFYIILQVTVSFFTAMGSPSLILIL 553
OATP1C1           IFYNCTCVGIAASKSGNSSGIVGRCQKDNGCPQMFLYFLVISVITSYTLSLGGIPGYILL 576
OATP2B1           FYTNCSCVVE------GNPVLAGSCDS--TCSHLVVPFLLLVSLGSALACLTHTPSFMLI 586
OATP3A1           -LTGCACLTT--VPAENATVVPGKCPS-PGCQEAFLTFLCVMCICSLIGAMAQTPSVIIL 561
OATP4A1           VYRDCSCIPQN-LSSGFGHATAGKCTSTCQRKPLLLVFIFVVIFFTFLS---SIPALTAT 602

                       *   ***     11          *          ***
                  ---------------  ----------
OATP1A2           LRCMKSEEKSLGVGLHTFCTRVFAGIPAPIYFGALMDSTCLHWGTLKCGESGACRIYDST 595
rOatp1a1          LRCVKSEEKSLGVGLHTFCIRVFAGIPAPVYFGALIDRTCLHWGTLKCGQRGACRMYDIN 595
rOatp1a3          LRCIKSEEKSLGIGIHAFCIRVFAGIPAPIYFGALIDRTCLHWGTQKCGAPGR-RMYDIN 594
rOatp1a4          LRCIKSEEKSLGVGLHAFCIRILAGIPAPIYFGALIDRTCLHWGTLKCGEPGACRMYDIN 594
rOatp1a5          LRCIKPEEKSLGIGLHAFCTRVFAGIPAPIYFGALIDRTCLHWGTLKCGEPGACRMYNIN 595
OATP1B1           VKIVQPELKSLALGFHSMVIRALGGILAPIYFGALIDTTCIKWSTNNCGTRGSCRTYNST 619
OATP1B3           VKIVQPELKALAMGFQSMVIRTLGGILAPIYFGALIDKTCMKWSTNSCGAQGACRIYNSV 619
rOatp1b2          MKSVQPELKSLAMGFHSLIIRALGGILAPIYYGAFIDRTCIKWSVTSCGKRGACRLYNSR 613
OATP1C1           LRCIKPQLKSFALGIYTLAIRVLAGIPAPVYFGVLIDTSCLKWGFKRCGSRGSCRLYDSN 636
OATP2B1           LRGVKKEDKTLAVGIQFMFLRILAWMPSPVIHGSAIDTTCVHWA-LSCGRRAVCRYYNND 645
OATP3A1           IRTVSPELKSYALGVLFLLLRLLGFIPPPLIFGAGIDSTCLFWS-TFCGEQGACVLYDNV 620
OATP4A1           LRCVRDPQRSFALGIQWIVVRILGGIPGPIAFGWVIDKACLLWQ-DQCGQQGSCLVYQNS 661
```



Figure 5. Multiple sequence alignment of human and rat OATPs/Oatps. The program CLUSTALW (21) was used to align the amino acid sequences of the 12 OATPs/Oatps for which functional data on ES transport are available. Transmembrane domains are shown by solid lines above the sequence alignment and are numbered continuously on the basis of hydropathy analysis. The PDZ consensus sequence in OATP1A2 is highlighted in purple and boxed. Histidine residues in OATP1A2 that were mutated to alanine and functionally characterized are marked by *. Lysine (marked by **) and arginine (marked by ***) residues that are found in either transmembrane domains or extracellular loops of OATP1A2 and that are conserved in at least 9 of the 12 OATPs/Oatps were mutated to alanine and functionally characterized. GenBank accession numbers for sequences in the alignment are NM_021094, NM_017111, D79981, NM_131096, NM_030838, NM_006446, NM_019844, NM_031650, NM_017435, NM_007256, NM_013272, and NM_016354.

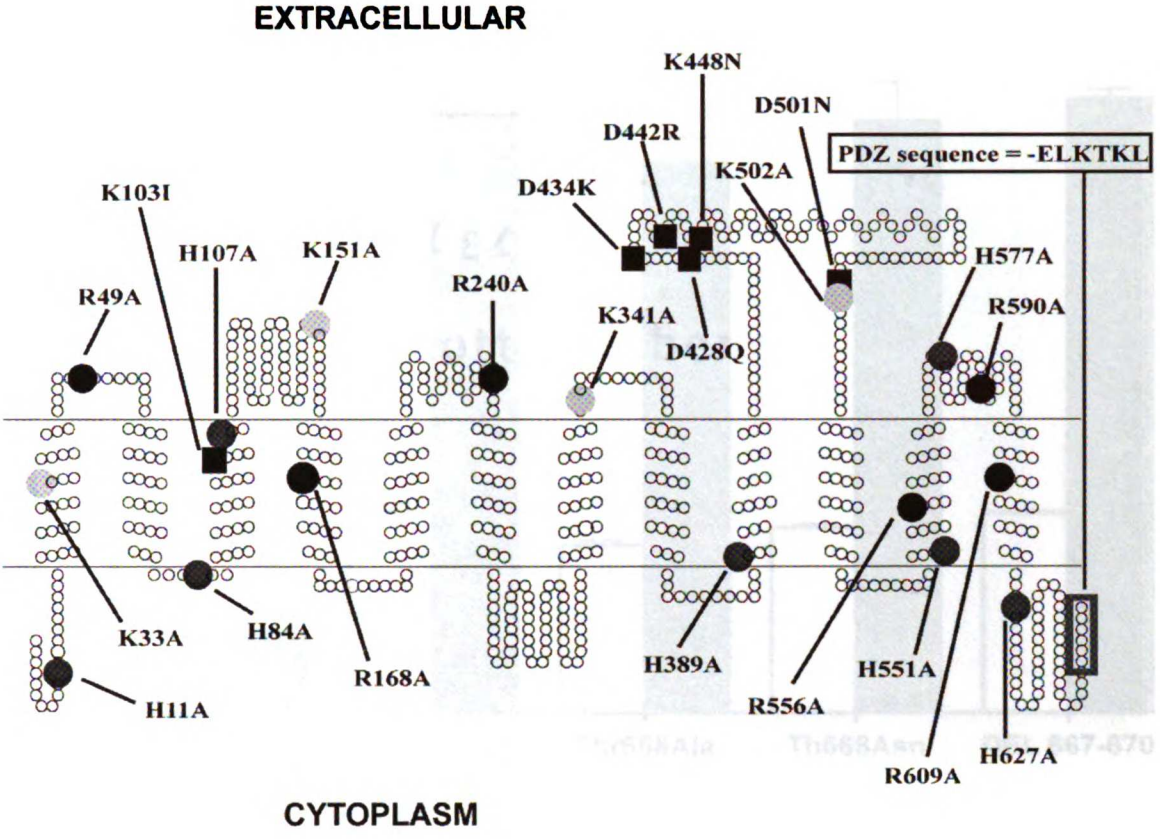

Figure 6. Predicted secondary structure model of OATP1A2. The PDZ consensus sequence is shown boxed. The 7 histidine residues, which were mutated to alanine, are shown in dark grey circles. The 6 arginine (black circles) and 4 lysine (light grey circles) residues, which were mutated to alanine, were selected based on their location in either transmembrane domains or extracellular loops of OATP1A2 and because they were conserved in at least 9 of the 12 OATPs/ rOatps. The 6 charged residues in OATP1A2 that were mutated to the corresponding uncharged or oppositely charged residues in rat Oatp1a1/Oatp1a4 are shown by black squares. The transmembrane topology diagram was constructed using TOPO [S. J. Johns (UCSF, San Francisco) and R. C. Speth (Washington State University, Pullman), transmembrane protein display software available at the UCSF Sequence Analysis Consulting Group website, http://www.sacs.ucsf.edu/TOPO/topo.html].

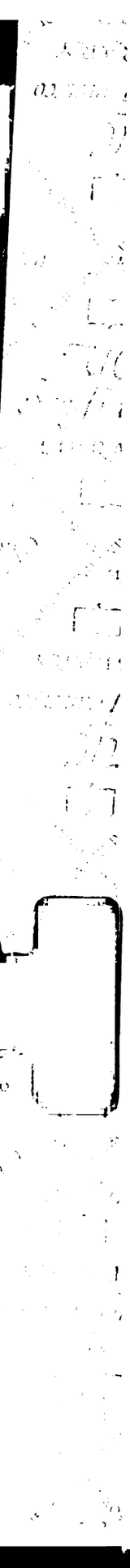

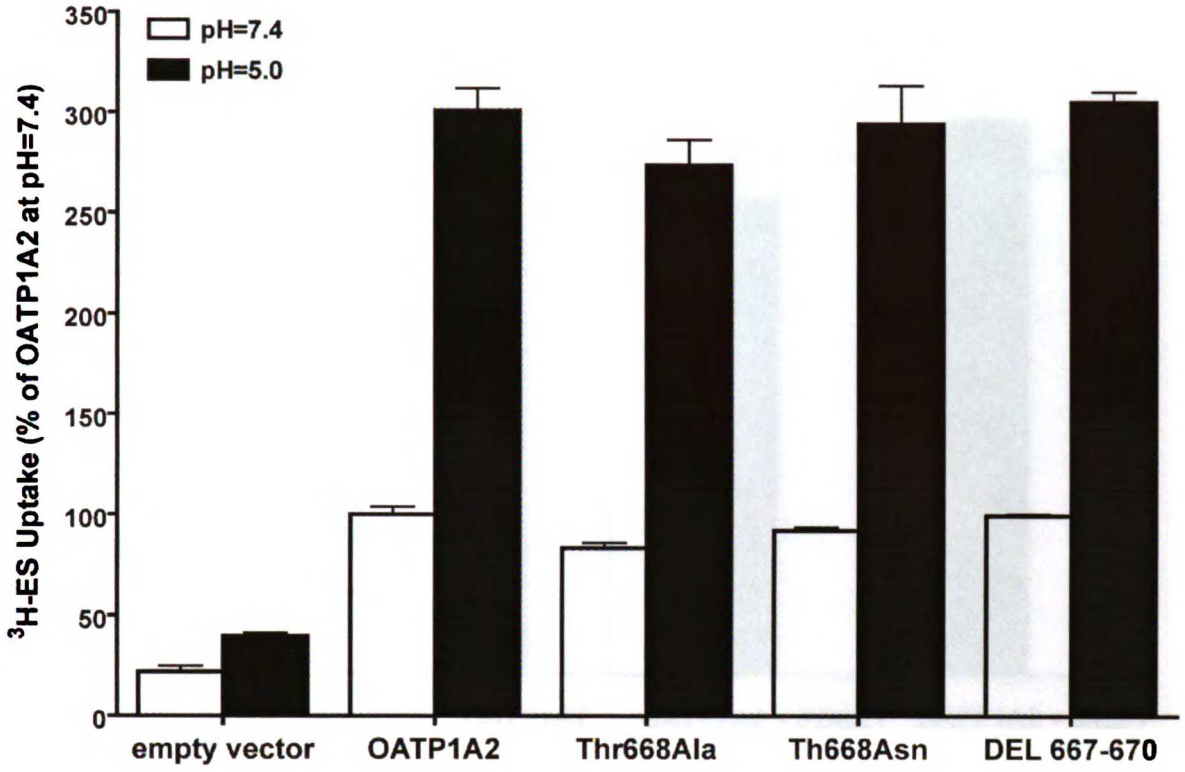

Figure 7. pH-Dependent transport of ES by C-terminus PDZ consensus sequence mutants of OATP1A2 in transiently transfected HEK293 cells. Uptake of 20 nM ^{3}H-ES in HEK293 cells transiently transfected with empty vector, OATP1A2, or C-terminus PDZ motif mutants (p. Thr668Ala, p. Thr668Asn, and p. DEL 667-670). Cells were pre-incubated in Na^+ buffer at pH 7.4 for 30 min. Transport was measured at pH 7.4 (white bars) or pH 5.0 (black bars) in Na^+ buffer over 2 min. Uptake is expressed as percentage of ES uptake by OATP1A2 transfected cells at pH 7.4. Data are representative of 3 independent experiments and each value represents the mean ± SE from 3 wells. P values were determined by comparing mutant to OATP1A2 reference uptake at each buffer pH using one-way ANOVA and Tukey's multi-comparison test with $p < 0.05$ as the criterion of significance.

UCSF LIBRARY

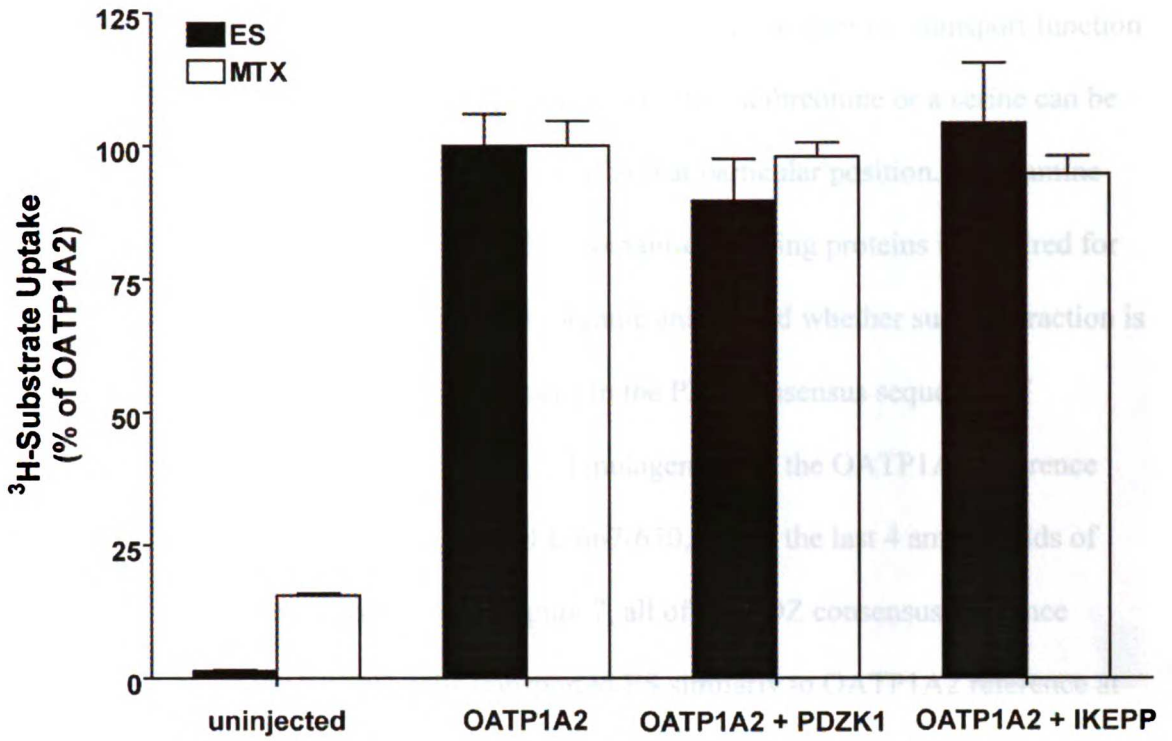

Figure 8. Overexpression of the PDZ proteins, PDZK1 and IKEPP, along with OATP1A2 does not enhance ES or MTX transport in *X. laevis* oocytes. Uptake of 20 nM ^{3}H-ES (white bars) or 0.2 μM ^{3}H-MTX (black bars) in oocytes expressing OATP1A2, OATP1A2 + PDZK1, or OATP1A2 + IKEPP. Oocytes were coinjected with equal concentrations (75 ng/50 nL) of OATP1A2 and PDZK1 or IKEPP cRNA. Transport was measured in Na^+ buffer at pH 7.4 over 60 min. Uptake is expressed as percentage of ES and MTX uptake, respectively, by OATP1A2 injected oocytes. Data shown are expressed as mean ± SE.



PDZ consensus sequence, but that change does not appears to alter the transport function of either ES or MTX, which is not surprising since either a threonine or a serine can be present in a Class I PDZ domain binding motif at that particular position. To examine whether interaction of OATP1A2 with PDZ domain-containing proteins is required for OATP1A2-mediated transport function of organic anions and whether such interaction is sensitive to extracellular pH, several mutants in the PDZ consensus sequence of OATP1A2 were constructed by site-directed mutagenesis of the OATP1A2 reference template: Thr668Ala, Thr668Asn, and DEL 667-670, where the last 4 amino acids of OATP1A2 were deleted. As shown in Figure 7, all of the PDZ consensus sequence mutants expressed in HEK293 cells transported ES similarly to OATP1A2 reference at both pH 7.4 and 5.0. Similar to wild-type OATP1A2, the transport of ES by the PDZ motif mutants was highly sensitive to extracellular pH. In addition, co-expression of either PDZK1 or IKEPP with OATP1A2 in oocytes did not result in enhanced transport of ES compared to that of oocytes expressing only OATP1A2 (Figure 8). The uptake of ES was 0.270 ± 0.017, 0.241 ± 0.021, 0.281 ± 0.031 pmol/oocyte/60 min and that of MTX was 0.119 ± 0.0066, 0.116 ± 0.0032, 0.113 ± 0.004 pmol/oocyte/60 min in oocytes expressing OATP1A2, OATP1A2 + PDZK1, OATP1A2 + IKEPP, respectively. Altogether these data suggest that the PDZ consensus sequence in OATP1A2 is not required for transport of organic anions and that the previously observed *in vitro* interaction of OATP1A2 with PDZ domain-containing proteins, such as PDZK1 and IKEPP, does not appear to be critical for the proper function of OATP1A2, at least in cellular assays.



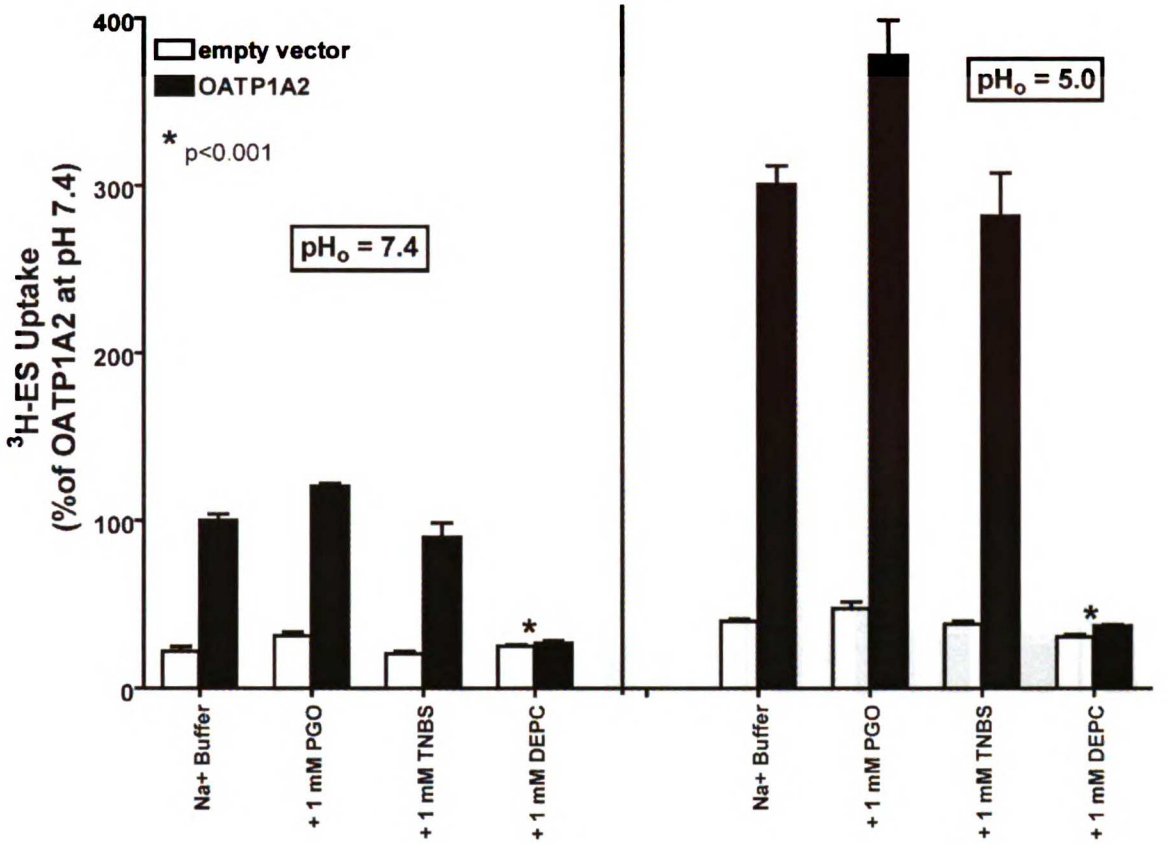

Figure 9. Effect of the amino acid-modifying reagents, PGO, TNBS, and DEPC on ES uptake in transiently transfected HEK293 cells. Uptake of 20 nM ^{3}H-ES in HEK293 cells transiently transfected with empty vector (white bars) or OATP1A2 (black bars). Cells were pre-incubated for 30 min with 1 mM PG, TNBS, or DEPC in Na^+ buffer at pH 7.4. Cells were washed three times with Na^+ buffer and transport was measured in Na^+ buffer at pH 7.4 or pH 5.0 over 2 min. Uptake is expressed as percentage of ES uptake by OATP1A2 transfected cells at pH 7.4 in the absence of amino acid-modifying agents. Each value represents the mean ± SE from 3 wells. P values were determined by comparing uptake in the presence to that in the absence of an amino acid-modifying reagent at each buffer pH using one-way ANOVA and Tukey's multi-comparison test with $p < 0.05$ as the criterion of significance.

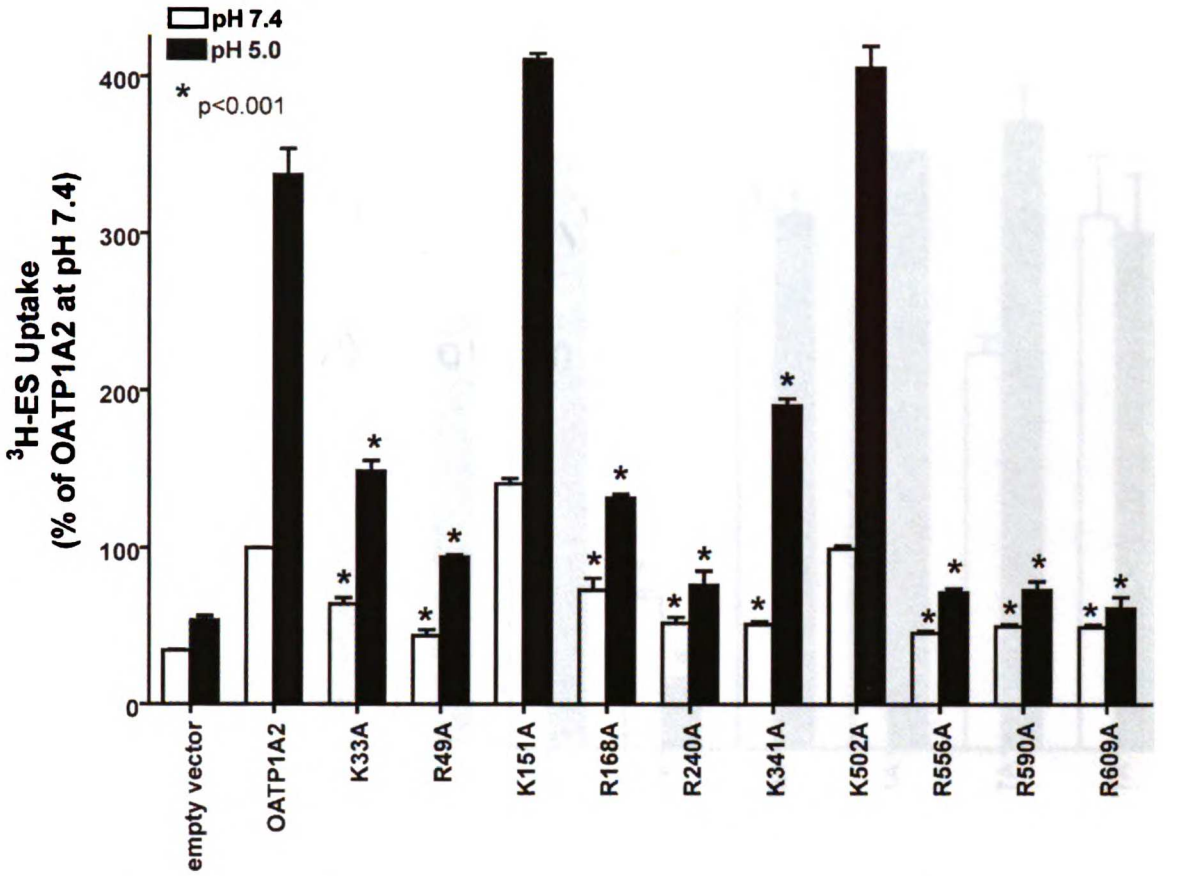

Figure 10. Functional effect of arginine and lysine replacements in OATP1A2 on ES transport in transiently transfected HEK293 cells. Uptake of 20 nM ^{3}H-ES in HEK293 cells transiently transfected with empty vector, OATP1A2, or mutants at arginine or lysine residues in OATP1A2, which were found in transmembrane domains or extracellular loops and were conserved across OATPs/rOatps. Transport was measured at pH 7.4 (white bars) or pH 5.0 (black bars) in Na^+ buffer over 2 min. Uptake is expressed as percentage of ES uptake by OATP1A2 transfected cells at pH 7.4. Each value represents the mean ± SE from 3 wells. P values were determined by comparing mutant to OATP1A2 reference uptake at each buffer pH using one-way ANOVA and Tukey's multi-comparison test with $p < 0.05$ as the criterion of significance.

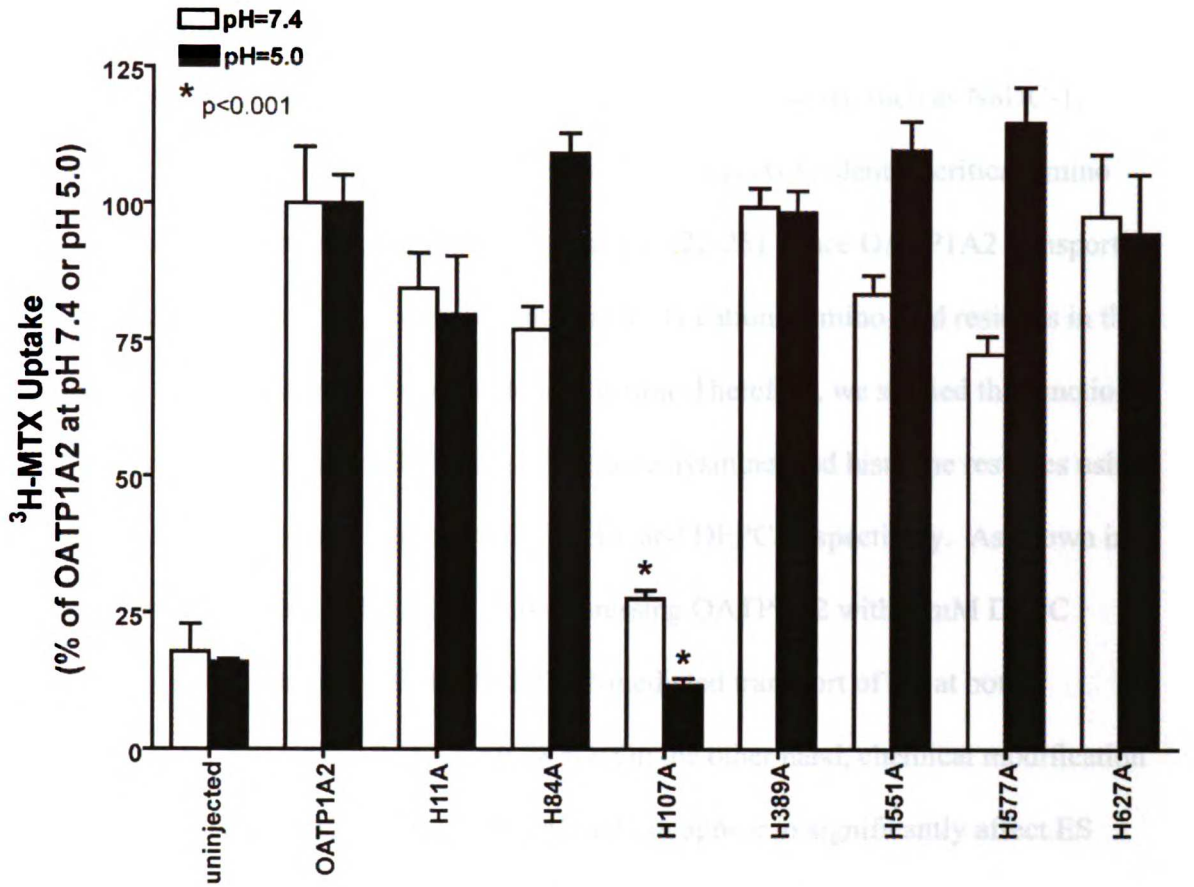

Figure 11. Functional analysis of the effect of single histidine replacement in OATP1A2 on MTX transport in *X. laevis* oocytes. Uptake of 0.2 μM ^{3}H-MTX in oocytes expressing OATP1A2 or the 7 histidine mutants. Transport was measured at pH 7.4 (white bars) or pH 5.0 (black bars) in Na^+ buffer over 2 min. Uptake is expressed as percentage of MTX uptake by OATP1A2 injected oocytes at pH 7.4 or pH 5.0 over 60 min. Each value represents the mean ± SE from 7-9 oocytes. P values were determined by comparing mutant to OATP1A2 reference uptake at each buffer pH using one-way ANOVA and Tukey's multi-comparison test with $p < 0.05$ as the criterion of significance.

UCSF LIBRARY

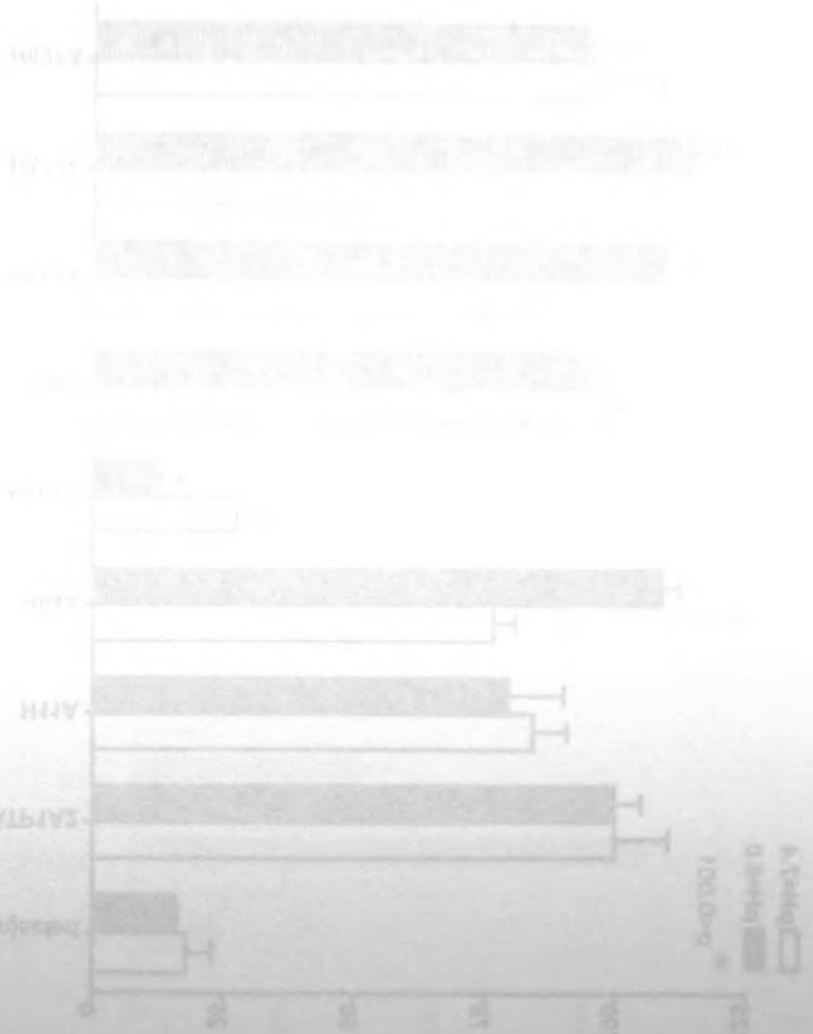

Chemical modification of histidine residues inhibits ES transport by OATP1A2

Site-specific chemical modification of transporter proteins, such as NaDC-1, OAT4, and PEPTs, has been used in several previous reports to identify critical amino acid groups that are required for substrate transport (22-25). Since OATP1A2 transports anionic compounds, it would be important to identify cationic amino acid residues in this transporter that are required for substrate interaction. Therefore, we studied the functional consequences of chemical modification of arginine, lysinine, and histidine residues using the amino acid-modifying reagents PGO, TNBS, and DEPC, respectively. As shown in Figure 9, pre-incubation of HEK293 cells expressing OATP1A2 with 1 mM DEPC significantly decreased ($p < 0.001$) OATP1A2-mediated transport of ES at both pH 7.4 (26.9 ± 1.5 %) and 5.0 (12.4 ± 0.28 %). On the other hand, chemical modification of arginine and lysine residues in OATP1A2 did not appear to significantly affect ES uptake. These data suggest that histidine residues in OATP1A2 may be primarily involved in interacting with organic anions and could be responsible for pH-dependent transport of organic anions.

Functional analysis of arginine, lysine, and histidine replacements in OATP1A2 on organic anion transport

To identify cationic residues in OATP1A2 that interact with organic anions, we initially selected arginine and lysine residues located in transmembrane domains and extracellular loops of OATP1A2 that were conserved across multiple human and rat OATPs/Oatps, which had been previously shown to transport ES (1, 2). Conservation was determined based on multiple sequence alignment of 12 OATPs/Oatps and an amino-

acid residue was selected for site-directed mutagenesis to alanine if it was completely or partially (*i.e.* a residue within the class of basic amino acids: arginine, lysine, or histidine) conserved across 9 of 12 members. As shown in Figures 5 and 6, there are 6 arginine (3 in transmembrane domains and 3 in extracellular loops) and 4 lysine (1 in a transmembrane domain and 3 in extracellular loops) residues in OATP1A2 that satisfy these requirements. In particular, K341 and R556 were completely conserved across all 12 OATPs/Oatps. As shown in Figure 10, the mutants R240A, R556A, R590A, and R609A were non-functional for ES transport at both pH 7.4 and pH 5.0 ($p < 0.001$). In addition, the mutants K33A (64.0 ± 4.1 %; 43.9 ± 2.1 %), R49A (43.7 ± 3.8 %; 27.9 ± 0.41 %), R168A (73.0 ± 7.8 %; 39.1 ± 0.73 %), and K341A (51.2 ± 1.9 %; 56.6 ± 1.3 %) showed significantly decreased uptake of ES ($p < 0.001$) compared to OATP1A2 at pH 7.4 and 5.0. In addition, all 7 histidines in OATP1A2 were mutated to alanine, since we observed that the histidine modifying reagent, DEPC, dramatically decreased ES transport by OATP1A2 (Figure 9) and histidines, therefore, could be necessary for the catalytic function of OATP1A2. We were also particularly interested in histidine residues, because they could play a critical role in enhancing transport of organic anions at acidic pH by improving the transporter affinity for anionic substrates, since the histidine side chain has a pKa of 6.0. As shown in Figures 5 and 6, 2 histidines were found in transmembrane domains, 1 in extracellular loops and 4 in intracellular loops. Of these, H84 was completely conserved across all 12 OATPs/Oatps. As shown in Figure 11, only the mutant H107A showed a dramatic decrease in MTX transport at both pH 7.4 and pH 5.0 ($p < 0.001$), while all other histidine mutants had similar transport function to OATP1A2 reference. Similar data were observed for ES transport (data not shown).

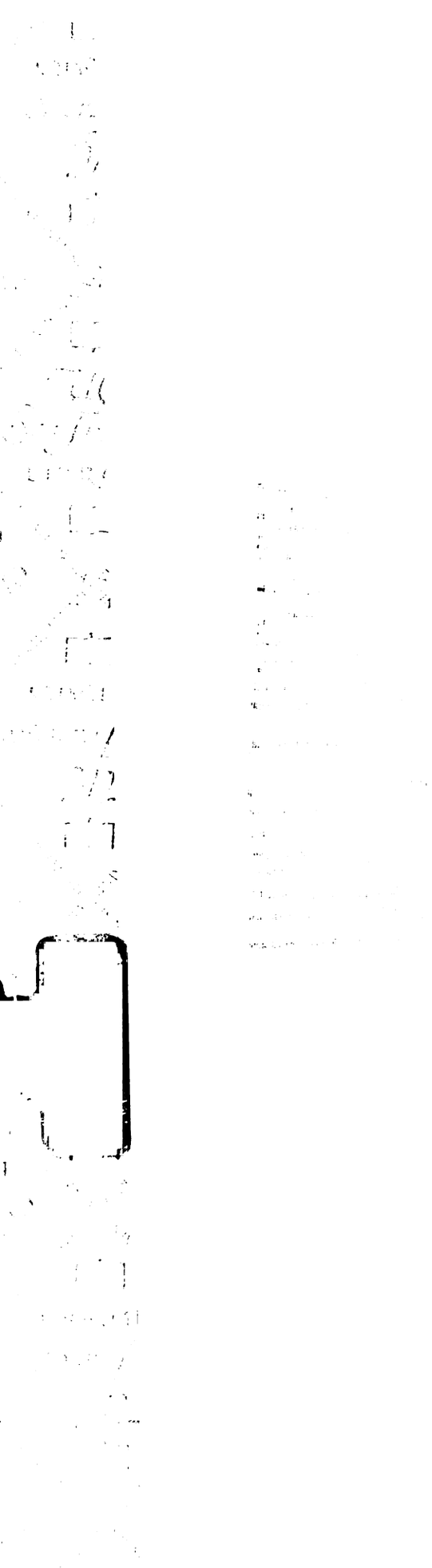

Altogether these data suggest that arginine residues in OATP1A2 appear to have critical structural roles as all 6 arginine mutants showed a dramatic decrease in the transport of ES. On the other hand, mutations at lysine and histidine residues seemed to be less detrimental to OATP1A2 transport function as 2 of 4 lysine mutants, K33A and K341A, resulted in partial decrease in ES uptake and 1 of 7 histidine mutants, H107A, was non-functional for ES and MTX.

Functional analysis of charged amino acid replacements in OATP1A2 to uncharged or oppositely charged ones in rOatp1a1/Oatp1a4 on ES transport

Previous functional studies with rat Oatp1a1 and Oatp1a4 have implicated the exchange of intracellular glutathione, bicarbonate, and/or hydroxyl ions, as the mechanism for organic anion transport across the membrane (11-14). Data presented in this report suggest that the transport mechanism for organic anions differs significantly between human and rat OATPs/rOatps, especially with respect to members in the 1A subfamily. Since human OATP1A2 is sensitive to extracellular pH but does not depend on the proton gradient to transport organic anions across the membrane (Figure 1 and 3, Table 1), charged amino acid residues in transmembrane domains and extracellular loops of OATP1A2 could be involved in the differential interaction with organic anions at acidic compared to physiological pH. Therefore, we selected cationic (lysine, arginine, or histidine) and anionic (aspartate or glutamate) residues if they were located in the transmembrane domains and extracellular loops of OATP1A2 and if the rat Oatp1a1 and Oatp1a4 sequences had uncharged or oppositely charged residues at the corresponding position (Figure 6 and 12). Six charged residues satisfied these requirements: K103 and

```
                                                                    1
OATP1A2          MGETEK-------RIETHRIR----------------CLSKLKMFLLAITCAFVSKTLS 36
rOatp1a1         MEETEK-------KIATQEGR----------------LFSKMKVFLLSLTCACLTKSLS 36
rOatp1a4         MGKSEK-------RVATHGVR----------------CFAKIKMFLLALTCAYVSKSLS 36

                                        2                           3
OATP1A2          GSYMNSMLTQIERQFNIPTSLVGFINGSFEIGNLLLIIFVSYFGTKLHRPIMIGIGCVVM 96
rOatp1a1         GVYMNSMLTQIERQFDISTSVAGLINGSFEIGNLFFIVFVSYFGTKLHRPVVIGIGCVIM 96
rOatp1a4         GTYMNSMLTQIERQFGIPTSIVGLINGSFEIGNLLLIIFVSYFGTKLHRPIMIGVGCAVM 96

                 *
OATP1A2          GLGCFLKSLPHFLMN--QYEYESTVSVSGNLSSNSFLCMENGTQILRPTQDPS------E 148
rOatp1a1         GLGCLLMSLPHFFMG--RYEYETTISPTGNLSSNSFLCMENRTQTLKPTQDPA------E 148
rOatp1a4         GLGCFLISLPHFLMG--QYEYET-ILPTSNVSSNSFFCVENRSQTLNPTQDPS------E 147

                                   4                          5
OATP1A2          CTKEVKSLMWVYVLVGNIVRGMGETPILPLGISYIEDFAKFENSPLYIGLVETGAIIGPL 208
rOatp1a1         CVKEMKSLMWICVMVGNIIRGIGETPIVPLGISYIEDFAKSENSPLYIGILEMGKVAGPI 208
rOatp1a4         CVKEMKSLMWIYVLVGNIIRGIGETPIMPLGISYIEDFAKSENSPLYIGILETGMTIGPL 207

                                                        6
OATP1A2          IGLLLASFCANVYVDTGFVNTDDLIITPTDTRWVGAWWFGFLICAGVNVLTAIPFFFLPN 268
rOatp1a1         FGLLLGSYCAQIYVDIGSVNTDDLTITPSDTRWVGAWWIGFLVCAGVNILTSIPFFFLPK 268
rOatp1a4         IGLLLASSCANIYVDIESVNTDDLTITPTDTRWVGAWWIGFLVCAGVNILTSFPFFFFPK 267

OATP1A2          TLPKEGLETNADIIK--------NENEDKQKEEVKKEKYGITKDFLPF------------ 308
rOatp1a1         ALPKKGQQENVAVTK--------DGKVEKYGGQAREENLGITKDFLTF------------ 308
rOatp1a4         TLPKEGLQENVDGTE--------NAKEKKHRKKAKEEKRGITKDFFVF------------ 307

                                 7                                 8
OATP1A2          ----MKSLSCNPIYMLFILVSVIQFNAFVNMISFMPKYLEQQYGISSSDAIFLMGIYNLP 364
rOatp1a1         ----MKRLFCNPIYMLFILTSVLQVNGFINKFTFLPKYLEQQYGKSTAEAIFLIGVYSLP 364
rOatp1a4         ----MKSLSCNPIYMLFILISVLQFNAFINSFTFMPKYLEQQYGKSTAEVVFLMGLYMLP 363

                                              9
OATP1A2          PICIGYIIGGLIMKKFKITVKQAAHIGCWLSLLEYLLYFLSFLMTCENSSVVGINTSYEG 424
rOatp1a1         PICLGYLIGGFIMKKFKITVKKAAYLAFCLSVFEYLLFLCHFMLTCDNAAVAGLTTSYKG 424
rOatp1a4         PICLGYLIGGLIMKKFKVTVKKAAHLAFWLCLSEYLLSFLSYVMTCDNFPVAGLTTSYEG 423
                   **   **       **     *
OATP1A2          IPQDLYVENDIFADCNVDCNCPSKIWDPVCG-NNGLSYLSACLAGCETSIGTGIN----M 479
rOatp1a1         VQHQLHVESKVLADCNTRCSCSTNTWDPVCG-DNGVAYMSACLAGCKKFVGTGTN----M 479
rOatp1a4         VQHQLYVENKVLADCNTRCNCSTNTWDPVCG-DNGLAYMSACLAGCEKSVGTGTN----M 478

                                        **                      10
OATP1A2          VFQNCSCI----QTSGNSSAVLGLCDKGPDCSLMLQYFLILSAMSSFIYSLAAIPGYMVL 535
rOatp1a1         VFQDCSCI----QSLGNSSAVLGLCKKGPECANRLQYFLILTIIISFIYSLTAIPGYMVF 535
rOatp1a4         VFQNCSCI----QSSGNSSAVLGLCNKGPDCANKLQYFLIIAIFGCFIYSLAGIPGYMVL 534

                                   11
OATP1A2          LRCMKSEEKSLGVGLHTFCTRVFAGIPAPIYFGALMDSTCLHWGTLKCGESGACRIYDST 595
rOatp1a1         LRCVKSEEKSLGVGLHTFCIRVFAGIPAPVYFGALIDRTCLHWGTLKCGQRGACRMYDIN 595
rOatp1a4         LRCIKSEEKSLGVGLHAFCIRILAGIPAPIYFGALIDRTCLHWGTLKCGEPGACRMYDIN 594
rOatp1a5         LRCIKPEEKSLGIGLHAFCTRVFAGIPAPIYFGALIDRTCLHWGTLKCGEPGACRMYNIN 595
```

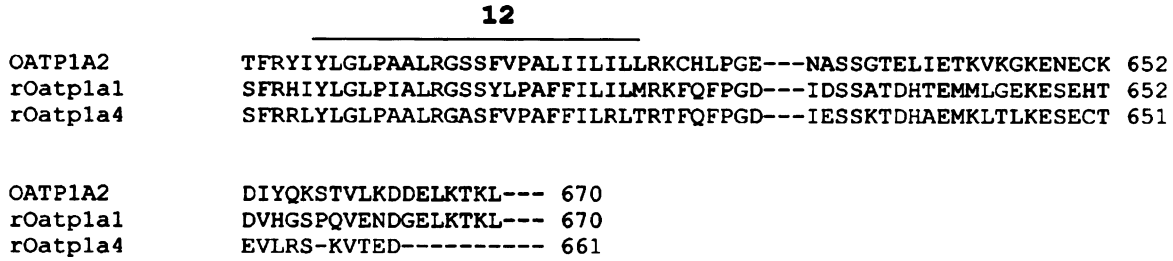

Figure 12. Multiple sequence alignment of human OATP1A2 and rat Oatp1a1 and Oatp1a4. The amino acid sequences of the human and rat OATPs/Oatps for which data on transport mechanism for organic anions is available were aligned using the program CLUSTALW (21). Transmembrane domains are identified by solid lines above the sequence alignment and are numbered continuously on the basis of hydropathy analysis. Cationic (bolded red) and anionic (bolded blue) amino acid residues in the transmembrane domains and extracellular loops of OATP1A2 which were mutated to the corresponding uncharged or oppositely charged residues in rat Oatp1a1/Oatp1a4 are labeled with * and **, respectively. GenBank accession numbers for sequences in the alignment are NM_021094, NM_017111, and NM_131096.

UCSF LIBRARY

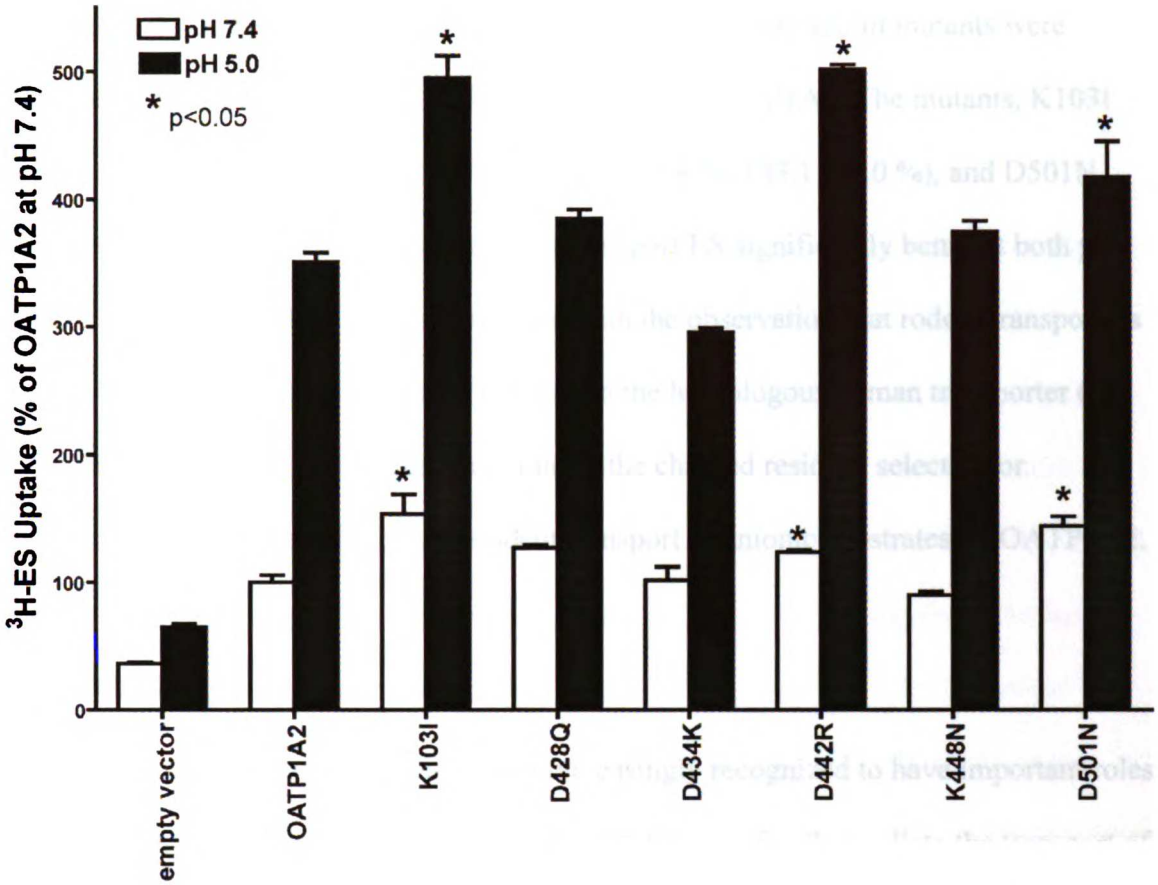

Figure 13. Functional effect of mutating conserved charged residues in OATP1A2 to the corresponding uncharged or oppositely charged ones in rat Oatp1a1/Oatp1a4 on ES transport in transiently transfected HEK293 cells. Uptake of 20 nM ^{3}H-ES in HEK293 cells transiently transfected with empty vector, OATP1A2, or mutants at charged residues in OATP1A2, which were found in transmembrane domains or extracellular loops. Transport was measured at pH 7.4 (white bars) or pH 5.0 (black bars) in Na^+ buffer over 2 min. Uptake is expressed as percentage of ES uptake by OATP1A2 transfected cells at pH 7.4. Each value represents the mean ± SE from 3 wells.

K448, and D428, D434, D442, and D501. As shown in Figure 13, all mutants were functional and had similar pH sensitivity compared to OATP1A2. The mutants, K103I (153.4 ± 15.4 %; 141.2 ± 4.9 %), D442R (123.7 ± 1.8 %; 143.1 ± 1.0 %), and D501N (144.0 ± 7.4 %; 119.0 ± 8.0 %) appeared to transport ES significantly better at both pH 7.4 and pH 5.0 ($p < 0.05$). This is consistent with the observation that rodent transporters tend to interact with some substrates better than the homologous human transporter (26, 27). Altogether these data suggest that none of the charged residues selected for mutagenesis are required for pH-dependent transport of anionic substrates by OATP1A2.

DISCUSSION

Xenobiotic transporters have been increasingly recognized to have important roles in drug efficacy and toxicity. Members of the OATP superfamily mediate the transport of many structurally diverse compounds in tissues relevant to drug disposition and response, such as the kidney, liver, intestine, and brain (1). However, the functional characterization of OATPs remains incomplete, especially in regards to the human members. Specifically, the mechanisms by which OATPs mediate substrate transport across the membrane is unresolved. Studies so far have predominantly focused on the driving forces for rodent Oatps. However, rodent Oatps, especially in the 1A subfamily, display significant differences in tissue expression and substrate specificities compared to OATP1A2 (1, 2), indicating that mechanistic studies performed with rodent transporters may not be reflective of the transport mechanisms of human OATPs. Therefore, in the present study we provide a comprehensive characterization of the mechanisms of

transport of organic anions by OATP1A2 and the structural determinants required for organic anion interaction with OATP1A2.

Functional analysis of pH-sensitive transport of ES by OATP1A2

Our data demonstrate that transport of ES by OATP1A2 is extremely sensitive to extracellular pH (Figure 1) and agree with a recent report showing that OATP1A2-mediated uptake of MTX was pH-dependent (10; and see Chapter 3). Uptake of ES is increased by as much as 4-fold at pH 5.0 compared to pH 7.4. The increased uptake at acidic extracellular pH is due to a significant increase in the affinity of ES for OATP1A2, with minor effects on the V_{max} (Figure 2). It is possible that the driving force for the pH-sensitive transport of organic anions by OATP1A2 could be provided by the proton gradient across the membrane. Our results with FCCP indicated that the driving force for transport of organic anions by OATP1A2 was not provided by the proton gradient across the membrane. Another human OATP transporter, OATP2B1, has been recently shown to be sensitive to extracellular pH (8, 9). OATP2B1-mediated transport of ES was higher at acidic pH due to a significant increase in V_{max} with no effect on the K_m and exhibited dependence on the proton gradient. The observed differences in the kinetic mechanisms of the effect of pH between the two human transporters, OATP1A2 and OAT2B1, are not known.

The apparent pH sensitivity of OATP1A2 might reflect the ionization state of the compounds tested rather than a specific effect of pH on the carrier. However, we believe that this is an unlikely explanation in the case of ES, since it has a pK_a of 2, which means that the majority exists in the mono-anionic form at both pH 7.4 and 5.0. We also previously observed a pH-dependent transport of MTX by OATP1A2, indicating that



increased transport at acidic pH is a general property of this transporter (10). Therefore, altogether these observations suggest that sensitivity of OATP1A2 to extracellular pH results from changes in the protonation state of amino acid side chains on the extracellular loops and/or transmembrane domains of this transporter, resulting in increased affinity of OATP1A2 for organic anions at acidic pH (Figure 2). OATP1A2 is expressed in several organs important for the disposition of organic anions, including the intestine, kidney, liver, and the blood brain barrier (1, 2). Our finding that transport of organic anions is dramatically higher at acidic extracellular pH, has important clinical implications in the absorption and elimination of organic anions drugs since the luminal pH of the intestine and kidney ranges from 4 to 7 and 4.5 to 8, respectively, and OATP1A2 is expressed on the apical membrane of intestinal and kidney tubule cells (1, 2, 5).

Effect of membrane potential on ES transport mediated by OATP1A2

Since several solute carrier transporters, such as OCT2, OCTN2, PEPT1, and MCT6, have been shown to utilize the potential gradient across the membrane to drive the pH-dependent transport of substrates (28-31), we examined whether transport of organic anions by OATP1A2 was sensitive to the membrane potential. Uptake of ES in OATP1A2 expressing cells was not significantly altered under depolarizing conditions (Figure 4) at either physiological or acidic pH, indicating that the pH-dependent transport mediated by OATP1A2 is not potential sensitive. These data suggest that the inside negative potential difference would not reduce uptake or enhance efflux of organic anions by OATP1A2.

Effect of intracellular GSH, HCO_3^-, or OH^- on ES uptake by OATP1A2

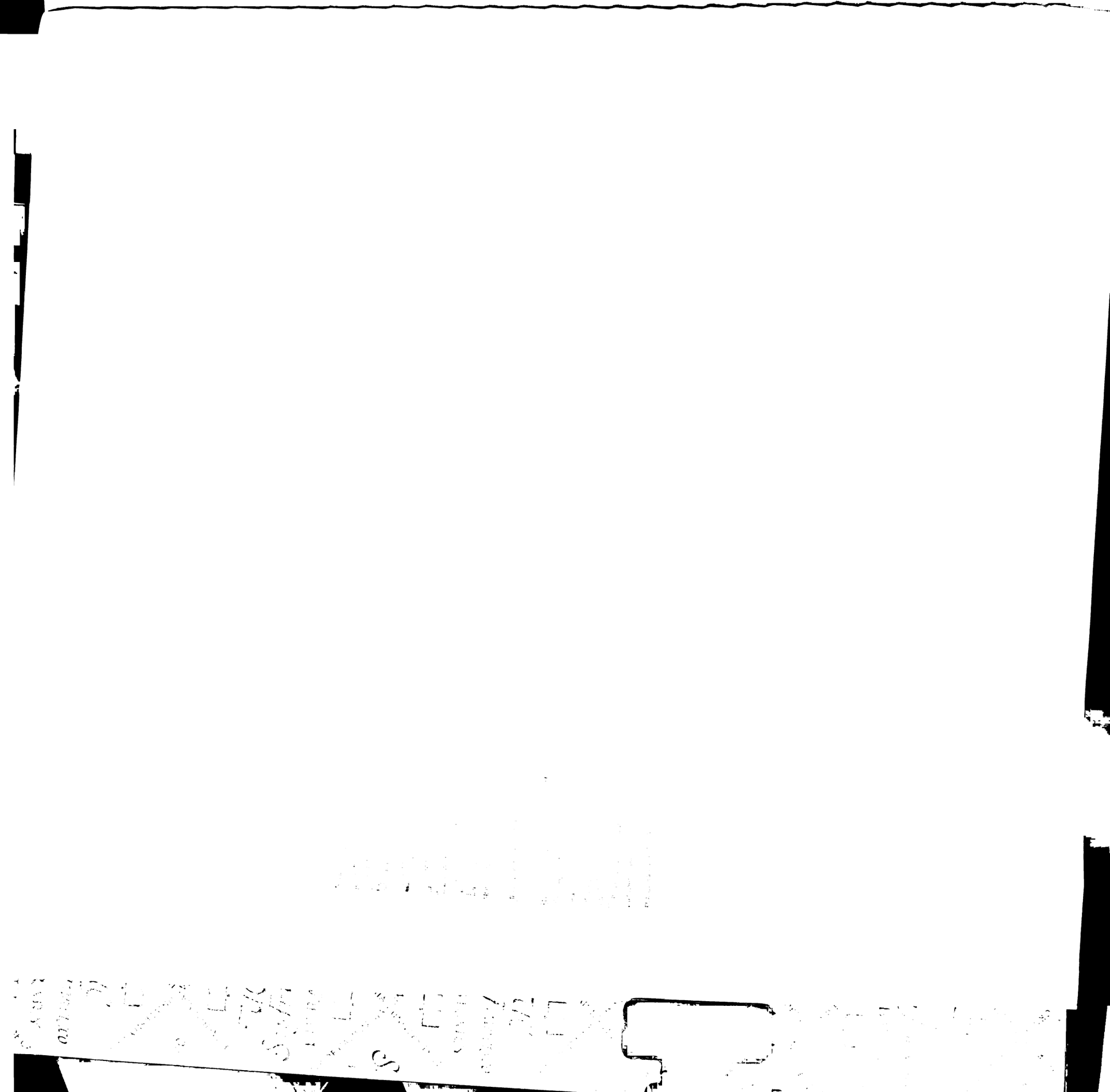

Intracellular loading of oocytes expressing OATP1A2 with various concentrations of GSH, HCO_3^-, or OH^- did not trans-stimulate ES uptake (Table 1) in contrast to previous studies with rat Oatp1a1 and Oatp1a4, which showed enhanced substrate transport occurring by exchange with intracellular GSH and HCO_3^- (11-13). The observed differences in the transport mechanisms of rat Oatps and human OATP1A2 may be explained by the fact that rat and human orthologs in the OATP1A family do not exist (1). The rodent Oatps arose through several gene duplications after divergence of rodent species from human (32). Thus each OATP1A family member may have its own functional role and may have evolved its own driving force.

Functional analysis of PDZ consensus sequence in C-terminus of OATP1A2 on organic anion transport

OATP1A2 has been recently shown to have a type I PDZ binding motif in the last four amino acids in the C-terminus (15, 16). PDZ domain-containing proteins can regulate membrane transporter function by stabilizing it at the cell surface and/or directly modulating the kinetics of substrate interaction (33). In fact, it was recently reported that mouse Oatp1a1 requires oligomerization with PDZK1 for proper expression on the hepatocyte surface (16). We found that all mutants in the PDZ consensus sequence transported ES in a pH-dependent manner similarly to OATP1A2 (Figure 5). In addition, co-expression of OATP1A2 with PDZ domain-containing proteins, such as PDZK1 and IKEPP, did not stimulate ES or MTX uptake (Figure 6). These findings suggest that the PDZ binding motif in OATP1A2 is not required for transport of organic anions at either acidic or physiologic extracellular pH and that the interaction of OATP1A2 with PDZ

domain-containing proteins does not appear to be critical for the proper function of this transporter.

Functional analysis of arginine, lysine, and histidine replacements in OATP1A2 on organic anion transport

The substrate binding site(s) of OATP1A2 is likely to contain positively charged amino acid side chains that interact with the negatively charged groups of organic anions. Our studies with side chain modifiers suggest that cationic residues, in particular histidines and possibly arginines, play a critical role in the transport mechanism of OATP1A2. Alanine substitution of the 6 conserved arginine residues, R49, R168, R240, R556, R590, and R609, in OATP1A2 had a dramatic functional effect on ES transport in HEK293 cells at both acidic and physiological pH (Figure 10). On the other hand, only 2 of 4 lysine residues and 1 of 7 histidine residues when mutated to alanine affected ES and/or MTX transport (Figure 10 and 11). These data suggest that arginine residues and selected lysine (K33 and K341) and histidine (H107) residues in OATP1A2 play critical structural and functional roles.

In contrast to many transporters, GFP tagging of OATP1A2 (at either the N or C terminus) produces a non-functional protein and other methods to detect the protein via tagged epitopes using confocal imaging have been unsuccessful (unpublished results in our laboratory). Thus, it could not be determined whether the decreased uptake of ES and/or MTX by the mutants generated in this study resulted from changes in cell surface expression and/or in the affinity of interaction with organic anion substrates.

Functional analysis of charged amino acid replacements in OATP1A2 to uncharged or oppositely charged ones in rOatp1a1/Oatp1a4 on ES transport

Since rat Oatp1a1 and Oatp1a4 appear to exhibit drastically different driving forces for substrate transport compared to human OATP1A2 (10-13), we analyzed the functional consequences of mutating charged residues in transmembrane domains and extracellular loops of OATP1A2 to the corresponding uncharged or oppositely charged residues in rat Oatp1a1/Oatp1a4. Six charged residues were found in transmembrane domains or extracellular loops of OATP1A2 (Figure 6 and 12) that were altered by site-directed mutagenesis to the corresponding rodent uncharged or oppositely charged residue: 2 were cationic (K103I and K448N) and 4 were anionic (D428Q, D434K, D442R, and D501N). All of the mutants transported ES at levels comparable to OATP1A2 and retained similar pH sensitivity to OATP1A2 (Figure 13). There are several possibilities that can help explain these findings: 1) other not yet identified residues in OATP1A2 are responsible for pH-dependent transport of organic anions, 2) a combination of residues in OATP1A2 that together are essential for sensitivity to extracellular pH, and/or 3) the residues critical for substrate interaction and those for sensitivity to extracellular pH are located in different domains of OATP1A2.

In summary, we determined that transport of organic anions by OATP1A2 is extremely sensitive to extracellular pH, but is not driven by the proton gradient, membrane potential across the membrane, or exchange with intracellular anions, such as GSH, HCO_3^-, or OH^-. In addition, we identified 6 arginine, 2 lysine, and 1 histidine residues in OATP1A2, that play important structural and/or functional roles in the transport of organic anions. Further studies are needed to specifically examine whether charged residues in OATP1A2 affect transporter expression, transporter turn-over rate, and/or the kinetics of interaction with organic anions, including clinically relevant drugs.

REFERENCES

1. Hagenbuch B, Meier PJ. Organic anion transporting polypeptides of the OATP/ SLC21 family: phylogenetic classification as OATP/ SLCO superfamily, new nomenclature and molecular/functional properties. Pflugers Arch 2004; **447**: 653-65.

2. Hagenbuch B, Meier PJ. The superfamily of organic anion transporting polypeptides. Biochim Biophys Acta 2003; **1609**: 1-18.

3. Kullak-Ublick GA, Hagenbuch B, Stieger B, Schteingart CD, Hofmann AF, Wolkoff AW, et al. Molecular and functional characterization of an organic anion transporting polypeptide cloned from human liver. Gastroenterology 1995; **109**: 1274-82.

4. Kullak-Ublick GA, Ismair MG, Stieger B, Landmann L, Huber R, Pizzagalli F, et al. Organic anion-transporting polypeptide B (OATP-B) and its functional comparison with three other OATPs of human liver. Gastroenterology 2001; **120**: 525-33.

5. Lee W, Glaeser H, Smith LH, Roberts RL, Moeckel GW, Gervasini G, et al. Polymorphisms in human organic anion-transporting polypeptide 1A2 (OATP1A2): implications for altered drug disposition and central nervous system drug entry. J Biol Chem 2005; **280**: 9610-7.

6. Su Y, Zhang X, Sinko PJ. Human organic anion-transporting polypeptide OATP-A (SLC21A3) acts in concert with P-glycoprotein and multidrug resistance protein 2 in the vectorial transport of Saquinavir in Hep G2 cells. Mol Pharm 2004; **1**: 49-56.

7. Gao B, Hagenbuch B, Kullak-Ublick GA, Benke D, Aguzzi A, Meier PJ. Organic anion-transporting polypeptides mediate transport of opioid peptides across blood-brain barrier. J Pharmacol Exp Ther 2000; **294**: 73-9.

8. Kobayashi D, Nozawa T, Imai K, Nezu J, Tsuji A, Tamai I. Involvement of human organic anion transporting polypeptide OATP-B (SLC21A9) in pH-dependent transport across intestinal apical membrane. J Pharmacol Exp Ther 2003; **306**: 703-8.

9. Nozawa T, Imai K, Nezu J, Tsuji A, Tamai I. Functional characterization of pH-sensitive organic anion transporting polypeptide OATP-B in human. J Pharmacol Exp Ther 2004; **308**: 438-45.

10. Badagnani I, Castro RA, Taylor TR, Brett CM, Huang CC, Stryke D, et al. Interaction Of Methotrexate With OATP1A2 And Its Genetic Variants. J Pharmacol Exp Ther 2006.

11. Satlin LM, Amin V, Wolkoff AW. Organic anion transporting polypeptide mediates organic anion/HCO3- exchange. J Biol Chem 1997; **272**: 26340-5.

12. Li L, Meier PJ, Ballatori N. Oatp2 mediates bidirectional organic solute transport: a role for intracellular glutathione. Mol Pharmacol 2000; **58**: 335-40.

13. Li L, Lee TK, Meier PJ, Ballatori N. Identification of glutathione as a driving force and leukotriene C4 as a substrate for oatp1, the hepatic sinusoidal organic solute transporter. J Biol Chem 1998; **273**: 16184-91.

14. Marin JJ, Mangas D, Martinez-Diez MC, El-Mir MY, Briz O, Serrano MA. Sensitivity of bile acid transport by organic anion-transporting polypeptides to intracellular pH. Biochim Biophys Acta 2003; **1611**: 249-57.

15. Kato Y, Yoshida K, Watanabe C, Sai Y, Tsuji A. Screening of the interaction between xenobiotic transporters and PDZ proteins. Pharm Res 2004; **21**: 1886-94.

UCSF LIBRARY

16. Wang P, Wang JJ, Xiao Y, Murray JW, Novikoff PM, Angeletti RH, et al. Interaction with PDZK1 is required for expression of organic anion transporting protein 1A1 on the hepatocyte surface. J Biol Chem 2005; **280**: 30143-9.

17. Giacomini KM, Markovich D, Werner A, Biber J, Wu X, Murer H. Expression of a renal Na(+)-nucleoside cotransport system (N2) in Xenopus laevis oocytes. Pflugers Arch 1994; **427**: 381-3.

18. Grundemann D, Gorboulev V, Gambaryan S, Veyhl M, Koepsell H. Drug excretion mediated by a new prototype of polyspecific transporter. Nature 1994; **372**: 549-52.

19. Sweet DH, Pritchard JB. rOCT2 is a basolateral potential-driven carrier, not an organic cation/proton exchanger. Am J Physiol 1999; **277**: F890-8.

20. Hung AY, Sheng M. PDZ domains: structural modules for protein complex assembly. J Biol Chem 2002; **277**: 5699-702.

21. Thompson JD, Higgins DG, Gibson TJ. CLUSTAL W: improving the sensitivity of progressive multiple sequence alignment through sequence weighting, position-specific gap penalties and weight matrix choice. Nucleic Acids Res 1994; **22**: 4673-80.

22. Pajor AM, Sun N, Valmonte HG. Mutational analysis of histidine residues in the rabbit Na+/dicarboxylate co-transporter NaDC-1. Biochem J 1998; **331 (Pt 1)**: 257-64.

23. Zhou F, Pan Z, Ma J, You G. Mutational analysis of histidine residues in human organic anion transporter 4 (hOAT4). Biochem J 2004; **384**: 87-92.

24. Chan BS, Bao Y, Schuster VL. Role of conserved transmembrane cationic amino acids in the prostaglandin transporter PGT. Biochemistry 2002; **41**: 9215-21.

UCSF LIBRARY

25. Fei YJ, Liu W, Prasad PD, Kekuda R, Oblak TG, Ganapathy V, et al. Identification of the histidyl residue obligatory for the catalytic activity of the human H+/peptide cotransporters PEPT1 and PEPT2. Biochemistry 1997; **36**: 452-60.

26. Gerstin KM, Dresser MJ, Giacomini KM. Specificity of human and rat orthologs of the concentrative nucleoside transporter, SPNT. Am J Physiol Renal Physiol 2002; **283**: F344-9.

27. Chernova MN, Jiang L, Friedman DJ, Darman RB, Lohi H, Kere J, et al. Functional comparison of mouse slc26a6 anion exchanger with human SLC26A6 polypeptide variants: differences in anion selectivity, regulation, and electrogenicity. J Biol Chem 2005; **280**: 8564-80.

28. Okuda M, Urakami Y, Saito H, Inui K. Molecular mechanisms of organic cation transport in OCT2-expressing Xenopus oocytes. Biochim Biophys Acta 1999; **1417**: 224-31.

29. Tamai I, Nakanishi T, Kobayashi D, China K, Kosugi Y, Nezu J, et al. Involvement of OCTN1 (SLC22A4) in pH-dependent transport of organic cations. Mol Pharm 2004; **1**: 57-66.

30. Kottra G, Daniel H. Bidirectional electrogenic transport of peptides by the proton-coupled carrier PEPT1 in Xenopus laevis oocytes: its asymmetry and symmetry. J Physiol 2001; **536**: 495-503.

31. Murakami Y, Kohyama N, Kobayashi Y, Ohbayashi M, Ohtani H, Sawada Y, et al. Functional characterization of human monocarboxylate transporter 6 (SLC16A5). Drug Metab Dispos 2005; **33**: 1845-51.

32. Cai SY, Wang W, Soroka CJ, Ballatori N, Boyer JL. An evolutionarily ancient Oatp: insights into conserved functional domains of these proteins. Am J Physiol Gastrointest Liver Physiol 2002; **282**: G702-10.

33. Kato Y, Watanabe C, Tsuji A. Regulation of drug transporters by PDZ adaptor proteins and nuclear receptors. Eur J Pharm Sci 2006; **27**: 487-500.

CHAPTER 6

ROLE OF GENETIC VARIATION IN KIDNEY TRANSPORTERS IN METHOTREXATE DISPOSITION AND TOXICITY

Introduction

Methotrexate (MTX) is a folate antimetabolite which has been successfully used in the treatment of patients with malignant and autoimmune diseases. Specifically, MTX is a cornerstone in the chemotherapy regimen for acute lymphoblastic leukemia (ALL), which is the most common type of cancer in children, representing nearly one third of all pediatric malignancies. MTX is most often included in the consolidation and continuation phases of ALL treatment, where it is given at high doses (1).

Although treatment of ALL with MTX results in high remission rates, MTX has several therapeutic problems that can influence both the efficacy and toxicity of this drug. One of the main clinical issues with MTX is that there is considerable inter-individual variability in the pharmacokinetic parameters of MTX, in particular the systemic and renal clearance (2-7). In addition, ALL patients can develop renal dysfunction, which is one of the most common toxicities following MTX therapy, especially at high doses (2, 8, 9). Acute renal toxicity caused by MTX results from tubular obstruction by crystal deposits of MTX and its main metabolite, 7-hydroxymethotrexate (7-OH-MTX) and direct glomerular damage caused by MTX (8). The subsequent nephrotoxicity decreases the elimination of MTX and increases the risk of severe multi-organ toxicities due to prolonged exposure of normal tissues to the antiproliferative effects of MTX. For these reasons, hydration and urine alkalinization are routinely used to minimize renal toxicity from MTX precipitation in the kidney tubules, which has reduced the incidence of severe

renal toxicity following high-dose MTX (HDMTX) to less than 1% (10, 11). Although severe nephrotoxicity with high-dose MTX is now rare, delayed MTX excretion as a result of an increase in serum creatinine (SCr) levels and/or a decrease in glomerular filtration rate (GFR) can occur in as many as 10-50% of ALL patients (11). This is reflected by elevated plasma MTX levels occurring 24 hours after MTX dosing which can then lead to severe system toxicity to other organs (6).

MTX is primarily excreted unchanged in the urine and its elimination occurs via saturable secretion and reabsorption mechanisms in the kidney, suggesting that membrane transporters expressed in the proximal and distal tubules of the kidney play a role in these processes (2, 7, 12-14). Over the years, many different laboratories have identified membrane transporters involved in the cellular transport of MTX (15-24). Among these, OAT1 (*SLC22A6*), OAT3 (*SLC22A8*), OAT4 (*SLC22A11*), OATP4C1 (OATP-H, *SLCO4C1*), RFC (*SLC19A1*), MRP2 (ABCC2), and MRP4 (ABCC4) are expressed in the proximal tubule, while OATP1A2 (OATP-A, *SLCO1A2*) and MRP3 (ABCC3) are expressed in the distal tubule (Figure 1). In addition, MRP5 (ABCC5) and BCRP (MXR, ABCG2) are present both in the proximal and distal tubule of the kidney.

Inter-individual variability in the efficacy, disposition, and toxicity of MTX can result from many factors, including physiological variables, concomitant diseases and drugs, diet, and exposure to the environment. Another critical factor that can influence variation in MTX therapy in ALL is an individual's genetic make-up. In fact, several studies have shown that genetic variation in the MTX transporter, RFC, and in several enzymes in the folate pathway, including gamma glutamyl hydrolase, 5,10-methylenetetrahydrofolate reductase, and thymidylate synthetase can have a clinical

impact on leukemia relapse and MTX-induced toxicities (25-31). However, little is known regarding the influence of genetic variation in membrane transporters that interact with MTX on the observed inter-individual variability in MTX therapy. Therefore, we undertook a preliminary pharmacogenetic analysis and a comprehensive pharmacopedemiological analysis of MTX disposition and toxicity in ALL, with a particular emphasis on the clinical impact of genetic variation in membrane transporters expressed in the kidney on MTX therapy. This study represents the largest analysis of the pharmacokinetics and toxicity of MTX in ALL, encompassing 565 patients for a total of 3930 courses.

Materials and Methods

Study Population

A total of 565 patients with newly diagnosed ALL were enrolled in St. Jude Children's Research Hospital Therapy studies XIII (N=265), XIV and XV (N=300) between 1991 and 1998. Subject selection and data collection was performed by Dr. Mary V. Relling's group with assistance from statisticians, Dr. Cheng Cheng, and Dr. Ching-Hon Pui. In protocol XIII patients received 10 courses of 2 g/m^2 of MTX given intravenously over 2 hours. Hydration with 5% dextrose and 40 mEq/L of $NaHCO_3$ in 0.25% normal saline at a rate of 200 $mL/m^2/h$ was given over 8 hours. Leucovorin (10 mg/m^2) was administered every 6 hours for 5 doses beginning 44 hours after starting MTX. The leucovorin dose was increased in patients who had MTX plasma concentrations greater than 0.8 μM at 42 hours after starting MTX and leucovorin

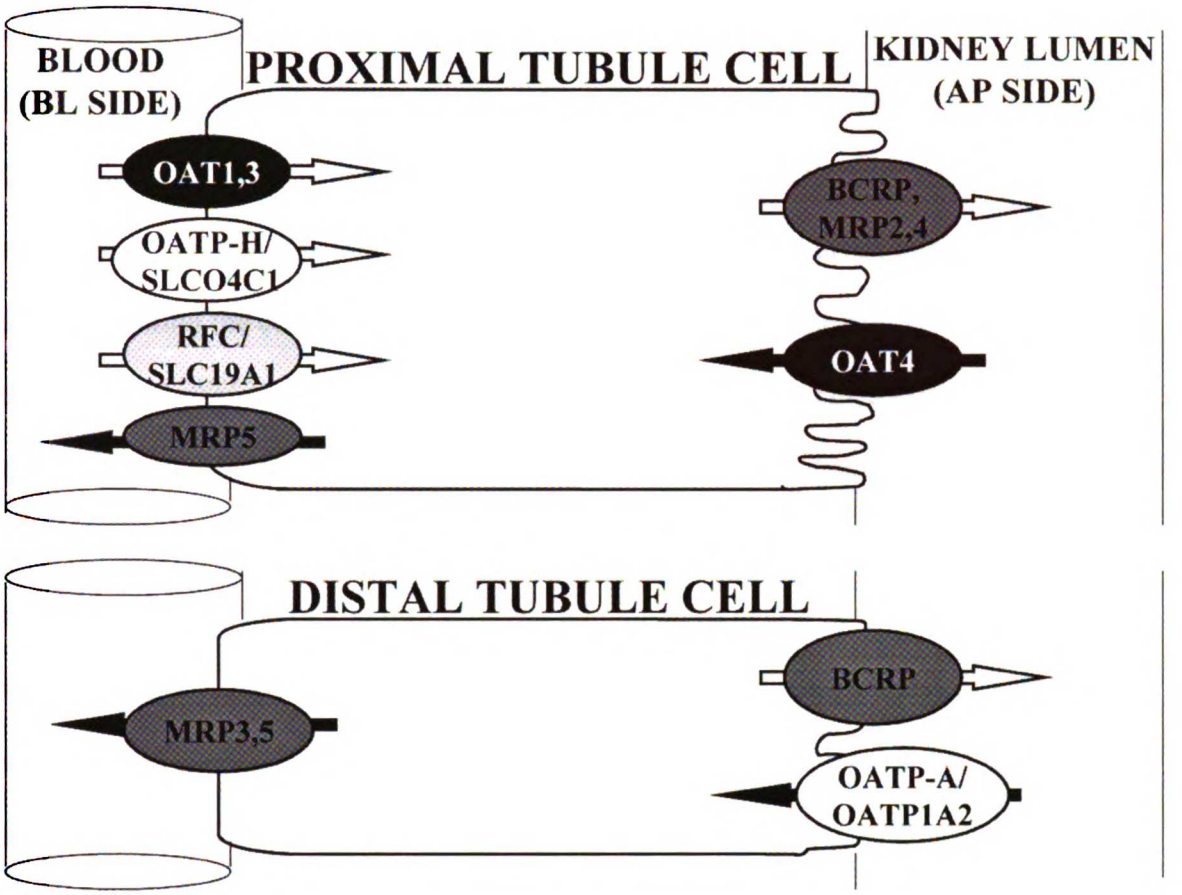

Figure 1. Diagram of membrane transporters expressed in the human proximal and distal tubule cells of the kidney that interact with MTX. Arrows provide the direction of MTX transport, with white filled arrows indicating secretion of MTX and black filled arrows indicating reabsorption of MTX. Color filled circles denote transporters belonging to a particular family of transporters, black for the OAT family, white for the OATP family, light gray for the SLC19 family, and dark gray for the ABC family.

treatment was continued until MTX concentrations fell below 0.1 μM. MTX, hydrocortisone, and cytarabine was administered intrathecally in an age-adjusted dose 6-7 hours prior to the MTX infusion. In protocol XIV and XV patients received 2.5 (low-risk patients) or 5 g/m^2 (standard or high-risk patients) of MTX given intravenously over 24 hours during the consolidation phase. Remission induction therapy prior to the consolidation phase included prednisone, vincristine, daunorubicin, asparaginase, etoposide, cytarabine and triple intrathecal regimen of hydrocortisone, MTC, and cytarabine. Hydration consisting of 5% dextrose and 40 mEq/L of $NaHCO_3$ in 0.25% normal saline at a rate of 200 mL/m^2/h was administered over 8 hours. Leucovorin (10 mg/m^2 for low-risk patients and 15 mg/m^2 for standard/high-risk patients) was administered every 6 hours for 5 doses beginning 44 hours after starting MTX. Leucovorin was increased in patients who had MTX plasma concentrations greater than 0.8 μM at 42 hours after starting MTX and leucovorin treatment was continued until MTX concentrations fell below 0.1 μM.

Pharmacokinetic Analysis

Plasma MTX concentrations were measured at 0, 3, 7, 23, and 44 hours from the start of MTX in protocol XIII or at 1, 6, 23, and 42 hours from the start of MTX in protocol XIV and XV. MTX concentrations were determined using a fluorescence polarization immunoassay (TDx/TDxFLx systems, Abbott Laboratories, IL). Pharmacokinetic parameters for a two-compartment model, including V_c (volume of distribution of the central compartment), K_{el} (elimination rate constant), K_{cp} (rate constant for MTX movement from central to peripheral compartment), and K_{pc} (rate constant for MTX movement from peripheral to central compartment), were estimated with a



Bayesian algorithm implemented in the Adapt II software based on the measured plasma MTX concentrations. The systemic clearance of MTX was calculated from V_c times K_{el} and MTX AUC (area under the concentration versus time curve) was determined from dose divided by systemic clearance.

Genotyping

A total of 23 single nucleotide polymorphisms (SNPs) in 6 kidney transporters (OAT3, OATP1A2, RFC, MRP2, MRP4, and BCRP), which are expressed in the kidney and interact with MTX are being genotyped using ABI TaqMan SNP Genotyping assays (Applied Biosystems, Foster City, CA). SNPs were selected based on several criteria: 1) a SNP had to have a minor allele frequency of 5% or greater in European-Americans and 2) a SNP had to alter the protein sequence of the transporter or 3) a SNP had to have been shown to alter the function of the protein *in vitro* or in cellular systems. Of the 23 SNPs, 11 will be tested for direct association with clinical phenotypes, while the remaining 14 are being genotyped to group patients according to the most common haplotypes. The 14 haplotype tagging SNPs were identified using the software program HaploBlockFinder V0.7. A total of 16 haplotypes in 4 kidney transporters (OAT3, OATP1A2, MRP2, and MRP4) were selected based on the criteria that they had to occur with a frequency of 5% or greater. SNP and haplotype frequencies were based on genotype data from an ethnically diverse population of 270 (N=247 in the case of MRP2) healthy individuals, which can be accessed at http://www.pharmgkb.org. Haplotypes were inferred from variant sites using the Bayesian statistical method of PHASE (32). Clinical phenotypes to be associated with SNPs and haplotypes in 6 kidney transporter genes include MTX

plasma concentrations 42 hours after dose, MTX systemic clearance, serum creatinine after start of MTX, and glomerular filtrarion rate after start of MTX.

Pharmacoepidemiological Analysis

The following demographics and clinical data were collected for analysis: age, race, gender, height (at start of each course), body surface area (at start of each course), serum creatinine (on day of or day before MTX start and between 18-48 hours after MTX start), bilirubin (on day of or day before MTX start and between 18-48 hours after MTX start), ALT (on day of or day before MTX start and between 18-48 hours after MTX start), AST (on day of or day before MTX start and between 18-48 hours after MTX start), and MTX plasma concentration at 42 hours after MTX start. In addition, GFR was estimated before and after MTX start using the pediatrics specific Schwartz formula (33, 34): GFR (mL/min) = K x height (in cm) / SCr, where K = 0.45 (for infants 1 year old or younger), 0.55 (for children 2-12 years of age and 13-21-year-old females), or 0.7 (for 13-21-year-old males). Pharmacokinetics, demographics, and clinical data were analyzed using two different statistical tests as implemented in GraphPad Prism 4 Software: Pearson Product Moment Correlation, Spearman Rank-Order Correlation, and unpaired Student's t-test.

Results

ALL study population

Our study population represents the largest number of ALL patients analyzed to date: of the 565 enrolled patients, 314 were male, 407 were European-Americans, and 107 were African-Americans. Demographics and clinical variables for the 565 ALL

Table 1. ALL patient characteristics

Characteristic	Median	Range
Age (years)	6.25	0.3-19.3
Height (cm)	113.7	14.1-186.8
Body surface area (m^2)	0.89	0.24-2.66
Serum creatinine (mg/dL)[1]	0.4	0.2-1.2
Glomerular filtration rate (mL/min/m^2)[1,2]	136.9	25.0-235.4
Total bilirubin (mg/dL)[1]	0.4	0.1-1.8
ALT (IU/L)[1]	25.0	4.0-324.0
AST (IU/L)[1]	32.3	14.5-263.0

[1]Clinical variables were measured on day of or one day before start of MTX. Normal values for serum creatinine (2-21 years of age) are 0.3-1.0 mg/dL, for glomerular filtration rate (2-21 years of age) are 133.0 ± 30.0 mL/min/1.73 m^2, for total bilirubin are 0-1.4 mg/dL, for ALT are 0-50 IU/L, and for AST are 0-60 IU/L.
[2]Glomerular filtration was estimated using the pediatric specific Schwartz formula (33, 34).

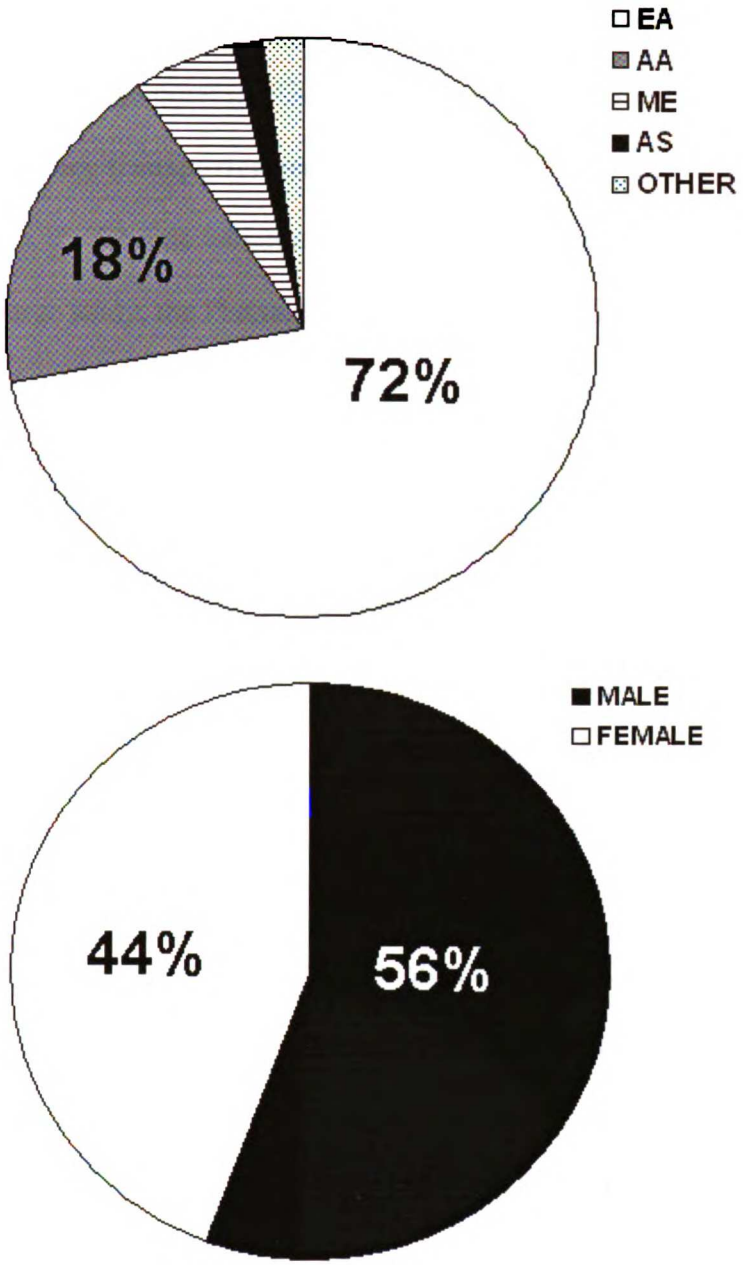

Figure 2. Ethnic and gender distribution of ALL population. EA refers to European-Americans, AA to African-Americans, ME to Mexican-Americans, and AS to Asian-Americans.

patients who received an average of 7 courses of MTX (range, 4 to 10 courses; total number of courses, 3930) are shown in Table 1 and Figure 2.

Kidney transporter genotyping

Genetic variation in 6 kidney transporter genes (Table 2) was analyzed as part of a large study, the Pharmacogenetics of Membrane Transporters project, whose goal is to identify variants in membrane transporter genes that contribute to differences in drug response and disposition. The coding exons, flanking intronic sequences, and in selected cases the promoter regions (*i.e.* MRP2) were screened in a collection of 270 (N=247 in the case of MRP2) ethnically diverse genomic DNA samples from healthy individuals. The data can be found at http://www.pharmgkb.org. OAT3 was selected because it is the most highly expressed organic anion transporter on the basolateral membrane of the proximal tubule acting to secrete MTX into the proximal tubule cells. OAT3 interacts with MTX with high affinity, and several drug-drug interactions involving MTX have been reported that occur via members of the OAT transporter family (22, 35-37). RFC was selected because it is also highly expressed on the basolateral membrane of the proximal tubule where it functions to secrete MTX into the proximal tubule cells and it has been shown to be a determinant of MTX efficacy in ALL (18). MRP2, MRP4, and BCRP on the other hand are highly expressed on the apical membrane of proximal tubule cells where they are actively involved in the transepithelial movement of MTX from the blood into the kidney lumen (16, 19, 38). Specifically, several naturally occurring variants in BCRP, including Val12Met and Gln141Lys, have been identified that exhibit decreased expression and/or efflux of anti-cancer drugs (39, 40). In addition, BCRP has been implicated in the drug-drug interaction between MTX and benzimidazoles (41),

UCSF LIBRARY

Table 2. Summary of 23 SNPs in 6 kidney membrane transporter genes

Transporter	SNP #	CDS Position[1]	Nucleotide Change	Amino Acid Position[1]	Amino Acid Change	Allele Frequency (%)[2]		
						Total (n=540)	EA (n=160)	AA (n=160)
SLC22A8								
	1.3	153	G→A	51	syn	15.7	5.1	40.0
	2.2	+79	G→C	N/A	N/A	25.9	16.0	36.2
	4.3	723	T→A	241	syn	19.9	24.4	9.0
	8.2	+81	G→A	N/A	N/A	16.0	17.1	7.7
SLCO1A2								
	1.1	**38**	**T→ C**	**13**	**Ile→Thr**	**6.3**	**16.3**	**2.5**
	3.1	-51	T→G	N/A	N/A	13.9	29.4	8.1
	5.2	**516**	**A→C**	**172**	**Glu→Asp**	**1.1**	**1.9**	**0.6**
	10.1	-22	G→A	N/A	N/A	6.9	13.8	3.1
SLC19A1								
	N/A	**80**	**G→A**	**27**	**Arg→His**	**44.3**	**N/A**	**N/A**
ABCC2[3]								
	P3	**-1549**	**G→A**	**N/A**	**N/A**	**40.7**	**43.0**	**48.5**
	P8	**-1023**	**G→A**	**N/A**	**N/A**	**15.4**	**10.5**	**13.5**
	P9	-1019	A→G	N/A	N/A	36.0	43.0	36.5
	P12	-24	C→T	N/A	N/A	13.6	19.5	6.0
	10.2	**1249**	**G→A**	**417**	**Val→Ile**	**15.8**	**17.0**	**17.0**
	25.4	**3563**	**T→A**	**1188**	**Val→Glu**	**5.9**	**7.5**	**6.5**
	28.2	3972	C→ T	1324	syn	30.9	38.3	27.3
	32.2	**4544**	**G→A**	**1515**	**Cys→Tyr**	**11.6**	**8.1**	**19.6**
ABCC4								
	8.2	**912**	**G→T**	**304**	**Lys→Asn**	**15.8**	**8.7**	**18.1**
ABCG2								
	1.1	**34**	**G→A**	**12**	**Val→Met**	**12.9**	**6.6**	**7.7**
	4.1	**421**	**C→A**	**141**	**Gln→Lys**	**16.7**	**8.1**	**1.3**
	9.1	-60	A→T	N/A	N/A	22.2	36.1	8.9
	12.3	+40	C→T	N/A	N/A	27.6	40.0	13.8
	14.1	-46	A→G	N/A	N/A	44.9	16.2	71.9

Data are available at http://www.pharmgkb.org. A population composed of 270 (N=247 in the case of ABCC2) ethnically diverse healthy individuals was used in the analysis. The variants shown in bold will be tested for direct association with clinical phenotypes.
[1]Positions are relative to the ATG start site for each gene.
[2]Allele frequencies were calculated from actual DNA samples sequenced. Total, entire sample; EA, European-American; AA, African-American; n, number of chromosomes.
[3]For ABCC2, the total number of chromosomes was 494 (EA=200; AA=200).

which can lead to severe MTX-induced clinical toxicity (*i.e.* omeprazole and pantoprazole). On the apical membrane of distal tubule cells, OATP1A2 is the only membrane transporter identified so far that is implicated in the saturable reabsorption of MTX from the kidney lumen back into the blood and several naturally occurring variants have been identified in this transporter, which exhibit altered cellular transport of MTX (15, 42).

As shown in Table 2, a total of 23 SNPs were selected in six kidney transporters, OAT3, OATP1A2, RFC, MRP2, MRP4, and BCRP, to be genotyped in the ALL study population. SNPs that we wanted to directly associate with MTX clinical phenotypes were chosen according to the following criteria: 1) the allele frequency of the minor allele had to be $\geq$ 5% in our healthy population used for initial screening of genetic variation in membrane transporters, and 2) the variant had to alter the protein sequence of the transporter, or 3) the variant had to have been shown to exhibit altered function in cellular assays. According to these criteria we identified 11 variants in 5 kidney transporters: Ile 13Thr and Glu172Asp in OATP1A2, Arg27His in RFC, P3, P8, Val417Ile, Val1188Glu, and Cys1515Tyr in MRP2, Lys304Asn in MRP4, and Val12Met and Gln141Lys in BCRP (Table 2). Furthermore, we identified an additional 12 variants to help differentiate among the 3-5 most common haplotypes in four kidney transporters (Figure 3), including *SLC22A8*, *SLCO1A2*, ABCC2, and ABCG2. Haplotypes were selected if they occurred with a frequency of at least 5% in the European-American population and were predicted using PHASE (32) in a population composed of 270 (N=247 in the case of ABCC2) ethnically diverse healthy individuals. As shown in Figure 3, all haplotypes in a particular

UCSF LIBRARY

SLC22A8 Haplotypes

Exon	1		2		3		4	5	6		8	9			10	Frequency of *SLC22A8* Haplotypes (%)	
Variable Site	G	G	G	G	C	C	T	T	A	G	G	G	G	G	C	EA	AA
*1																47.5	25.9
*2							A									23.4	7
*3			G								A					15.2	1.3
*4		A														5.1	24.1

SLCO1A2 Haplotypes

Exon	1	2			3		4	5		7		8	9	10		11	12				13	14		Frequency of *SLCO1A2* Haplotypes (%)	
Variable Site	T	A	A	T	T	T	A	A	A	G	C	C	A	C	T	G	A	T	A	C	A	T	A	C	G	EA	AA
*1																										62.7	40.0
*2					G										A											12.0	3.1
*3	C				G																					15.8	1.9

ABCC2 Haplotypes

Exon	P											2		3	6	7	8	9	10		11	13	14	16	19	21	22	23	24	25		26	27	28		29		30		31		32		Frequency of ABCC2 Haplotypes (%)	
Variable Site	T	G	A	G	C	G	A	C	G	G	T	A	C	G	G	A	G	C	G	T	C	T	T	T	C	G	T	T	G	G	T	C	T	A	C	C	C	C	C	G	G	G	G	C	G	C	G	EA	AA
*1																																														14.1	7.6
*2			A								G	T																						T											17.2	4.3
*3																																													6.1	3.3
*4																			A																										10.1	2.2
*6			A								G																							T											9.1	3.8

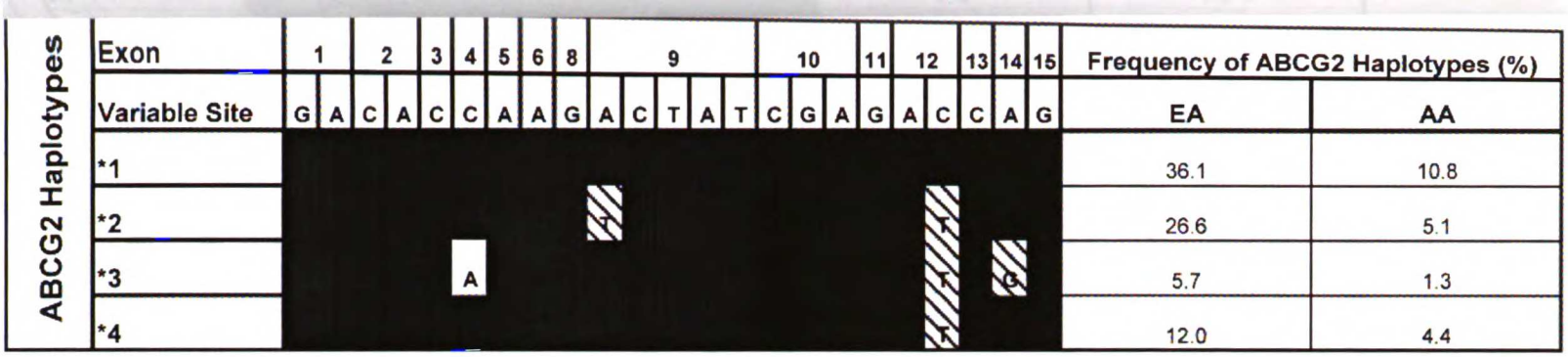

Figure 3. Structure and population frequency of the most common haplotypes in 4 kidney transporters (*SLC22A8*, *SLCO1A2*, ABCC2, and ABCG2), which are used to subgroup the ALL population. The first row shows the exons of the gene; the second row contains the sequence of the reference allele at each variable site. Each of the subsequent rows shows the 3-5 most common haplotypes based on their frequency in European-Americans. A black filled square is used to indicate that there is no change from the reference allele; a gray filled square shows a synonymous change in the coding region; a white filled square indicates a non-synonymous change; a diagonally striped square denotes a change at a non-coding site. Letters in the squares indicate the base pair change. Haplotypes were predicted using PHASE software version 1.0.1 (32) in a separate population composed of 270 (N=247 in the case of ABCC2) ethnically diverse healthy individuals. Frequencies of the haplotypes in the European-American (EA) and African-American (AA) ethnic groups are given as percentages.

transporter gene except for the reference haplotype, which is the one occurring at the highest frequency in all populations, contained non-coding and/or synonymous variants. In addition, a few haplotypes also contained a variant which altered the protein sequence of the transporter. A total of four haplotypes were identified in *SLC22A8*, which occurred with a frequency of $\geq$ 5% in European-Americans. None of the *SLC22A8* haplotypes contained a protein-altering variant. A total of three haplotypes were selected in *SLCO1A2* and haplotype *3 contained the protein-altering variant Ile13Thr. Five haplotypes were identified in ABCC2 and haplotype *4 contained the Val417Glu variant, while 4 haplotypes were selected in ABCG2, with haplotype *3 having the Gln141Lys variant.

Genotyping of our ALL study population for the nine SNPs and 16 haplotypes in six kidney transporters is ongoing. The clinical variables we plan to test for association include MTX plasma concentrations 42 hours after dose, MTX systemic clearance, serum creatinine after start of MTX, and glomerular filtration rate after start of MTX. We plan to perform association analyses by testing whether the average value (i.e. mean and/or median) of a particular clinical phenotype significantly differs among the three genotype and/or haplotype groups for each transporter variant and/or haplotype identified in our ALL patients.

Pharmacoepidemiological analysis of ALL population

Following MTX treatment, a considerable number of ALL patients can exhibit delayed elimination of MTX and variable MTX pharmacokinetic parameters and this is a significant clinical problem because it requires additional hospitalization for monitoring and more aggressive rescue therapy which can negate MTX anti-tumor effects (7, 11). As

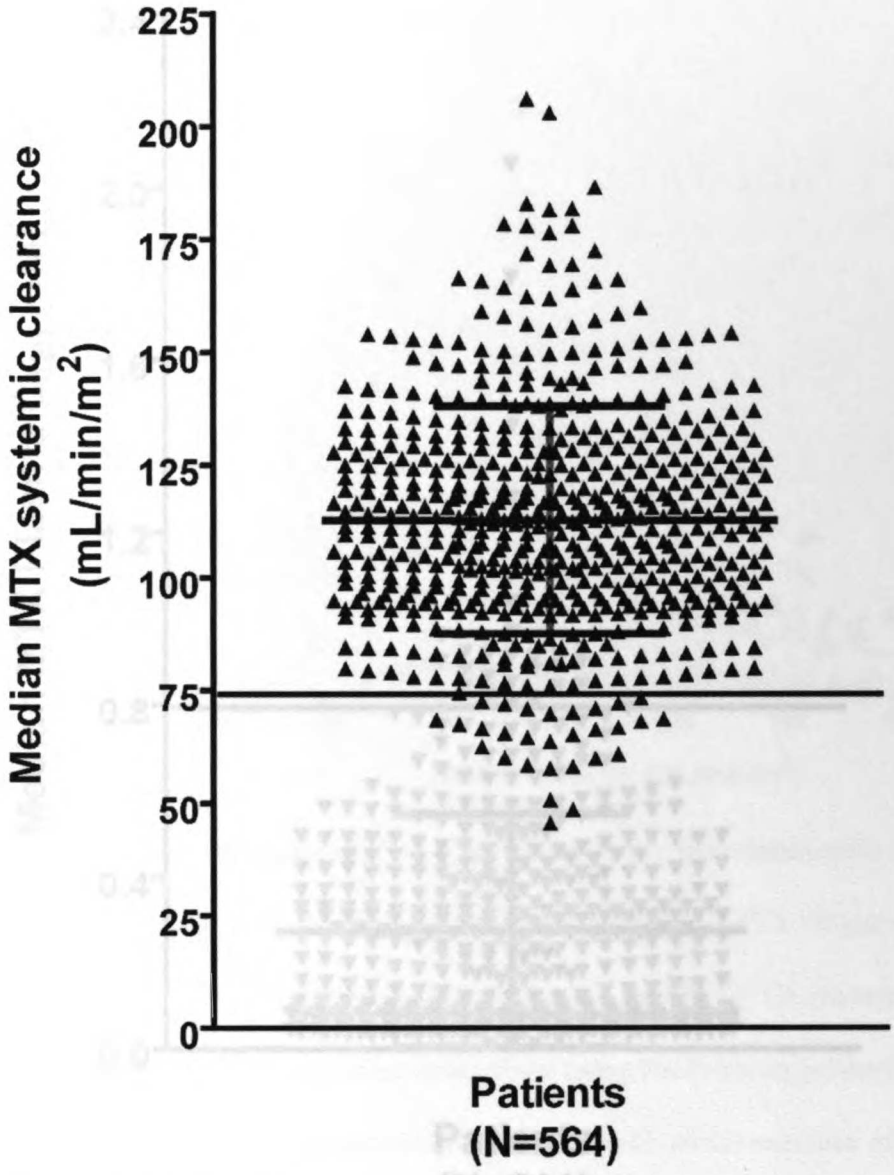

Figure 4. Median MTX systemic clearance estimated in 564 ALL patients. Patients received an average of 7 MTX courses and the median was calculated from all of the MTX CL measurements available for each patient. The mean ± SD for MTX CL is 113 ± 25.3 mL/min/m^2. MTX CL was estimated from measured plasma MTX concentrations following the MTX infusion using a Bayesian algorithm implemented in the Adapt II software. Patients (30 of 564) with MTX CL below 75 mL/min/m^2 exhibited delayed excretion.

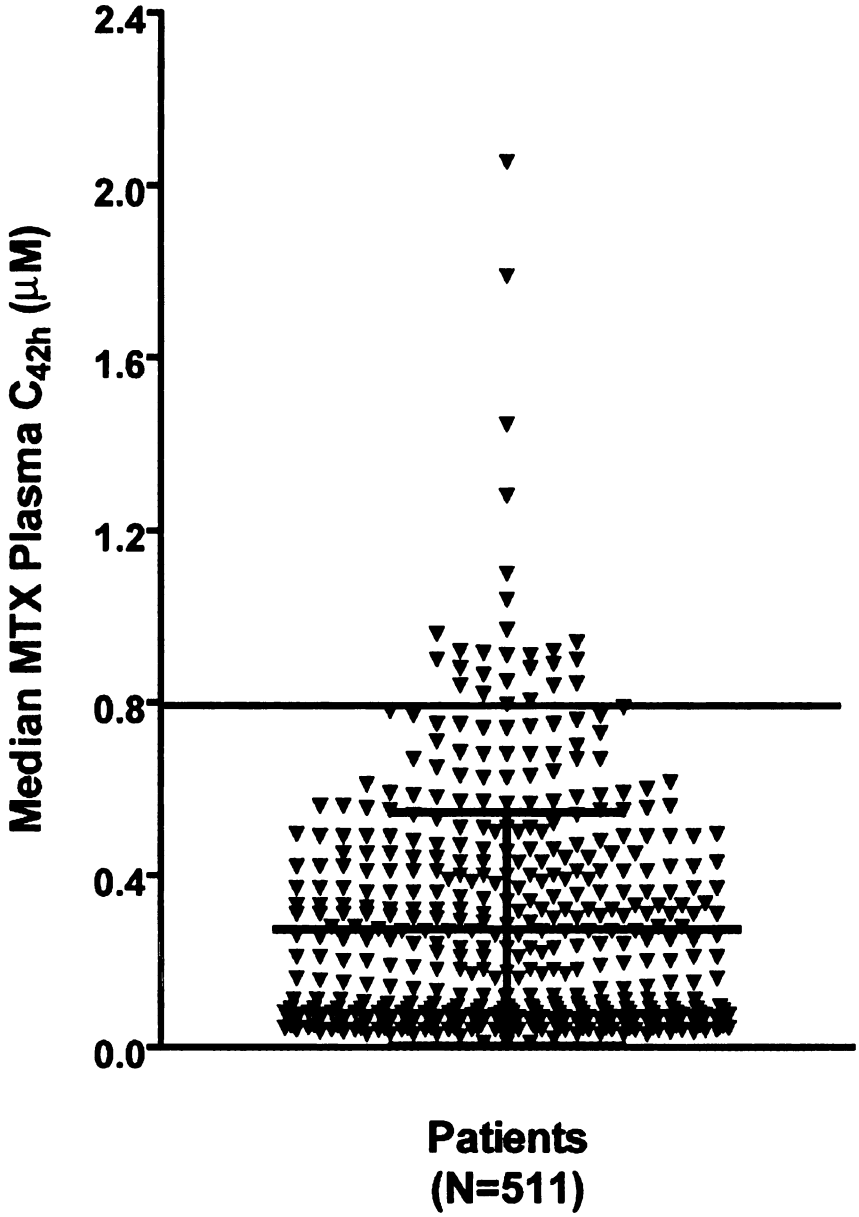

Figure 5. Median plasma MTX concentration measured 42 hours after start of MTX infusion in 511 ALL patients. Patients received an average of 7 MTX courses and the median was calculated from all of the MTX plasma C_{42h} measurements available for each patient. The mean ± SD for MTX plasma C_{42h} is 0.275 ± 0.27 μM. A MTX plasma C_{42h} > 0.8 μM is considered high-risk and has been associated with the development of severe systemic toxicity (6).

UCSF LIBRARY

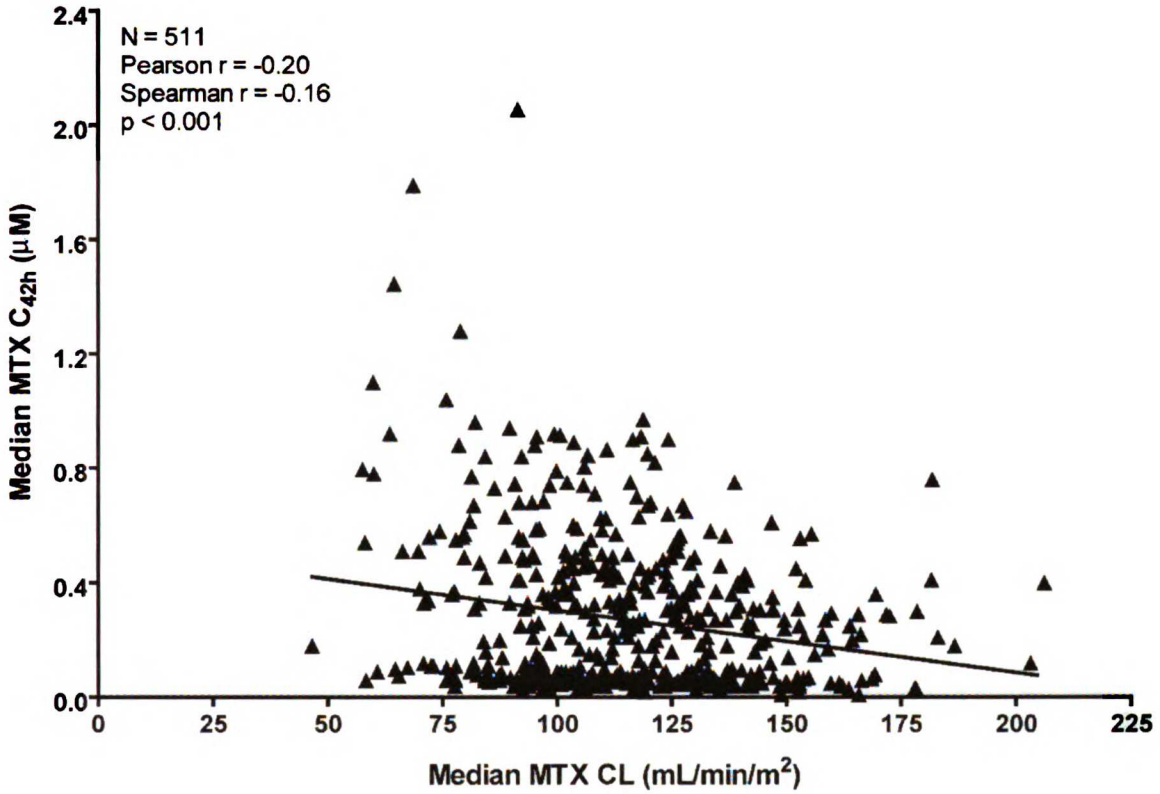

Figure 6. Median plasma MTX C_{42h} is negatively correlated with median MTX CL in 511 ALL patients. Patients received an average of 7 MTX courses and the median was calculated from all of the MTX plasma C_{42h} and MTX CL measurements available for each patient. P values were determined using the Pearson product moment correlation and Spearman rank-order correlation, with $p < 0.05$ as the criterion of significance.

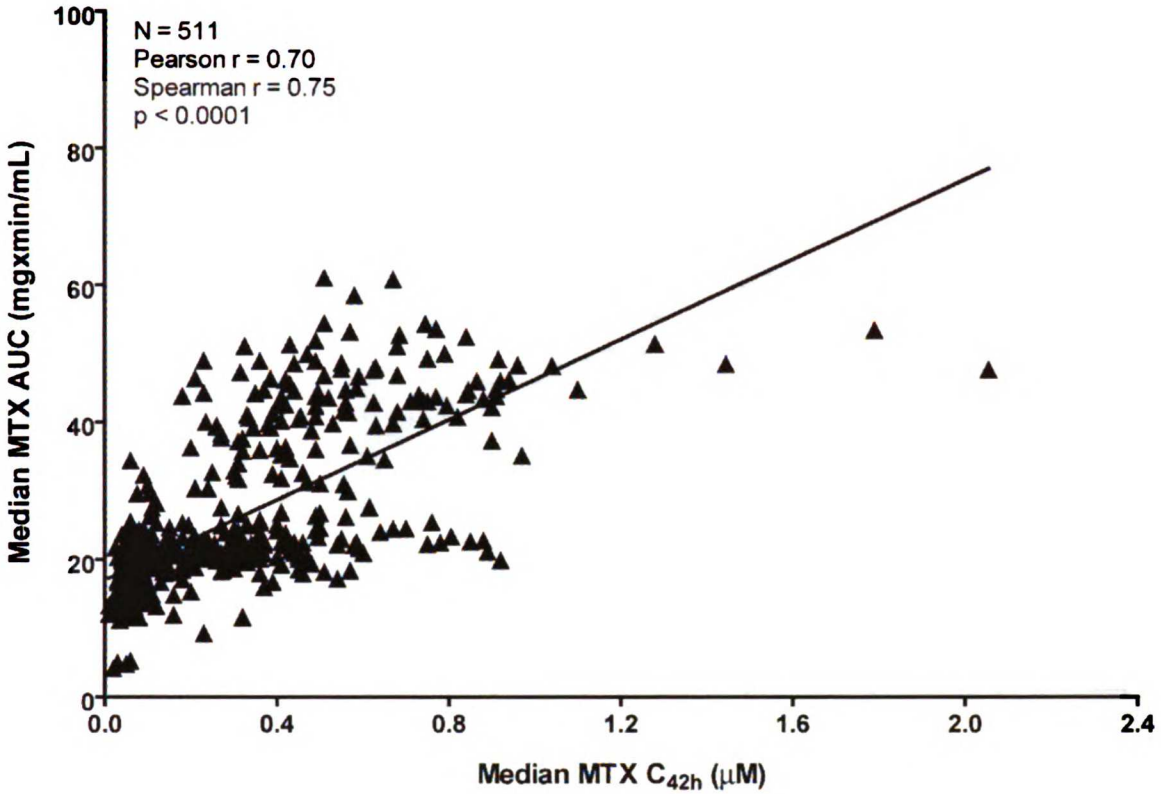

Figure 7. Median MTX AUC is positively correlated with plasma MTX C_{42h} in 511 ALL patients. Patients received an average of 7 MTX courses and the median was calculated from all of the MTX plasma C_{42h} and MTX AUC measurements available for each patient. P values were determined using the Pearson product moment correlation and Spearman rank-order correlation, with $p < 0.05$ as the criterion of significance.

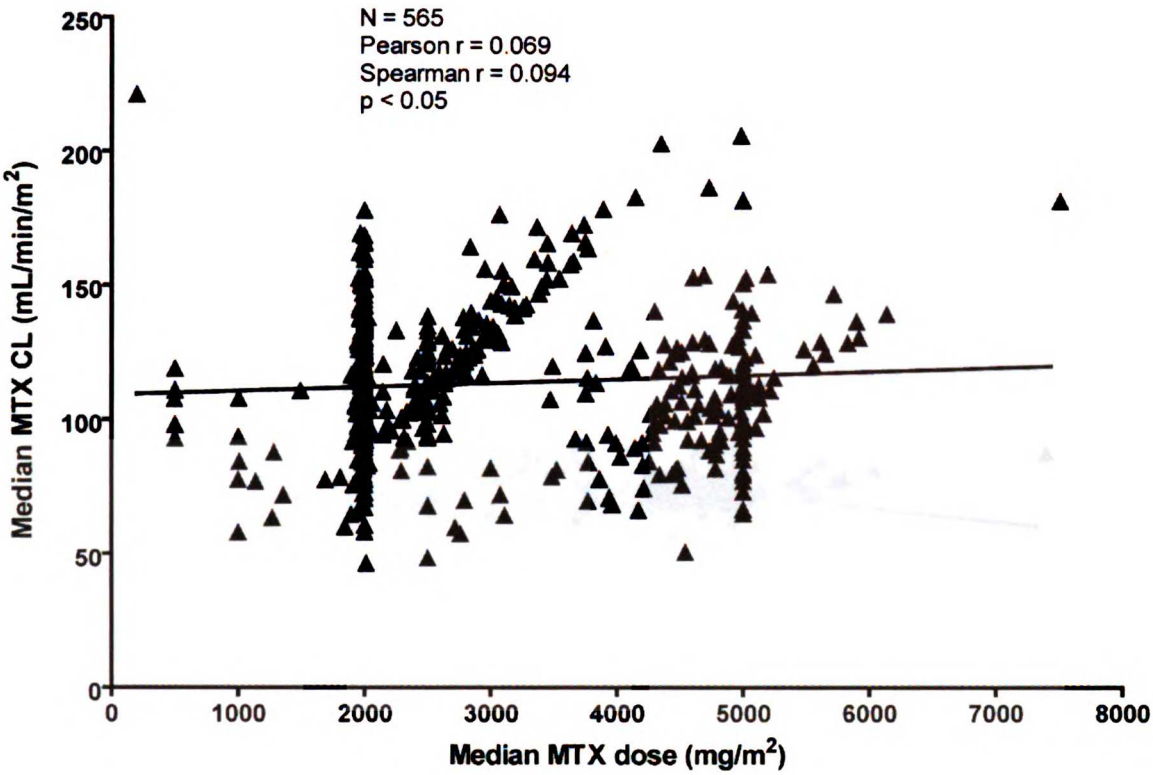

Figure 8. Median MTX CL is positively correlated with MTX dose in 565 ALL patients. Patients received an average of 7 MTX courses and the median was calculated from all of the MTX CL and MTX dose measurements available for each patient. P values were determined using the Pearson product moment correlation and Spearman rank-order correlation, with $p < 0.05$ as the criterion of significance.

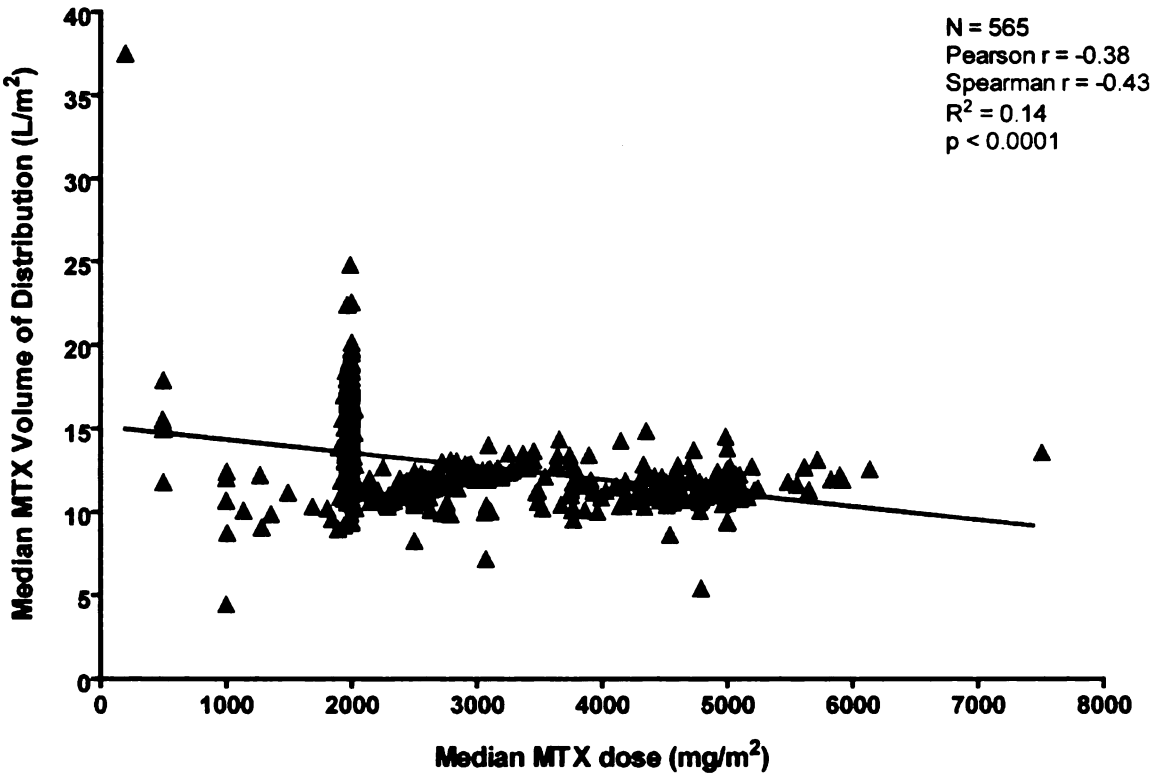

Figure 9. Median MTX volume of distribution for the central compartment (V_c) is negatively correlated with plasma MTX dose in 565 ALL patients. Patients received an average of 7 MTX courses and the median was calculated from all of the MTX V_c and MTX dose measurements available for each patient. P values were determined using the Pearson product moment correlation and Spearman rank-order correlation, with $p < 0.05$ as the criterion of significance.

shown in Figure 4, systemic MTX clearance (CL) was estimated in 564 ALL patients after each course of MTX. Median values of MTX CL were calculated for each patient from all their MTX courses and it was determined that MTX CL can vary by as much as 5-fold (range, 45.5 to 206.2 mL/min/m^2). As many as 30 (5.3%) ALL patients had MTX CL below 75 mL/min/m^2, indicating that these patients exhibit delayed MTX elimination and would require a decrease in MTX dose as well as more aggressive rescue treatment to avoid serious systemic toxicities.

MTX plasma concentrations following the start of infusion have been used to monitor ALL patients to reduce and/or prevent systemic toxicity to the kidney, GI tract, and the hematopoietic and central nervous system. In particular, MTX concentrations above 0.8 μM at 42 hours following the start of MTX have been associated with increased risk of serious toxicity (6). As shown in Figure 5, 27 out of 511 (5.3%) ALL patients exhibited MTX plasma $C_{42h} \geq 0.8$ μM, suggesting that these patients are at increased risk of MTX-induced severe systemic toxicities. In our ALL population, we observed that low systemic CL of MTX was significantly correlated ($p < 0.001$) with elevated high-risk MTX plasma C_{42h} and that MTX plasma C_{42h} were in turn strongly correlated with increased exposure to MTX, that is elevated MTX AUC (Figure 6 and 7) . These findings suggest that delayed elimination of MTX can lead to elevated high-risk plasma levels of MTX and subsequently increased exposure of normal tissues and cells to the cytotoxic effect of MTX, resulting in severe systemic toxicities.

It was observed in the ALL study population that MTX CL significantly increased ($p < 0.05$) as the MTX dose increased (Figure 8). Since 60-90% of MTX is excreted unchanged in the urine (2), this finding suggests that MTX renal excretion is non-linear

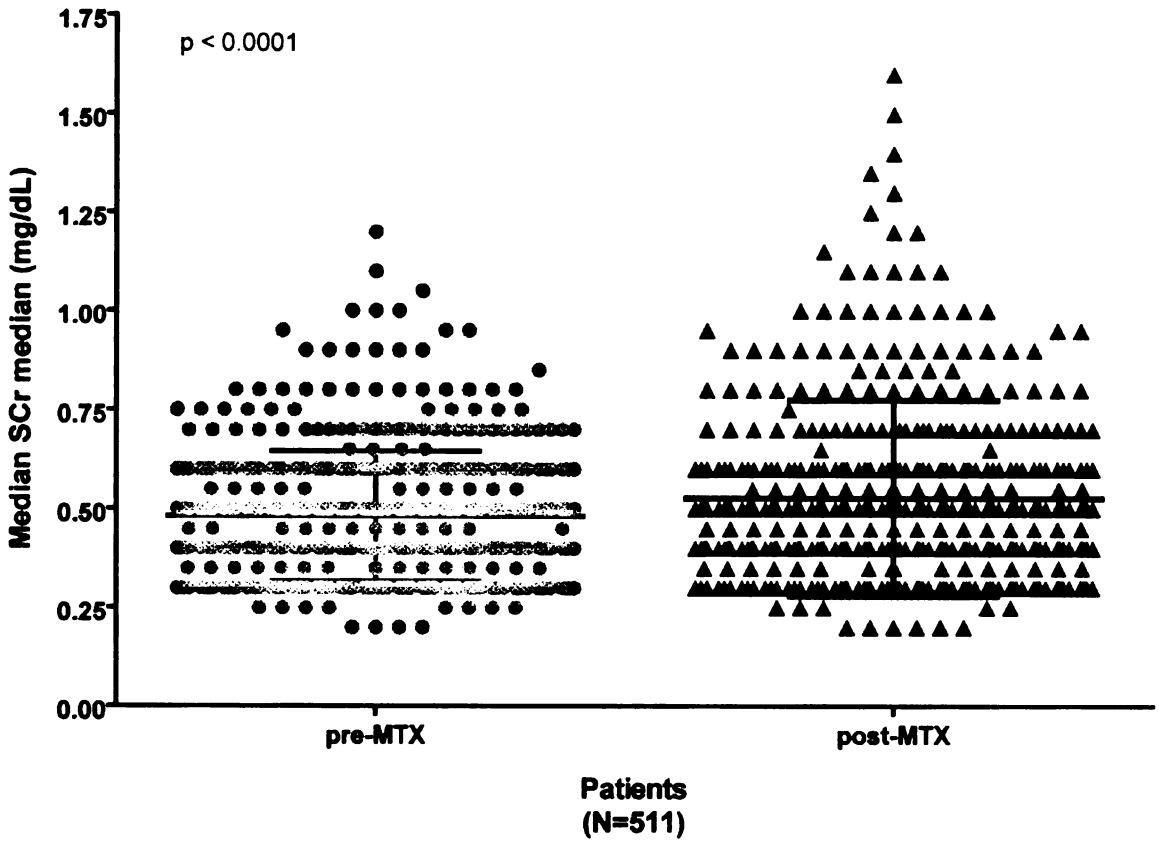

Figure 10. Median SCr measured before and after MTX in 511 ALL patients. Patients received an average of 7 MTX courses and the median was calculated from all of the SCr measurements available for each patient. SCr was measured the day of or the day before the MTX infusion and between 18 to 48 hours after starting MTX. The mean ± SD for median SCr before MTX (gray circles) is 0.48 ± 0.16 mg/dL, while after MTX (black triangles) is 0.53 ± 0.25 mg/dL ($p < 0.0001$). Normal SCr values vary by age and are between 0.3-0.7 mg/dL in children 2-12 years of age. P values were determined using the paired Student t-test, with $p < 0.05$ as the criterion of significance.

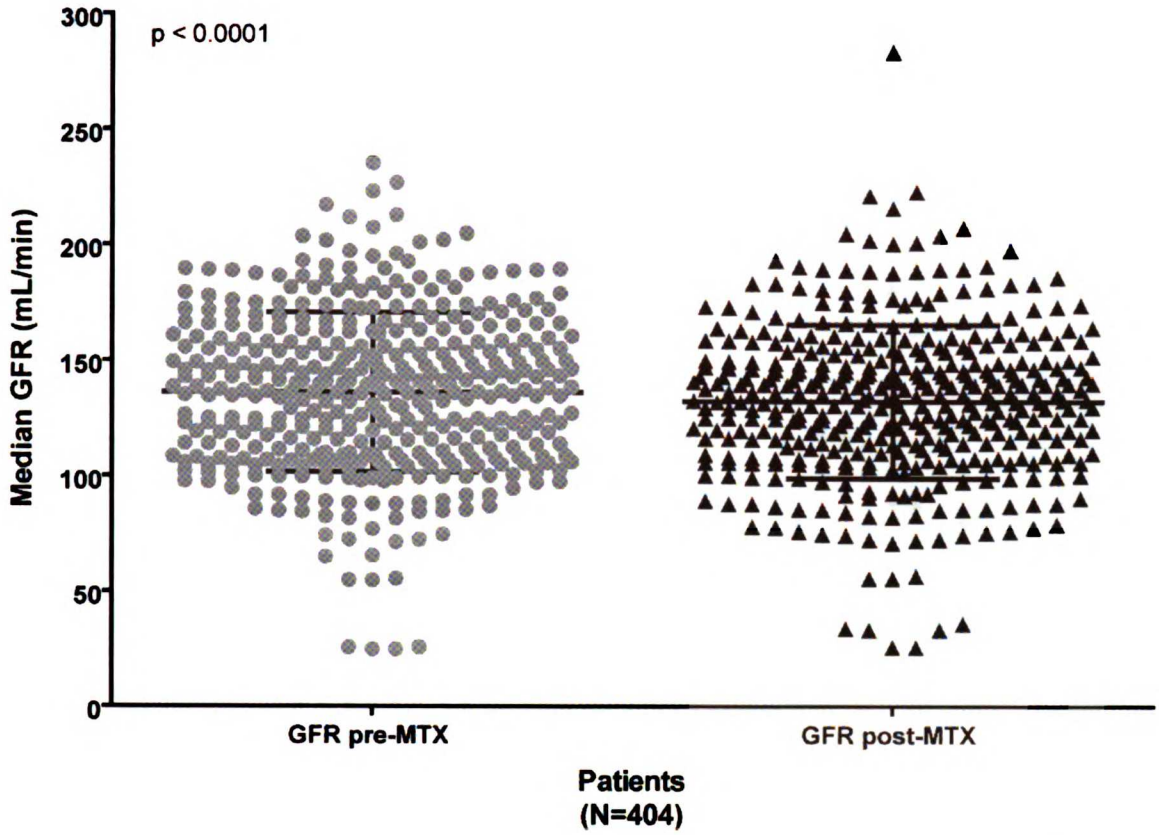

Figure 11. Median GFR measured before and after MTX in 404 ALL patients. Patients received an average of 7 MTX courses and the median was calculated from all of the GFR measurements available for each patient. GFR was estimated using the pediatric specific Schwartz formula (33, 34). The mean ± SD for median GFR before MTX (gray circles) is 136 ± 34.5 mL/min/m^2, while after MTX (black triangles) is 132 ± 33.3 mL/min/m^2 ($p < 0.0001$). Thirty-nine of 404 ALL patients had MTX GFR below 90 mL/min/m^2 (*i.e.* a 25% reduction) while nine of 404 ALL patients exhibited MTX GFR below 60 mL/min (*i.e.* a 50% reduction) after MTX. Normal GFR values vary by age and are between 100-150 mL/min/m^2 in children 2-12 years of age. P values were determined using the paired Student t-test, with $p < 0.05$ as the criterion of significance.

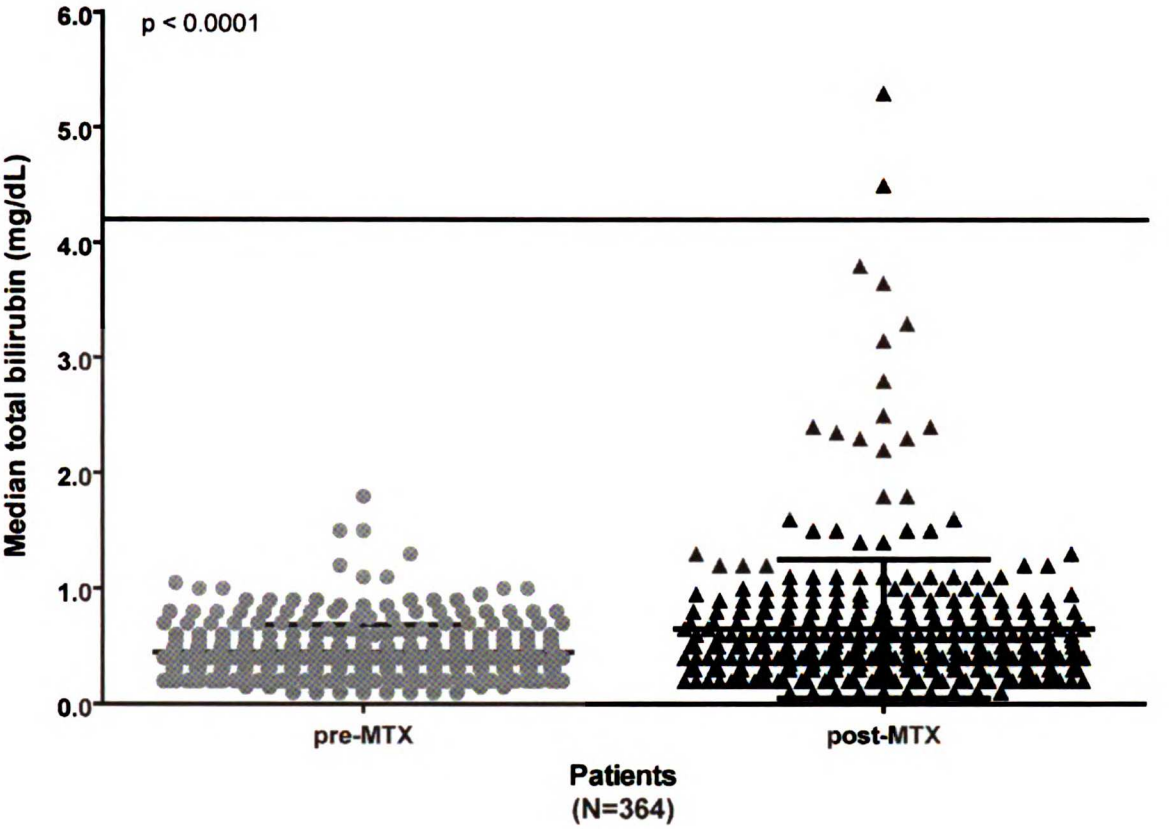

Figure 12. Median total bilirubin measured before and after MTX in 364 ALL patients. Patients received an average of 7 MTX courses and the median was calculated from all of the total bilirubin measurements available for each patient. Total bilirubin was measured the day of or the day before the MTX infusion and between 18 to 48 hours after starting MTX. The mean ± SD for median total bilirubin before MTX (gray circles) is 0.45 ± 0.24 mg/dL, while after MTX (black triangles) is 0.65 ± 0.60 mg/dL ($p < 0.0001$). Normal total bilirubin values range from 0-1.4 mg/dL in pediatrics. The solid black line indicates total bilirubin levels of three times the upper limit of normal (*i.e.* 4.2 mg/dL) or greater, which is indicative of liver dysfunction. P values were determined using the paired Student t-test, with $p < 0.05$ as the criterion of significance.

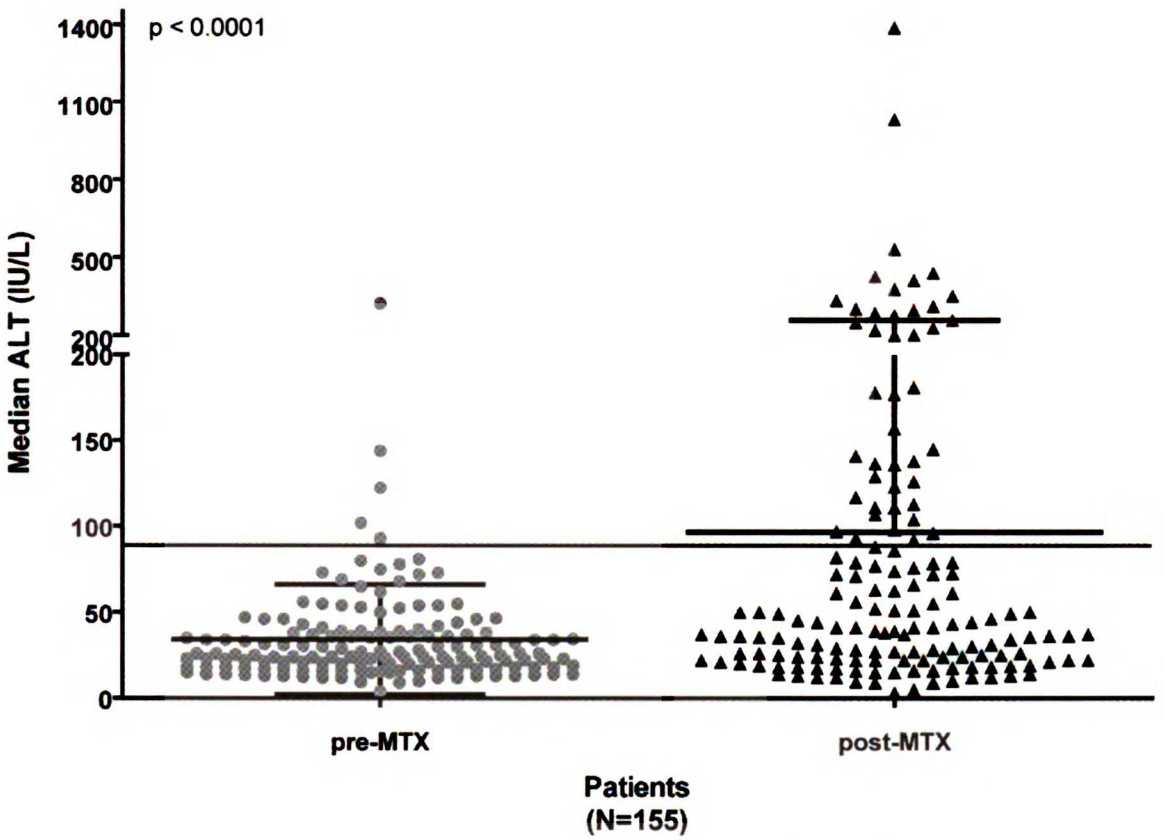

Figure 13. Median ALT measured before and after MTX in 155 ALL patients. Patients received an average of 7 MTX courses and the median was calculated from all of the ALT measurements available for each patient. ALT was measured the day of or the day before the MTX infusion and between 18 to 48 hours after starting MTX. The mean ± SD for median ALT before MTX (gray circles) is 34.1 ± 31.9 IU/L, while after MTX (black triangles) is 96.8 ± 163 IU/L ($p < 0.0001$). Normal ALT values range between 0-30 IU/L in pediatrics. The solid black line indicates total ALT levels of three times the upper limit of normal (*i.e.* 90 IU/L) or greater, which is indicative of liver dysfunction. P values were determined using the paired Student t-test, with $p < 0.05$ as the criterion of significance.

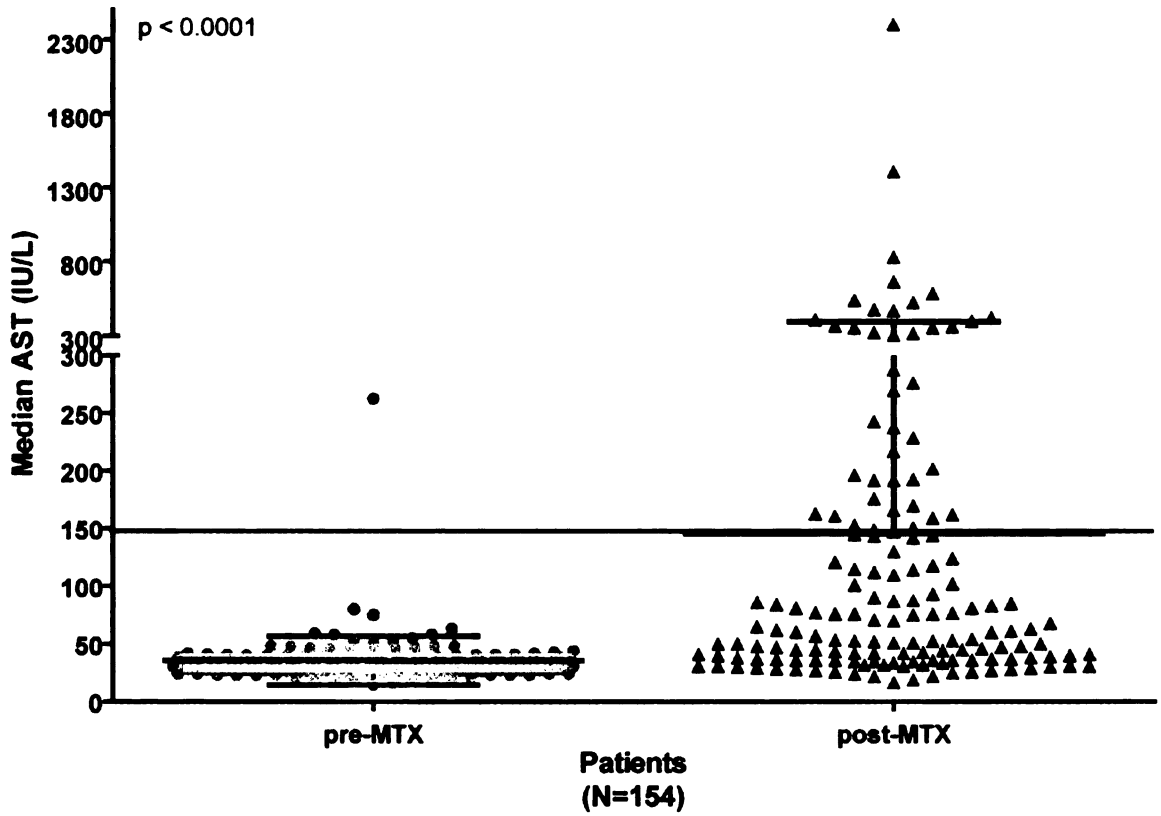

Figure 14. Median AST measured before and after MTX in 154 ALL patients. Patients received an average of 7 MTX courses and the median was calculated from all of the AST measurements available for each patient. AST was measured the day of or the day before the MTX infusion and between 18 to 48 hours after starting MTX. The mean ± SD for median AST before MTX (gray circles) is 35.6 ± 21.1 IU/L, while after MTX (black triangles) is 145.7 ± 253 IU/L ($p < 0.0001$). Normal AST values range from 0-50 IU/L in pediatrics. The solid black line indicates total AST levels of three times the upper limit of normal (*i.e.* 150 IU/L) or greater, which is indicative of liver dysfunction. P values were determined using the paired Student t-test, with $p < 0.05$ as the criterion of significance.

due to active saturable reabsorption, which has been previously reported for low-dose oral MTX used in psoriasis (12). In addition, there was a strong and significant ($p < 0.0001$) inverse relationship between MTX volume of distribution for the central compartment (V_c) and MTX dose, suggesting that MTX and/or its minor metabolite 7-OH-MTX exhibit saturable tissue protein-binding resulting in nonlinear distribution of MTX (Figure 9).

Toxicities associated with MTX administration include nephrotoxicity, neurotoxicity, myelosuppression, mucositis, and less commonly hepatotoxicity (2). We measured in our ALL study population clinical biomarkers of renal (SCr and GFR) and hepatic (total bilirubin, ALT, and AST) function to determine whether these were negatively affected following MTX treatment. Following treatment with MTX, twenty-four of 511 (4.7%) ALL patients exhibited an increase of $\geq$ 50% in their SCr, which is indicative of kidney damage. As shown in Figure 10, SCr significantly increased ($p< 0.0001$) after MTX treatment compared to before the start of the MTX infusion. In parallel, GFR, which was estimated using the pediatric specific Schwartz formula (33, 34), was significantly ($p<0.0001$) lower after MTX treatment compared to before MTX was started (Figure 11). These findings suggest that MTX appears to negatively impact renal function, which could result in variable disposition of MTX and increased risk of severe systemic toxicities. In addition, we observed that ALL patients exhibited an approximately 1.5-fold increase in total bilirubin, 3-fold increase in ALT, and 4-fold increase in AST following MTX treatment (Figure 12-14), suggesting that MTX also has a negative impact on hepatic function, which could put ALL patients at increased risk of severe systemic toxicities and result in highly variable MTX pharmacokinetics.

Discussion

Chemotherapy regimens in ALL generally employ high-dose MTX infusions during the consolidation and continuation phase (1). Despite its successful use in ALL treatment, patients treated with MTX exhibit substantial inter-individual variability in their response to and disposition of MTX (2, 4, 7). In addition, a considerable number of ALL patients develop severe systemic toxicities following MTX, which usually affect the GI tract, kidney, liver, and the hematopoietic and central nervous system (2). Several previous studies have shown that genetic variation in the enzymes of the folate pathway can have a negative impact on MTX therapy in ALL, especially with respect to leukemia relapse and development of treatment-related toxicities (25-31). However, the influence of genetic variation in membrane transporters that are responsible for the uptake and efflux of MTX in human tissues on the efficacy, disposition, and toxicity of MTX in ALL has not been addressed. Since MTX is primarily excreted unchanged in the urine and its elimination depends on saturable secretion and reabsorption in the kidney, it is reasonable to hypothesize that genetic variation in membrane transporters that are expressed in proximal and distal tubule cells and that interact with MTX (Figure 1) contributes to the observed clinical variability in MTX therapy. Therefore, our study provides the most extensive pharmacogenetic and pharmacoepidemiological analysis to date of MTX pharmacokinetics and MTX-induced toxicities in ALL patients.

We selected single nucleotide polymorphisms and haplotypes in 6 kidney transporters (OAT3, OATP1A2, RFC, MRP2, MRP4, and BCRP) known to interact with MTX to determine their impact on MTX disposition and toxicity in ALL. This represents the largest number of genetic variants being analyzed for clinical effects in the largest

number of ALL patients. Our plan is to test for significant differences in clinical phenotypes (*i.e.* MTX plasma concentrations 42 hours after dose, MTX systemic clearance, serum creatinine after start of MTX, and glomerular filtrarion rate after start of MTX) among genotype and/or haplotype groups for each transporter variant and/or haplotype identified in ALL patients. The genotyping and genetic association analysis of our ALL study population is currently ongoing.

Several unique and clinically important findings were observed in our comprehensive pharmacoepidemiological analysis of the ALL study population treated with an average of 7 courses of high-dose MTX. Treatment with MTX resulted in highly variable systemic MTX CL and plasma levels of MTX measured 42 hours following the start of the infusion (Figure 4 and Figure 5). A significant number of ALL patients (~ 5%) exhibited delayed elimination of MTX, elevated high-risk MTX plasma levels, and increased exposure to MTX. In fact, we observed in our study that MTX CL was negatively correlated ($p < 0.001$) with plasma MTX C_{42h}, which in turn was positively correlated ($p < 0.0001$) with MTX AUC (Figure 6 and Figure 7), suggesting that patients with delayed excretion of MTX can develop high-risk elevated levels of MTX in the blood which can then lead to the accumulation of MTX in normal tissues exposing them to the cytotoxic effects of MTX and resulting in severe systemic toxicity. These findings are consistent with previous studies, which analyzed a smaller set of ALL patients, identifying demographics and clinical variables that can contribute to MTX-induced toxicities (11, 43, 44).

We also observed that the systemic CL of MTX significantly increased ($p < 0.05$) as the MTX dose increased, suggesting that MTX exhibits non-linear pharmacokinetics

when given at high-doses in ALL patients (Figure 8). Specifically, MTX appears to have non-linear elimination due to saturation of active reabsorption mechanisms in the kidney. Interestingly, in sub-group analysis we determined for the first time that total MTX CL correlated more strongly with MTX dose in female (Spearman $r = 0.19$; $p < 0.005$) and African-American (Spearman $r = 0.25$; $p < 0.05$) patients (data not shown). The fact that systemic MTX CL exhibits non-linearity is consistent with the majority of a MTX dose being excreted unchanged in the urine and saturable transport mechanisms being responsible for the secretion and reabsorption of MTX in the kidney (2, 7, 12-14). Non-linear renal CL of MTX as a result of saturation of renal tubular reabsorption was previously reported in a small study where MTX was given orally at low doses in psoriatic patients (12). The authors determined from the relationship between cumulative amount of MTX excreted in the urine and MTX exposure and between renal CL of MTX and MTX Cmax that non-linear renal elimination kinetics occurred with MTX C_{max} of 2 μM or higher (12). Although the correlation between total CL of MTX and MTX dose in the total ALL population was weak in this study (Figure 8), our findings provide a unique analysis of a larger population with a different disease where patients received high doses of MTX intravenously.

Interestingly, we observed for the first time in ALL patients that the volume of distribution of MTX for the central compartment (*i.e.* V_c) significantly decreased ($p<0.0001$) as the MTX dose increased, suggesting saturation of protein binding in tissues (Figure 9). MTX and 7-OH-MTX are approximately 50% and 90% bound to albumin in serum, respectively (2, 45). It was determined in a small study of patients with various neoplastic diseases that binding of MTX to serum albumin becomes non-linear

with MTX concentrations of 50 μM or greater, resulting in the disproportional elevation of free MTX levels (46). Our findings are consistent with previous studies reporting significant increases in the unbound fraction of MTX and non-linear pharmacokinetics when MTX was co-administered with other drugs (47-49), suggesting that MTX and/or 7-OH-MTX can be displaced from their binding sites on serum and tissue proteins.

MTX therapy can lead to severe toxicity to a variety of organs in ALL patients, including the kidney, GI tract, hematopoietic system, central nervous system, and less commonly the liver (1, 2). Therefore, in our study we analyzed the effect of MTX treatment on clinical biomarkers for renal and hepatic function. We observed that MTX had a negative impact on renal function since it resulted in a significant increase ($p<0.0001$) in SCr and a significant decrease ($p<0.0001$) in GFR in ALL patients following treatment with MTX. Specifically, twenty-four of 404 ALL patients in our study showed an increase of 50% or greater in their SCr following treatment with MTX (Figure 10), which is considered a clinical sign of impaired kidney function. In addition, thirty-nine of 404 ALL patients in our study exhibited GFR values between 60 and 89 mL/min (*i.e.* a 25% reduction in GFR from the normal range) after treatment with MTX, which indicates mild kidney damage, while nine of 404 ALL patients had GFR values between 15 and 59 mL/min (*i.e.* a 50% reduction in GFR from the normal range) after MTX (Figure 11), which signifies moderate to severe kidney damage. None of our ALL patients had GFR values of less than 15 mL/min after treatment with MTX, which is a sign of kidney failure. Our findings are consistent with previous studies, where a much smaller number of ALL patients was analyzed, showing that SCr and GFR can be useful predictors of delayed MTX elimination and MTX-induced nephrotoxicity (8, 9, 12, 50,

51). Detrimental changes in clinical biomarkers of renal function during MTX therapy, such as those observed in our study, are clinically significant because they can result in variable MTX disposition and put ALL patients at risk of developing not only nephrotoxicity but other systemic toxicities since MTX and its minor metabolite are predominantly eliminated by the kidney.

We observed for the first time that MTX appears to negatively affect clinical biomarkers of hepatic function, including total bilirubin, ALT, and AST in ALL patients. Specifically, the mean of the per-patient median total bilirubin increased from 0.45 ± 0.24 mg/dL to 0.65 ± 0.60 mg/dL after MTX, while the mean of the per-patient median ALT increased from 34.1 ± 31.9 IU/L to 96.8 ± 163 IU/L after MTX, and the mean of the per-patient median AST increased from 35.6 ± 21.1 IU/L to 145.7 ± 253 IU/L (Figure 12-14). A total of 43 (27.7%) of 155 and 40 (25.8%) of 155 ALL patients exhibited increases of at least three times the upper limit of normal, which is indicative of liver damage, in their ALT and AST, respectively, following treatment with MTX. These findings suggest that approximately 25% of ALL patients are at risk of developing MTX-induced hepatotoxicity. Our data are consistent with previous studies that investigated the common occurrence of hepatic dysfunction following weekly low-dose oral MTX therapy in the treatment of rheumathoid arthritis and psoriasis (52, 53). To date, however, there has been very little investigation of the effect of high-dose intravenous MTX therapy in ALL on liver function and toxicity and our study provides the first preliminary evidence of damaging effects of MTX on the liver.

In summary, our pharmacoepidemiological analyses in ALL patients treated with high-dose MTX suggest that MTX pharmacokinetics is non-linear and highly variable

and that severe systemic toxicities as a result of increased exposure to MTX are related to both elevated blood levels of MTX and delayed elimination of MTX. In addition, both renal and hepatic function in ALL patients appears to be adversely affected by MTX, which could lead to variable MTX disposition and result in MTX-induced nephrotoxicity and hepatotoxicity. Our follow-up pharmacogenetic analysis will provide insights on the contribution of genetic variation in membrane transporters that are expressed in the kidney and that interact with MTX on the observed clinical variability in MTX disposition and toxicity.

References

1. Carroll WL, Bhojwani D, Min DJ, Raetz E, Relling M, Davies S, et al. Pediatric acute lymphoblastic leukemia. Hematology (Am Soc Hematol Educ Program) 2003: 102-31.

2. Goodman LS, Hardman JG, Limbird LE, Gilman AG. Goodman & Gilman's the pharmacological basis of therapeutics. 10th / ed. New York: McGraw-Hill Medical Pub. Division; 2001.

3. Christophidis N, Louis WJ, Lucas I, Moon W, Vajda FJ. Renal clearance of methotrexate in man during high-dose oral and intravenous infusion therapy. Cancer Chemother Pharmacol 1981; **6**: 59-64.

4. Huffman DH, Wan SH, Azarnoff DL, Hogstraten B. Pharmacokinetics of methotrexate. Clin Pharmacol Ther 1973; **14**: 572-9.

5. Skoglund KA, Soderhall S, Beck O, Peterson C, Wennberg M, Hayder S, et al. Plasma and urine levels of methotrexate and 7-hydroxymethotrexate in children with ALL during maintenance therapy with weekly oral methotrexate. Med Pediatr Oncol 1994; **22**: 187-93.

6. Stoller RG, Hande KR, Jacobs SA, Rosenberg SA, Chabner BA. Use of plasma pharmacokinetics to predict and prevent methotrexate toxicity. N Engl J Med 1977; **297**: 630-4.

7. Shen DD, Azarnoff DL. Clinical pharmacokinetics of methotrexate. Clin Pharmacokinet 1978; **3**: 1-13.

8. Perazella MA. Crystal-induced acute renal failure. Am J Med 1999; **106**: 459-65.

9. Perazella MA. Drug-induced renal failure: update on new medications and unique mechanisms of nephrotoxicity. Am J Med Sci 2003; **325**: 349-62.

10. Christensen ML, Rivera GK, Crom WR, Hancock ML, Evans WE. Effect of hydration on methotrexate plasma concentrations in children with acute lymphocytic leukemia. J Clin Oncol 1988; **6**: 797-801.

11. Relling MV, Fairclough D, Ayers D, Crom WR, Rodman JH, Pui CH, et al. Patient characteristics associated with high-risk methotrexate concentrations and toxicity. J Clin Oncol 1994; **12**: 1667-72.

12. Hendel J, Nyfors A. Nonlinear renal elimination kinetics of methotrexate due to saturation of renal tubular reabsorption. Eur J Clin Pharmacol 1984; **26**: 121-4.

13. Bourke RS, Chheda G, Bremer A, Watanabe O, Tower DB. Inhibition of renal tubular transport of methotrexate by probenecid. Cancer Res 1975; **35**: 110-6.

14. Huang KC, Wenczak BA, Liu YK. Renal tubular transport of methotrexate in the rhesus monkey and dog. Cancer Res 1979; **39**: 4843-8.

15. Badagnani I, Castro RA, Taylor TR, Brett CM, Huang CC, Stryke D, et al. Interaction Of Methotrexate With OATP1A2 And Its Genetic Variants. J Pharmacol Exp Ther 2006.

16. Chen ZS, Robey RW, Belinsky MG, Shchaveleva I, Ren XQ, Sugimoto Y, et al. Transport of methotrexate, methotrexate polyglutamates, and 17beta-estradiol 17-(beta-D-glucuronide) by ABCG2: effects of acquired mutations at R482 on methotrexate transport. Cancer Res 2003; **63**: 4048-54.

17. Fujita T, Urban TJ, Leabman MK, Fujita K, Giacomini KM. Transport of drugs in the kidney by the human organic cation transporter, OCT2 and its genetic variants. J Pharm Sci 2006; **95**: 25-36.

18. Ganapathy V, Smith SB, Prasad PD. SLC19: the folate/thiamine transporter family. Pflugers Arch 2004; **447**: 641-6.

19. Hooijberg JH, Peters GJ, Assaraf YG, Kathmann I, Priest DG, Bunni MA, et al. The role of multidrug resistance proteins MRP1, MRP2 and MRP3 in cellular folate homeostasis. Biochem Pharmacol 2003; **65**: 765-71.

20. Ito K, Oleschuk CJ, Westlake C, Vasa MZ, Deeley RG, Cole SP. Mutation of Trp1254 in the multispecific organic anion transporter, multidrug resistance protein 2 (MRP2) (ABCC2), alters substrate specificity and results in loss of methotrexate transport activity. J Biol Chem 2001; **276**: 38108-14.

21. Takeda M, Khamdang S, Narikawa S, Kimura H, Hosoyamada M, Cha SH, et al. Characterization of methotrexate transport and its drug interactions with human organic anion transporters. J Pharmacol Exp Ther 2002; **302**: 666-71.

22. Uwai Y, Saito H, Inui K. Interaction between methotrexate and nonsteroidal anti-inflammatory drugs in organic anion transporter. Eur J Pharmacol 2000; **409**: 31-6.

23. Wielinga P, Hooijberg JH, Gunnarsdottir S, Kathmann I, Reid G, Zelcer N, et al. The human multidrug resistance protein MRP5 transports folates and can mediate cellular resistance against antifolates. Cancer Res 2005; **65**: 4425-30.

24. Zeng H, Chen ZS, Belinsky MG, Rea PA, Kruh GD. Transport of methotrexate (MTX) and folates by multidrug resistance protein (MRP) 3 and MRP1: effect of polyglutamylation on MTX transport. Cancer Res 2001; **61**: 7225-32.

25. Krajinovic M, Costea I, Chiasson S. Polymorphism of the thymidylate synthase gene and outcome of acute lymphoblastic leukaemia. Lancet 2002; **359**: 1033-4.

26. Chango A, Emery-Fillon N, de Courcy GP, Lambert D, Pfister M, Rosenblatt DS, et al. A polymorphism (80G->A) in the reduced folate carrier gene and its associations with folate status and homocysteinemia. Mol Genet Metab 2000; **70**: 310-5.

27. Laverdiere C, Chiasson S, Costea I, Moghrabi A, Krajinovic M. Polymorphism G80A in the reduced folate carrier gene and its relationship to methotrexate plasma levels and outcome of childhood acute lymphoblastic leukemia. Blood 2002; **100**: 3832-4.

28. Cheng Q, Wu B, Kager L, Panetta JC, Zheng J, Pui CH, et al. A substrate specific functional polymorphism of human gamma-glutamyl hydrolase alters catalytic activity and methotrexate polyglutamate accumulation in acute lymphoblastic leukaemia cells. Pharmacogenetics 2004; **14**: 557-67.

29. Frosst P, Blom HJ, Milos R, Goyette P, Sheppard CA, Matthews RG, et al. A candidate genetic risk factor for vascular disease: a common mutation in methylenetetrahydrofolate reductase. Nat Genet 1995; **10**: 111-3.

30. Molloy AM, Daly S, Mills JL, Kirke PN, Whitehead AS, Ramsbottom D, et al. Thermolabile variant of 5,10-methylenetetrahydrofolate reductase associated with low red-cell folates: implications for folate intake recommendations. Lancet 1997; **349**: 1591-3.

31. Ulrich CM, Yasui Y, Storb R, Schubert MM, Wagner JL, Bigler J, et al. Pharmacogenetics of methotrexate: toxicity among marrow transplantation patients varies with the methylenetetrahydrofolate reductase C677T polymorphism. Blood 2001; **98**: 231-4.

32. Stephens M, Smith NJ, Donnelly P. A new statistical method for haplotype reconstruction from population data. Am J Hum Genet 2001; **68**: 978-89.

33. Schwartz GJ, Feld LG, Langford DJ. A simple estimate of glomerular filtration rate in full-term infants during the first year of life. J Pediatr 1984; **104**: 849-54.

34. Schwartz GJ, Gauthier B. A simple estimate of glomerular filtration rate in adolescent boys. J Pediatr 1985; **106**: 522-6.

35. Uwai Y, Taniguchi R, Motohashi H, Saito H, Okuda M, Inui K. Methotrexate-loxoprofen interaction: involvement of human organic anion transporters hOAT1 and hOAT3. Drug Metab Pharmacokinet 2004; **19**: 369-74.

36. Nozaki Y, Kusuhara H, Endou H, Sugiyama Y. Quantitative evaluation of the drug-drug interactions between methotrexate and nonsteroidal anti-inflammatory drugs in the renal uptake process based on the contribution of organic anion transporters and reduced folate carrier. J Pharmacol Exp Ther 2004; **309**: 226-34.

37. Koepsell H, Endou H. The SLC22 drug transporter family. Pflugers Arch 2004; **447**: 666-76.

38. Konig J, Hartel M, Nies AT, Martignoni ME, Guo J, Buchler MW, et al. Expression and localization of human multidrug resistance protein (ABCC) family members in pancreatic carcinoma. Int J Cancer 2005; **115**: 359-67.

39. Mizuarai S, Aozasa N, Kotani H. Single nucleotide polymorphisms result in impaired membrane localization and reduced atpase activity in multidrug transporter ABCG2. Int J Cancer 2004; **109**: 238-46.

40. Morisaki K, Robey RW, Ozvegy-Laczka C, Honjo Y, Polgar O, Steadman K, et al. Single nucleotide polymorphisms modify the transporter activity of ABCG2. Cancer Chemother Pharmacol 2005; **56**: 161-72.

41. Breedveld P, Zelcer N, Pluim D, Sonmezer O, Tibben MM, Beijnen JH, et al. Mechanism of the pharmacokinetic interaction between methotrexate and benzimidazoles: potential role for breast cancer resistance protein in clinical drug-drug interactions. Cancer Res 2004; **64**: 5804-11.

42. Lee W, Glaeser H, Smith LH, Roberts RL, Moeckel GW, Gervasini G, et al. Polymorphisms in human organic anion-transporting polypeptide 1A2 (OATP1A2): implications for altered drug disposition and central nervous system drug entry. J Biol Chem 2005; **280**: 9610-7.

43. Kishi S, Griener J, Cheng C, Das S, Cook EH, Pei D, et al. Homocysteine, pharmacogenetics, and neurotoxicity in children with leukemia. J Clin Oncol 2003; **21**: 3084-91.

44. Rubnitz JE, Relling MV, Harrison PL, Sandlund JT, Ribeiro RC, Rivera GK, et al. Transient encephalopathy following high-dose methotrexate treatment in childhood acute lymphoblastic leukemia. Leukemia 1998; **12**: 1176-81.

45. Slordal L, Sager G, Huseby NE, Aarbakke J. Distribution of 7-hydroxymethotrexate in human blood. J Pharm Pharmacol 1988; **40**: 50-2.

46. Steele WH, Lawrence JR, Stuart JF, McNeill CA. The protein binding of methotrexate in the serum of patients with neoplastic disease. Cancer Chemother Pharmacol 1981; **7**: 61-4.

47. Tracy TS, Krohn K, Jones DR, Bradley JD, Hall SD, Brater DC. The effects of a salicylate, ibuprofen, and naproxen on the disposition of methotrexate in patients with rheumatoid arthritis. Eur J Clin Pharmacol 1992; **42**: 121-5.

48. Stewart CF, Fleming RA, Germain BF, Seleznick MJ, Evans WE. Aspirin alters methotrexate disposition in rheumatoid arthritis patients. Arthritis Rheum 1991; **34**: 1514-20.

49. Ferrazzini G, Klein J, Sulh H, Chung D, Griesbrecht E, Koren G. Interaction between trimethoprim-sulfamethoxazole and methotrexate in children with leukemia. J Pediatr 1990; **117**: 823-6.

50. Skarby T, Jonsson P, Hjorth L, Behrentz M, Bjork O, Forestier E, et al. High-dose methotrexate: on the relationship of methotrexate elimination time vs renal function and serum methotrexate levels in 1164 courses in 264 Swedish children with acute lymphoblastic leukaemia (ALL). Cancer Chemother Pharmacol 2003; **51**: 311-20.

51. Murry DJ, Synold TW, Pui CH, Rodman JH. Renal function and methotrexate clearance in children with newly diagnosed leukemia. Pharmacotherapy 1995; **15**: 144-9.

52. West SG. Methotrexate hepatotoxicity. Rheum Dis Clin North Am 1997; **23**: 883-915.

53. Thomas JA, Aithal GP. Monitoring liver function during methotrexate therapy for psoriasis: are routine biopsies really necessary? Am J Clin Dermatol 2005; **6**: 357-63.

CHAPTER 7

SUMMARY AND CONCLUSIONS

It is widely recognized that there is considerable variation in how patients respond to drug therapy, with some individuals showing no efficacy, others exhibiting exaggerated responses, and still others having severe toxicities (1). It has been established that inter-patient variability in drug therapy is often much greater than intra-patient variation, suggesting that genetic factors are important determinants of drug response and may account for between 20 and 95% of the variability in the efficacy and disposition of drugs (2). Most of the early pharmacogenetics research has focused on assessing the functional role and clinical impact of variation in drug metabolizing enzymes, such as CYP2D6 (3, 4). More recent studies have begun to examine the functional and clinical consequences of genetic variation in other proteins that interact with drugs, such as drug transporters and drug receptors, on the observed inter-individual variability in drug therapy (3, 5-11).

In particular, membrane transporters play critical roles in controlling the cellular levels of endogenous nutrients (*i.e.* nucleotides, amino acids, sugars, vitamins, and hormones), neurotransmitters, xenobiotics, and therapeutics, thereby modulating both whole-body homeostasis and drug disposition. Transport proteins have been shown to be expressed in absorptive and excretory tissues, including enterocytes, hepatocytes, and tubular epithelial cells of the kidneys, where they determine the absorption and elimination of a wide range of drugs (8, 9, 11, 12). In addition, membrane transporters

have also been located in peripheral tissues and at blood tissue barrier sites, such as the blood-brain, blood-placenta, and blood-testis barrier, where they control the distribution, efficacy, and toxicity of therapeutic compounds (8, 9, 11-13).

It is well recognized that the major obstacles in cancer treatment are intrinsic and acquired drug resistance and drug-induced toxicities (14). In this context, membrane transporters that interact with drugs, along with drug metabolizing enzymes, are important determinants of the pharmacokinetics and pharmacodynamics of anti-cancer drugs, influencing the response and toxicity of cancer patients to chemotherapy (Figure 1). The major goals of the work presented in this dissertation were to identify and characterize membrane transporters that interact with anti-cancer drugs, and to analyze their genetic and functional diversity as a first step towards determining their contribution to inter-individual variability in the efficacy, disposition, and toxicity of anti-cancer drugs.

Nucleoside analogs, including cladribine and fludarabine, are administered therapeutically in the treatment of neoplasms affecting the hematopoietic system (15). Although these anti-cancer drugs are highly efficacious, a significant portion of patients exhibits intrinsic resistance to chemotherapy (16, 17). In Chapter 2, it was hypothesized that the heterogeneous response to chemotherapy with nucleoside analogs can be explained, at least in part, by inter-individual variability in the expression and/or activity of nucleoside transporters. In particular, we focused on the genetic and functional analysis of the human concentrative nucleoside transporter 3 (CNT3; *SLC28A3)*, because this transporter interacts with a broad range of endogenous nucleosides and nucleoside

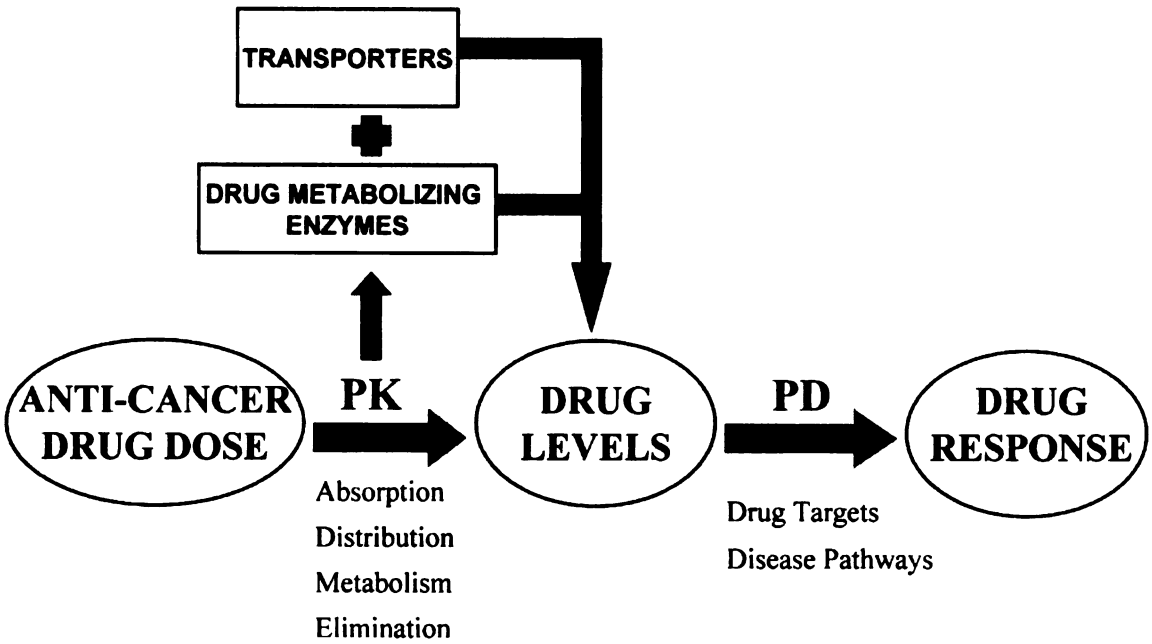

Figure 1. Determinants of anti-cancer drug action. An individual's response (*i.e.* efficacy and/or toxicity) to an anti-cancer drug depends on pharmacokinetic processes, including drug absorption, distribution, metabolism and elimination, and pharmacodynamic effects at the drug target and/or disease pathway. Transporters and drug metabolizing enzymes expressed throughout the body are critical in controlling blood and tissue specific levels of drugs, thereby affecting their pharmacokinetic properties. Inter-individual variability in anti-cancer therapy (*i.e.* efficacy, disposition, and/or toxicity) can result from naturally occurring variation in genes that influence pharmacokinetic and/or pharmacodynamic processes.

analogs and is expressed on the apical membrane of epithelial cells in absorptive and excretory tissues (18, 19).

Using an ethnically diverse population of 270 healthy individuals, a total of 56 variable sites were identified in the exons and flanking intronic regions of *SLC28A3* by the Pharmacogenetics of Membrane Transporters Project. Twelve of the sixteen coding region variants had not been previously reported. Ten resulted in amino acid changes and three of these had total allele frequencies of ≥ 1%. Nucleotide diversity (π) at non-synonymous and synonymous sites of *SLC28A3* was estimated to be 1.81×10^4 and 18.13×10^4, respectively, suggesting that this gene is under negative selection. A total of 35 haplotypes, six of which occurred with a total frequency of ≥ 5%, were estimated using PHASE (20). The common non-synonymous variant, p. Tyr113Cys, was present in a common haplotype, which was found in all ethnic groups.

All non-synonymous variants, constructed by site-directed mutagenesis and expressed in *Xenopus laevis* oocytes, transported purine and pyrimidine model substrates, except for c. 1099G>A (p. Gly367Arg). This rare variant alters an evolutionarily conserved site in the putative substrate recognition domain of CNT3. The presence of three additional evolutionarily conserved glycine residues in the vicinity of p. Gly367Arg that are also conserved in human paralogs suggest that these glycine residues are critical in the function of the concentrative nucleoside transporter family. In addition, it was determined that CNT3 interacts with cladribine and fludarabine with affinities (K_m) of approximately 300 and 1000 μM, respectively.

The genetic analysis and functional characterization of CNT3 variants suggest that this transporter does not tolerate non-synonymous changes and is important for

human fitness. It remains to be determined whether genetic variation in other regions of *SLC28A3* contribute to the observed variation in the clinical response to nucleoside analogs in leukemia patients.

Methotrexate (MTX) is used in patients with malignant and autoimmune diseases (15). MTX is an organic anion, which is primarily excreted unchanged in the urine. Its elimination has been shown to depend on both saturable secretory and reabsorptive mechanisms, implicating membrane transporters expressed in the kidney in these processes (21-24). Since it was recently determined that the organic anion transporting polypeptide, OATP1A2 (OATP-A; *SLCO1A2*), is expressed on the apical membrane of distal tubule cells (25), it was hypothesized in Chapter 3 that OATP1A2 interacted with MTX, controlling the reabsorption of this drug in the kidney and thereby influencing the systemic and tissue levels of MTX. In particular, we focused on characterizing the interaction of MTX with OATP1A2, on identifying naturally occurring variants in OATP1A2, and examining MTX interaction with protein-altering variants in OATP1A2.

We observed that MTX uptake was saturable with a K_m of approximately 450 μM in *Xenopus laevis* oocytes expressing OATP1A2. Our finding that MTX transport was enhanced in acidic pH has important clinical implications in the absorption and elimination of MTX, since the luminal pH of the intestine and kidney, where OATP1A2 is expressed, can range from 4 to 8. Interestingly, another human OATP transporter, OATP2B1, which is highly expressed on the apical membrane of intestinal cells, was recently shown to be sensitive to extracellular pH, but unlike OATP1A2, its pH-dependent transport depended on the proton gradient (26, 27).

Using an ethnically diverse population of 270 healthy individuals, a total of 41 variable sites were identified in the exons and flanking intronic region of *SLCO1A2*. Eleven variants altered the protein sequence of OATP1A2 and of these seven were newly discovered. Six protein-altering variants had allele frequencies of ≥ 1% in at least one ethnic group.

All of the protein-altering variants in OATP1A2 were constructed by site-directed mutagenesis and functionally characterized in *Xenopus laevis* oocytes. It was determined that 4 protein-altering variants in OATP1A2 exhibited altered transport of the model compound, estrone-3-sulfate (ES), and/or MTX. The common variant, p. Ile13Thr, was hyperfunctional for ES and MTX and showed a 2-fold increase in the V_{max} for ES. The common variant, p. Glu172Asp exhibited reduced maximal transport capacity for ES and MTX. p. Arg168Cys was hypofunctional and p. Asn277DEL was non-functional.

Because of its expression on the apical membrane of the distal tubule and in other tissues (*i.e.* liver, blood-brain barrier, and intestine) relevant to MTX disposition and toxicity (28-30), these findings suggest that OATP1A2 may play a role in active tubular reabsorption of MTX and in MTX-induced toxicities. Furthermore, genetic variation in OATP1A2 may have important pharmacokinetic and toxicological implications. Future studies are needed to assess the clinical consequences of genetic variation in OATP1A2, especially with respect to MTX therapy.

The organic anion transporters (OAT; *SLC22A6-8* and *SLC22A10-11*) have been shown to modulate the tubular secretion and renal elimination of MTX (23, 31, 32). In addition, OATs have been implicated in a variety of clinically relevant drug-drug interactions involving MTX and other organic anion drugs (23, 33-37). Among OATs,

human OAT3 (*SLC22A8*) is the most abundantly expressed on the basolateral membrane of proximal tubule cells in the kidney (38, 39). Therefore, in Chapter 3 we examined the genetic and functional diversity of OAT3 in ethnically diverse populations to better understand the genetic factors that can contribute to inter-individual variability in MTX therapy.

Using an ethnically diverse population of 270 healthy individuals, a total of 26 naturally occurring variants were identified in the exons and flanking intronic regions of *SLC22A8*. Ten of 26 variable sites led to a change in the protein sequence of OAT3; of these 3, p. Val281Ala, p. Ile305Phe, and p. Val448Ile, were polymorphisms occurring at a frequency of $\geq$ 1% in an ethnic group, while 6 (p. Phe129Leu, p. Gln239DEL, p. Ile260Arg, p. Arg277Trp, p. Ala310Val, and p. Ala399Ser) were singletons, meaning they were found only once in 540 chromosomes. The ratio of nucleotide diversity for non-synonymous sites to that for synonymous sites (π_{NS}/π_S) was 0.05 for *SLC22A8* compared to a previous estimate of 0.23 for 24 transporter genes (40), suggesting that OAT3 is under significant purifying selection acting against amino-acid changes. A total of 20 haplotypes in *SLC22A8* were estimated using PHASE (20), and of those 5 had total frequencies of $\geq$ 5% and occurred in all ethnic groups. The common protein-altering variants p. Val281Ala and p. Ile305Phe were each found in an ethnic specific haplotype, while p. Val448Ile was found in a haplotype, which was present in 3 of 4 ethnic groups.

OAT3 was shown to exhibit a saturable uptake of MTX with a K_m of 75 μM. Five of ten protein-altering variants in OAT3 exhibited altered uptake of MTX Specifically, p. Arg149Ser, p. Gln239DEL, and p. Ile260Arg were non-functional, while p. Phe129Leu and p. Arg277Trp exhibited half of the transport activity compared to OAT3 reference.

With the exception of p. Arg277Trp, all of the protein-altering variants with altered transport function occurred at evolutionarily conserved (EC) sites, suggesting that substitutions at EC sites are likely to be deleterious for OAT3 transport function.

Our genetic and functional studies indicate that OAT3 likely plays an important role in the active secretion of MTX in the kidney and that protein-altering variants in OAT3 may contribute to inter-individual variation in MTX disposition and toxicity. The functional analysis of genetic variants in OAT3 and other transporters (41-45), such as CNT3 (Chapter 2), suggests that rare variants should often be given higher priority when selecting polymorphisms for pharmacogenetics studies. Further studies should be done to address the clinical impact of genetic variants in OAT3 to MTX elimination and toxicity in the kidney and brain.

A considerable number of studies have reported on the tissue distribution and substrate specificity of rodent and human Oatps/OATPs (28, 29). However, the driving force of substrate transport across the membrane for human OATPs is still poorly understood. Since it was determined in Chapter 3 that OATP1A2 mediates the pH-dependent transport of organic anions, such as MTX, in Chapter 5 we examined in detail the mechanisms of transport of organic anions by OATP1A2 as well as the structural determinants in OATP1A2 that are required for its transport function.

We determined that the K_m of ES for OATP1A2 at pH 5.0 decreased by 7-fold compared to pH 7.4, with minor changes in the maximal transport rate, suggesting that extracellular acidic pH enhances the affinity of OATP1A2 for organic anions. Using a proton ionophore, we determined that the pH-dependent transport of ES and MTX was not driven by the proton gradient across the membrane. In addition, the pH-dependent

transport of organic anions by OATP1A2 was not dependent on the membrane potential and intracellular anions, such as HCO_3^-, OH^-, and GSH, did not appear to be exchanged for extracellular organic anion substrates.

Since ES and MTX are organic anions, we analyzed whether cationic residues in OATP1A2 (*i.e.* arginine, lysine, and histidine) were required for OATP1A2-mediated transport of organic anions using amino acid modifying reagents and site-directed mutagenesis of evolutionarily conserved cationic residues found in transmembrane domains and extracellular loops of OATP1A2. Chemical modification of histidine residues abolished cellular uptake of ES by OATP1A2, suggesting that histidines in OATP1A2 are critical for its transport function. The mutants R49, R168A, R240A, R556A, R590A, R609A, K33A, K341A, and H107A exhibited dramatic reductions in the cellular accumulation of ES and/or MTX, suggesting that these residues in OATP1A2 have important structural and functional roles.

Our mechanistic and functional studies indicate that OATP1A2 plays an important role in the pH-dependent absorption and elimination of organic anion drugs, such as MTX, thereby influencing their tissue-specific disposition and toxicity. Further studies should be directed at identifying additional residues in OATP1A2 that are required for its transport function as well as residues in OATP1A2 that impart pH-sensitivity in the interaction with organic anions. In addition, it remains to be determined whether charged residues in OATP1A2 alter transporter expression, transporter turn-over rate, and/or the kinetics of interaction with organic anions.

MTX has been extensively used in the treatment of childhood acute lymphoblastic leukemia (ALL) (46). Despite resulting in high remission rates, MTX has several

therapeutic problems that can influence its efficacy and toxicity, including variable pharmacokinetics and renal dysfunction (15, 22, 32, 47-49). MTX elimination occurs via saturable secretion and reabsorption mechanisms in the kidney, suggesting that membrane transporters expressed in the proximal and distal tubules of the kidney are involved in these processes (15, 21-24). In Chapter 6, we expanded upon the genetic and functional analyses discussed in Chapter 3 and Chapter 4 to examine whether genetic variation in kidney transporters that interact with MTX contributes to the observed clinical variability in MTX disposition and toxicity.

A total of 565 patients with newly diagnosed ALL were enrolled at St. Jude Children's Research Hospital between 1991 and 1998 and received between 4 and 10 courses of high-dose MTX infusions. The majority of ALL patients were male and of European-American ethnicity.

To determine whether genetic variation in membrane transporters expressed in the kidney is a factor in the observed variability in MTX pharmacokinetics and toxicity, we selected 11 single nucleotide polymorphisms and 16 haplotypes in six kidney transporters (OAT3, OATP1A2, RFC, MRP2, MRP4, and BCRP) to be associated with MTX systemic clearance (CL), MTX plasma concentrations 42 hours after dosing (C_{42h}), and biomarkers of renal function (serum creatinine (SCr) and glomerular filtration rate (GFR)). These studies are ongoing.

Pharmacoepidemiological analyses in ALL patients treated with high-dose MTX indicated that 5% of ALL patients exhibited elevated high-risk MTX C_{42h}. The elevated high-risk MTX C_{42h} was found to be correlated with low MTX CL and increased exposure to MTX (AUC), which is clinically significant because it can lead to the

accumulation of MTX in normal cells and tissues exposing them to the cytotoxic effects of MTX and can result in the development of severe systemic toxicities. In addition, it was observed that MTX pharmacokinetics is non-linear, where MTX CL increases, while MTX volume of distribution (V_c) decreases with increasing MTX dose, suggesting the presence of saturable renal reabsorption processes and saturable tissue protein binding. Furthermore, it was determined that MTX appears to negatively affect renal function, since ALL patients exhibited a significant increase in SCr and a significant decrease in GFR after exposure to MTX. Biomarkers for hepatic function, including total bilirubin, ALT, and AST, appeared to be adversely affected by MTX, since ALL patients showed significant increases in all three clinical parameters following exposure to MTX. These findings are clinically important, because MTX effects on renal and hepatic function could contribute to variable MTX disposition and result in nephrotoxicity and hepatotoxicity.

By generating hypotheses, the studies in this chapter have expanded our knowledge regarding the variability in MTX pharmacokinetics and the impact of MTX on renal and hepatic function in ALL patients. In addition, we have selected genetic variants and haplotypes in six membrane transporters that are expressed in proximal and distal tubule cells of the kidney that will be used in future studies to determine whether genetic variation in kidney transporters is associated with inter-individual variability in MTX disposition and toxicity.

Membrane transporter proteins act as gatekeepers in cells and tissues of the human body controlling the uptake and efflux of endogenous nutrients and clinically used

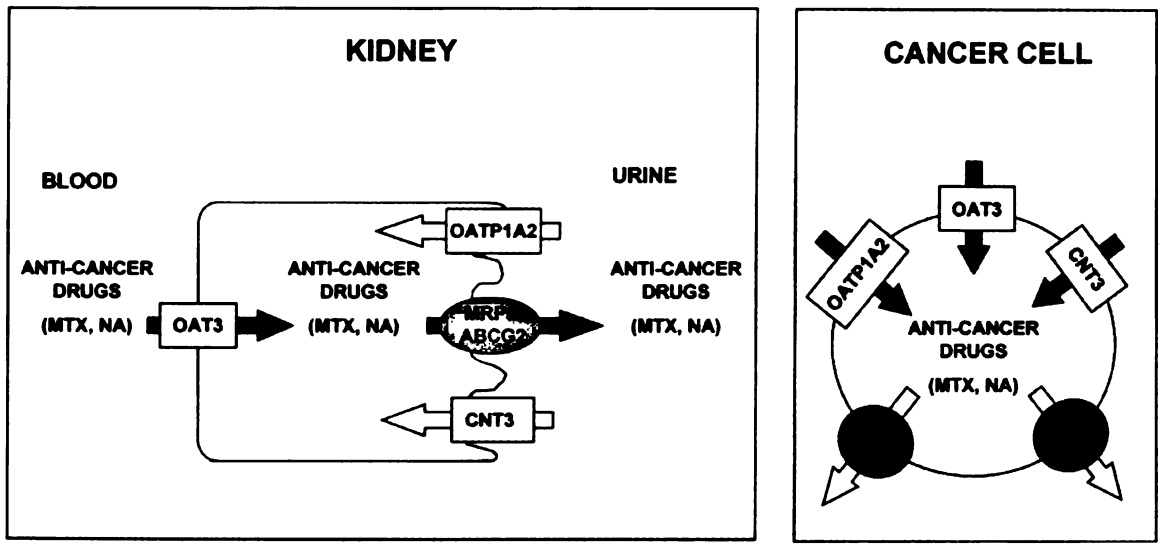

Figure 2. Schematic diagram depicting disposition of anti-cancer drugs in the kidney (left panel) and cancer cells (right panel) based on findings from Chapter 2, 3, and 4. Left panel, anti-cancer drugs are actively secreted into kidney tubule cells and actively reabsorbed from urine by solute carrier (SLC) and/or ATP-binding cassette (ABC) transporters. Black arrows show secretion processes, while white arrows indicate reabsorption processes. MTX is actively secreted into proximal tubule cells by OAT3 and into the kidney lumen via MRPs and BCRP (50, 51) (Chapter 4). MTX is reabsorbed from the urine in the distal tubule by OATP1A2 (Chapter 3). Nucleoside analogs, such as cladribine and fludarabine, are secreted into the kidney lumen by MRPs (52, 53) and reabsorbed from the urine into proximal tubule cells via CNT3 (Chapter 2). Right panel, anti-cancer drug efficacy is influenced by uptake (SLC) and efflux (ABC) transporters expressed in cancer cells. Black arrows denote drug uptake, while white arrow indicate drug efflux from the cancer cell. MTX is transported into cancer cells by OAT3 and OATP1A2, while it is effluxed out by MRPs and BCRP (50, 54-59) (Chapter 3 and 4). Nucleoside analogs gain access into cancer cells via CNT3 and are effluxed out by MRPs (52, 53)(Chapter 2). Transporters belonging to the SLC superfamily are shown in white

rectangles, while those belonging to the ABC superfamily are indicated by gray circles. Arrows provide the direction of anti-cancer drug transport. MTX, methotrexate; NA, nucleoside analog; MRP, multi-drug resistance related protein; ABCG2, breast cancer related protein or BCRP.

drugs. As exemplified in Figure 2, transporters that are expressed in target organs, such as cancer cells, and in tissues important for drug disposition, including the kidney, liver, and intestine, are critical determinants of the efficacy and toxicity of drugs (11, 12). It has been shown that there is considerable inter-individual variability in drug response and drug-induced toxicities and a significant portion of such variation can be explained by an individual's genes (2). Studies presented in Chapter 2-6 of this dissertation provide significant contributions to the fields of drug transport and pharmacogenetics. Membrane transporters, including CNT3, OATP1A2, and OAT3, were functionally characterized for their interaction with anti-cancer drugs to demonstrate their roles in controlling systemic and tissue levels of chemotherapeutic agents. In addition, the genetic and functional diversity of membrane transporter proteins, including CNT3, OATP1A2, and OAT3, was examined in detail to demonstrate how genetic variation in membrane transporters can influence inter-individual variability in the efficacy, disposition, and toxicity of anti-cancer drugs. Future studies are needed to further elucidate the clinical consequences of genetic and functional variation in membrane transporters on homeostasis of endogenous nutrients and drug therapy.

References

1. Evans WE, Relling MV. Pharmacogenomics: translating functional genomics into rational therapeutics. Science 1999; **286**: 487-91.

2. Kalow W, Endrenyi L, Tang B. Repeat administration of drugs as a means to assess the genetic component in pharmacological variability. Pharmacology 1999; **58**: 281-4.

3. Meyer UA. Pharmacogenetics - five decades of therapeutic lessons from genetic diversity. Nat Rev Genet 2004; **5**: 669-76.

4. Weinshilboum R. Inheritance and drug response. N Engl J Med 2003; **348**: 529-37.

5. Evans WE, McLeod HL. Pharmacogenomics--drug disposition, drug targets, and side effects. N Engl J Med 2003; **348**: 538-49.

6. Kerb R. Implications of genetic polymorphisms in drug transporters for pharmacotherapy. Cancer Lett 2006; **234**: 4-33.

7. Fischer V, Einolf HJ, Cohen D. Efflux transporters and their clinical relevance. Mini Rev Med Chem 2005; **5**: 183-95.

8. Gerloff T. Impact of genetic polymorphisms in transmembrane carrier-systems on drug and xenobiotic distribution. Naunyn Schmiedebergs Arch Pharmacol 2004; **369**: 69-77.

9. Kim RB. Transporters and xenobiotic disposition. Toxicology 2002; **181-182**: 291-7.

10. Roden DM, George AL, Jr. The genetic basis of variability in drug responses. Nat Rev Drug Discov 2002; **1**: 37-44.

11. Ayrton A, Morgan P. Role of transport proteins in drug absorption, distribution and excretion. Xenobiotica 2001; **31**: 469-97.

12. Lee VH. Membrane transporters. Eur J Pharm Sci 2000; **11 Suppl 2**: S41-50.

13. Cordon-Cardo C, O'Brien JP, Boccia J, Casals D, Bertino JR, Melamed MR. Expression of the multidrug resistance gene product (P-glycoprotein) in human normal and tumor tissues. J Histochem Cytochem 1990; **38**: 1277-87.

14. Efferth T, Volm M. Pharmacogenetics for individualized cancer chemotherapy. Pharmacol Ther 2005; **107**: 155-76.

15. Goodman LS, Hardman JG, Limbird LE, Gilman AG. Goodman & Gilman's the pharmacological basis of therapeutics. 10th / ed. New York: McGraw-Hill Medical Pub. Division; 2001.

16. Pott C, Hiddemann W. Purine analogs in the treatment of chronic lymphocytic leukemia. Leukemia 1997; **11 Suppl 2**: S25-8.

17. Robak T. The role of nucleoside analogues in the treatment of chronic lymphocytic leukemia-lessons learned from prospective randomized trials. Leuk Lymphoma 2002; **43**: 537-48.

18. Ritzel MW, Ng AM, Yao SY, Graham K, Loewen SK, Smith KM, et al. Molecular identification and characterization of novel human and mouse concentrative Na+-nucleoside cotransporter proteins (hCNT3 and mCNT3) broadly selective for purine and pyrimidine nucleosides (system cib). J Biol Chem 2001; **276**: 2914-27.

19. Mangravite LM, Badagnani I, Giacomini KM. Nucleoside transporters in the disposition and targeting of nucleoside analogs in the kidney. Eur J Pharmacol 2003; **479**: 269-81.

20. Stephens M, Smith NJ, Donnelly P. A new statistical method for haplotype reconstruction from population data. Am J Hum Genet 2001; **68**: 978-89.

21. Hendel J, Nyfors A. Nonlinear renal elimination kinetics of methotrexate due to saturation of renal tubular reabsorption. Eur J Clin Pharmacol 1984; **26**: 121-4.

22. Shen DD, Azarnoff DL. Clinical pharmacokinetics of methotrexate. Clin Pharmacokinet 1978; **3**: 1-13.

23. Bourke RS, Chheda G, Bremer A, Watanabe O, Tower DB. Inhibition of renal tubular transport of methotrexate by probenecid. Cancer Res 1975; **35**: 110-6.

24. Huang KC, Wenczak BA, Liu YK. Renal tubular transport of methotrexate in the rhesus monkey and dog. Cancer Res 1979; **39**: 4843-8.

25. Lee W, Glaeser H, Smith LH, Roberts RL, Moeckel GW, Gervasini G, et al. Polymorphisms in human organic anion-transporting polypeptide 1A2 (OATP1A2): implications for altered drug disposition and central nervous system drug entry. J Biol Chem 2005; **280**: 9610-7.

26. Kobayashi D, Nozawa T, Imai K, Nezu J, Tsuji A, Tamai I. Involvement of human organic anion transporting polypeptide OATP-B (SLC21A9) in pH-dependent transport across intestinal apical membrane. J Pharmacol Exp Ther 2003; **306**: 703-8.

27. Nozawa T, Imai K, Nezu J, Tsuji A, Tamai I. Functional characterization of pH-sensitive organic anion transporting polypeptide OATP-B in human. J Pharmacol Exp Ther 2004; **308**: 438-45.

28. Hagenbuch B, Meier PJ. The superfamily of organic anion transporting polypeptides. Biochim Biophys Acta 2003; **1609**: 1-18.

29. Hagenbuch B, Meier PJ. Organic anion transporting polypeptides of the OATP/ SLC21 family: phylogenetic classification as OATP/ SLCO superfamily, new nomenclature and molecular/functional properties. Pflugers Arch 2004; **447**: 653-65.

30. Gao B, Hagenbuch B, Kullak-Ublick GA, Benke D, Aguzzi A, Meier PJ. Organic anion-transporting polypeptides mediate transport of opioid peptides across blood-brain barrier. J Pharmacol Exp Ther 2000; **294**: 73-9.

31. Liegler DG, Henderson ES, Hahn MA, Oliverio VT. The effect of organic acids on renal clearance of methotrexate in man. Clin Pharmacol Ther 1969; **10**: 849-57.

32. Huffman DH, Wan SH, Azarnoff DL, Hogstraten B. Pharmacokinetics of methotrexate. Clin Pharmacol Ther 1973; **14**: 572-9.

33. McLeod HL. Clinically relevant drug-drug interactions in oncology. Br J Clin Pharmacol 1998; **45**: 539-44.

34. Nozaki Y, Kusuhara H, Endou H, Sugiyama Y. Quantitative evaluation of the drug-drug interactions between methotrexate and nonsteroidal anti-inflammatory drugs in the renal uptake process based on the contribution of organic anion transporters and reduced folate carrier. J Pharmacol Exp Ther 2004; **309**: 226-34.

35. Takeda M, Khamdang S, Narikawa S, Kimura H, Hosoyamada M, Cha SH, et al. Characterization of methotrexate transport and its drug interactions with human organic anion transporters. J Pharmacol Exp Ther 2002; **302**: 666-71.

36. Uwai Y, Saito H, Inui K. Interaction between methotrexate and nonsteroidal anti-inflammatory drugs in organic anion transporter. Eur J Pharmacol 2000; **409**: 31-6.

37. Uwai Y, Taniguchi R, Motohashi H, Saito H, Okuda M, Inui K. Methotrexate-loxoprofen interaction: involvement of human organic anion transporters hOAT1 and hOAT3. Drug Metab Pharmacokinet 2004; **19**: 369-74.

38. Koepsell H, Endou H. The SLC22 drug transporter family. Pflugers Arch 2004; **447**: 666-76.

39. Burckhardt BC, Burckhardt G. Transport of organic anions across the basolateral membrane of proximal tubule cells. Rev Physiol Biochem Pharmacol 2003; **146**: 95-158.

40. Leabman MK, Huang CC, DeYoung J, Carlson EJ, Taylor TR, de la Cruz M, et al. Natural variation in human membrane transporter genes reveals evolutionary and functional constraints. Proc Natl Acad Sci U S A 2003; **100**: 5896-901.

41. Owen RP, Gray JH, Taylor TR, Carlson EJ, Huang CC, Kawamoto M, et al. Genetic analysis and functional characterization of polymorphisms in the human concentrative nucleoside transporter, CNT2. Pharmacogenet Genomics 2005; **15**: 83-90.

42. Owen RP, Lagpacan LL, Taylor TR, De La Cruz M, Huang CC, Kawamoto M, et al. Functional characterization and haplotype analysis of polymorphisms in the human equilibrative nucleoside transporter, ENT2. Drug Metab Dispos 2006; **34**: 12-5.

43. Leabman MK, Huang CC, Kawamoto M, Johns SJ, Stryke D, Ferrin TE, et al. Polymorphisms in a human kidney xenobiotic transporter, OCT2, exhibit altered function. Pharmacogenetics 2002; **12**: 395-405.

44. Fujita T, Urban TJ, Leabman MK, Fujita K, Giacomini KM. Transport of drugs in the kidney by the human organic cation transporter, OCT2 and its genetic variants. J Pharm Sci 2006; **95**: 25-36.

45. Badagnani I, Chan W, Castro RA, Brett CM, Huang CC, Stryke D, et al. Functional analysis of genetic variants in the human concentrative nucleoside transporter 3 (CNT3; SLC28A3). Pharmacogenomics J 2005; **5**: 157-65.

46. Carroll WL, Bhojwani D, Min DJ, Raetz E, Relling M, Davies S, et al. Pediatric acute lymphoblastic leukemia. Hematology (Am Soc Hematol Educ Program) 2003: 102-31.

47. Christophidis N, Louis WJ, Lucas I, Moon W, Vajda FJ. Renal clearance of methotrexate in man during high-dose oral and intravenous infusion therapy. Cancer Chemother Pharmacol 1981; **6**: 59-64.

48. Skoglund KA, Soderhall S, Beck O, Peterson C, Wennberg M, Hayder S, et al. Plasma and urine levels of methotrexate and 7-hydroxymethotrexate in children with ALL during maintenance therapy with weekly oral methotrexate. Med Pediatr Oncol 1994; **22**: 187-93.

49. Stoller RG, Hande KR, Jacobs SA, Rosenberg SA, Chabner BA. Use of plasma pharmacokinetics to predict and prevent methotrexate toxicity. N Engl J Med 1977; **297**: 630-4.

50. Breedveld P, Zelcer N, Pluim D, Sonmezer O, Tibben MM, Beijnen JH, et al. Mechanism of the pharmacokinetic interaction between methotrexate and benzimidazoles: potential role for breast cancer resistance protein in clinical drug-drug interactions. Cancer Res 2004; **64**: 5804-11.

51. Vlaming ML, Mohrmann K, Wagenaar E, de Waart DR, Elferink RP, Lagas JS, et al. Carcinogen and anticancer drug transport by Mrp2 in vivo: studies using Mrp2 (Abcc2) knockout mice. J Pharmacol Exp Ther 2006; **318**: 319-27.

52. Ritter CA, Jedlitschky G, Meyer zu Schwabedissen H, Grube M, Kock K, Kroemer HK. Cellular export of drugs and signaling molecules by the ATP-binding cassette transporters MRP4 (ABCC4) and MRP5 (ABCC5). Drug Metab Rev 2005; **37**: 253-78.

53. Wijnholds J, Mol CA, van Deemter L, de Haas M, Scheffer GL, Baas F, et al. Multidrug-resistance protein 5 is a multispecific organic anion transporter able to transport nucleotide analogs. Proc Natl Acad Sci U S A 2000; **97**: 7476-81.

54. Chen ZS, Robey RW, Belinsky MG, Shchaveleva I, Ren XQ, Sugimoto Y, et al. Transport of methotrexate, methotrexate polyglutamates, and 17beta-estradiol 17-(beta-D-glucuronide) by ABCG2: effects of acquired mutations at R482 on methotrexate transport. Cancer Res 2003; **63**: 4048-54.

55. Hooijberg JH, Peters GJ, Assaraf YG, Kathmann I, Priest DG, Bunni MA, et al. The role of multidrug resistance proteins MRP1, MRP2 and MRP3 in cellular folate homeostasis. Biochem Pharmacol 2003; **65**: 765-71.

56. Ito K, Oleschuk CJ, Westlake C, Vasa MZ, Deeley RG, Cole SP. Mutation of Trp1254 in the multispecific organic anion transporter, multidrug resistance protein 2 (MRP2) (ABCC2), alters substrate specificity and results in loss of methotrexate transport activity. J Biol Chem 2001; **276**: 38108-14.

57. Konig J, Hartel M, Nies AT, Martignoni ME, Guo J, Buchler MW, et al. Expression and localization of human multidrug resistance protein (ABCC) family members in pancreatic carcinoma. Int J Cancer 2005; **115**: 359-67.

58. Wielinga P, Hooijberg JH, Gunnarsdottir S, Kathmann I, Reid G, Zelcer N, et al. The human multidrug resistance protein MRP5 transports folates and can mediate cellular resistance against antifolates. Cancer Res 2005; **65**: 4425-30.

59. Zeng H, Chen ZS, Belinsky MG, Rea PA, Kruh GD. Transport of methotrexate (MTX) and folates by multidrug resistance protein (MRP) 3 and MRP1: effect of polyglutamylation on MTX transport. Cancer Res 2001; **61**: 7225-32.

UCSF LIBRARY

San Francisco Public Library
7539359
3 1378 00753 9359
For reference
Not to be taken from the room.